Symposia Biologica Hungarica 18

MATHEMATICAL MODELS OF METABOLIC REGULATION

Akadémiai Kiadó, Budapest

MATHEMATICAL MODELS OF METABOLIC REGULATION

18

MATHEMATICAL MODELS OF METABOLIC REGULATION

Edited by

T. KELETI and S. LAKATOS

(Symposia Biologica Hungarica 18)

This volume comprises the papers delivered at the FEBS Advanced Course No. 27 held after the 9th Meeting of the Federation of European Biochemical Societies in 1974. The reports of the lecturers give an overall picture of the present state of their research fields including so far unpublished results.

The papers deal with the biochemical aspects of the regulation of metabolic pathways and the possibilities of mathematical modelling of such systems. Special attention is devoted to the key enzymes and enzyme systems, further to the interaction of these enzymes and membranes as well as to the biochemical, biophysical and mathematical descriptions of kinetic analysis of the metabolic processes.

The volume is recommended for those actively engaged in biochemical and biophysical research but it may be useful also for mathematicians, physicists, biologists and medical workers who are interested in the current problems and trends of metabolic regulation.

AKADÉMIAI KIADÓ
Publishing House of the
Hungarian Academy of Sciences
BUDAPEST

ISBN 963 05 0919 9

Symposia
Biologica
Hungarica
18

Symposia Biologica Hungarica

Redigit

T. KELETI et S. LAKATOS

Vol. 18

AKADÉMIAI KIADÓ, BUDAPEST 1976

MATHEMATICAL MODELS OF METABOLIC REGULATION

Edited by

T. KELETI

Enzymology Department, Institute of Biochemistry,
Hungarian Academy of Sciences, Budapest, Hungary

and

S. LAKATOS

Enzymology Department, Institute of Biochemistry,
Hungarian Academy of Sciences, Budapest, Hungary

AKADÉMIAI KIADÓ, BUDAPEST 1976

The FEBS Advanced Course No. 27 was held at Dobogókő,
1—5 September, 1974

ISBN 963 05 0919 9

Printed in Hungary

CONTENTS

LIST OF CONTRIBUTORS

ACHILLES, W. Institute of Physiological Chemistry, Friedrich Schiller University, Jena, GDR

BELLMANN, K. Central Institute of Cybernetics and Information Processes, Acad. Sci. GDR, 1199 Berlin-Adlershof, Rudower Chaussee

BÖTTNER, R. Central Institute of Cybernetics and Information Processes, Acad. Sci. GDR, 1199 Berlin-Adlershof, Rudower Chaussee

BUBLITZ, R. Institute of Physiological Chemistry, Friedrich Schiller University, Jena, GDR

CUMME, G. Institute of Physiological Chemistry, Friedrich Schiller University, Jena, GDR

ENDRENYI, L. Department of Pharmacology and Department of Preventive Medicine and Biostatistics, University of Toronto, Toronto M5S 1A8, Canada

FAJSZI, Cs. Institute of Biophysics, Biological Research Center of the Hungarian Academy of Sciences, Szeged, Hungary

FRUNDER, H. Institute of Physiological Chemistry Friedrich Schiller University, Jena, GDR

HEINRICH, R. Humboldt-Universität zu Berlin, Institut für physiologische und biologische Chemie, Berlin, DDR

HORN, A. Institute of Physiological Chemistry Friedrich Schiller University, Jena, GDR

KELETI, T. Enzymology Department, Institute of Biochemistry, Hungarian Academy of Sciences, Budapest, Hungary

KNIJNENBURG, A. Central Institute of Cybernetics and Information Processes, Acad. Sci. GDR 1199 Berlin-Adlershof, Rudower Chaussee

KURGANOV, B. I. Institute for Vitamin Research, Moscow, USSR

NEUMANN, H. Central Institute of Molecular Biology, Acad. Sci. GDR, Berlin-Buch, Lindenberger Weg

PRAJDA, N. Laboratory for Experimental Oncology and Department of Pharmacology, Indiana University School of Medicine, Indianapolis, Indiana, USA 46202

RAPOPORT, T. A. Akademie der Wissenschaften der DDR, Zentralinstitut für Molekularbiologie, Bereich Bioregulation, Berlin-Buch, DDR

REICH, J. G. Zentralinstitut für Molekularbiologie, Bereich Methodik und Theorie, Berlin-Buch, DDR

Ricard, J. Laboratoire de Physiologie Cellulaire Végétale Associé au C. N. R. S. Université d'Aix-Marseille, Centre de Luminy, 13288 Marseille Cedex 2. France

Weber, G. Laboratory for Experimental Oncology and Department of Pharmacology, Indiana University School of Medicine, Indianapolis, Indiana, USA 46202

Williams, J. C. Laboratory for Experimental Oncology and Department of Pharmacology, Indiana University School of Medicine, Indianapolis, Indiana, USA 46202

Wright, B. Boston Biomedical Research Institute, Boston, Ma. USA

I. MODELLING OF THE KINETIC AND REGULATORY BEHAVIOUR OF ENZYMES

Symp. Biol. Hung. 18, pp. 11–30 (1974)

STATISTICAL PROBLEMS OF KINETIC MODEL BUILDING

L. ENDRENYI

Department of Pharmacology and Department of Preventive Medicine and Biostatistics, University of Toronto, Toronto M5S 1A8, Canada

ROLE AND LIMITATIONS OF STATISTICS IN MODEL BUILDING

Statistical methods are utilized with increasing frequency for the evaluation of quantitative data. They are, of course, often very useful. Indeed, one aim of this brief review is to call attention to their applicability. At the same time, thoughtless application of any useful technique or method can lead to misinterpretations, exercises in futility and dangerous misunderstandings. Therefore, it may be worthwhile to delimit the place of statistical procedures in kinetic and in general, in quantitative investigations.

Certainly, it is pointless to ask for the statistical evaluation of data when the conclusions are obvious anyway. Thus, the presence or absence of "statistical significances" can be meaningless when phenomena are clearly observed. After all, the use of statistics in the biological sciences is only a fairly recent custom, and many very valuable observations have been made and conclusions reached without resorting to such "sophisticated" procedures.

Thus it may not be useful to apply statistical methods for the evaluation of data which are practically error-free or involve only very small errors. Similarly, statistics can be of little help in the presence of very scattered, poor observations. Artificial manipulation or "massaging" of such data can only mislead an unwary investigator.

Statistical methods are applied most fruitfully with moderately scattered data. They can be used very effectively and efficiently indeed in the vast range of studies admitting this condition. Substantial information can frequently be extracted which would be inaccessible to other methods.

Nevertheless, like any technique, statistical analysis of experimental data has its limitations and will not provide an all-embracing solution, a panacea to all kinetic modelling problems. Consequently, it is a dangerous practice (seen with increasing frequency in the literature) to rely for analysis solely on numerical, statistical solutions and computer printouts. These methods should not be used blindly but with great deal of common sense, ideally in conjunction with traditional procedures, including linearizations and replots which frequently provide at least guidance for the interpretation of the observations. The continuous interplay between statistical computations and graphical evaluations is very strongly recommended.

STRATEGY OF MODEL BUILDING

A scientific investigation is performed presumably in order to learn about a biological, chemical, physical, etc. phenomenon. Certainly, at the conclusion of the study, and possibly at its commencement, assumptions, hypotheses are made which characterize the phenomenon. As a result, a biological, chemical, physical, etc. model is visualized.

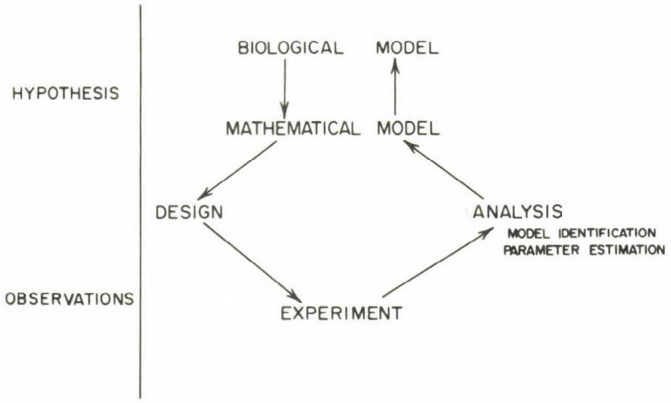

Fig. 1. General strategy of model building.

For the purpose of quantitative studies, this model can be described in mathematical terms. The resulting expressions, the mathematical models, can characterize simply straight-line, linear relationships or they can be much more complicated, such as a system of differential equations.

The hypothesis of a mathematical model should be justified and characterized on the basis of observations. Usually experiments are designed, performed and analyzed for this purpose. Therefore, the experiment and its analysis have two main purposes: First, the validity of the mathematical model must be evaluated, for example, by testing the linearity of a supposedly straight-line relationship. Adoption of a mathematical model implies also conclusions about the validity of the biological model, since computations based on the observations at least do not argue against it.

Once a model is tentatively accepted, interest centers on the evaluation of its constants. Actually in practice, the computations involving model identification and parameter estimation are usually pursued simultaneously. In principle, however, these two processes should be carefully distinguished not only in order to clarify the principal purpose of the investigation (a very important requirement, not always considered), but also because the efficient experimental design for estimations and for validity tests may not be the same (Hill, Hunter and Wichern, 1968).

The repeated cycle between model hypothesis and experimentation, including the design and analysis of the latter, is a basic characteristic of scientific investigations (Box and Hunter, 1962). It is illustrated in Fig. 1.

As an illustrative example, the Briggs-Haldane model for simple enzymic reactions will be considered:

$$E + S \rightleftharpoons ES \longrightarrow E + P$$

The corresponding mathematical model, the Michaelis-Menten equation, describes the relationship between the reaction velocity (v) and the substrate concentration (c):

$$v = \frac{Vc}{K_m + c} \quad .$$

The expression characterizes a rectangular hyperbola with two constants: The maximal velocity (V) and the so-called Michaelis constant (K_m).

In order to characterize a particular enzymic system, an investigator performs an experiment with N observations. The observed reaction velocities,

$$v_i = \frac{Vc_i}{K_m + c_i} \quad , \qquad i = 1,2,\ldots,N,$$

are not free of experimental errors (e_i) which are superimposed on the unknown true velocities, so that

$$v_i = v + e_i \quad .$$

As will be described later, the model can be analyzed by several methods. These include the various well-known linearizations of the hyperbola which can be utilized to test the validity of the mathematical, and therefore of the biological model (the Michaelis-Menten equation and Briggs-Haldane mechanism, respectively). This approach (which is, as will be seen, not necessarily the best one) relies on the evaluation of the actually observed linearity of the transformed observation.

The linearizations and the corresponding plots can be utilized also for the estimation of the two parameters. This is a customary procedure but, as will be seen, certainly not a recommended one.

PURPOSES OF MODEL BUILDING

Investigations into the characteristics of models (i.e., model building studies) are pursued for two main reasons. The first driving force is man's quest for knowledge, his search for insight into manifestations of nature. Therefore, he wishes to establish the features of various phenomena, to describe the mechanisms of processes, including those of chemical reactions, and to evaluate the magnitude of natural constants, including those of equilibrium and rate constants.

The second principal motivation for developing models lies in their utilization. For example, they can be applied for interpolation, and to some extent even for extrapolation and, therefore, for prediction.

But merely for prediction we do not necessarily require models based on natural, e.g. biological foundations. In principle, superficial but appropriately descriptive and sufficiently accurate characterizations would be quite satisfactory. Thus, we can distinguish two kinds of models: Those fundamentally relying on natural principles, including those based on mechanisms of processes (mechanistic or deterministic models), and those in which such foundations are more tenous or perhaps even entirely absent. Such empirical models may simply involve, in part or entirely, past experience concerning the properties and behaviour of the investigated system.

The mathematical form of a mechanistic model reflects, of course, features of the underlying natural models. An example is the already mentioned Michaelis-Menten equation. In contrast, empirical models may be described by very simple expressions, such as polynomials which may contain coefficients having no physical meaning at all.

The methodology of statistical analysis of the experiment, in particular that of parameter estimation, follows the division between the two model types. As will be indicated in greater detail later, parameter estimation must be performed with much greater care when insight into a model is desired than with the interest of the investigator restricted merely to the prediction of responses.

FACTORS AFFECTING MODEL IDENTIFICATION AND PARAMETER ESTIMATION

Quite naturally all investigators want to obtain information as reliably and as efficiently about the studied models as possible. It is, therefore, necessary to consider the main factors influencing the effectiveness of model validity tests and of parameter estimation. These include

i) the properties of the experimental error;
ii) the experimental design; and
iii) the method of evaluation.

The development and evaluation of models is assisted very substantially if the investigator pays thorough attention to these factors. In order to emphasize this important point, the recommended considerations and actions are summarized in Table 1. They will be analyzed now in some detail.

Table 1.

Investigators' approach to factors influencing the effectiveness of model building

Factor	Action expected of investigator
Experimental error Constant absolute error? Constant relative error?	Recognizes characteristics
Experimental design Number of observations Range of observations Scaling of observations	Carefully chooses optimum
Method of analysis Nonlinear regression Weighting? Linear transformations, graphs	Selects principal method Uses combination

CHARACTERISTICS OF THE EXPERIMENTAL ERROR

It is assumed in most model building procedures, including those based on the methods of least squares, that the experimental errors are present only in the dependent but not in the independent variables, that they are random and have constant variance independently of the magnitudes of the variables and that, for the evaluation of statistical significance tests and confidence limits, they follow the normal, Gaussian distribution. Failure of one or more of these assumptions can lead to inadequate and misleading results.

Deviations from the assumption of normally distributed errors are rather difficult to detect. For example, plots of the estimated errors (the residuals, to be discussed later) in cumulative normal grids require a large number of observations (Daniel and Wood, 1971). Fortunately, results of analyses are believed to be quite robust against moderate divergences from normality.

The assumption of randomness implies that the various observations and their errors are independent of each other, with no correlations among them. This is often reasonably correct in the case of binding or steady-state rate equations. However, as illustrated in Fig. 2, correlations

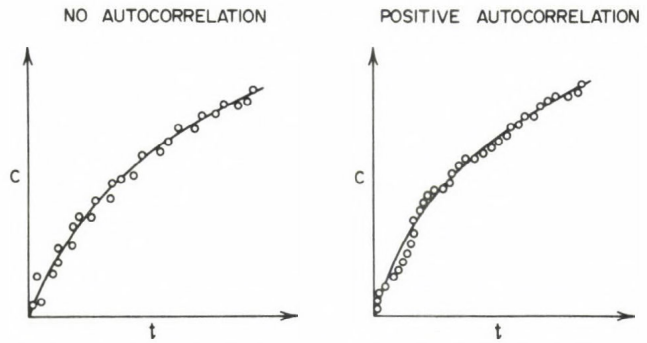

Fig. 2. Illustration of autocorrelated observations for concentration measurements of an accumulating product with time.

between consecutive time-dependent observations can be very high. The consequences of such autocorrelations (which are estimated by the corresponding observed serial correlations; Kendall and Stuart, 1966) are generally small (Suranyi, 1973) and therefore neglected. Still, it is worth pointing out that apparent serial correlations can be brought about by unusual, outlying data points. Therefore, detection of outliers is aided by the analysis of error correlations (Reich, 1974).

Among the characteristics of experimental errors, the assumption of their constant variance is particularly important since divergences from its validity have very strong effects on the outcome of model identification tests and parameter estimations. Fortunately, as we shall see later, deviations from this condition can be fairly conveniently evaluated and corrections can be made for these.

Very frequently, the absolute magnitude of the experimental error tends not to remain the same in the whole range of the investigation (corresponding to the assumption of constant error variance) but increases proportionately with the value of the response (the reaction velocity in kinetic studies). Actually, in this case, the ratio of the error to the response, i.e. the relative error, i.e. the coefficient of variation remains

constant, which is a very usual condition.

Therefore, it is important that the investigator should make a serious effort to recognize the trend in the error behaviour (cf. Table 1). In particular, he should evaluate whether the absolute or the relative

Table 2.

Principal types of error behaviour

Absolute error σ_i	Relative error σ_i/v_i
Constant	Decreases with v
Increases with v	Constant

v_i: Reaction velocity predicted at i-th observation.

σ_i: Expected standard deviation of i-th observation.

error remains constant in his experiment (Table 2). Residual plots, which will be described later, can be applied to advantage for this purpose.

EXPERIMENTAL DESIGN

The design of the experiments has very strong influence on the effectiveness of model identification (Box and Hill, 1967) and parameter estimation (Box and Lucas, 1959). Therefore, whenever possible, the investigator should select the most efficient design for the task (cf. Table 1). In particular, the components of the design should be considered, including

i) the number of observations (N);
ii) the range of the measurements; and
iii) the arrangement or spacing of the independent variable.

Increasing the number of observations improves, of course, the effectiveness of all aspects of model building (when correctly executed, see later). The final number will be the result of a compromise between the desired excellence of the results and the increasing expense in time, effort and funds.

The effect of the observational range on the outcome of the model building may be more surprising since efficiency can frequently be improved not by expanding but, on the contrary, by restricting the range of experimentation. For example, in hyperbolic kinetic or binding studies, with constant absolute observational errors, the effectiveness of parameter estimation is improved when the measurements are restricted to relative velocities not lower than 0.2 or to fractional bindings not lower than 0.4 (Endrenyi and Kwong, 1972).

This is illustrated in Fig. 3. With constant absolute error, both the precision and the bias of the parameters improve when the range of the observations is restricted at the lower end. In contrast, with constant relative errors such confinement would be ruinous since, under this error condition, the precision and accuracy of the estimated parameters improve by widening the range of observations.

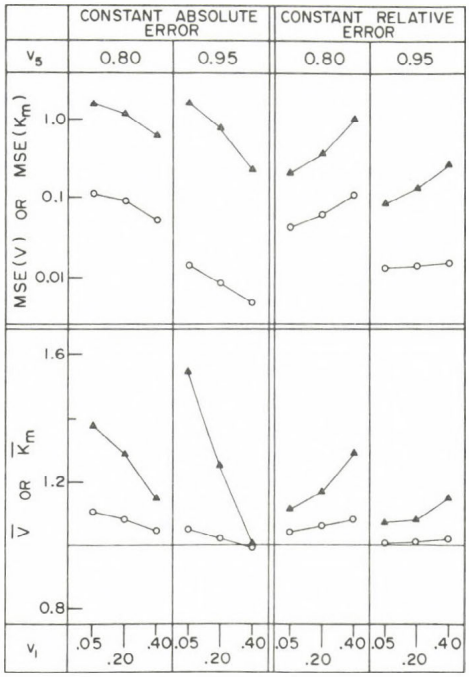

Fig. 3. Effect of experimental design on the precision and accuracy of kinetic parameters which are estimated by nonlinear regression.

Each point represents the averaged result of 100 computer simulated experiments with N=5 observations, with the concentrations uniformly spaced, and true parameters V = 1.0 and K_m = 1.0. Either constant absolute error of σ_i = 0.10 or constant relative error of σ_i = 0.20 v_i was assumed in the experiments. In the latter case the parameters were evaluated by weighted nonlinear least-squares calculations.

The open circles show estimates of V, the dark triangles refer to those of K_m.

The lower half of the diagram provides a measure of the bias (deviation from the true value of unity) in the average value of the estimated parameters. The upper half illustrates MSE, the mean square parameter error averaging the variances of the estimated parameters, which is a measure of their precision (reproducibility).

The smallest and largest relative velocities, v_1 and v_5, are indicated on the bottom and at the top of the diagram, respectively.

Such considerable contrasts between effective experimental designs emphasize again the great importance of the necessity for recognizing the error behaviour of the observations.

Restricting the range of observations does not agree with the usual conduct of the investigations. For the explanation we have to return to the already stressed two main purposes of mechanistic model building: Model identification and parameter estimation. The desirability, under certain conditions, of restricting the range of measurements has been concluded for the efficient evaluation of the two parameters. This has

implied that we have been reasonably certain of the applicability of the Michaelis-Menten equation. If, however, the appropriateness of the model is to some extent in question then readings have to be obtained also at lower concentrations in order to evaluate, for instance, the absence of sigmoidicity. Ideally again a compromise should be reached in which some observations aim at demonstrating the applicability of the hyperbolic model while the remaining ones evaluate the parameters in the most efficient way using the most effective design for this purpose.

METHOD OF ANALYSIS

By far the most frequently technique of statistical model building is the method of least squares since, as we shall see later, it has many favourable properties.

Initially, an arbitrary set of values is selected for the model parameters. From these, on the basis of the model, responses (reaction velocities) are calculated which are compared with the observed responses. The basis of the comparison is the so-called sum of squares (SS) which is the sum of the squared differences between the observations (v_i) and the corresponding values predicted from these models ($\hat{v}_i$),

$$SS = \Sigma(v_i - \hat{v}_i)^2 \quad .$$

By selecting new values for the parameters, the predicted responses and, therefore, the sum of squares can be recalculated. As the best values, those parameters will be chosen which yield the smallest of all possible sum of squares. These estimated, least-squares parameters are designated by a "hat" mark over them.

In the example of the Michaelis-Menten equation, the two parameters, V and K_m, can be systematically varied to obtain their least-squares values, $\hat{V}$ and $\hat{K}_m$, corresponding to the minimum sum of squares,

$$SS = \Sigma\left(v_i - \frac{\hat{V}c_i}{\hat{K}_m + c_i}\right)^2 \quad .$$

As mentioned above, corrections can be made if changes in the error variance are recognized. In this case, the sum of squares is weighted before minimization,

$$SS_w = \Sigma w_i(v_i - \hat{v}_i)^2 \quad ,$$

with weights (w_i) inversely proportional to the variance of the error,

$$w_i \propto 1/\sigma_i^2 \quad .$$

If, for example, the relative error of observations is constant throughout the range of experimentation then the standard deviation is proportional to the response (which is estimated by the predicted response),

$$\sigma_i \propto \hat{v}_i$$

and the weight is inversely proportional to the square of the predicted response,

$$w_i \alpha 1/\hat{v}_i^2 .$$

Therefore, the minimized sum of squares is now

$$SS_w = \Sigma(v_i - \hat{v}_i)^2 / \hat{v}_i^2 .$$

It must be emphasized concerning the selection of weights that they should be based on a scheme of error behaviour (e.g., constant absolute or constant relative errors) involving the entire set of observations since this gives reasonable confidence in their validity. The weights should not rely merely on replicate readings obtained at a given experimental condition (at a given set of independent variables; Ottaway, 1973) since their reliability would be very limited. The reason for this, in statistical language, is that they would be based on very few degrees of freedom.

The calculations, based on the method of least squares are quite straightforward if the model is linear in all of its parameters since, in this case, the parameters and the corresponding minimum sum of squares can be computed from explicit formulas. If, however, the model is not linear with respect to all of its parameters, then the sum of squares must be minimized by iterative calculations. Naturally, such nonlinear regression analyses are facilitated by the use of computers.

The Michaelis-Menten model is linear in one of its parameters, V, but not linear with respect to the other, K_m. Thus, its analysis should involve nonlinear regression computations (Wilkinson, 1961; Cleland, 1963, 1967; Bliss and James, 1966).

Traditionally, evaluations of the Michaelis-Menten equation have been based on one of its linear transformations. These have been used both for model identification and parameter estimation. Their analysis can be purely graphical or again the method of least squares may be applied. Consequently, as will be discussed, there is a selection among the analytical methods (which is in fact much wider). Therefore, the investigator can and should choose the best, most effective procedure among these (cf. Table 1). An even more preferable approach, especially in studies of complex systems, utilizes more than a single procedure. Without exception, each of these has limitations. Reliance on only a computational or solely on a graphical method can be very dangerous. Consequently, mutual confirmation of the conclusions and quantitative results by a variety of methods is very desirable. This procedure is strongly recommended and urged.

PROBLEMS OF NONLINEAR REGRESSION COMPUTATIONS

To recapitulate, in nonlinear regression analysis the model parameter values are varied until they yield the smallest sum of squares value. Therefore, we are searching for an absolute minimum on a surface of sum of squares plotted against the appropriate parameter values (Fig. 4).

Several computational schemes have been devised which explore the surface, seeking its minimum. The task of such optimization routines is easy when the surface itself is smooth with nearly ellipsoidal sections indicating almost linear characteristics (Fig. 4a). At other times, however, the surface is bent, elongated, "banana-shaped" (Fig. 4b). The search for

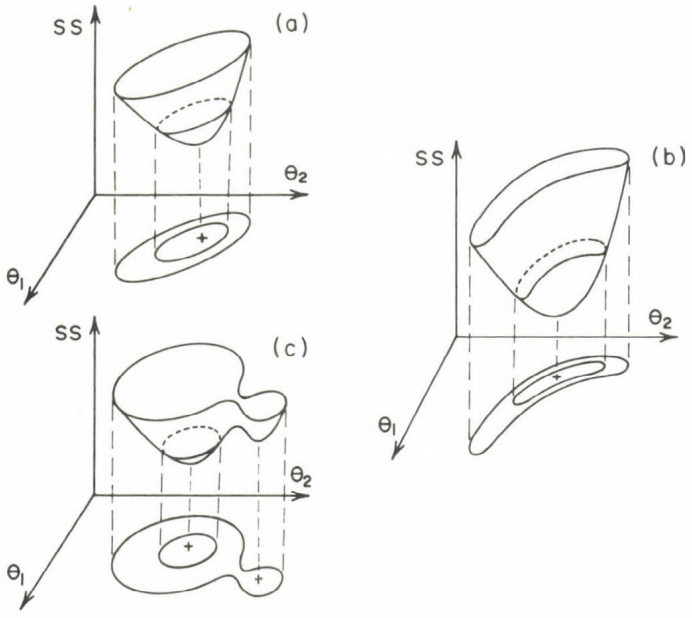

Fig. 4. Sum of squares surfaces. The sum of squares (SS) is plotted against the corresponding parameter values (θ_1 and θ_2). Projections of the surfaces (corresponding to their sections) are shown in the plane of the parameters. This contains also the parameter combination indicated by + which yields the minimum SS.
(a) Surface with almost elliptical sections and, therefore, with nearly linear characteristics. (b) Elongated, bent, strongly nonlinear surface. (c) Surface with a local and an absolute minimum.

its minimum is much more difficult, often frustrating. Still other surfaces have more than one minimum (Fig 4c). Their exploration may falsely stop at a local minimum instead of going on to the true absolute minimum.

There are many general and very useful computer programs and packages attempting to remedy these difficulties (for example, Cornish-Bowden and Koshland, 1970; Atkins, 1971; Reich et al., 1972, for kinetic purposes). All of them can conveniently be used for most model building problems. However, none of the routines can solve all difficult situations and none can claim to provide the all-round best procedure.

The problem of multiple minima was already mentioned. As a result, the user is never quite certain of reaching the smallest sum of squares, the absolute minimum. This problem of uniqueness can be overcome by starting the exploration of the surface at several points, that is, by assuming initially several different sets of parameters. They should yield repeatedly the same final set of constants.

It should be emphasized that the assumed error behaviour with the corresponding weights determines the shape of the sum of squares surface. Consequently, the minimum and the least-squares parameters are fixed by

supposing, for example, the condition of constant absolute or constant relative error but they do not involve the assumption of any kind of error distribution.

RESIDUAL PLOTS, TEST OF ERROR BEHAVIOUR

After reaching the minimum, the various assumptions made earlier must be tested. Very important among these is the hypothesis of random errors having constant variance which is evaluated most frequently by the very useful residual plots. These contrast (weighted) residuals with the various independent variables, with the observed or the predicted response or with the time sequence of the observations (Draper and Smith, 1966; Daniel and Wood, 1971, pp. 27-32). Systematic deviations, nonrandom trends indicate the inadequacy of the assumed model.

The weighted residuals are (Box and Hill, 1974)

$$\sqrt{w_i}\ \text{(observed response - predicted response)}$$

$$= \sqrt{w_i}\ (v_i - \hat{v}_i)$$

for reaction velocities.

For example, if a hyperbola is fitted to kinetic data which actually characterize a system with positive deviations from hyperbolic behaviour (for instance, a system described by a sigmoidal rate curve) then systematic

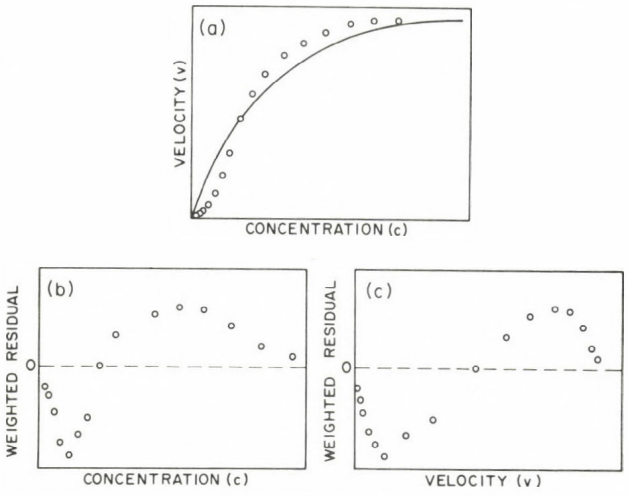

Fig. 5. Residual plots demonstrating the inadequateness of an assumed model. (a) Hyperbolic rate curve fitted to observations involving a nonhyperbolic kinetic system. (b) Residuals plotted against the independent variable or (c) against the observations show systematic trends, i.e., deviations from randomness.

trends are noted in the observed residual plot (Fig. 5). Advantages of the plot include its being illustrative and very sensitive. This is useful since, for example, positive nonhyperbolicities are not necessarily indicated by the appearance of sigmoidicity (Ainsworth, 1968; Endrenyi, Chan and

Wong, 1971).

Residual plots can be applied not only in order to aid model identification, but also to characterize the observational error and, in particular, to distinguish between the two main types of error behaviour.

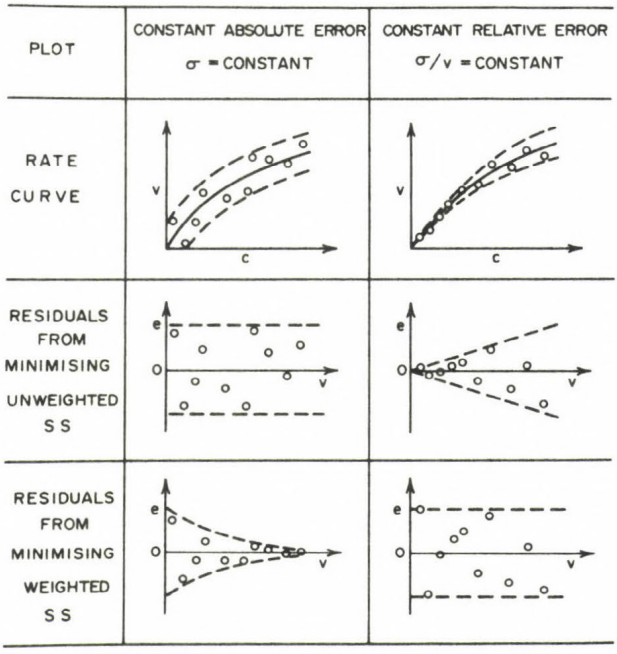

Fig. 6. Residual plots testing the behaviour of the experimental error. The two rate curve plots illustrate the two main types of error behaviour: constant absolute error or constant relative error. If a rate equation is fitted to the data by assuming the former error condition then the residuals conforming with the error behaviour show randomness in a horizontal band. Conflict with the true error behaviour is revealed by a widening belt. Similarly, randomness is indicated when the curve-fitting based on the assumption of constant relative errors corresponds to the true error properties, while a narrowing error band suggests disagreement with the error hypothesis.

As illustrated in Fig. 6, a given set of observations can be fitted successfully by least-squares curves based on the assumption constant absolute and then by constant relative error. The assumption corresponding to the true error behaviour yields a plot in which the residuals with the appropriate weights are randomly placed in a horizontal band. In contrast, by using weights not corresponding to the true error behaviour, characteristically non-random plots are obtained. For instance, assuming in the computations constant relative errors when, in fact, the absolute magnitude of the errors tends to remain constant, the band of residuals narrows. The reverse situation is indicated by exactly the opposite pattern: If a system is actually characterized by constant relative errors but the data are fitted by assuming constant absolute errors, then the residuals are in a wedge-shaped, widening zone.

Various formal schemes have been proposed for the evaluation of error behaviour. These include the use of transformations (Box and Cox, 1964), the regression of the absolute value of the residuals (e) against the response (Glejser, 1969), and an F-test comparing the sum of the squares of the last residuals in an ordered sequence against the sum of the squares of the initial residuals (Goldfeld and Quandt, 1965),

$$F = (e_N^2 + e_{N-1}^2 + \ldots) \; / \; (e_1^2 + e_2^2 + \ldots) \quad .$$

Kwong (1972) compared these methods and concluded that the F-test was most powerful. He recommended that the first and last m points of the sequence should be included in the test where m is the integer part of (N+3)/4 . For example, with N=10 observations, m = Int(13/4) = 3 , and

$$F = (e_{10}^2 + e_9^2 + e_8^2) \; / \; (e_1^2 + e_2^2 + e_3^2) \quad .$$

The performance of the test has not been compared with those of the residual plots. Their use is very strongly recommended both for model identification and for the evaluation of error behaviour.

MODEL IDENTIFICATION

We return now to the main tasks of model building: Model identification and parameter estimation for the characterization of mechanistic models and for prediction.

Some approaches have already been mentioned which are useful for the identification of models. They included the application of residual plots which could indicate incompatibility with the assumed model. Serial correlations were noted to indicate disagreement with some of the assumptions made or to suggest the presence of outliers.

Some other useful criteria have been summarized by Bártfai and Mannervik (1972). These include the success of nonlinear regression computations and examination of the estimated parameter values. Slowness or failure of the computer routine to converge, from several initial points, to a minimum raises suspicion about the validity of the model. Similarly, doubts are caused by unreasonable values of the estimated parameters or by their relatively large standard errors. (It has occasionally been suggested that negative parameter estimates, which could not characterize kinetic or equilibrium constants, would be restricted simply by constraining the range of accessible values. It is firmly believed that this approach would merely evade but not solve the problem. As we shall now see, negative estimates of constants actually call attention at their dispensability.) Convergence problems, unreasonable parameter values or large errors are often manifestations of the same problem: The presence of redundant parameters. Eliminating these from the model will frequently cure the anomalies (Box and Jenkins, 1970; Reich and Zinke, 1974). Redundance is indicated also when the information matrix has very small eigenvalues.

The variance of the observational errors estimated from the minimum sum of squares provides further evidence of the adequacy of the model. If an independent measure of the errors is available, for instance, from replicate observations, then the two estimates can be compared. Substantial, "significant" difference between the two estimates suggests a deficiency of the investigated model.

If an independent error estimate is not available then the use of the sum of squares is restricted to comparing the plausibility of the various alternative models. The sums of squares yielded by the different models

can be contrasted and the expression giving rise to the smallest value accepted as most likely to be correct. The procedure has been described for rate equations by Pettersson and Pettersson (1970) and applied by Bártfai et al. (1973) and Augustinsson et al. (1974). It is worth emphasizing again that assumption of the appropriate error behaviour is critical in all statistical modelling calculations.

Occasionally high values of multiple correlation coefficients are presented to demonstrate the acceptability of a model. This is quite meaningless for a number of reasons. For one, it is quite possible to have a curve fitting, in general, very well to the data points and still yielding non-random residuals.

As mentioned earlier, several approaches are available to many modelling problems. Returning for illustration to the example of the Michaelis-Menten equation, its identification may involve not only statistical but, in fact more usually, graphical procedures. These evaluate the presence or absence of linearity in one of the transformed plots of the hyperbola. However, comparison of the various methods (Moosavi and Endrenyi, 1974) indicates that, when least-squares methods are used for analysis, decisions based on (weighted) nonlinear regression are much more powerful than the analysis of the transformation. However, purely graphical evaluations should not be dismissed. Non-hyperbolicities are quite sensitively detected by the Eadie-Hofstee (or by the equivalent Scatchard) plot. The most frequently used Lineweaver-Burk plot is inferior because of its extreme insensitivity (Moosavi and Endrenyi, 1974).

PARAMETER ESTIMATION FOR PREDICTION

The main and often unstated aim of many investigations is to characterize sufficiently a system in order to enable the satisfactorily accurate interpolation and prediction of its responses. Certainly, this seems to be the case in various branches of kinetics. Many chemical kinetic data find application in the practice of chemical engineers designing reactors and other plant units; drug kinetic observations and constants are used primarily for the characterization and prediction of drug responses under various conditions; enzyme kinetic results are utilized for predicting features of metabolic regulatory systems.

If prediction of responses is recognized as the primary purpose of an investigation then the requirements for the design, execution and analysis of the experiments become different, generally less stringent. This is illustrated (Fig. 7) again on the example of hyperbolic kinetic experiments described by the Michaelis-Menten equation. If prediction is required only in the low concentration, first-order region (as is frequently the case, for example, in pharmacokinetic applications) then the observations may also be restricted to this range. However, such an experimental design does not permit evaluation of the maximal velocity, V, and therefore the Michaelis-Menten constant, K_m, can be estimated also with only great uncertainty. The diagram illustrates two pairs of parameters which describe the linear portion equally well. This indicates that one parameter is actually redundant. The linear part of the rate curve can indeed be characterized by a single constant, the ratio of V/K_m.

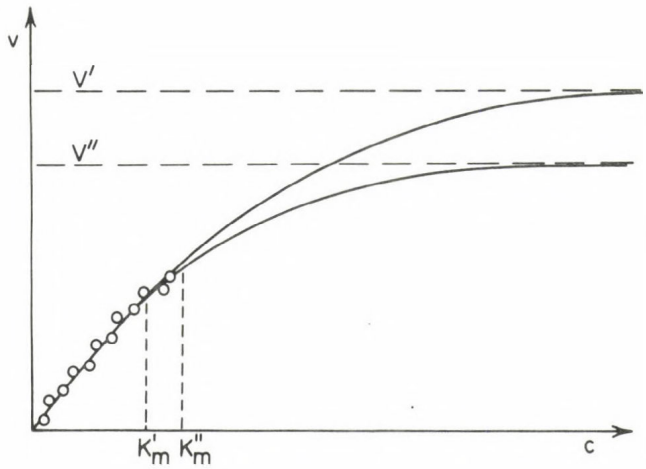

Fig. 7. Use of unsatisfactorily estimated parameters for prediction.
Response prediction is required only in the approximately linear range of the hyperbola and, therefore, observations are restricted to this range. From these, the maximum velocity (V) and, therefore, the Michaelis constant (K_m) can be evaluated only very imprecisely. Consequently, the two pairs of constants, (V',K_m') and (V'',K_m''), are plausible but uncertain estimates. Still, both pairs provide good prediction in the desired region.
One parameter, V/K_m, is sufficient to characterize the rate curve in its linear range, while one constant is redundant. Consequently, redundant parameters can be applied for response prediction. However, they should not be utilized for mechanistic modelling.

Thus, it is quite appropriate (even if not too elegant) to use a model containing redundant parameters for purposes of prediction. After all, we are not really interested now in the constants or their errors. They merely serve as a means for the main purpose of the investigation, prediction. This is in sharp contrast with the study of mechanistic models: We wish to know their parameters with high precision. Consequently, redundant constants will be excluded from deterministic models.

ESTIMATION OF MECHANISTIC MODEL PARAMETERS

As just indicated, evaluation of mechanistic models requires the inclusion of the smallest possible number of interpretable parameters. This principle of parsimony (Tukey, 1961) means that the mathematical representation of an otherwise plausible model would have to be simplified. For example, it may not be possible to evaluate some constants of mechanistically interpretable higher-degree rate equations and, therefore, these may have to be represented by the less complex, more superficial Hill equation (Hurst, 1974; Reich and Zinke, 1974). The situation may arise simply because of the given true magnitude of the natural model constants. For instance, stepwise equilibrium constants and most cumulative formation constants of the Adair equation, which characterizes most binding systems, cannot be evaluated in the presence of strong positive cooperativities (Endrenyi and Kwong, 1973).

Several methods are frequently available for the assessment of model constants. Again, they include not only statistical but also often very useful graphical procedures. The relative merits of these procedures have been evaluated only in a few instances. For example, various approaches estimating the two Michaelis-Menten parameters have been compared in computer simulations (Dowd and Riggs, 1965; Colquhoun, 1969; Endrenyi and Kwong, 1972). As illustrated in Table 3 for two specific experimental designs, the precision (reproducibility) and accuracy (correctness) of parameters obtained by nonlinear regression and from the various linear transformations were noted. Quite consistently, the customarily and still most usually used double reciprocal Lineweaver-Burk plot yielded extremely poor results.

Among the linear plots derived from the hyperbolic expression, the reverse of the Hanes plot, the contrast of c against c/v , gave the best results when the absolute experimental error was constant. This plot excelled also with constant relative errors but only with harmonic and, to some extent, with geometric spacing (Endrenyi and Kwong, 1972). The parameters obtained by this linearization have frequently more favourable properties than those based on (weighted) nonlinear regression.

Nevertheless, nonlinear least-squares analysis has advantageous features which recommend its use with asymptotically large samples: The estimated parameters are efficient (have the smallest possible variance), consistent (essentially, unbiased) and normally distributed (Hartley and Booker, 1965; Jennrich, 1969; Malinvaud, 1970). For practical purposes it is probably more important that the optimality of these parameter estimates does not deteriorate badly at small sample sizes (Endrenyi and Kwong, 1972). This means also that the parameters obtained by (weighted) nonlinear regression are comparatively robust, that is, while they may not give the best possible results, they will never give very poor, misleading or imprecise answers either. This feature strongly suggests the use of the (weighted) nonlinear least-squares method.

Some alternative procedures evaluating the Michaelis-Menten parameters have been described recently. They include the separate estimation of the two parameters on the basis of paired observations (Miguel Merino, 1974; Fajszi and Endrenyi, 1974), and an ingenious graphical procedure determining the constants in parameter space and using nonparametric methods for their assessment (Eisenthal and Cornish-Bowden, 1974).

The evaluation of model constants requires ascertaining not only the magnitudes of the parameters but also their errors. Unfortunately, this principle is not always followed. At any rate, even the separately expressed parameter errors contain incomplete and somewhat misleading information. For illustration, Fig. 8b shows the separate 99% confidence limits of the two Michaelis-Menten parameters evaluated in an experiment. Confidence limits estimated jointly for the two constants are also displayed in the diagram. The separate limits contain an extensive range of parameter combinations which are excluded by the joint limits. On the other hand, some further admissible pairs of constants would not be considered by the separate limits.

The joint limits are slanted upwards thereby indicating that the two parameters are correlated in the positive direction. This is reasonable since together with a larger V value we would expect to determine also a larger K_m value.

Table 3.

Accuracy and precision of Michaelis-Menten parameters estimated by various methods[a]

	Method of estimation		Geometric				Arithmetic			
			V		K_m		V		K_m	
	y	x	Mean	RMS[b]	Mean	RMS	Mean	RMS	Mean	RMS
Constant absolute error										
(d)	1/v	1/c	287.1	*[c]	535.0	*	76.8	*	28.2	*
(e)	v	v/c	85.2	23.6	71.6	49.3	98.5	20.6	101.3	55.7
(f)	c/v	c	108.6	28.4	132.3	85.2	108.9	26.9	136.8	95.8
	1/c	1/v	101.8	*	95.6	*	96.0	*	92.0	*
(g)	v/c	v	95.6	*	72.3	*	218.0	*	487.1	*
(h)	c	c/v	96.3	20.0	98.2	60.8	97.0	19.7	97.2	69.7
(i)	v	c	104.9	23.8	115.6	71.0	107.9	30.2	128.9	108.7
Constant relative error										
(d)	1/v	1/c	106.0	*	117.0	*	109.6	*	137.5	*
(e)	v	v/c	92.7	21.5	85.7	40.9	96.6	20.5	93.8	49.6
(f)	c/v	c	106.1	22.6	120.0	64.1	103.0	28.3	117.6	98.4
	1/c	1/v	139.3	*	177.2	*	97.5	*	95.7	*
(g)	v/c	v	124.5	299.0	151.5	504.9	126.4	*	171.7	*
(h)	c	c/v	96.9	17.9	95.6	51.3	88.5	20.4	70.0	71.8
(i)	v	c	109.4	26.5	124.9	82.8	110.3	37.0	132.6	130.3
(j)	v(w)	c	103.6	29.3	109.4	58.4	105.9	24.6	117.0	60.4

(a) 750 computer simulated experiments were performed with 5 observations spaced, between relative velocities of 0.20 and 0.80, either in a geometric or in arithmetic progression of concentrations. The true values of the two parameters were assumed to be 100. With constant absolute errors, the standard deviation $\sigma = 10$, with constant relative errors $\sigma_i = 0.20 v_i$.

(b) RMS: Root mean square of the estimated parameter, the square root of the average observed parameter variance.

(c) * indicates RMS > 1000.

(d) Lineweaver, H. and Burk, D. (1934). J. Am. Chem. Soc. 56, 658.

(e) Eadie, G.S. (1942). J. Biol. Chem. 146, 85; Hofstee, B.H.J. (1952). Science 116, 329.

(f) Hanes, C.S. (1932). Biochem. J. 26, 1406.

(g) Scatchard, G. (1949). Ann. N.Y. Acad. Sci. 51, 660.

(h) Endrenyi and Kwong (1972).

(i) Nonlinear regression.

(j) Weighted nonlinear regression.

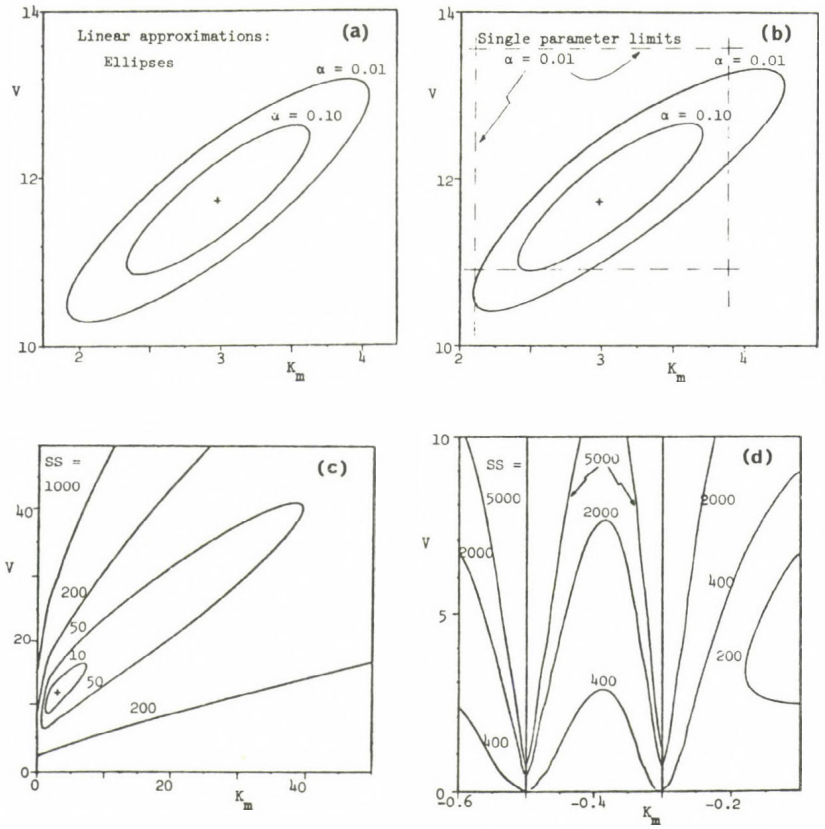

Fig. 8. Separate and joint parameter confidence limits.

Approximate 90 and 99% confidence limits (α=0.10 and 0.01, respectively) to a given set of hyperbolic kinetic observations based (a) on elliptical contours (linear approximation), and (b) on sum-of-squares contours. The latter are nearly elliptical. The second diagram includes also the 99% limits estimated separately for the two parameters. They include a large range of parameter pairs which is excluded by the joint limits.

(c) The approximately elliptical shape of the sum-of-squares contours is distorted further away from the minimum which is indicated by a + sign. (d) Contours in the inadmissible region of negative K_m values.

The joint confidence limits actually represent a given, constant value of the sum of squares. Consequently, as comparison of Figs. 8b and 8c indicates, the elliptical shape of the sum-of-squares contours (projected sections of the sum-of-squares surface) are gradually distorted with increasing distance from the minimum. This can be seen further in Fig. 8d which shows contours at negative K_m values.

In spite of their usefulness, confidence and sum-of-squares contours have scarcely been applied until now.

SUMMARY

1. An investigator must know very clearly the primary purpose of his/her investigation. In particular, it should be realized whether the observations aim mainly at the future prediction of the responses (empirical models) or at gaining insight into natural phenomena, including mechanisms of processes (mechanistic or deterministic models).

2. The effective design and analysis of experiments depend on their purposes: (a) prediction, (b) identification of mechanistic models, or (c) evaluation of their parameters. Response prediction does not necessarily require precisely estimated parameters and it may rely on redundant constants.

3. Features and procedures of model building are illustrated on the example of the hyperbolic Michaelis-Menten equation which characterizes the Briggs-Haldane mechanism of simple enzymic reactions.

4. Designing the experiments in accordance with their primary purpose assists their evaluation and can substantially improve the reliability of the conclusions. For instance, provided that the absolute observational error tends to remain constant throughout the range of experimentation, the precision and accuracy of the estimated Michaelis-Menten equation improve by restricting the range of observations to relative velocities exceeding at least the 0.2.

5. Analysis by the method of least squares requires that the error behaviour (for instance, constant absolute or constant relative error) be known or at least assumed. The experimental design and the conclusions reached by the analysis can be vastly different depending on the actual and assumed error structure. Assumptions about the distribution of errors are required only for the calculation of confidence limits and statistical significance tests.

6. Residual plots are very useful for testing the validity of an assumed model and for evaluating the error behaviour.

7. Especially in more complex systems, graphical and statistical procedures frequently supplement each other. Each method has its limitations. Therefore, conclusions concerning model validity and parameter values should be reached by the joint application of several procedures.

ACKNOWLEDGEMENT

This work was supported by the Medical Research Council of Canada.

REFERENCES

Ainsworth, S. (1968). J. Theor. Biol. 19, 1.
Atkins, G.L. (1971). Biochim. Biophys. Acta 252, 405.
Augustinsson, K.B., Bártfai, T. and Mannervik, B. (1974). Biochem. J. 141, 825.
Bártfai, T., Ekwall, K. and Mannervik, B. (1973). Biochemistry 12, 387.
Bártfai, T. and Mannervik, B. (1972). FEBS Letters 26, 252.
Bliss, C.I. and James, A.T. (1966). Biometrics 22, 573.
Box, G.E.P. and Cox, D.R. (1964). J. Roy. Stat. Soc. B26, 211.
Box, G.E.P. and Hill, W.J. (1967). Technometrics 9, 57.
Box, G.E.P. and Hill, W.J. (1974). Technometrics 16, 385.
Box, G.E.P. and Hunter, W.G. (1962). Technometrics 4, 301.
Box, G.E.P. and Jenkins, G.M. (1970). in "Time Series Analysis, Forecasting and Control" (Holden-Day, San Francisco), pp. 248-250.
Box, G.E.P. and Lucas, H.L. (1959). Biometrika 46, 77.

Cleland, W.W. (1963). Nature 198, 463.
Cleland, W.W. (1967). Adv. Enzymol. 29,1.
Colquhoun, D. (1969). Appl. Statist. 18, 130.
Cornish-Bowden, A. and Koshland, D.E., Jr. (1970). Biochemistry 9, 3325.
Daniel, C. and Wood, F.S. (1971). in "Fitting Equations to Data" (Wiley-Interscience, New York) pp. 28-29, 34-43.
Dowd, J.E. and Riggs, D.S. (1965). J. Biol. Chem. 240, 863.
Draper, N.R. and Smith, H. (1966). in "Applied Regression Analysis" (Wiley, New York), pp. 86-93.
Eisenthal, R. and Cornish-Bowden, A. (1974). Biochem. J. 139, 715.
Endrenyi, L., Chan, M.S. and Wong, J.T.F. (1971). Can. J. Biochem. 49, 581.
Endrenyi, L. and Kwong, F.H.F. (1972). in "Analysis and Simulation of Biochemical Systems", eds. H.C. Hemker and B. Hess (North-Holland, Amsterdam), p. 219.
Endrenyi, L. and Kwong, F.H.F. (1973). Acta Biol. Med. Germ. 31, 495.
Fajszi, Cs. and Endrenyi, L. (1974). FEBS Letters 44, 240.
Glejser, H. (1969). J. Am. Stat. Assoc. 64, 316.
Goldfeld, S.M. and Quandt, R.E. (1965). J. Am. Stat. Assoc. 60, 539.
Hartley, H.O. and Booker, A. (1965). Ann. Math. Stat. 36, 638.
Hunter, W.G., Hill, W.J. and Wichern, D.W. (1968). Technometrics 10, 145.
Hurst, R.O. (1974). Can. J. Biochem. 52, 1137.
Jennrich, A.I. (1969). Ann. Math. Stat. 40, 633.
Kendall, M.G. and Stuart, A. (1966). in "The Advanced Theory of Statistics" (Hafner, New York), Vol. 3, pp. 361-362, 403-404.
Kwong, F.H.F. (1972). M.Sc. Thesis, University of Toronto, pp. 73-90.
Malinvaud, E. (1970). Ann. Math. Stat. 41, 956.
Miguel Merino, F. (1974). Biochem. J. 143, 93.
Moosavi, S.F.H. and Endrenyi, L. (1974). Proc. Can. Fed. Biol. Soc. 17, 162.
Ottaway, J.H. (1973). Biochem. J. 134, 729.
Pettersson, G. and Pettersson, I. (1970). Acta Chem. Scand. 24, 1275.
Reich, J.G. (1974). Studia Biophys. 42, 165.
Reich, J.G., Wangermann, G., Falck, M. and Rohde, K. (1972). Eur. J. Biochem. 26, 368.
Reich, J.G. and Zinke, I. (1974). Studia Biophys. 43, 91.
Suranyi, G. (1973). M.Sc. Thesis, University of Toronto, pp. 45-53.
Tukey, J.W. (1961). Technometrics 3, 191.
Wilkinson, G.N. (1961). Biochem. J. 80, 324.

Symp. Biol. Hung. 18, pp. 31—45 (1974)

REGULATORY PROPERTIES OF DISSOCIATING AND ASSOCIATING ENZYME SYSTEMS

B.I.Kurganov

Institute for Vitamin Research, Moscow, USSR

INTRODUCTION

All allosteric enzymes possess a subunit structure. At certain conditions they reveal the possibility to dissociate into individual subunits which are usually enzymatically inactive. On the other hand, the molecules of allosteric enzymes often contain the additional association sites whose saturation occurs at association of protein molecules. The typical situation is that the similar association is accompanied by diminution of specific enzyme activity owing to steric screening of active sites.

The displacement of equilibrium between oligomeric enzyme forms under the influence of metabolites is one of the allosteric mechanisms of enzyme regulation in vivo (Datta et al.,1964; Kurganov,1967,1968; Nichol et al.,1967; Frieden, 1967,1968; Bonsignore et al.,1968; LéJohn et al.,1969; Constantinides and Deal,1969; Stancel and Deal,1969). It is worth noting that the regulatory characteristics of polymerising allosteric enzyme systems (the shape of the dependences of enzymatic reaction rate on concentration of substrate

or allosteric effector, the character of combined action of allosteric ligands on enzymatic activity and so on) depends on enzyme concentration.

The kinetic approaches to analysis of kinetic behaviour of dissociating and associating allosteric enzyme systems were elaborated by Kurganov (1967,1968). These approaches allow to prove the existence of allosteric interactions mediated by the displacement of equilibrium between oligomeric enzyme forms under the influence of substrates and allosteric effectors and isolate allosteric interactions in individual oligomeric forms. The separation of such two types of allosteric interactions becomes possible if one analyses the set of the dependences of specific enzyme activity on enzyme concentrations obtained at various fixed concentrations of substrate and allosteric effectors.

Taking into account the great importance of the dependences of specific enzyme activity (i.e. initial velocity of enzymatic reaction divided by enzyme concentration) on concentration of enzyme at analysis of kinetic behaviour of dissociating and associating allosteric enzyme systems, I decided to devote my report to the discussion of the character of specific enzyme activity versus enzyme concentration plots for polymerising enzyme systems of different types.

ASSOCIATING ENZYME SYSTEMS OF THE TYPE MONOMER $\rightleftharpoons$ N-MER

The dependence of specific enzyme activity on enzyme concentration is determined by three parameters for the associating enzyme systems of the type monomer $\rightleftharpoons$ N-mer. These

parameters are the specific enzyme activity of monomer, a_1, the specific enzyme activity of N-mer, a_N, and the association constant for the equilibrium monomer $\rightleftarrows$ N-mer, K_N (K_N = [N-mer]/[monomer]^N). If the equilibrium between monomer and N-mer is rapid in comparison with the over-all enzymatic process, the association constant K_N is the apparent constant which depends on concentrations of allosteric ligands. Specific enzyme activity and total enzyme concentration calculated on monomer are connected by the following relationship in the case of system monomer $\rightleftarrows$ N-mer (Kurganov,1973):

$$(a_1-a_N)^{N-1}(a_1-a) - NK_N[E]_o^{N-1}(a-a_N)^N = 0 \qquad (1)$$

In Fig.1 the dependences of relative specific enzyme activity on dimensionless enzyme concentration $\sqrt[N-1]{K_N[E]_o}$ are represented in logarithmic coordinates for dissociating and associating enzyme systems of the type inactive monomer $\rightleftarrows$ active tetramer (a) and active monomer $\rightleftarrows$ inactive tetramer (b). Similar standard plots may be superposed on experimental data represented in logarithmic coordinates. This procedure enables to estimate association constant and the specific enzyme activities of oligomeric forms for the enzyme systems of the type monomer $\rightleftarrows$ N-mer where one of the oligomeric enzyme forms is catalytically inactive.

ASSOCIATING ENZYME SYSTEMS OF THE TYPE MONOMER $\rightleftarrows$ DIMER $\rightleftarrows$ TETRAMER

The cases have been discussed when only one of the oligomeric forms is enzymatically active.

a) inactive monomer $\rightleftarrows$ inactive dimer $\rightleftarrows$ active tetramer

Specific enzyme activity and total molar enzyme concentration calculated on monomer are connected by the following relationship (Kurganov,1973):

$$1 + \sqrt[4]{\frac{4aK_1^2[E]_o}{a_4K_2}} - \left(1 - \frac{a}{a_4}\right)\sqrt[4]{\frac{4a_4K_1^2K_2[E]_o^3}{a}} = 0 \qquad (2)$$

where a_4 is the specific enzyme activity of tetramer, K_1 and K_2 are association constants for the equilibria monomer $\rightleftarrows$ dimer and dimer $\rightleftarrows$ tetramer respectively. Specific enzyme activity increases with increasing enzyme concentration. The

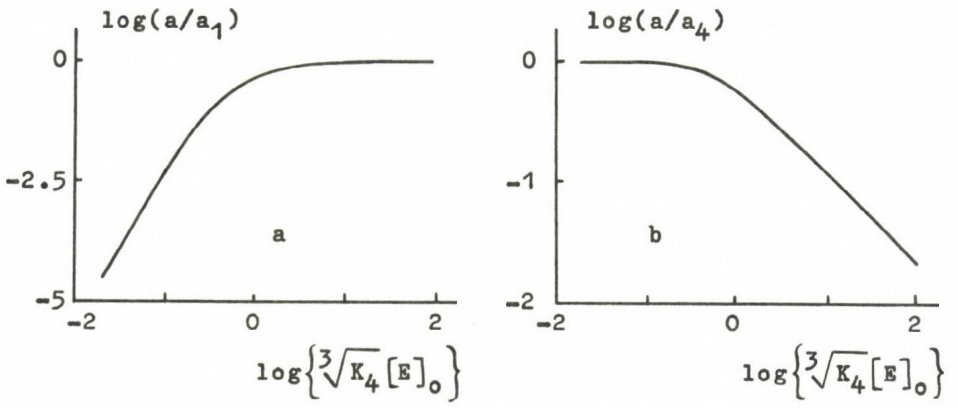

Fig.1. The associating enzyme system of the type monomer $\rightleftarrows$ tetramer (N=4).

The dependences of relative specific enzyme activity (a/a_4 and a/a_1 respectively) on dimensionless enzyme concentration $\sqrt[3]{K_4}[E]_o$ for enzyme systems of the types inactive monomer $\rightleftarrows$ active tetramer (a) and active monomer $\rightleftarrows$ inactive tetramer (b). a_1 and a_4 are the specific enzyme activities of monomer and tetramer respectively.

plots of a vs $[E]_o$ are sigmoidal and sigmoidicity increases with decreasing value of K_1/K_2 ratio (Fig.2).

b) inactive monomer $\rightleftarrows$ active dimer $\rightleftarrows$ inactive tetramer

$$1 - \frac{a}{a_2} - \sqrt{\frac{a}{2a_2K_1[E]_o}} - K_2[E]_o\left(\frac{a}{a_2}\right)^2 = 0 \qquad (3)$$

where a_2 is the specific enzyme activity of dimer. Specific enzyme activity passes through a maximum with increasing enzyme concentration (Fig.3).

c) active monomer $\rightleftarrows$ inactive dimer $\rightleftarrows$ inactive tetramer

$$(1-a/a_1)^2 - 2K_1[E]_o\,(a/a_1)^2 - 4K_1^2K_2[E]_o^3(a/a_1)^4 = 0 \qquad (4)$$

where a_1 is the specific enzyme activity of monomer. Specific enzyme activity decreases with increasing enzyme concentration. At $K_1/K_2 < 0.04343$ the plots of a vs $[E]_o$ are sigmoidal (Fig.4).

ASSOCIATING ENZYME SYSTEMS WITH LINEAR INDEFINITE TYPE OF ASSOCIATION

Let us discuss the associating enzyme systems of the types $M \rightleftarrows M_2 \rightleftarrows M_3 \rightleftarrows \ldots$ (I) and $2M \rightleftarrows D \rightleftarrows D_2 \rightleftarrows D_3 \rightleftarrows \ldots$ (II). In the systems of the first type monomer (M) has two association sites and is able to form polymer having indefinite length. In the systems of the second type dimer (D) which is in equilibrium with monomer forms linear associates D_i.

Model Ia

Monomer has two association sites which are overlapped with active sites in such a manner that half of total number of

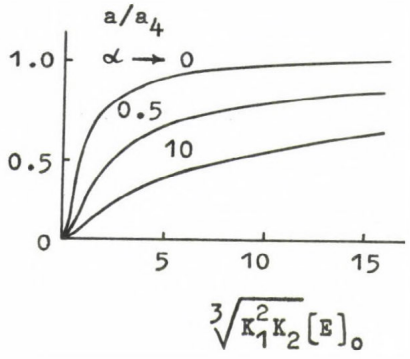

Fig.2. Associating enzyme system of the type inactive monomer ⇌ inactive dimer ⇌ active tetramer.
The dependences of relative specific enzyme activity a/a_4 on dimensionless enzyme concentration $\sqrt[3]{K_1^2K_2}[E]_o$ calculated by means of Eq.(2) at various values of $\alpha = K_1/K_2$.

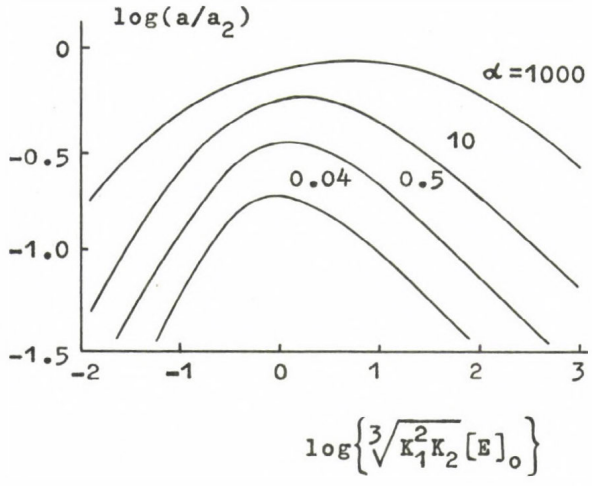

Fig.3. Associating enzyme system of the type inactive monomer ⇌ active dimer ⇌ inactive tetramer.
The dependences of relative specific enzyme activity a/a_2 on dimensionless enzyme concentration $\sqrt[3]{K_1^2K_2}\,x$ $x[E]_o$ calculated by means of Eq.(3) at various values of $\alpha = K_1/K_2$.

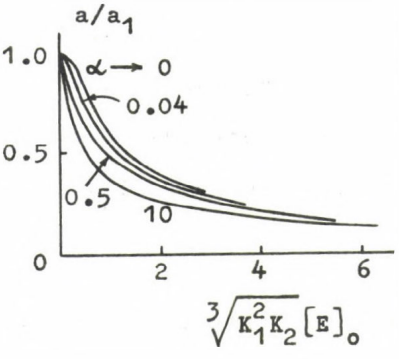

Fig.4. Associating enzyme system of the type active monomer ⇌ inactive dimer ⇌ inactive tetramer.
The dependences of relative specific enzyme activity a/a_1 on dimensionless enzyme concentration $\sqrt[3]{K_1^2K_2}[E]_o$ calculated by means of Eq.(4) at various values of $\alpha = K_1/K_2$.

active sites of the monomer is sterically screened in each of two contacts of monomer with its neighbours. In this model associate M_i and monomer M have the same number of active sites accessible to substrate. Let us assume that active sites accessible to substrate in each of oligomeric forms are identical and independent and the association constants for each association step ($K_i=[M_i]/[M][M_{i-1}]$) are identical (these constants are designated by $\bar{K}$). Let a_1 be the specific enzyme activity of free monomer. The specific enzyme activity calculated on monomer for associate M_i will be equal to a_1/i.

For associating enzyme system under discussion the dependences of specific enzyme activity on total molar enzyme concentration calculated on monomer has simple form (Kurganov, 1974):

$$a = \frac{2a_1}{1 + \sqrt{1+4\bar{K}[E]_o}} \qquad (5)$$

In accordance with this expression specific enzyme activity decreases with increasing enzyme concentration and becomes proportional to $[E]_o^{-1/2}$ at relatively high values of $[E]_o$ (Fig.5).

The model of linearly associating enzyme system with steric screening of active sites was used by Kempfle et al. (1972) for description of the dependence of rate of glutamate oxidation catalyzed by beef liver glutamate dehydrogenase on enzyme concentration (Fig.6). Using the data of the work of Eisenberg and Tomkins (1968) Kempfle and co-workers drew the conclusion that the specific activity calculated on

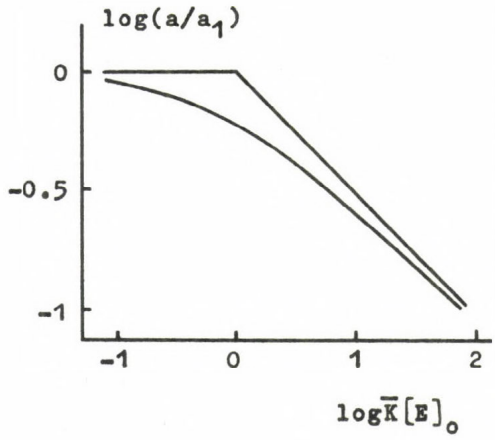

Fig.5. Model Ia (associating enzyme system of the type $M \rightleftarrows M_2 \rightleftarrows M_3 \rightleftarrows \ldots$ with steric screening of equivalent and independent active sites in the course of association).
The dependences of relative specific enzyme activity, a/a_1, on dimensionless enzyme concentration $\bar{K}[E]_o$ calculated by means of Eq.(5).

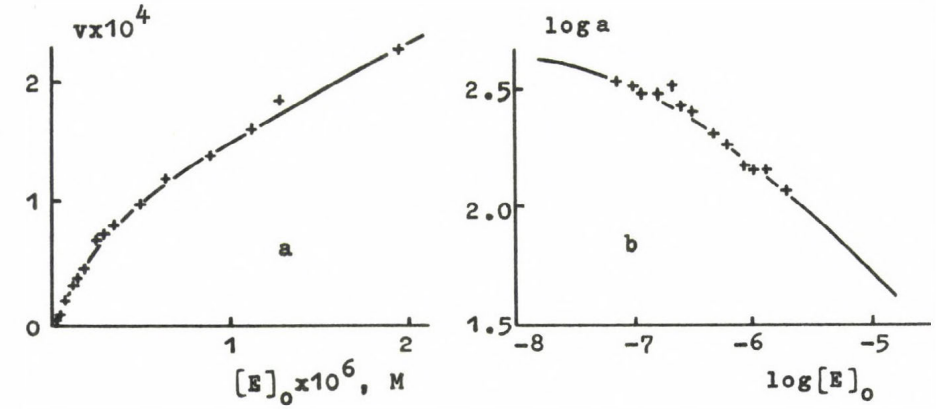

Fig.6. The dependence of rate, v, of glutamate oxidation catalyzed by beef liver glutamate dehydrogenase on enzyme concentration (a) (Kempfle et al.,1972) and the plot of specific enzyme activity, a, on enzyme concentration constructed by us in logarithmic coordinates (b).
Solid lines for both Figures are calculated by means of Eq. (5) at a_1=430 moles of NADH per min per mole of enzyme and $\bar{K} = 5 \times 10^6$ M^{-1}. The dimension of v is moles of NADH per liter per min and dimension of a is moles of NADH per min per mole of enzyme. The molecular weight of the enzyme is accepted to be equal to 312 000. 0.1 M phosphate buffer, pH 7.6. 0.1 mM EDTA, 10^{-2} M L-glutamate, 10^{-3} M NAD. 25°C.

oligomeric form M_1 remains constant in the course of association. Taking into account that the association constants for individual steps of association of beef liver glutamate dehydrogenase are identical (Dessen and Pantaloni,1969; Chun and Kim,1969; Chun et al.,1969; Reisler et al.,1970; Markau et al.,1971), we can expect the validity of Eq.(5), if one assumes, of course, that active sites accessible to substrate in each oligomeric form are identical and independent. The upper Figure represents the dependence of velocity of enzymatic reaction catalyzed by glutamate dehydrogenase on enzyme concentration obtained by Kempfle and co-workers (1972). In lower Figure the dependence of specific enzyme activity of glutamate dehydrogenase on enzyme concentration constructed by us in logarithmic coordinates is shown. The solid curve is theoretical one. It is seen that the experimental data may be satisfactorily described at the following values of parameters: the specific enzyme activity of free "monomer" (with molecular weight 312 000) is equal to 430 moles of NADH per minute per mole of "monomer" and the association constant is equal to 5×10^6 M^{-1}.

Model Ib

The type of active sites screening is the same as one in the Model Ia but it is assumed that active sites are interacting and the character of active sites interaction in free monomer and in associate is different. In this model two parameters are necessary for characterization of enzyme activity of oligomeric forms, namely a_1 (the specific enzyme activity of

free monomer) and $\bar{a}_2$ ($\bar{a}_2/i$ is the specific enzyme activity of associate M_i calculated on monomer).

The dependence of specific enzyme activity on enzyme concentration for the Model Ib has the following form:

$$a = a_1 \frac{4}{(1+\sqrt{1+4\bar{K}[E]_o})^2} + \bar{a}_2 \frac{2(\sqrt{1+4\bar{K}[E]_o}-1)}{(1+\sqrt{1+4\bar{K}[E]_o})^2} \qquad (6)$$

At $\bar{a}_2/a_1 > 2$ the dependence of specific enzyme activity on enzyme concentration passes through a maximum with increasing enzyme concentration (Fig.7). It is worth noting that the slopes of the linear asymptotes at sufficiently high enzyme concentrations are equal to -0.5.

Model Ic

Let us assume that at complete saturation of association sites of monomer not all of the active sites but m of them are sterically screened ($m < n$). The number of active sites in associate M_i is equal to $[in-(i-1)m]$. If active sites are identical and independent and if catalytic efficiencies of active sites accessible to substrate in linear associate M_i, on the one hand, and in free monomer, on the other hand, are identical, the dependence of specific enzyme activity on enzyme concentration has the following form:

$$a = a_1 \left(1 - \frac{m}{n} + \frac{2m/n}{1+\sqrt{1+4\bar{K}[E]_o}}\right) \qquad (7)$$

The plots of $\log a$ vs $\log [E]_o$ have plateau in the regions of relatively low and relatively high enzyme concentrations

respectively. The slope of tangent in the inflection point is equal to -0.067, -0.111 and -0.168 at m/n=1/3, 1/2 and 2/3 respectively (Fig.8).

Model IIa

The active dimer which is in equilibrium with inactive monomer is able to form linear associates having indefinite length. Let K_1 be the apparent association constant for the equilibrium monomer $\rightleftarrows$ dimer and $\bar{K}_2$ be the apparent association constant for the equilibrium $D + D_{i-1} \rightleftarrows D_i$. It is assumed that active sites in dimer are identical and independent and that association of dimers does not result in steric screening of active sites. Such model was suggested by Hofer (1971) for association of phosphofructokinase from rabbit skeletal muscles.

For the Model IIa specific enzyme activity and total molar enzyme concentration are connected by the following relationship:

$$1 - \frac{a}{a_2} - \frac{\sqrt{a_2 + 2a\bar{K}_2[E]_o} - a_2}{\bar{K}_2[E]_o \sqrt{2aK_1[E]_o}} = 0 \qquad (8)$$

where a_2 is the specific enzyme activity of dimer. The shape of the dependence of specific enzyme activity on enzyme concentration is determined by the ratio of association constants. In Fig.9 the theoretical dependences of relative specific enzyme activity, a/a_2, on dimensionless enzyme concentration $\sqrt[3]{K_1^2\bar{K}_2}[E]_o$ are represented at various values of $K_1/\bar{K}_2$ ratio. When this ratio is less than 0.08 these dependences

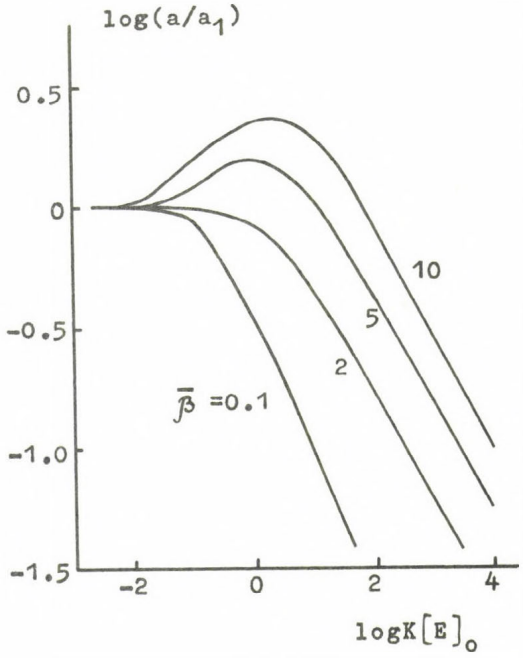

Fig.7. Model Ib (associating enzyme system of the type $M \rightleftarrows M_2 \rightleftarrows M_3 \rightleftarrows \ldots$ with steric screening of interacting active sites in the course of association).
The dependences of relative specific enzyme activity, a/a_1, on dimensionless enzyme concentration, $\bar{K}[E]_o$, calculated by means of Eq. (6) at various values of $\bar{\beta} = \bar{a}_2/a_1$.

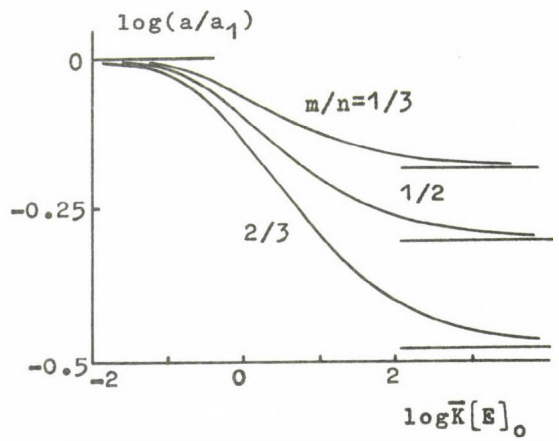

Fig.8. Model Ic (associating enzyme system of the type $M \rightleftarrows M_2 \rightleftarrows M_3 \rightleftarrows \ldots$ with steric screening of m of n independent and equivalent active sites in the course of association. The dependences of relative specific enzyme activity a/a_1 on dimensionless enzyme concentration $\bar{K}[E]_o$ calculated by means of Eq.(7) at various values of m/n.

become sigmoidal.

Model IIb

It is assumed that active dimer has two association sites which are overlapped with active sites in such a manner that half of the total number of active sites of dimer is sterically screened in each of two contacts of dimer by its neighbours. If active sites accessible to substrate in free dimer and associates D_i are identical and independent, the following relationship connects a and $[E]_o$:

$$1 + \sqrt{aK_1[E]_o(2a_2+a\bar{K}_2[E]_o)}\left(\frac{2a_2 + a\bar{K}_2[E]_o}{2a_2^2} - \frac{1}{a}\right) = 0 \quad (9)$$

Specific enzyme activity passes through a maximum with increasing enzyme concentration (Fig.10). The slope of asymptotes in logarithmic coordinates is equal to 1 at $[E]_o \rightarrow 0$ and -0.5 at $[E]_o \rightarrow \infty$.

In conclusion, I should like to emphasize that the reliable analysis of the dependences of specific enzyme activity on enzyme concentration is possible only when association of the enzyme is studied independently using physical methods.

SUMMARY

The shape of dependences of specific enzyme activity on enzyme concentration has been analysed for associating enzyme systems of the types monomer $\rightleftarrows$ N-mer, monomer $\rightleftarrows$ dimer $\rightleftarrows$ tetramer and for associating enzyme systems with linear indefinite type of association.

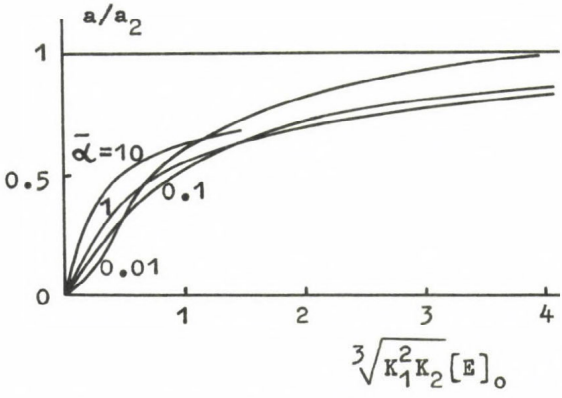

Fig.9. Model IIa (associating enzyme system of the type $2M \rightleftarrows D \rightleftarrows D_2 \rightleftarrows D_3 \rightleftarrows \ldots$ where M is inactive and specific enzyme activity of D does not change in the course of association).
The dependences of relative specific activity, a/a_2, on dimensionless enzyme concentration $\sqrt[3]{K_1^2\bar{K}_2}[E]_o$ calculated by means of relationship (8) at various values of $\bar{\alpha}=K_1/\bar{K}_2$.

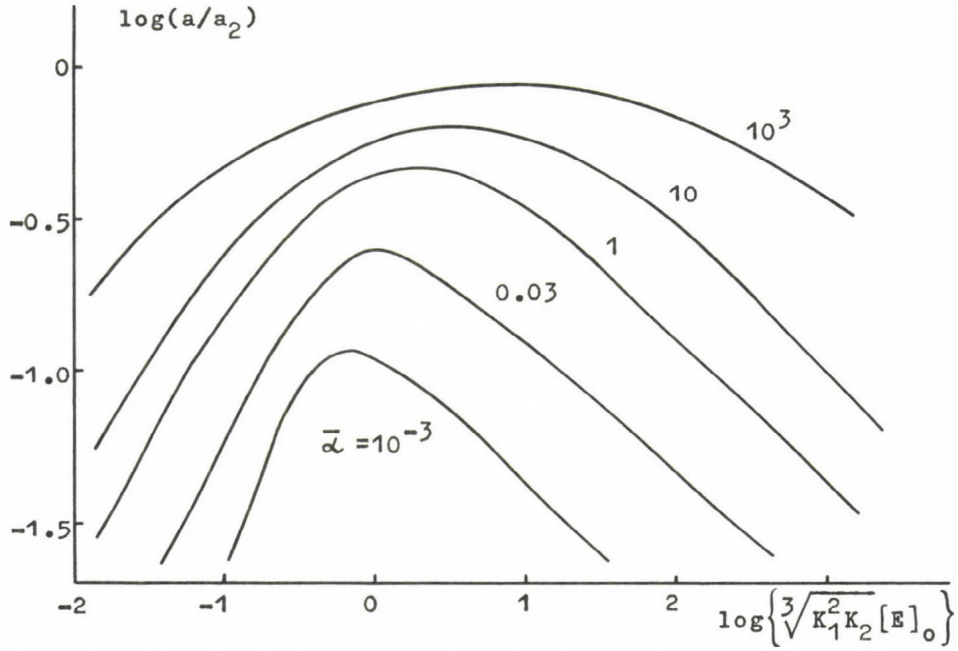

Fig.10. Model IIb (associating enzyme system $2M \rightleftarrows D \rightleftarrows D_2 \rightleftarrows D_3 \rightleftarrows \ldots$ where M is inactive and association of D is accompanied by steric screening of active sites).
The dependences of relative specific activity a/a_2 on dimensionless enzyme concentration $\sqrt[3]{K_1^2\bar{K}_2}[E]_o$ calculated by means of relationship (9) at various values of $\bar{\alpha}=K_1/\bar{K}_2$.

REFERENCES

Bonsignore,A., de Flora,A., Mangiarotti,M.A., Lorenzoni,I., Cancedda,R. and Dina,D. (1968). Ital. J. Biochem. 17, 90.

Chun,P.W. and Kim,S.J. (1969). Biochemistry 8, 1633.

Chun,P.W., Kim,S.J. and Stanley,C.A. (1969). Biochemistry 8, 1625.

Constantinides,S.M. and Deal,W.C., Jr. (1969). J. Biol. Chem. 244, 5695.

Datta,P., Gest,H and Segal,H.L. (1964). Proc. Natl. Acad. Sci. US 51, 125.

Dessen,P and Pantaloni,D. (1969). Eur. J. Biochem. 8, 292.

Eisenberg,H. and Tomkins,G.M. (1968). J. Mol. Biol. 31,37.

Frieden,C. (1967), J. Biol. Chem. 242, 4045.

Frieden,C. (1968). In: Regulation of enzyme activity and allosteric interactions, eds. E.Kvamme and A.Pihl (Universitetsforlaget, Oslo) p.59.

Frieden,C. (1971). Ann. Rev. Biochem. 40, 653.

Hofer, H.W. (1971). Hoppe-Seyler's Z. Physiol Chem. 352,997.

Kempfle,M., Mosebach, K.O. and Winkler,H. (1972). FEBS Letters 19, 301.

Kurganov,B.I. (1967). Chemistry and technology of polymers 11, 140.

Kurganov,B.I. (1968). Molec. Biol. 2, 430.

Kurganov,B.I. (1973). Molec. Biol. 7, 429.

Kurganov,B.I. (1974). Molec. Biol. 8, 525.

LéJohn,H.B., McCrea,B.E., Suzuki,I. and Jackson,S. (1969). J. Biol. Chem. 244, 2484.

Markau,K., Schneider,J. and Sund,H. (1971). Eur. J. Biochem. 24, 393.

Nichol,L.W., Jackson,W.J.H. and Winzor,D.J. (1967). Biochemistry 6,2449.

Reisler,E., Pouyet,J. and Eisenberg,H. (1970). Biochemistry 9,3095.

Stancel,G.M. and Deal,W.C.,Jr. (1969). Biochemistry 8, 4005.

Symp. Biol. Hung. 18, pp. 47–76 (1974)

PROBLEMS OF TWO-SUBSTRATE ENZYME KINETICS THE CONCEPT OF ENZYME MEMORY

Jacques Ricard

Laboratoire de Physiologie Cellulaire Végétale Associé au C.N.R.S. Université d'Aix-Marseille, Centre de Luminy, 13288 Marseille Cedex 2. France.

One of the classical problems of multi-substrate enzyme kinetics is to determine whether there is an order in the addition of the substrates and the release of the products during an enzyme reaction [1-7]. This matter has been recently revived by the emergence of a new concept : that of enzyme memory [8,9]. The aim of this lecture is to discuss this problem in connection with a possible regulatory behavior of some monomeric enzymes.

In Figure 1 are presented two possible reaction schemes for substrate binding on a two-substrate monomeric enzyme. If the enzyme binds the substrates in an obligatory order, the reaction model is said to be ordered. One substrate (A for instance) will be the first to be bound and the other one (B) will be second.

If the free enzyme can bind the substrates in either order, the reaction mechanism is defined as a random one. In the reaction schemes of Figure 1 we take into account only the binding of the substrates. All the steps following the addition of substrates (transformation of substrates into products, release of the products) have been expressed by an apparent rate constant k^*.

Obviously, an ordered mechanism can be considered as a limiting case of a random mechanism, and one may wonder whether the term "ordered mechanism" has any physical significance for a given real enzyme. Here , this term will be used in its operational meaning. Since most, if not all, ordered mechanisms are in fact random mechanisms considerably shifted

towards one reaction path, the term "ordered mechanism" will be used to indicate a mechanism in which one reaction path only can be experimentally detected. When both reaction paths are experimentally detectable a mechanism will be defined as random.

At this stage of the lecture it is of interest to speculate about the possible structural significance of the concept of ordered mechanism. The fact that the free enzyme molecule cannot bind the second substrate to any appreciable extent suggests that the binding of the first substrate molecule induces a conformational change that allows the binding of the second substrate. Ordered binding of substrates and ordered release of products are thus likely to be associated with sequential conformation changes of the enzyme molecule. But these sequential conformation changes might in turn generate "memory" phenomena. If the enzyme "recalls" for a while the conformation stabilized by the last product after its desorption, then the free enzyme will appear under two different conformation states, giving rise to deviations from classical Michaelian behavior. This point will be discussed at length in this paper.

I - KINETIC METHODS OF DISCRIMINATING BETWEEN ORDERED AND RANDOM MECHANISMS

There are several kinetic methods that allow one to decide whether a reaction mechanism is ordered or random : the analysis of product inhibition [6,7], the evaluation of isotope exchange [10-12] and the use of alternative substrates [13,14] . Only the last method will be discussed in the present lecture.

Let us suppose that the ordered mechanism of Figure 1 is in initial steady-state conditions, whereas the random mechanism of the same Figure is in a pseudo-equilibrium state. Both mechanisms then give rise to the same type of rate equation that can be written as

$$(1) \qquad \frac{[E]_0}{v} = \Phi_0 + \frac{\Phi_A}{[A]} + \frac{\Phi_B}{[B]} + \frac{\Phi_{AB}}{[A][B]}$$

where the Φ are groupings of rate constants (the so-called Dalziel cefficients), $[E]_0$ the total enzyme concentration and v the initial steady-state or pseudo-equilibrium rate. Thus the kinetic schemes of Figure 1 are

indistinguishable on the basis of a classical kinetic study. They are defined as homeomorphic.

The principle of the alternative substrates method rests on the kinetic analysis of the transformation of a substrate in the presence of an analogue of that substrate, which is taken as a competitive inhibitor of the reaction. If, for instance, A is the substrate and A' the alternative substrate, the method will use rate determination of the disappearance of A in the presence of A'. This can usually be achieved by the use of a coupled assay. Models of Figure 1 in the presence of an alternative substrate of A, A', can be written as shown in Figure 2. For the ordered model of Figure 2, the reciprocal rate equation describing the transformation of A in the presence of A' can be written as

$$\frac{[E]_0}{v} = \Phi_0 + \frac{\Phi_A}{[A]} + \frac{\Phi_B}{[B]} + \frac{\Phi_{AB}}{[A][B]} + \frac{[A']}{[A]}\left\{\Phi_A + \frac{\Phi_{AB}}{[B]}\right\} \tag{2}$$

$$\cdot \frac{\Phi'_0}{\Phi'_{A'}} \quad \frac{\Phi'_B/\Phi'_0 + [B]}{\Phi'_{A'B}/\Phi'_{A'} + [B]}$$

where v is the initial steady-state rate of reaction for A, Φ and Φ' the kinetic coefficients of the substrate and the alternative substrate, respectively. The explicit formulation of these kinetic coefficients is

$$\Phi_0 = \frac{1}{k^*} \qquad \Phi'_0 = \frac{1}{k^{*\prime}} \qquad \Phi_A = \frac{1}{k_1} \qquad \Phi'_{A'} = \frac{1}{k'_1}$$

$$\Phi_B = \frac{k_{-2} + k^*}{k^* k_2} \qquad \Phi_{B'} = \frac{k'_{-2} + k^{*\prime}}{k^{*\prime} k'_2} \tag{3}$$

$$\Phi_{AB} = \frac{k_{-1}(k^* + k_{-2})}{k_1 k_2 k^*} \qquad \Phi'_{A'B} = \frac{k'_{-1}(k^{*\prime} + k'_{-2})}{k'_1 k'_2 k^{*\prime}}$$

If the random mechanism of Figure 2 is in pseudo-equilibrium state, the reciprocal rate equation (the reciprocal rate of transformation of A in the presence of A') is

$$(4)\qquad \frac{[E]_0}{v} = \Phi_0 + \frac{\Phi_A}{[A]} + \frac{\Phi_B}{[B]} + \frac{\Phi_{AB}}{[A][B]} + \frac{[A']}{[A]}\left\{\Phi'_0 + \frac{\Phi'_B}{[B]}\right\}\frac{\Phi_{AB}}{\Phi'_{A'B}}$$

where the Φ and Φ' are still the kinetic coefficients of the substrate and the alternative substrate respectively. They are expressed as

$$\Phi_0 = \frac{1}{k^*} \qquad \Phi'_0 = \frac{1}{k^{*\prime}} \qquad \Phi_A = \frac{1}{k^* K_4} \qquad \Phi'_{A'} = \frac{1}{k^{*\prime} K'_4}$$

$$(5)\qquad \Phi_B = \frac{1}{k^* K_3} \qquad \Phi'_B = \frac{1}{k^{*\prime} K'_3}$$

$$\Phi_{AB} = \frac{1}{k^* K_1 K_2} \qquad \Phi'_{A'B} = \frac{1}{k^{*\prime} K'_1 K'_2}$$

A compulsory order model with B' as alternative substrate, is presented in Figure 3. The reciprocal rate equation is now

$$(6)\qquad \frac{[E]_0}{v} = \Phi_0 + \frac{\Phi_A}{[A]} + \frac{\Phi_B}{[B]} + \frac{\Phi_{AB}}{[A][B]} + \frac{[B']}{[B]}\left\{\Phi'_0 + \frac{\Phi'_A}{[A]}\right\}\frac{\Phi_B}{\Phi'_{B'}}$$

The Φ and Φ' are still the kinetic coefficients of the substrate and the alternative substrate. Their expression is similar to that already given (expressions 3).

Inspection of equations (2), (4), and (6) indicates , at least in theory, a possibility of discriminating among ordered and random mechanisms. From equation (2) (with A' being the alternative substrate) it is obvious that the reciprocal plots should be linear with regard to the first substrate A but curvilinear with respect to the second substrate B. Some possible shapes of the reciprocal plots obtained by computer simulation are presented in Figure 4. If, on the other hand, the alternative substrate is B', an analogue of the second substrate B, or if the mechanism is random, the reciprocal plots are always linear.

Although very simple at first sight, the direct use of rate equations (2), (4), and (6) can give rise to misleading interpretations

because a non-linear rate equation can, under certain conditions, generate linear or quasi-linear plots with regard to $1/[B]$. Expression (2) is the equation of a hyperbola that has an oblique asymptote

$$\frac{[E]_0}{v} = \Phi_0 + \frac{\Phi_A}{[A]} + \frac{\Phi_B}{[B]} + \frac{\Phi_{AB}}{[A][B]} + \frac{[A']}{[A]}$$

(9)

$$\cdot \left\{ \frac{\Phi_{AB}\,\Phi'_B}{\Phi'_{A'B}[B]} + \frac{\Phi_A \Phi'_B}{\Phi'_{A'B}} + \frac{\Phi_{AB}\,\Phi'_0}{\Phi'_{A'B}} - \frac{\Phi_{AB}\,\Phi'_{A'}\,\Phi'_B}{\Phi'^2_{A'B}} \right\}$$

and a vertical asymptote

(10)

$$\frac{1}{[B]} = -\frac{\Phi'_{A'B}}{\Phi'_{A'}}$$

Equation (2) can generate straight plots $[E]_0/v$ against $1/[B]$ in two cases : first, when the hyperbola is degenerate, and second when a large part of the hyperbola asymptotically approaches its oblique asymptote. It can be shown after some algebra that there are two degeneracy conditions of the hyperbola

(11)

$$\frac{\Phi'_B}{\Phi'_0} = \frac{\Phi'_{A'B}}{\Phi'_{A'}}$$

$$\frac{\Phi'_{A'B}}{\Phi'_{A'}} = \frac{\Phi_{AB}}{\Phi_A}$$

If either the first or the second degeneracy condition holds, equation (2) becomes

(12)

$$\frac{[E]_0}{v} = \Phi_0 + \frac{\Phi_A}{[A]} + \frac{\Phi_B}{[B]} + \frac{\Phi_{AB}}{[A][B]} + \frac{[A']}{[A]} \left\{ \Phi_A + \frac{\Phi_{AB}}{[B]} \right\} \frac{\Phi'_B}{\Phi'_{A'B}}$$

or

$$(13)\quad \frac{[E]_0}{v} = \Phi_0 + \frac{\Phi_A}{[A]} + \frac{\Phi_B}{[B]} + \frac{\Phi_{AB}}{[A]\,[B]} + \left\{\frac{[A']}{[A]}\right\}\left\{\Phi'_0 + \frac{\Phi'_B}{[B]}\right\}\frac{\Phi_{AB}}{\Phi'_{A'B}}$$

If both degeneracy conditions simultaneously hold, then rate equations (12) and (13) become identical.

The reciprocal plot approaches the oblique asymptote when

$$(14)\quad \Phi'_{A'}\,\Phi'^{2}_{A'B} >> \frac{[A']}{[A]}\left(\Phi'_{A'}\Phi'_B - \Phi'_0\,\Phi'_{A'B}\right)\left(\Phi_A\Phi'_{A'B} - \Phi_{AB}\,\Phi'_{A'}\right)$$

Obviously, a sufficient, but by no means necessary, condition is that

$$(15)\quad \frac{[A']}{[A]\Phi'^{2}_{A'B}}\left(\Phi'_{A'}\,\Phi'_B - \Phi'_0\,\Phi'_{A'B}\right)\left(\Phi_A\,\Phi'_{A'B} - \Phi_{AB}\,\Phi'_{A'}\right) \equiv 0$$

Each of the degeneracy conditions fulfills identity (15). Some linear plots obtained from an ordered model involving an alternative substrate A' of the first substrate (A) are presented in Figure 4.

When the two reaction routes involving, respectively, the substrate and the alternative substrate are independent, as occurs with the ordered model of Figure 2, there is no obligatory relation between the Φ (the kinetic coefficients of the substrate) and the Φ' (the kinetic coefficients of the alternative substrate). If a relation between these coefficients holds, it is purely fortuitous. The second degeneracy condition (11) is an example of such a fortuitous relation. But if the alternative substrate is B' or if the mechanism is random, then the two reaction routes are not independent but have a step in common. The occurence of this common step gives rise to obligatory relations between the Φ and the Φ'. These obligatory relations are termed constraint conditions. For a compulsory order model with an alternative substrate of the second substrate (model of Figure 3), there are two constraint conditions

$$(16)\quad \Phi'_A = \Phi_A \qquad \frac{\Phi'_{AB'}}{\Phi'_{B'}} = \frac{\Phi_{AB}}{\Phi_B}$$

and for a random model such as that of Figure 2, only one constraint condition

$$\frac{\Phi_{A'B}}{\Phi_{A'}} = \frac{\Phi_{AB}}{\Phi_{A}} \tag{17}$$

has to be fulfilled.

The above theoretical developments make it possible, in most cases, to choose a kinetic scheme. This screening necessitates the independent evaluation of the kinetic coefficients Φ and Φ' pertaining to the substrate and to the alternative substrate; then the use of the above equations allows the choosing of a model. The screeming can also be done in a systematic way by using diagnostic rules [14].

To give an example, we will apply these rules to the transfer reaction catalyzed by yeast hexokinase. It has been stated by different research groups that the primary Lineweaver-Burk plots are compatible with the initial rate equation

$$\frac{[E]_0}{v} = \Phi_0 + \frac{\Phi_H}{[H]} + \frac{\Phi_{MA}}{[MA]} + \frac{\Phi_{H.MA}}{[H][MA]} \tag{18}$$

where H is the hexose (glucose, fructose, or mannose), MA the chelate $MgATP^{2-}$, and Φ the kinetic coefficients pertaining to glucose, fructose, or mannose phosphorylation and determined from pH-stat experiments. The values obtained are given in Table 1. Since $\Phi_{MA}(Glc) \neq \Phi_{MA}(Fru)$ and $\Phi_{MA}(Glc) \neq \Phi_{MA}(Man)$, a compulsory order mechanism with $MgATP^{2-}$ as the first substrate can be ruled out. For a random model, constraint condition (8) should hold for any alternative substrate. Now, it is seen from Table 1 that

$$\frac{\Phi_{H.MA}}{\Phi_H}(Glc) \neq \frac{\Phi_{H.MA}}{\Phi_H}(Man) \tag{19}$$

Therefore, the constraint condition is not fulfilled with glucose or mannose. A random model is thus incompatible with the results of Table 1. The only way to interpret the above data is to consider that the binding

of the substrates on the hexokinase is ordered with glucose being bound first. This is in agreement with a previous interpretation [15,16].

An additional possibility of checking a given model is to plot the reciprocal of the specific rate measured experimentally in the presence of the alternative substrate, and, independently, to calculate that reciprocal rate by means of a given rate equation such as (2), (4), or (6). Such a calculation necessitates the independent evaluation of the kinetic coefficients Φ and Φ' for the substrate and for the alternative substrate, respectively. Obviously, if the points obtained experimentally lie on the theoretical plot, this can be taken as an additional argument in favor of the proposed reaction scheme. Results of Figure 5 clearly show that the predictions of an ordered binding of substrates on yeast hexokinase correspond exactly to the reaction-rate measurements in the presence of an alternative substrate, either fructose or mannose. Notice in Figure 5, that an ordered mechanism with an alternative substrate (fructose or mannose) of the first substrate (glucose) generates linear primary plots. This is caused, in each of the above cases, by the occurence of a degeneracy condition. With fructose as an alternative substrate, the degeneracy condition is

$$(20) \qquad \frac{\Phi_{H.MA}}{\Phi_H}\,(Glc) = \frac{\Phi_{H.MA}}{\Phi_H}\,(Fru)$$

and with mannose

$$(21) \qquad \frac{\Phi_{MA}}{\Phi_0}\,(Man) = \frac{\Phi_{H.MA}}{\Phi_H}\,(Man)$$

We think that the alternative substrate method is one of the most powerful tools for elucidating reaction sequences.

II - ENZYME MEMORY

From a kinetic point of view, the regulatory behavior of an enzyme usually appears as a departure from classical Michaelian behavior. The most frequent deviations are an upward ("positive cooperativity") or

a downward ("negative cooperativity") curvature of the reciprocal plots. These deviations are usually considered as the immediate consequence of subunit interactions [17-20]. Moreover, it is obvious that the random binding of substrates on a rigid-or nearly rigid-monomeric enzyme can, also in theory, generate deviations from Michaelian behavior. However, to the best of our knowledge, these deviations have never been found for any real enzyme. This is probably due to the frequent occurrence of asymptotic or degeneracy conditions [7,21,22,14] similar to those already discussed. But it is also possible to explain departure from Michaelis-Menten behavior of one-site enzymes by the occurrence of conformational transitions between enzyme forms. Thus far, two types of models have been proposed a priori to explain non-Michaelian behavior of one-substrate monomeric enzymes.

The first model [23] assumes the existence of a pre-equilibrium between two enzyme forms that both bind the substrate without further conformational change as shown in Figure 6. If the conformational transitions are slow with respect to the other steps, this system will generate non-linear reciprocal plots [23]. A more complete scheme including the enzyme-product complexes has also been proposed [24,25]but its basic features are the same.

The second model that was put forward [26] to explain non-Michaelian kinetics of one-substrate enzymes, assumes the existence of a "memory" in the enzyme.That is the protein molecule, after catalysis, is released in the conformation stabilized by the substrate (Figure 6). It is now our aim to discuss at length the kinetic and the thermodynamic bases of this enzyme memory, and to show that this concept applies to a real enzyme : wheat germ hexokinase L I.

A - The mnemonical transition

An enzyme exhibiting memory phenomena is defined as a mnemonical enzyme. If one looks at the Rabin scheme in Figure 6, one notes that this scheme has to be modified for two reasons :

- since the enzyme is considered to recall for a while the conformation stabilized by the last ligand, it is obvious that this

ligand is a product and that the enzyme-product(s) complex(es) has(have) to be inserted in the reaction scheme;

- an additional difficulty of the Rabin scheme is that it violates the principle of microscopic reversibility. Thus, the free enzyme interconversion has to be considered as reversible. But then this reversibility raises the difficult question of whether the departure from Michaelian behavior is due to enzyme memory or rather to a shift of the pre-equilibrium between the two free enzyme conformations as represented in the Frieden [23], or in the Ainslie et al [24] schemes (Figure 6). The discussion of this problem will now be the focus of our interest.

One of the basic ideas of this lecture is to consider that the non-Michaelian behavior of some monomeric enzymes rests on a special type of conformational transition, which we call the mnemonical transition. Three requirements have to be fulfilled to produce such a transition :

- the free enzyme exists in two conformational states (the circle and the rhombus of Figure 7) in equilibrium;

- the collision of a ligand L with either of these enzyme forms induces a new conformation (the square of Figure 7) which is required for proper ligand binding;

- another ligand M can be bound competitively, at the same site on one form only (the rhombus of Figure 7) without any further conformation change.

Thus, the scheme of Figure 6 combines induced-fit phenomena (steps 2 and 3) with the existence of a pre-equilibrium shifted by the binding of a ligand (steps 1 and 4). Now, if this mnemonical transition is inserted into an ordered reaction scheme, in such a way that L is the first substrate and M the last product, one gets a generalization of the Rabin scheme that takes into account the two above remarks. For instance, if the mnemonical transition is a component of an ordered two-substrate, two-product mechanism, one has the situation depicted in Figure 8.

It is of interest now to go back to the molecular basis of deviations from Michaelis kinetics exhibited by a mnemonical enzyme. For a polymeric enzyme, departure from linear reciprocal plots is usually considered

as the consequence of quaternary constraints and active-site interactions. For a one-sited mnemonical enzyme the non-Michaelian behavior appears as a consequence of a cooperation between two different conformation states of the same protein in the overall reaction process. It is obvious that, as for cooperativity between sites, the cooperation between conformation states of the enzyme can be positive or negative. This point will be discussed later on.

B - Mnemonical two-substrate, two-product enzymes

In the absence of any product, the reciprocal reaction rate of the model of Figure 9 can be written in either of the two following forms

$$\frac{[E]_0}{v} = \frac{(\alpha_1+\alpha_2[B])\frac{1}{[A]^2} + (\beta_1+\beta_2[B])\frac{1}{[A]} + (\gamma_1+\gamma_2[B])}{\delta[B]\frac{1}{[A]}+\varepsilon[B]} \tag{22}$$

$$\frac{[E]_0}{v} = \frac{\alpha_1+\beta_1[A]+\gamma_1[A]^2}{\delta[A]+\varepsilon[A]^2}\frac{1}{[B]} + \frac{\alpha_2+\beta_2[A]+\gamma_2[A]^2}{\delta[A]+\varepsilon[A]^2}$$

The coefficients $\alpha,\beta,\gamma,\delta,\varepsilon$ are groupings of rate constants and are defined in Table 2. The reciprocal plots are linear with respect to $1/[B]$, but not with regard to $1/[A]$. An example of this type of behavior, simulated by computer, is shown in Figure 9. It is to be noted that the linear plots do not intersect at the same point. The secondary plots derived from the analysis of the straight lines of Figure 9 exhibit an interesting property. Although the intercepts $\imath$ are not a linear function of $1/[A]$, the slopes σ give a straight line when replotted against $1/[A]$. As a matter of fact one has

$$\imath = \frac{\alpha_2\frac{1}{[A]^2} + \beta_2\frac{1}{[A]} + \gamma_2}{\delta\frac{1}{[A]}+\varepsilon} \tag{23}$$

(23) $$\sigma = \frac{\alpha_1}{\delta} \frac{1}{[A]} + \frac{\beta_1\delta - \alpha_1\varepsilon}{\delta^2}$$

Again this situation can be illustrated by computer simulation (Figure 10).

An interesting point is to determine whether the first reciprocal rate equation (22) can predict inhibition by excess substrate when $[E]_0/v$ is plotted against $1/[A]$. If the expression of the first derivative (with respect to $1/[A]$) is evaluated, one sees that all the terms of the numerator are positive. Thus, the reciprocal rate equation cannot exhibit any extreme and the mnemonical transition cannot give rise to substrate inhibition. The second derivative (with respect to $1/[A]$) of the same rate equation can be written, after some rearrangement, as

(24) $$\left(\frac{[E]_0}{v}\right)'' = \frac{2k^3k_1^2k_2^3k_4^3k_5k_6k_3^3(k_6-k_1)}{(\delta \frac{1}{A} + \varepsilon)^3}$$

Depending on the respective values of k_6 and k_1, the reciprocal plots are linear , concave up or down. This is exemplified by the computer outputs of Figure 11. Since the reciprocal plots cannot exhibit any extreme it is possible to express the extent of cooperation between the two enzyme forms by the numerical value of the second derivative when $1/[A]$ approaches zero. This extent of cooperation Γ is shown to be

(25) $$\Gamma = \frac{2k_5}{k_1k_6^2}(k_6 - k_1)$$

If $[E]_0$ is expressed in seconds, the extent of cooperation Γ is expressed in sM^2. A point of cardinal importance is that the expression of Γ rests on three rate constants only, thus the concentration of the second substrat B does not effect the cooperation of the two enzyme forms. However, one may wonder whether the products modify the curvature of the plots. In the presence of product P, again all the terms in the numerator of the first derivative (with respect to $1/[A]$) of the new reciprocal-rate equation are positive, and the expression of Γ is still equation (25). In the presence of the second product Q, one gets a new reciprocal-rate equation ha-

ving a first derivative with only positive terms in the numerator. But now the extent of cooperation is dependent upon the concentration of Q; one has

$$\Gamma = \frac{2k_5}{k_1 k_6^2} \{(k_6 - k_1) - k_1 K_4 [Q]\} \quad (26)$$

where K_4 is the dissociation constant (k_{-4}/k_4) of the product Q from the enzyme surface. Obviously, if

$$k_6 > k_1 \ (1+K_4[Q]) \quad (27)$$

the cooperation in the presence of Q is positive, and if

$$k_6 < k_1 \ (1+K_4 \ [Q]) \quad (28)$$

the cooperation is negative. If, in the absence of any product, the cooperation was negative, the product Q strengthens that cooperation. If the cooperation was positive, in the absence of Q, the product Q lowers, or even reverses, the cooperation.This interesting property is exemplified in Figures 12 and 13.

C - Thermodynamic aspects of enzyme memory

The expression of the extent of cooperation is unchanged whatever the number of substrates and products, and can be written for any mnemonical transition in its most general form as

$$\Gamma = \frac{2k_T}{k_L k_L'^2} (k_L' - k_L) \quad (29)$$

The significance of the three rate constants k_T, k_L, k_L' is to be found in the general scheme of Figure 7. In that form, it is obvious that the concavity of the reciprocal plots, that is, the extent of cooperation between enzyme forms (the circle and the rhombus), is independent of the equilibrium constant between these enzyme forms, but is the consequence of enzyme memory. As a general rule the substrates , and all but the last product, do not affect the cooperation. In the presence of the last pro-

duct M (Figure 7), and regardless of the number of substrates and products, the extent of cooperation becomes

$$\Gamma = \frac{2k_T}{k_L k_L'^2} \{k_L' - k_L (1 + K_M [M])\} \quad (30)$$

where K_M is the dissociation constant of the enzyme-M complex. Γ is thus a linear function of the concentration of M.

Since the sign of the cooperation rests on the respective values (in the absence of M) of only two rate constants, k_L and k_L', it is of interest to discuss briefly the thermodynamic grounds of cooperation for mnemonical enzymes. The free energy of activation associated with the two rate constants k_L and k_L' can be split into two components :

- an ideal binding component, $\Delta G_B^{\neq}$, that is, the free energy of activation for binding without taking into account the conformation change;

- an ideal transconformation, $\Delta G_T^{\neq}$ or $\Delta G_{T'}^{\neq}$, that is, the free energy of activation for conformational change apart from binding effects.

Neither of these thermodynamic contributions can have a negative value and one gets

$$\Delta G_L^{\neq} = \Delta G_B^{\neq} + \Delta G_T^{\neq}$$
$$\Delta G_{L'}^{\neq} = \Delta G_B^{\neq} + \Delta G_{T'}^{\neq} \quad (31)$$

By comparing the two equations, it is obvious that if

$$k_L' > k_L \quad (32)$$

then

$$\Delta G_{T'}^{\neq} < \Delta G_T^{\neq} \quad (33)$$

Conversely, if

$$k_L' < k_L \quad (34)$$

then

(35) $$\Delta G_{T'}^{\neq} > \Delta G_{T}^{\neq}$$

Obviously, the positivity or negativity of the cooperation between the two conformation states rests on the respective values of the free energies of activation of the two transconformation processes as shown in Figure 14.

D- Wheat germ hexokinase L I as a mnemonical enzyme

Four isohexokinases have been isolated from wheat germ and obtained in a homogeneous state [27]. Two of them (L I and L II) have a molecular weight of 50,000, the two others (H I and H II) a molecular weight of 110,000. Both L I and L II are made up of only one polypeptide chain.

It can be shown, by equilibrium dialysis experiments, that L I binds [^{14}C] glucose, but not [^{14}C] $MgATP^{2-}$. This result is similar to that previously obtained with yeast hexokinase [28-31]. It suggests that the binding of substrates is essentially ordered [15,16], glucose being bound first. Both the Klotz and Scatchard plots show the existence of one binding site for glucose per enzyme molecule. In addition, these plots are linear (Figure 15). However, if the Lineweaver-Burk plots are linear with regard to $MgATP^{2-}$, they exhibit a downward curvature with regard to glucose (Figure 16). If the slopes of the primary plots II of Figure 16, are replotted against the reciprocal of glucose, one has a straight line, but if the intercepts are replotted against 1/[glucose] one gets a curve (Figure 17). This is exactly what is expected with a mnemonical model. The effects of the products, glucose-6-phosphate and $MgADP^{-}$, on the primary reciprocal plots expressed with respect to glucose are presented in Figure 18. Obviously, these effects are very different. Glucose-6-phosphate increases the concavity of the plots, whereas $MgATP^{2-}$ does not. This can be more clearly seen by estimating the Γ values of the plots, and plotting these values (expressed in sM^{2}) against either glucose-6-phosphate or $MgADP^{-}$ concentrations (Figure 19). The extent of cooperation Γ increases linearly with glucose-6-phosphate concentration, whereas it is independent of $MgADP^{-}$ concentration. The whole set of above results clearly allows one to conclude that wheat germ hexokinase L I is a

mnemonical enzyme, that glucose is the first substrate, and glucose-6-phosphate the last product. The simplest scheme consistent with these conclusions is presented in Figure 20. Other kinetic results, which are not presented here, demonstrate that a random model is incompatible with the available data.

Since conformational equilibria involved in the mnemonical transition are considered to be the explanation of the departure from Michaelian behavior, shifting or altering these equilibria by slight concentrations of denaturating agents would modify or even suppress the concavity of the primary plots. This is what is obtained when urea or sodium dodecylsulfate (SDS) are used (Figure 21). The linearization of the Lineweaver-Burk plots ("desensitization") by urea and SDS is clearly in accord with the existence of the conformational transitions required for enzyme memory.

E - Can the mnemonical transition be considered as a device for the regulation of metabolic processes ?

Obviously, an enzyme can be defined as regulatory when it effectively regulates a metabolic pathway through conformational transitions. It is not yet possible to decide whether a mnemonical monomeric enzyme, such as hexokinase L I, is regulatory or not, because of the lack of physiological studies on the relevant metabolic pathways (in this case, glycolysis in the wheat germ). However, a conclusion that can be drawn from this study is that enzyme memory represents a possible device for the regulation of metabolic processes. Since the mnemonical transition can give rise either to an upward or downward curvature of the reciprocal plots, the "advantages" of enzyme memory are similar to those exhibited by allosteric enzymes (sharp response of the enzyme for a narrow range of substrate concentration) or by enzymes exhibiting negative cooperativity (comparatively high reaction rate for very low substrate concentration). However, the mnemonical enzymes exhibit a unique property : that of having their "regulatory behavior" modulated by the last product of the reaction sequence. This property implies that, compared with a Michaelian enzyme, the mnemonical enzyme can be more weakly inhibited by the product at low substrate concentration than at high substrate concentration . Since many enzymes in the cell catalyze

the transformation of a substrate in the presence of the corresponding product the mnemonical transition is a device that can represent an "advantage" evolved for the control of a metabolic chain.

AKNOLEDGEMENTS - The author wishes to thank his associates, G.Noat, J.C. Meunier, J.Buc, C.Got and M. Borel for their participation in this work.

REFERENCES.

1. Dalziel K. (1958) Trans. Farad. Soc. 54, 1247.
2. Dalziel, K. (1957) Acta Chem. Scand. 11, 1706.
3. Dalziel, K. (1962) Biochem. J. 84, 244.
4. Dalziel, K. (1965) Biochem. J. 100, 34.
5. Alberty, R.A. (1953) J. Amer. Chem. Soc. 75, 1928.
6. Alberty, R.A. (1958) J. Amer. Chem. Soc. 80, 1777.
7. Cleland, W.W. (1970) In: The Enzymes, ed. P.D. Boyer (Academic Press, New York) Vol. 2, p. 1.
8. Ricard, J., Meunier, J.C. and Buc, J. (1974) Eur. J. Biochem 49, 195.
9. Meunier, J.C., Buc, J., Navarro, A. and Ricard, J. (1974) Eur. J. Biochem. 49, 209.
10. Boyer, P.D. (1959) Arch. Biochem. Biophys. 82, 387.
11. Boyer, P.D. and Silverstein, E. (1963) Acta Chem. Scand. 17, 195.
12. Britton, H.G. (1966) Arch. Biochem. Biophys. 117, 167.
13. Rudolph, F.B. and Fromm, H.J. (1970) Biochemistry, 9, 4660.
14. Ricard, J., Noat, G., Got, C. and Borel, M. (1972) Eur. J. Biochem. 31, 14.
15. Noat, G., Ricard, J., Borel, M. and Got, C. (1968) Eur. J. Biochem. 5, 55.
16. Noat, G., Ricard, J., Borel, M. and Got, C. (1970) Eur. J. Biochem. 13, 347.
17. Whitehead, E. (1970) Progress Biophys. 21, 321
18. Teipel, J. and Koshland, D.E. (1969) Biochemistry, 8, 4656.
19. Ricard, J., Mouttet, C. and Nari, J. (1974) Eur. J. Biochem. 41, 479.
20. Nari, J., Mouttet, C., Fouchier, F. and Ricard, J. (1974) Eur. J. Biochem. 41, 499.
21. Pettersson, G. (1969) Acta Chem. Scand. 23, 2717.
22. Pettersson, G. and Nylen, V. (1972) Acta Chem. Scand. 26, 420.
23. Frieden, C. (1970) J. Biol. Chem. 245, 5788.
24. Ainslie, R.E., Shill, J.R. and Neet, K.E. (1972) J. Biol. Chem. 247, 7088.
25. Rübsamen, H., Klandker, R. and Witzel, H. (1974) Hoppe-Seyler's Z. Physiol. Chem. 355, 1.
26. Rabin, B.R. (1967) Biochem. J. 102, 22c.
27. Meunier, J.C., Buc, J. and Ricard, J (1971) Febs Lett. 14,

25.

28. Colowick, S.P. and Womack, F.C. (1969) J. Biol. Chem. 244, 774.

29. Colowick, S.P., Womack, F.C. and Nielsen, J. (1969) In: The Role of Nucleotides, eds. H.M. Kalckar, H. Klenow, M. Ottessen, A. Munch-Petersen and J.H. Taysen (Munksgaard Copenhagen) p. 15.

30. Noat, G., Ricard, J., Borel, M. and Got, C. (1969) Eur. J. Biochem. 11, 406.

31. Roustan, C., Brevet, A., Pradel, L.A. and Van Thoai, N. (1974) Eur. J. Biochem. 44, 353.

Table 1

The kinetic coefficients pertaining to glucose, fructose and mannose phosphorylation determined from pH-stat experiments.

The values given in this table are least-square estimations of the kinetic coefficients with their standard errors. For yeast hexokinase, the screening among two-substrate models is partly based on the following facts: (a) the values of Φ_{MA}, for glucose and fructose or glucose and mannose, are significantly different; (b) the values of $\Phi_{H.MA}/\Phi_H$ for glucose and mannose are significantly different.

Substr.H	Φ_0	Φ_H	Φ_{MA}	$\Phi_{H.MA}$	Φ_{MA}/Φ_0	$\Phi_{H.MA}/\Phi_H$
	ms	mM.ms	mM.ms	mM^2. ms	mM	mM
Glucose	1.30≠0.10	0.20≠0.03	0.50≠0.04	0.100≠0.020	0.38≠0.07	0.50≠0.12
Fructose	0.39≠0.05	0.68≠0.09	0.14≠0.02	0.324≠0.035	0.36≠0.10	0.47≠0.10
Mannose	1.70≠0.10	0.16≠0.01	0.18≠0.02	0.016≠0.002	0.10≠0.02	0.10≠0.02

Table 2

Explicit formulation of the kinetic parameter of equation (22).

Kinetic parameter	Equation
α_1	$= k_4 (kk_3 + k_{-2}k_3 + k'k_{-2})(k_{-1} + k_{-6})(k_5 + k_{-5})$
α_2	$= kk_2k_3k_4 (k_5 + k_{-5})$
α_3	$= k'k_{-2}k_{-3} (k_5 + k_{-5})(k_{-1} + k_{-6})$
α_4	$= k_{-4}k_{-5} (k_{-1} + k_{-6})(kk_3 + k'k_{-2} + k_{-2}k_3)$
α_5	$= kk_2k_3k_{-4}k_{-5}$
β_1	$= k_4 (kk_3 + k_{-2}k_3 + k'k_{-2})(k_1k_5 + k_1k_{-6} + k_{-1}k_6 + k_{-5}k_6)$
β_2	$= k_2 (k_1k_5 + k_{-5}k_6)(kk_4 + k'k_4 + k_3k_4 + kk_3) + kk_1k_2k_3k_4$
β_3	$= k'k_{-2}k_{-3} (k_{-1}k_6 + k_1k_5 + k_{-5}k_6 + k_1k_{-6})$
β_4	$= k_2k_{-3} (k + k')(k_1k_5 + k_{-5}k_6)$
β_5	$= k_1k_{-4}k_{-6} (k'k_{-2} + k_{-2}k_3 + kk_3)$
β_6	$= kk_1k_2k_3k_{-4}$
γ_1	$= k_1k_4k_6 (k'k_{-2} + k_{-2}k_3 + kk_3)$
γ_2	$= k_1k_2k_6 (k_3k_4 + k'k_4 + kk_4 + kk_3)$
γ_3	$= k'k_1k_{-2}k_{-3}k_6$
γ_4	$= k_1k_2k_{-3}k_6 (k + k')$
δ	$= kk_2k_3k_4 (k_1k_5 + k_{-5}k_6)$
ε	$= kk_1k_2k_3k_4k_6$

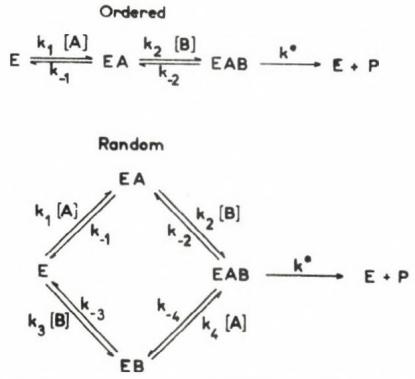

ig. 1. Ordered and random mechanisms for a two-substrate enzyme

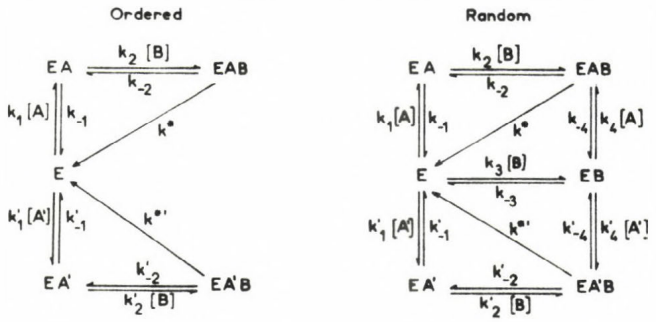

Fig. 2. Ordered and random mechanisms with an alternative substrate of A.

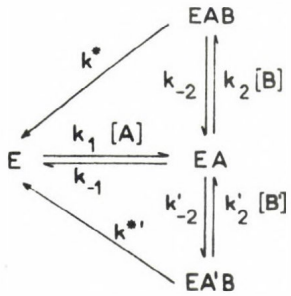

Fig. 3. Ordered mechanism with an alternative substrate of B.

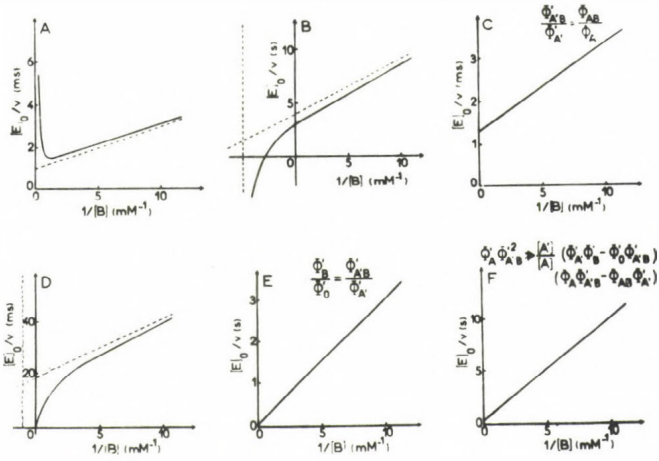

Fig. 4. Theoretical plots for an ordered model with an alternative substrate (A') of the first substrate (A).

Plots C, E, F correspond to degeneracy or asymptotic conditions. The numerical values of kinetic coefficients can be found elsewhere [14].

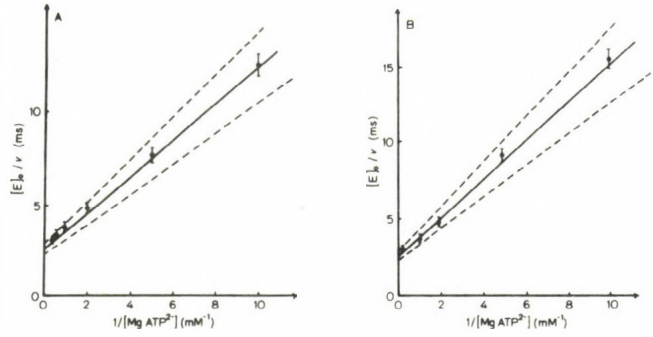

Fig. 5. Reciprocal plots of glucose phosphorylation in the presence of an alternative substrate.

(A) Alternative substrate is fructose; (B) alternative substrate is mannose. The plots are theoretical. They have been computed with rate equation (2) and the values of the kinetic coefficients Φ and Φ'. Points are experimental. Dotted lines correspond to the enveloppe of expected error.

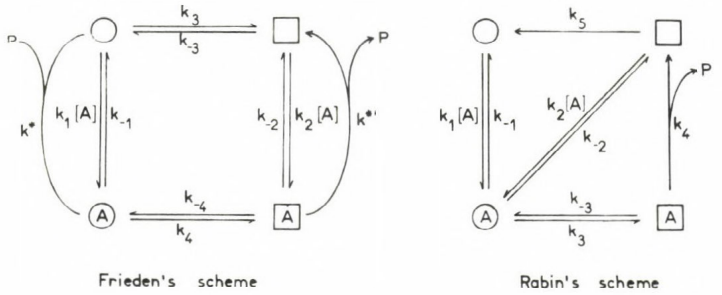

Fig. 6. Rabin and Frieden schemes of conformational transitions for a one-substrate enzyme.

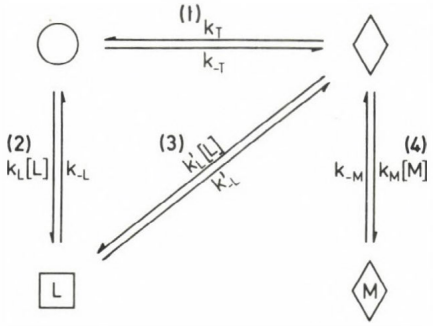

Fig. 7. The mnemonical transition.

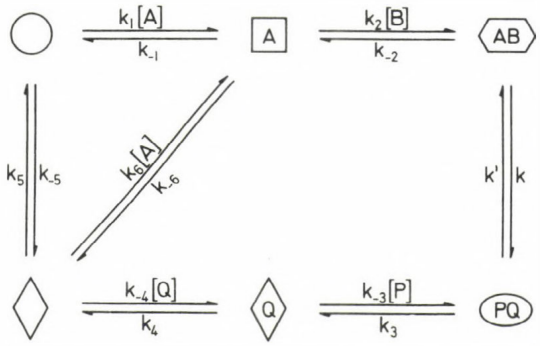

Fig. 8. The mnemonical transition for a two-substrate, two-product monomeric enzyme.

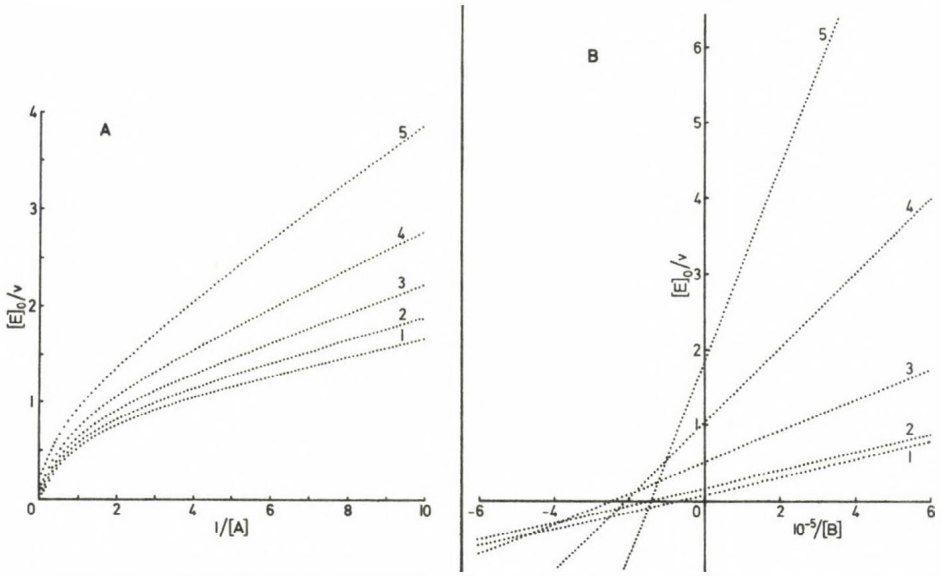

Fig. 9. Some possible shapes (computer outputs) of the reciprocal plots for a two-substrate, two-product mnemonical enzyme.

The numerical values of the rate constants and substrate concentration are to be found elsewhere [8].

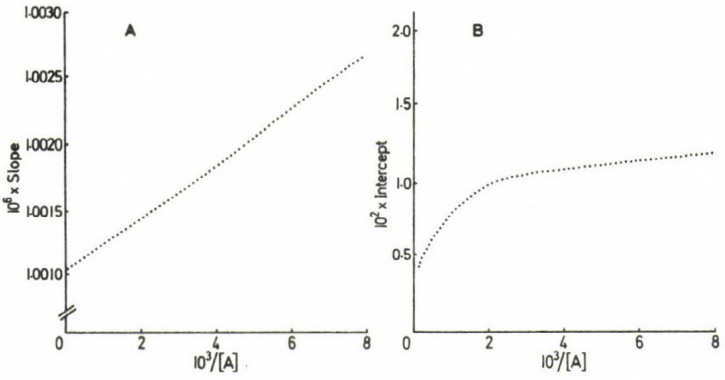

Fig. 10. Secondary plots (computer outputs) for a two-substrate, two-product mnemonical enzyme.

The values of the rate constants are given elsewhere [8].

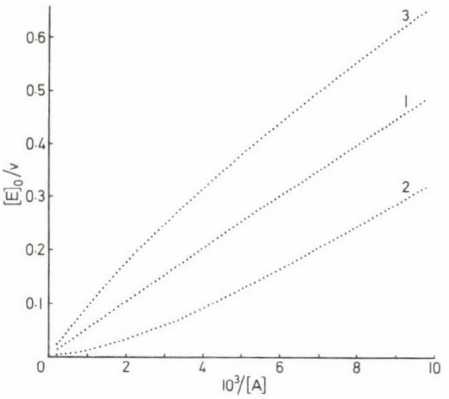

Fig. 11. Cooperation of a two-substrate, two-product mnemonical enzyme.

(1) Michaelian behavior, (2) positive cooperation, (3) negative cooperation. The values of the rate constants can be found elsewhere [8].

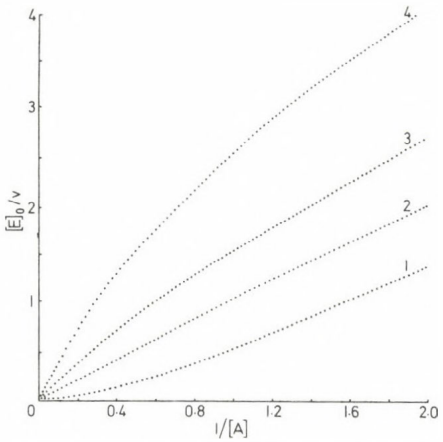

Fig. 12. Reversal of cooperation by the last product (computer outputs).

(1) no product, (2), (3), (4) increasing concentrations of Q. The values of the rate constants and the concentrations of the product can be found elsewhere [8].

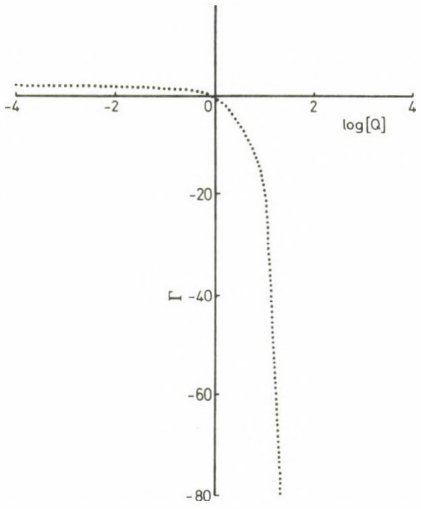

Fig. 13. Effect of the last product on the extent of cooperation (computer outputs).

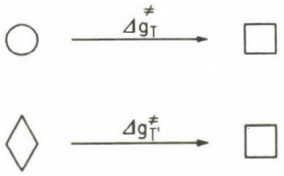

$\Delta g_{T'}^{\neq} > \Delta g_T^{\neq}$ Negative cooperation

$\Delta g_{T'}^{\neq} < \Delta g_T^{\neq}$ Positive cooperation

$\Delta g_{T'}^{\neq} = \Delta g_T^{\neq}$ Michaelian behaviour

Fig. 14. Thermodynamic grounds of cooperation for mnemonical enzymes.

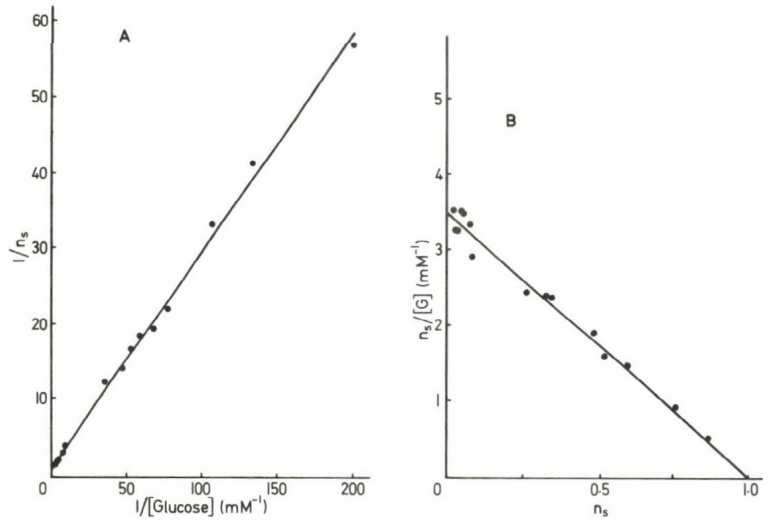

Fig. 15. Binding of $[^{14}C]$ glucose on wheat hexokinase L I.
A Klotz plot, B Scatchard plot.

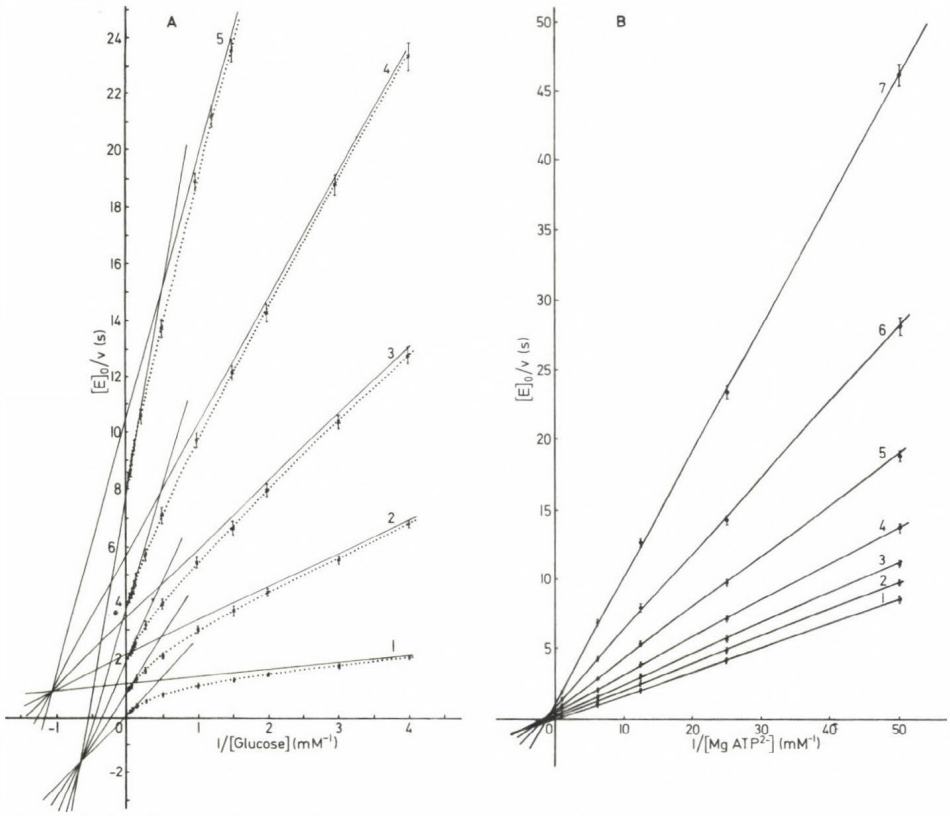

Fig. 16. Primary plots of glucose phosphorylation by wheat germ hexokinase

L I.
A Curves 1-5 are obtained for decreasing concentrations of $MgATP^{2-}$.
B Plots 1-7 are obtained for decreasing concentrations of glucose.
Experimental conditions can be found elsewhere [9].

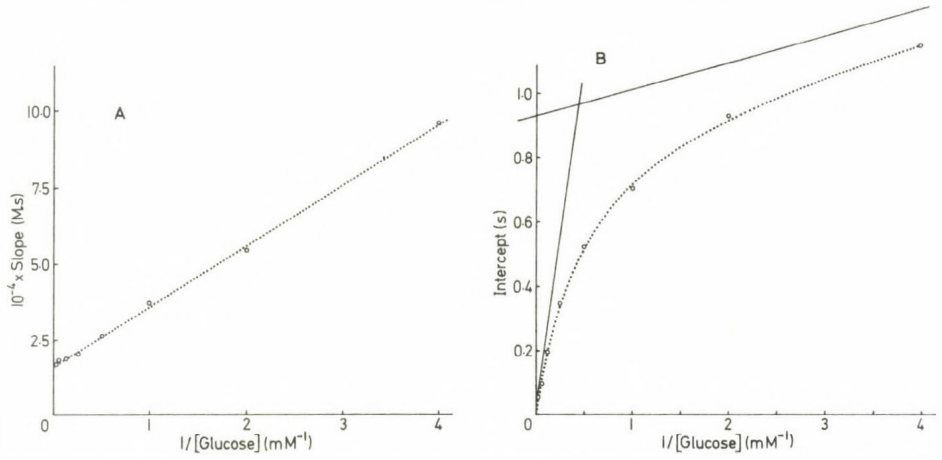

Fig. 17. Replot of intercepts and slopes of Fig. 16 against the reciprocal of glucose concentration.

See ref [9].

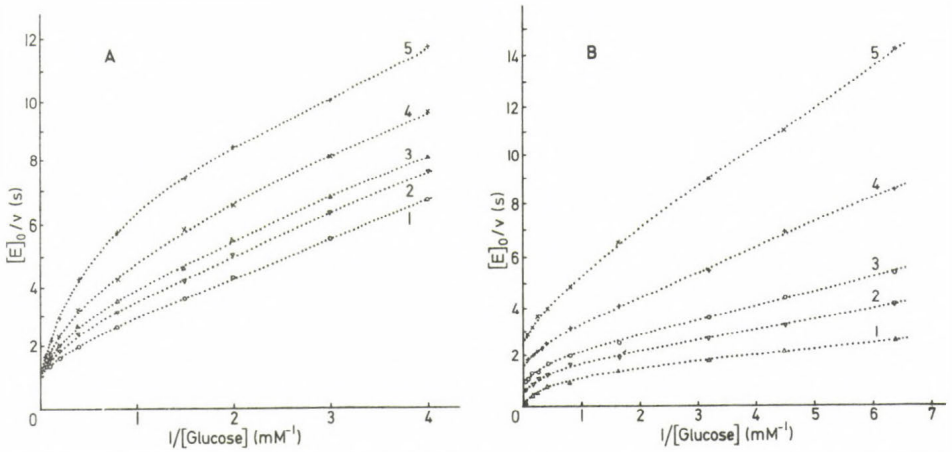

Fig. 18. Inhibitory effect of reaction products on the reciprocal reaction rate plotted against the reciprocal of glucose concentration.

(A) Inhibitory effect of glucose-6-phosphate. Curve (1) no glucose-6-phosphate, curves (2)-(5) increasing concentrations of glucose-6-phosphate.

(B) Inhibitory effect of $MgATP^{2-}$. Curve (1) no $MgATP^{2-}$, curves (2)-(5) increasing concentrations of $MgATP^{2-}$.

Experimental conditions can be found in ref [9].

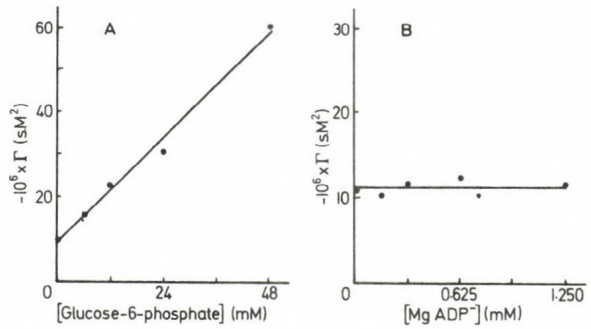

Fig. 19. Effect of products on the extent of cooperation.
(A) Effect of glucose-6-phosphate.
(B) Effect of $MgATP^{2-}$.

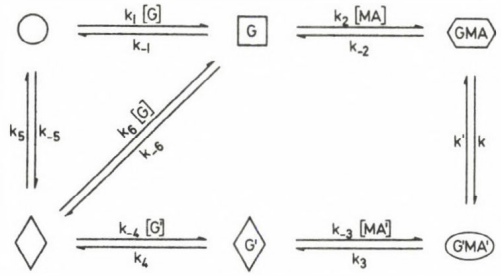

Fig. 20. The mnemonical model for wheat germ hexokinase L I.
G, MA, MA', G' represent glucose, $MgATP^{2-}$, $MgADP^-$ and glucose-6-phosphate.

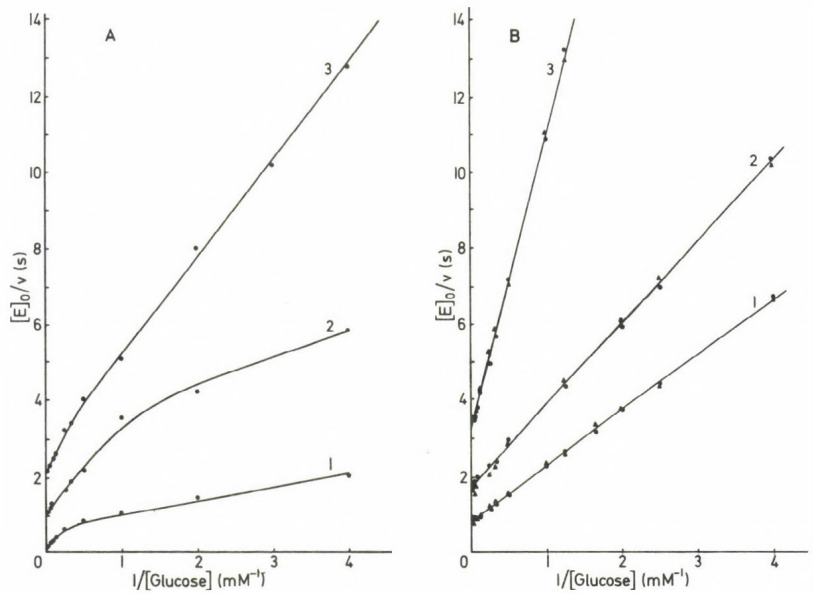

Fig. 21. Desensitization of wheat hexokinase L I.
(A) Primary plots exhibiting the curvature.
(B) Suppression of curvature by urea (▲) or SDS (●).
Experimental conditions can be found in ref [9].

Symp. Biol. Hung. 18, pp. 77–103 (1974)

METHODS OF ANALYSIS OF DOUBLE INHIBITION EXPERIMENTS

Cs. Fajszi

Institute of Biophysics, Biological Research Center of the Hungarian Academy of Sciences, Szeged, Hungary

1. Introduction

The use of specific modifiers can provide a lot of useful information about the active and regulatory sites of an enzyme, about the binding of the substrate to the enzyme. The simultaneous use of two inhibitors has been proved to be an even more powerful tool in elucidating the interaction not only between the substrate and the enzyme, but also between the substrate and the modifiers, and between the modifiers themselves. This method can demonstrate the possible steric changes in the enzyme during the binding of the substrate, and can help in mapping and localization of the binding groups.

These, and several other, advantages of the double inhibition studies were recognized some twenty years ago, and a number of such studies were performed with the use of purely competitive and purely noncompetitive inhibitors (Slater and Bonner, 1952; Loewe, 1957; Yagi and Ozawa, 1960; Yonetani and Theorell, 1964; Mares-Guia and Shaw, 1965; Berezin and Martinek, 1967; Berezin et al., 1967a,b; Silonova et al., 1969; Reynolds et al., 1970; Wermuth and Brodbeck, 1973; Semenza and Balthazar, 1974). Various methods were elaborated to decide whether there is a full competition between the two inhibitors or not (Loewe, 1957; Yagi and Ozawa, 1960; Yonetani and Theorell, 1964; Semenza and Balthazar, 1974). For the case of two purely competitive inhibitors the measure of competition between the inhibitors is given by an interaction constant, which

can be determined from the experiments (Yonetani and Theorell, 1964).

The aim of this paper is to generalize these methods to the case of other types of pure inhibitors (uncompetitive and mixed type), and also to partial inhibitors. More concretely, methods are presented for the determination of the parameters which do not occur in experiments with a single inhibitor, namely, the dissociation constants of the complexes containing both inhibitors - and hence the interaction constants of the two inhibitors in these complexes -, and also the rate constant of product formation from the ESI_1I_2 complex, if it exists

As a first step, we want to decide whether ther is a full competition between the inhibitors, i.e. whether the interaction constants equal infinity or have a finite value.

The second step will be the determination of the exact value of the interaction constants.

2. Independence of the inhibitors, or synergism/antagonism

When two modifiers act simultaneously on an enzyme reaction, the summary effect can equal the sum of the effects of the individual modifiers - in this case we say that the modifiers act independently. In other cases one modifier can strengthen or weaken the effect of the other. This is called synergism and antagonism, respectively. Such cases are often met in drug interactions (Loewe, 1957), and in the regulation of metabolic pathways (Atkinson, 1966; Stadtman, 197o).

These questions will not dealt in this paper with. It is, however, necessary to underline that the independence or interdependence of the action of two inhibitors must not be mixed with the value of the interaction constants. The interaction constant characterizes only the change of affinity of an inhibitor towards the enzyme or the enzyme-substrate complex, in the presence of a second inhibitor. On the other hand, synergism or antagonism is related to the change of the rate of product formation.

Another argument against the equivalency of these notions is the following. The interaction constants are constants,

characterizing the two inhibitors, while the effect of the inhibitors on the reaction rate depends on the concentration of the ligands. Thus, in some cases between the same two inhibitors we can find synergism at one substrate concentration and antagonism at other (Fajszi and Keleti, 1975).

Third, it was shown (Keleti and Fajszi, 1971) that for the independence of two inhibitors it is necessary but not sufficient their independent binding to E and ES. In addition one of the inhibitors must be noncompetitive with the substrate, and, besides this, one of the inhibitors must be pure inhibitor or they must independently influence the rate of product formation from the ESI_1I_2 complex.

3. Terminology

In the subsequent, we will speak everywhere about inhibitors, but the same reasoning applies to any modifier whose action is described by analoguous equations.

We deal only with single-substrate enzymes, which follow the Michaelis-Menten equation. For every inhibitor, the enzyme is supposed to have a single binding site.

An inhibitor is called pure, when the ESI complex is not formed, or it is inactive. In the case of a partial inhibitor this complex is active. In the plot of 1/v versus the concentration of the inhibitor (at fixed substrate concentration) a pure inhibitor yields a straight line, while a partial one yields a hyperbola.

A competitive inhibitor influences the affinity of the enzyme towards the substrate, and not the rate of the breakdown of the ES complex. A noncompetitive inhibitor influences the rate of breakdown, and not the affinity. An inhibitor of the mixed type influences both the rate and the affinity. A special type is the uncompetitive inhibitor, which can not be bound by the free enzyme, only by the ES complex.

4. General mechanism of double inhibitions

In the general case, if two inhibitors interact with an enzyme, the following complexes can be formed (assuming that

all complexes contain the enzyme, i.e. complexes I_1I_2, SI_1, SI_2, or SI_1I_2 are not formed): ES, EI_1, EI_2, ESI_1, ESI_2, EI_1I_2, ESI_1I_2, where E is the enzyme, S the substrate, I_1 and I_2 are the inhibitors. In the general case, product (P) will be formed from complexes ES, ESI_1, ESI_2 and ESI_1I_2. The general mechanism in graphical form is shown in Fig. 1.

Fig.1. Scheme of the general mechanism of double inhibitions

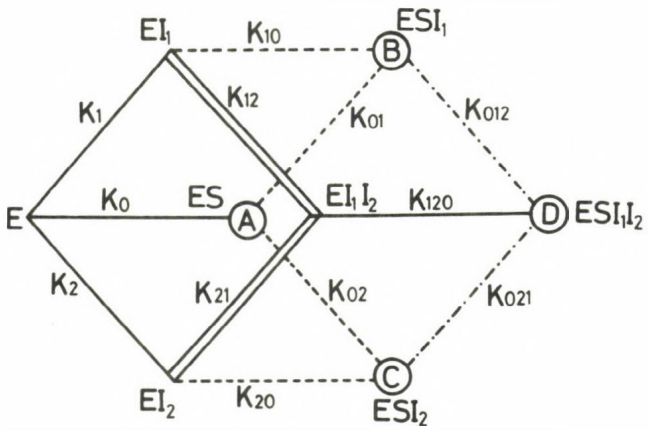

The vertices of the scheme correspond to the different complexes and to the free enzyme, as indicated. An edge between two vertices represents a reversible elementary step, the equilibrium constant of which is also indicated.

Broken lines show the elementary steps where the substrate and one of the inhibitors may interact; double lines, where the inhibitors interact on the free enzyme; and dotted lines, where the two inhibitors interact on the enzyme-substrate complex.

Circled symbols indicate complexes from which the product is formed.

The equilibrium constants of the reversible elementary steps are expressed as dissociation constants. In the indices of K's 0 corresponds to the substrate, 1 to I_1, and 2 to I_2. From the complex dissociates the ligand, corresponding to the last digit in the index of the dissociation constant. E.g.,

$$K_{20} = \frac{[EI_2][S]}{[ESI_2]}, \quad K_{02} = \frac{[ES][I_2]}{[ESI_2]}.$$

Product is formed in the following reactions (assumed irreversible), with the rate constants at the right:

A. $ES \longrightarrow E + P$, $\quad k_m = V_m/[E]_T$

B. $ESI_1 \longrightarrow EI_1 + P$, $\quad k_1 = V_1/[E]_T$

C. $ESI_2 \longrightarrow EI_2 + P$, $\quad k_2 = V_2/[E]_T$

D. $ESI_1I_2 \longrightarrow EI_1I_2 + P$, $\quad k_3 = V_3/[E]_T$

where V_m, V_1, V_2, V_3 are the maximum velocities of reactions A, B, C, D, respectively, and $[E]_T$ is the total enzyme concentration:

$$[E]_T = [E]+[ES]+[EI_1]+[EI_2]+[ESI_1]+[ESI_2]+[EI_1I_2]+[ESI_1I_2].$$

The initial rate of the formation of product is

$$v_{12} = k_m[ES] + k_1[ESI_1] + k_2[ESI_2] + k_3[ESI_1I_2] =$$
$$= (V_m[ES] + V_1[ESI_1] + V_2[ESI_2] + V_3[ESI_1I_2])/[E]_T$$

In the special cases some of the complexes may not exist, and/or some substrate-containing complexes are inactive (i.e. k_1, k_2 or k_3 equal 0). According to these restrictions the rate equation becomes simpler. This simplification will be used in the estimation of the interaction constants.

5. Interaction constants of the two inhibitors

In the general mechanism the following equalities hold between the dissociation constants:

$$K_0K_{01}K_{012}=K_0K_{02}K_{021}=K_1K_{10}K_{012}=K_1K_{12}K_{120}=K_2K_{20}K_{021}=K_2K_{21}K_{120}.$$

Hence we may derive the following relations (among others):

$$K_1K_{12} = K_2K_{21} \quad \text{and} \quad K_{01}K_{012} = K_{02}K_{021},$$

i.e.

$$\frac{K_{12}}{K_2} = \frac{K_{21}}{K_1} = \alpha$$ - the interaction constant of the two inhibitors on the free enzyme,

and

$\frac{K_{012}}{K_{02}} = \frac{K_{021}}{K_{01}} = \beta$ - the interaction constant of the two inhibitors on the enzyme-substrate complex.

Thus, α and β express the effect of the binding of one inhibitor to the enzyme and the enzyme-substrate complex, respectively, on the binding of the other inhibitor to these complexes. Their meaning is summarized in Table 1.

Table 1. The meaning of interaction constants

Value of interaction constant	Binding of one inhibitor
$\alpha=1$ or $\beta=1$	is independent of the binding of the other
$\alpha=\infty$ or $\beta=\infty$	excludes the binding of the other (full competition between the inhibitors)
$1<\alpha<\infty$ or $1<\beta<\infty$	hinders the binding of the other
$0<\alpha<1$ or $0<\beta<1$	facilitates the binding of the other

In all cases α refers to the interaction of the inhibitors on the free enzyme, and β to that on the ES complex. Of course, α makes sense only if complexes EI_1 and EI_2 exist. Similarly, β has meaning only if complexes ESI_1 and ESI_2 exist.

6. The rapid equilibrium rate equations

When rapid equilibrium conditions prevail, i.e. the elementary step/s/ of product formation is /are/ rate limiting, the concentration of different complexes can be expressed as follows:

$$[ES] = \frac{es}{K_0}, \quad [EI_1] = \frac{ei_1}{K_1}, \quad [EI_2] = \frac{ei_2}{K_2},$$

$$[ESI_1] = \frac{esi_1}{K_0 K_{01}}, \quad [ESI_2] = \frac{esi_2}{K_0 K_{02}},$$

$[EI_1I_2] = \frac{ei_1i_2}{K_1K_{12}}$ or $\frac{ei_1i_2}{K_2K_{21}}$ or $\frac{ei_1i_2}{\alpha K_1K_2}$, according to whether only the EI_1, only the EI_2, or both these complexes exist,

respectively.

$[ESI_1I_2] = \frac{esi_1i_2}{K_0K_{01}K_{012}}$ or $\frac{esi_1i_2}{K_0K_{02}K_{021}}$ or $\frac{esi_1i_2}{\beta K_0K_{01}K_{02}}$, according to whether only the ESI_1, only the ESI_2, or both these complexes exist, respectively.

Here e, s, i_1 and i_2 is the concentration of E, S, I_1 and I_2, respectively.

The initial rate of the formation of product is, in reciprocal form:

I.) When both I_1 and I_2 are pure inhibitors:

$$\frac{1}{v_{12}} = \frac{1}{V_m}\{(1+\frac{i_1}{K_1}+\frac{i_2}{K_2}+\frac{i_1i_2}{\beta K_{01}K_{02}})+\frac{K_0}{s}(1+\frac{i_1}{K_1}+\frac{i_2}{K_2}+\frac{i_1i_2}{\alpha K_1K_2})\} \quad (1)$$

II.) When I_1 is pure and I_2 partial inhibitor:

$$\frac{1}{v_{12}} = \frac{(1+\frac{i_1}{K_{01}}+\frac{i_2}{K_{02}}+\frac{i_1i_2}{\beta K_{01}K_{02}})+\frac{K_0}{s}(1+\frac{i_1}{K_1}+\frac{i_2}{K_2}+\frac{i_1i_2}{\alpha K_1K_2})}{V_m+V_2\frac{i_2}{K_{02}}} \quad (2)$$

III.) When both I_1 and I_2 are partial inhibitors:

$$\frac{1}{v_{12}} = \frac{(1+\frac{i_1}{K_{01}}+\frac{i_2}{K_{02}}+\frac{i_1i_2}{\beta K_{01}K_{02}})+\frac{K_0}{s}(1+\frac{i_1}{K_1}+\frac{i_2}{K_2}+\frac{i_1i_2}{\alpha K_1K_2})}{V_m+V_1\frac{i_1}{K_{01}}+V_2\frac{i_2}{K_{02}}+V_3\frac{i_1i_2}{\beta K_{01}K_{02}}} \quad (3)$$

These equations were written up with the use of α and β. If some of them has no sense, then instead of αK_1K_2 one has to put K_1K_{12} or K_2K_{21}, whichever has meaning, and instead of $\beta K_{01}K_{02}$: $K_{01}K_{012}$ or $K_{02}K_{021}$.

When I_1 is a pure inhibitor, it is natural to assume, that the ESI_1I_2 complex (if exists) is inactive, i.e. $k_3 = o$. If, however, product can be formed also from this complex, then the rate equation will be of type III., with $V_1=0$ (and, perhaps, $V_2=0$). Cases I., II. and III. can easily be separated on the basis of plots of $1/v_{12}$ against i_1 or i_2 (Table 2).

Table 2. Differentiation of cases I., II. and III.

case	plot of $1/v_{12}$ against	
	i_1 at fixed i_2 and s	i_2 at fixed i_1 and s
I.	straight line	straight line
II.	straight line	hyperbola
III.	hyperbola	hyperbola

7. Full competition between the inhibitors

The first question we want to decide is whether there is a full competition between the inhibitors. Full competition means that the binding of one inhibitor to E or ES excludes the binding of the other, i.e. nor EI_1I_2, neither ESI_1I_2 exist. In the case of full competition between the inhibitors α and/or β (whichever has meaning) equal infinity. When nor α neither β has meaning, i.e. when I_1 is purely competitive ($K_{01}=\infty$) and I_2 is uncompetitive ($K_2=\infty$), then one expects that none of the complexes containing both inhibitors exists. This case will also be referred to as full competition in contrast with the case when EI_1I_2 exists in spite of the uncompetitive type of I_2. This may occur if I_1 contains the groups which make possible for I_2 to bind to the ES complex, e.g. I_1 is a structural analogue of the corresponding part of the substrate, and thus I_2 behaves, in relation to EI_1, as a non-uncompetitive effector.

To decide whether there is a full competition between the inhibitors, several methods were proposed. (Their formal treatment see in the Appendix).

7.1. The isobolograms of Loewe(1957)

Isobols are equi-effective combinations of active substances plotted on graphs whose coordinates are the concentrations of the substances. In our case the coordinates are i_1 and i_2, and the isobols correspond to combinations of the inhibitors yielding (at fixed substrate concentration) a constant v_{12} (or v_{12}/v_0) value. (v_0 = the initial rate in the absence of the inhibitors).

Although this method was used only for the analysis of two purely competitive inhibitors, in fact it can be used for any combination of pure or partial inhibitors.

When nor EI_1I_2, neither ESI_1I_2 exist, the isobols are straight lines.

In case I. the straight lines, corresponding to different values of v_{12}, are parallel, as shown in Fig. 2.

In case II. the straight lines have a common intercept, with negative i_2-coordinate (Fig. 3.).

In case III. all the above isobol patterns can occur,

even with v_{12} growing in the direction, opposite to that shown by the arrows. One more possibility is shown in Fig. 4.

Fig. 2. Isobologram, indicating full competition in case I.

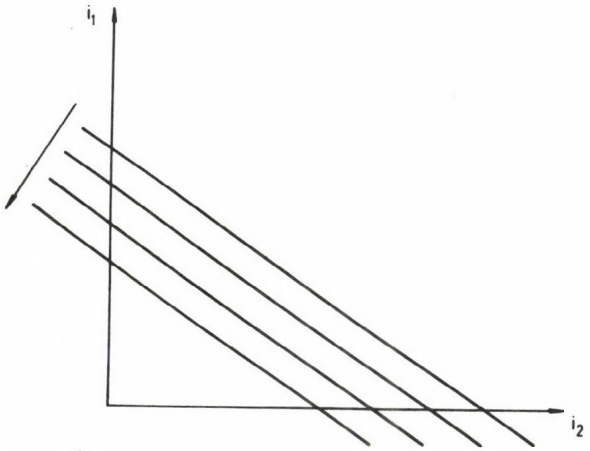

The different straight lines correspond to different v_{12} values. The arrow shows the direction of increasing v_{12}.

(Such pattern can occur also in case III.)

When at least one of the EI_1I_2 and ESI_1I_2 complexes exists, the isobols are hyperbolae, in some cases with a straight line among them. So this case can easily be distinguished from the case of full competition.

7.2. Method of Yagi and Ozawa(196o)

It can be used only for case I. Plotting $1/v_{12}$ (or v_0/v_{12}) against the concentration of one of the inhibitors (e.g., i_1) at fixed i_2/i_1 ratio, and fixed substrate concentration, we obtain a straight line, when nor EI_1I_2, neither ESI_1I_2 exist, and a second order curve in other cases.

Fig. 3. Isobolograms, indicating full competition in case II.

a.) If I_2 inhibits at the given substrate concentration

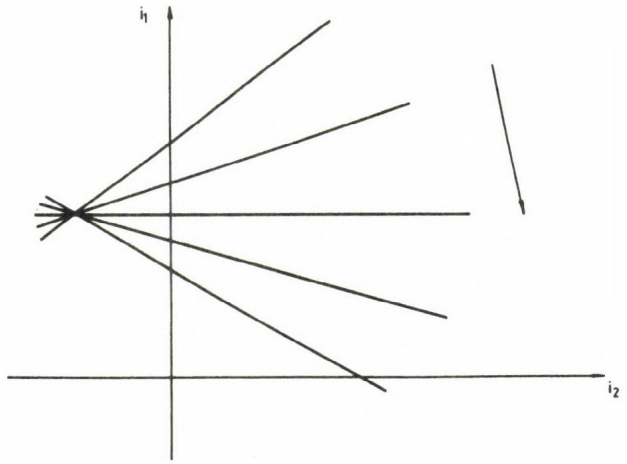

b.) If I_2 activates at the given substrate concentration

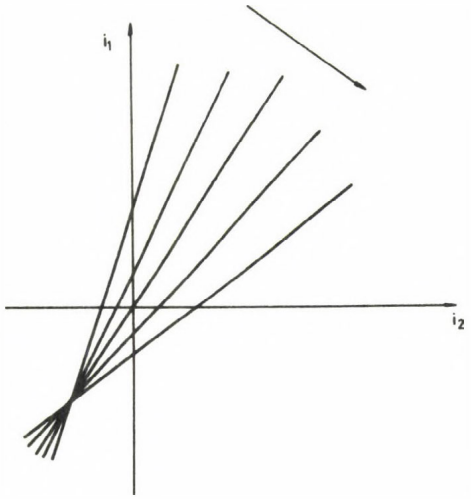

The different straight lines correspond to different v_{12} values. The arrows show the direction of increasing v_{12}.

(Such patterns can occur also in case III.)

Fig. 4. Additional isobologram, indicating full competition in case III.

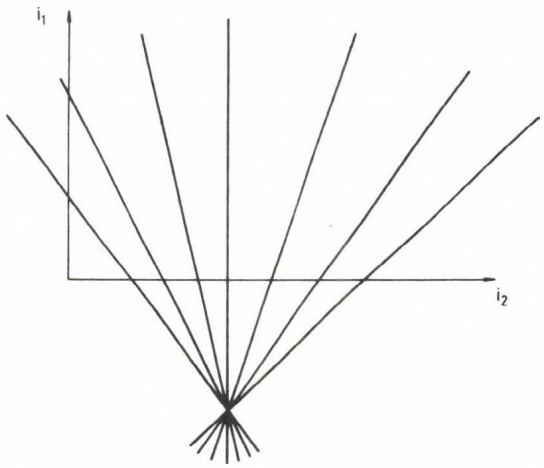

The different straight lines correspond to different v_{12} values.

7.3. Method of Yonetani and Theorell(1964) (see also Semenza and Balthazar, 1974).

This method is designated also for case I. only. If we plot $1/v_{12}$ (or v_0/v_{12}) versus i_1 at constant i_2 and s, the result will be a straight line. Repeating this for different values of i_2, at the same fixed s, we obtain a family of straight lines. The lines are parallel if nor EI_1I_2 neither ESI_1I_2 exist, while in the other cases they have a common intercept, which, in many cases, can be used for the exact determination of α and β. (See 9.1.).

7.4. Extension of the method of Hunter and Downs(1945) to the case of two inhibitors

This is also a generally applicable method, not only for pure inhibitors. It requires the plotting of $i_1 . \frac{v_{12}}{v_0 - v_{12}}$ versus i_1 at constant s, and fixed i_2/i_1 ratio. The result will differ in cases I., II. and III. The plot yields:

in case I.: a constant, when there is a full competition

between the inhibitors, and hyperbola in other cases;

in case II.: a straight line, not constant, if there is a full competition, and hyperbola or constant otherwise;

in case III.: a straight line, not constant, when there is a full competition between the inhibitors. Else the result may be a curve, or a constant, or even a straight line. A straight line, however, can occur for at most two specific values of i_2/i_1. When plotting is performed for other ratios, the result will be no more a straight line.

7.5. Generalized method of Webb(1963)

Very similar situation occurs by the use of the plot of $v_0/(v_0-v_{12})$ versus $1/i_1$ at fixed i_2/i_1, and constant s.

This method, however, seems less sensitive in the detection of full competition, than the previous one.

7.6. Immediate method for case I.

For case I. there is an immediate method of deciding whether both EI_1I_2 and ESI_1I_2 are absent. When this is the case,

$$\frac{1}{v_{12}} + \frac{1}{v_0} = \frac{1}{v_1} + \frac{1}{v_2} \quad .$$

(Here v_1 is the initial rate in the presence of I_1 only, while v_2 is that in the presence of I_2 only).

8. Determination of the interaction constants

When some of the EI_1I_2 and ESI_1I_2 complexes exists, then the interaction constants can provide information about the binding groups on the enzyme molecule, about the binding of the substrate, etc. (See in details in Keleti and Fajszi,1971)

This question was rosen (and solved) for two purely competitive inhibitors by Yonetani and Theorell(1964). For other combinations of inhibitors the problem was investigated by Keleti and Fajszi(1971). For the case of two pure inhibitors α and/or β can relatively easily be determined exactly. When one or both of the inhibitors inhibits only partially, this is a harder task. In many cases it seems enough to decide whether the binding of one inhibitor is independent from, hinders, or facilitates the binding of the other (i.e. the interaction

constant is equal to, greater than, or less than unity, respectively).

We shall treat cases I., II. and III. separately. Mathematical derivation of the following results is also given in the Appendix.

9. Case I.: Two pure inhibitors

9.1. Method of Yonetani and Theorell(1964)

$1/v_{12}$ vs. i_1 at different values of i_2 and fixed s (called plot A) gives a series of straight lines which are parallel when nor EI_1I_2 neither ESI_1I_2 exist, and have a common intercept if at least one of these complexes exists. The situation is quite analoguous in the plot of $1/v_{12}$ vs. i_2 at different i_1's and fixed s (called plot B).

Generally, the coordinates of the common intercept depend, in a nonlinear manner, on s. The exceptions, when the x-coordinate of the common intercept is constant, independently of s, are summarized in Table 3.

Table 3. Constant common intercepts in the plots of Yonetani and Theorell

inhibition type of I_1	I_2	EI_1I_2	ESI_1I_2	x-coordinate of the common intercept in plot A	plot B
C	C	+	-	$-\alpha K_1$	$-\alpha K_2$
C	NC	+	-		$-\alpha K_2$
C	U	+	-		$-K_{12}$
NC	U	-	+	$-\beta K_{01}$	
U	U	-	+	$-\beta K_{01}$	$-\beta K_{02}$
NC	NC for $\alpha=\beta$	+	+	$-\alpha K_1$	$-\alpha K_2$

Inhibition types: C = purely competitive, NC = purely noncompetitive, U = purely uncompetitive. An empty place in the table means that α and/or β can not be determined immediately from the coordinates of the common intercept.

For other combinations of inhibitors secondary plots (see 9.2.), or other methods (e.g., 9.3.) are to be used.

9.1.1.

When both I_1 and I_2 are purely noncompetitive inhibitors, let us denote the coordinates of the common intercept by (x_A, y_A) in plot A, and by (x_B, y_B) in plot B. (In fact, $y_A = y_B$). Then

$$K_1 . V_m . \frac{y_A}{x_A} = K_2 V_m . \frac{y_B}{x_B} = (1 - \frac{1}{\beta}) + \frac{K}{s}(1 - \frac{1}{\alpha}) \qquad (4)$$

whence α and β can be obtained, plotting y_A/x_A or y_B/x_B against $1/s$.

9.2. Determination of α and β from secondary plots

In the plot of $1/v_{12}$ vs. $1/s$ let a be the intercept on the ordinate, and b the slope of the straight line, i.e. $1/v_{12} = a + b.(1/s)$.

a vs. i_1 at constant i_2 is linear. For different i_2 values the straight lines are parallel, if ESI_1I_2 does not exist (β has no meaning, or $\beta=\infty$). They have a common intercept with coordinates $(-\beta K_{01}, \frac{1-\beta}{V_m})$, if $\beta<\infty$. From the ordinate of this common intercept one can decide whether the binding of one inhibitor to the ES complex hinders or facilitates the binding of the other: A positive ordinate corresponds to $0<\beta<1$, while a negative ordinate to $\beta>1$. Moreover, this common intercept is on a fixed straight line, determined by the parameters of I_1 alone (see Fig. 5).

If β has no meaning, but the ESI_1I_2 complex exists, the coordinates of the common intercept are $(-K_{021}, 1/V_m)$, when $K_{01}=\infty$, and $(0, 1/V_m)$, when $K_{02}=\infty$. In this case K_{012} can be determined from the plot of a vs. i_2 at different i_1's.

b vs. i_1 for different i_2's are parallel, if EI_1I_2 does not exist. Else they have a common intercept, whose coordinates are $(-\alpha K_1, \frac{K}{V_m}(1-\alpha))$, if $\alpha<\infty$. This common intercept is also on a fixed straight line (see Fig. 6).

In the exceptional cases, when α has no meaning, but EI_1I_2 exists, the common intercept is: $(-K_{21}, K_0/V_m)$, when

Fig. 5. Fixed straight line for the determination of β from secondary plot

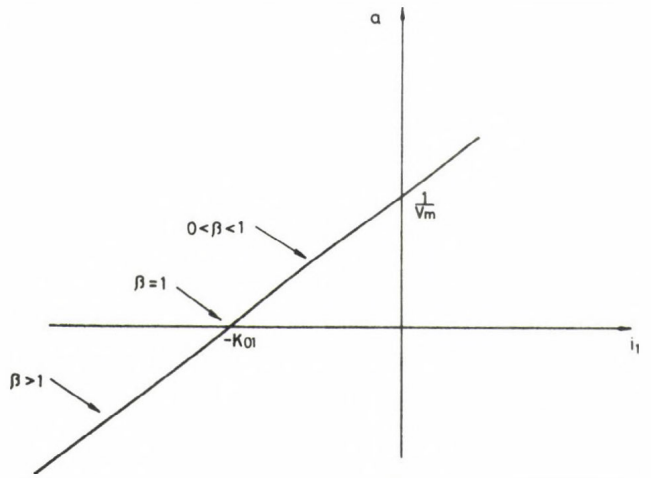

Fig. 6. Fixed straight line for the determination of α from secondary plot

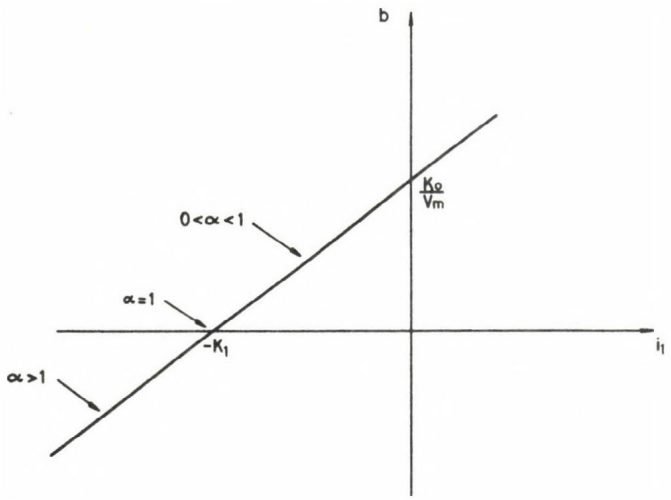

$K_1=\infty$, and $(0, K_0/V_m)$, if $K_2=\infty$. In this latter case K_{12} can be determined from the plot of b vs. i_2 at different i_1's.

9.3. Immediate method

$\frac{1}{i_1 i_2}(\frac{1}{v_{12}} - \frac{1}{v_2} - \frac{1}{v_1} + \frac{1}{v_0})$ vs. $\frac{1}{s}$ is a straight line with slope $\frac{K_0}{V_m}\cdot\frac{1}{\alpha K_1 K_2}$, and intercept on the ordinate $\frac{1}{V_m}\cdot\frac{1}{\beta K_{01} K_{02}}$.

10. Case II.: One pure and one partial inhibitor

10.1. Saturation by the partial inhibitor ($i_2\to\infty$)

Let $v_{12}^{/sat2/}$ be the initial velocity when saturated by the partial inhibitor I_2. Then $1/v_{12}^{/sat2/}$ vs. $1/s$ at different i_1's gives straight lines, which are parallel, when EI_1I_2 does not exist. Else, from $1/v^{/sat2/} = a + b.(1/s)$, b vs. i_1 is a straight line which intercepts the abscissa at $-\alpha K_1$, when α has meaning; at $-K_{21}$, when $K_1=\infty$; and at 0, when $K_2=\infty$. In the latter case K_{12} can be determined from the slope of b vs. i_1, equal to $K_0K_{02}/V_2K_1K_{12}$.

a is constant, when ESI_1I_2 does not exist. Else a vs. i_1 intercepts the abscissa at $-\beta K_{01}$, if β has meaning; and at $-K_{021}$, if $K_{01}=\infty$.

Another possibility is plotting $1/v_{12}^{/sat2/}$ vs. i_1 at different fixed values of s. The straight lines will be parallel, with slope $\frac{1}{V_2}\cdot\frac{1}{\beta K_{01}}$, if EI_1I_2 does not exist. Else they have a common intercept with coordinates $\left(-\alpha K_1; \frac{1}{V_2}(1 - \frac{\alpha K_1}{\beta K_{01}})\right)$.

10.2. Without saturation

10.2.1.

$\frac{1}{i_1}(\frac{1}{v_{12}} - \frac{1}{v_2})$ vs. $\frac{1}{s}$ gives a straight line: $= a + b.\frac{1}{s}$.

1. If it is constant, independently of s and i_2 (i.e. a=const, b=0), then $K_I=\infty$, EI_1I_2 does not exist, and $\beta=V_m/V_2$.

2. If there are different constants for different i_2's (i.e. b=0, $a\neq$ const), then $K_1=\infty$, EI_1I_2 does not exist, and the plot of $a/(a-a_0)$ vs. $1/i_2$ intercepts the abscissa at $-1/\beta K_{02}$. (Here a_0 = the intercept on the ordinate at i_2=0, i.e. that of the straight line $\frac{1}{i_1}(\frac{1}{v_1} - \frac{1}{v_0})$ vs. $\frac{1}{s}$).

3. If $b \neq 0$, then let c denotes the intercept on the abscissa of the original straight line (i.e. $c = -a/b$). If $c \equiv c_0$, then $\alpha K_2 = \beta K_{02}$, and α and β can be obtained from the plot of $a/(a-a_0)$ against $1/i_2$. If c varies with i_2, then $1/(c-c_0)$ vs. $1/i_2$ intercepts the abscissa at $-1/\alpha K_2$, while $c/(c-c_0)$ vs. $1/i_2$ intercepts the abscissa at $-1/\beta K_{02}$.

10.2.2.

$\frac{1}{v_{12}}$ vs. $\frac{1}{s}$ at different i_1's and fixed i_2 are parallel, if $K_1=\infty$ and EI_1I_2 does not exist. Else they have a common intercept, whose x-coordinate equals the above c.

11. Case III.: Two partial inhibitors

The saturation of the enzyme with one or both inhibitors is proposed. The analysis can be performed in the following sequence:

1. If $1/v_{12}^{/sat2/}$ vs. i_1 and $1/v_{12}^{/sat1/}$ vs. i_2 both are straight lines, then ESI_1I_2 does not exist ($\beta=\infty$), or it is inactive ($V_3=0$). $1/v_{12}^{/sat2/}$ vs. $1/s$ is also a straight line: $1/v_{12}^{/sat2/} = a + b.(1/s)$. When $\beta=\infty$, a is constant. When $\beta\neq\infty$, $V_3=0$, then a vs. i_1 intercepts the abscissa at $-\beta K_{01}$. In both cases b vs. i_1 intercepts the abscissa at $-\alpha K_1$.

2. When $\beta<\infty$ and $V_3>0$, then let us denote by c the intercept on the abscissa of the plot of $1/v_{12}^{/sat2/}$ vs. $1/s$. If c changes with i_1, then the abscissa-intercept of $1/(c-c_0)$ vs. $1/i_1$ equals $-1/\alpha K_1$, while that of $c/(c-c_0)$ vs. $1/i_1$ equals $-1/\beta K_{01}$. The remaining parameter, V_3, can be determined according to §3 or §4.

If $c \equiv c_0$, then $\alpha K_1 = \beta K_{01}$. Then one can use quite analoguously the abscissa-intercept of $1/v_{12}^{/sat1/}$ vs. $1/s$, which depends on i_2 unless $\alpha K_2 = \beta K_{02}$.

In this latter case let a be the ordinate-intercept of $1/v_{12}^{/sat2/}$ vs. $1/s$. a does not change with i_1, if $V_2=V_3$. In this case we use the ordinate-intercept of $1/v_{12}^{/sat1/}$ vs. $1/s$, in function of i_2. It seems quite improbable that for any two effectors $V_1=V_2=V_3$, and $\alpha K_1=\beta K_{01}$ and $\alpha K_2=\beta K_{02}$, at the same time.

3. If the ordinate-intercept of $1/v_{12}^{/sat2/}$ vs. $1/s$, α, depends on i_1, then $1/(\alpha-\alpha_0)$ vs. $1/i_1$ intercepts the abscissa at $-(V_3/V_2)(1/\beta K_{01})$, while $\alpha/(\alpha-\alpha_0)$ vs. $1/i_1$ intercepts the abscissa at $-1/\beta K_{01}$, whence both V_3 and β can be determined.

4. When the enzyme is saturated by both inhibitors,

$$\frac{1}{v_{12}^{/sat1,2/}} = \frac{1}{V_3}\left(1 + \frac{K_0}{s}\cdot\frac{\beta K_{01}K_{02}}{\alpha K_1 K_2}\right)$$

and hence V_3 can be determined as the ordinate-intercept in plotting this against $1/s$.

12. Conclusions

In the analysis of the effect of two simultaneously applied inhibitors (generally: modifiers) the following sequence of actions can be recommended.

1. From the analysis of the uninhibited reaction one obtains V_m and K_0.

2. Analysing the two inhibitors separately, V_1, K_1 and K_{01}, and V_2, K_2 and K_{02} can be obtained, and the type of the two inhibitors cleared up.

3. By the simultaneous application of both inhibitors one checks if case I., II. or III. is encountered. For this purpose a few series of experiments are needed, in which i_1 and s are fixed, while i_2 varies. In another few series i_2 and s are fixed, while i_1 varies. (See 6.).

4. In the following step one decides if there is a full competition between the inhibitors. For this purpose in case I. when one of the inhibitors is purely competitive, or purely uncompetitive, the method of Yonetani and Theorell can be recommended, using the same series of experiments and the same plots as in step 3. (See 7.3.).

5. For other combinations of the inhibitors (and even for those in step 4) the method of Loewe can be used (see 7.1.). In cases I. and II. from the straight lines of $1/v_{12}$ vs. i_1 (plot of step 3) the (i_1,i_2) pairs, yielding the same v_{12} value, can be easily obtained.

6. In case III. the plots of step 3 yield hyperbolae, whence the determination of the (i_1,i_2) pairs would be impre-

cise. Thus it is better to plot $1/v_{12}$ vs. $1/s$ at different fixed (i_1,i_2) pairs, this yielding straight lines. This requires, however, a lot of experimental work, since the concentration of all three ligands are to be varied (in contrast with the preceeding steps, where s could be kept constant).

7. Therefore, it seems better to use in case III. the extension of the method of Hunter and Downs (see 7.4.). It can be performed on the same set of data as in step 3, if the concentrations of I_1 and I_2 are properly chosen. For sake of a sure decision it is better, however, to repeat this step for at least two different substrate concentrations.

8. In case of full competition the analysis is over. If some of the EI_1I_2 and ESI_1I_2 complexes exist, the exact value of α and/or β can be determined by the methods of 9., 10. and 11.

In case I., if possible, method of Yonetani and Theorell is to be used, since it requires no other experiments as those performed in step 3.

In case II. the saturation with the partial inhibitor seems to require less new experiments, since only two concentrations have to be varied.

APPENDIX

Let us denote $1/v_{12}$ by w. Beside this, let us introduce the following notations:

$$a = 1 + \frac{K_0}{s}\ ,\quad b_1 = \frac{1}{K_{01}} + \frac{K_0}{s}\cdot\frac{1}{K_1}\ ,\quad b_2 = \frac{1}{K_{02}} + \frac{K_0}{s}\cdot\frac{1}{K_2}\ ,$$

$$c = \frac{1}{\beta K_{01}K_{02}} + \frac{K_0}{s}\cdot\frac{1}{\alpha K_1 K_2}\ ,\quad d = V_m\ ,\quad e_1 = V_1/K_{01},$$

$$e_2 = V_2/K_{02},\quad f = \frac{V_3}{\beta K_{01}K_{02}}\ .$$

Obviously, a, b_1, b_2 and d are positive, while c, e_1, e_2 and f are positive or zero.

Using this notation, the initial velocity can be expressed as follows:

without inhibitors: $v_0 = \frac{d}{a}$;

in the presence of one inhibitor: $v_j = \frac{d + e_j i_j}{a + b_j i_j}$ $(j=1,2)$;

where $e_j=0$ corresponds to a pure inhibitor, while $e_j>0$ to a partial one;

in the presence of both inhibitors:

$$v_{12} = \frac{d + e_1 i_1 + e_2 i_2 + f i_1 i_2}{a + b_1 i_1 + b_2 i_2 + c i_1 i_2} \qquad (5)$$

where full competition between the two inhibitors is expressed by c=0, and in this case necessarily also f=0. (Generally, $e_j=0$ involves also f=0).

For pure inhibitors $v_j<v_0$. The same is true for most of the partial inhibitors. There are, however, some types of partial inhibitors, which inhibit at certain concentrations of the substrate, and activate at others (Frieden, 1964). If one of the inhibitors is of such a type, then the substrate concentration for the measurements has to be chosen so that $v_j \neq v_0$.

$v_j<v_0$ is equivalent to $\frac{d + e_j i_j}{a + b_j i_j} < \frac{d}{a}$,

whence

$$da + ae_j i_j < ad + b_j d i_j$$

$$ae_j i_j < db_j i_j$$

$$ae_j < db_j\ .$$

1. Isobolograms (Loewe, 1957)

The equation of isobols is obtained by expressing from Eqs.(1)-(3) - or, which is the same, Eq.(5) - i_1 as a function of i_2, at fixed s.

Case I., c=0: $i_1 = \frac{wd - a}{b_1} - \frac{b_2}{b_1} i_2$

The isobols are parallel straight lines, with slope $\frac{b_2}{b_1}$, and with ordinate-intercept $\frac{wd-a}{b_1}$, decreasing, as w decreases, i.e. as v_{12} increases.

Case I., c>0: $i_1 = \frac{(wd-a) - b_2 i_2}{b_2 + c i_2}$

The isobols are hyperbolae with asymptotes $i_1 \equiv -b_2/c$ and $i_2 \equiv -b_1/c$.

Case II., c=0: $i_1 = \frac{wd-a}{b_1} + \frac{we_2-b_2}{b_1} i_2$

- straight lines, both the slope and the ordinate intercept of which decreases as v_{12} increases. These straight lines intercept at the point with coordinates

$$i_1^o = \frac{b_2 d - a e_2}{b_1 e_2} \quad , \quad i_2^o = -\frac{d}{e_2} \ .$$

i_2^o is always negative. i_1^o is positive, if $v_2 < v_0$, while it is negative, if $v_2 > v_0$.

Case II., c>0: $i_1 = \frac{(wd-a) + (we_2-b_2).i_2}{b_1 + c i_2}$

The isobols are hyperbolae, with asymptotes $i_1 \equiv (we_2-b_2)/c$ and $i_2 \equiv -b_1/c$, the former changing with v_{12}. If $b_1 e_2 > dc$, then among these hyperbolae there is also a straight line, parallel with the abscissa: $i_1 = \frac{b_1 b_2 - ac}{b_1 e_2 - cd}$.

Case III., c=0: the isobols are determined by the following relationship:

$$0 = (wd-a) + i_1(we_1-b_1) + i_2(we_2-b_2)$$

$$0 = (wd-a) + i_1 e_1 (w - \frac{b_1}{e_1}) + i_2 e_2 (w - \frac{b_2}{e_2})$$

If $b_1/e_1 = b_2/e_2$, then $w \neq b_1/e_1$, and $w - \frac{b_1}{e_1} = w - \frac{b_2}{e_2}$, whence

$$i_1 = \frac{wd - a}{b_1 - we_1} - \frac{e_2}{e_1} . i_2$$

The isobols are parallel straight lines with slope $-e_2/e_1$.

If $b_1/e_1 \neq b_2/e_2$, then the isobols are straight lines with a common intercept $i_1^o = \frac{db_1 - ae_1}{b_2 e_1 - b_1 e_2}$, $i_2^o = \frac{db_2 - ae_2}{b_1 e_2 - b_2 e_1}$.

If $v_0>v_1$ and $v_0>v_2$, then the numerators both in i_1^o and i_2^o are positive, while the denominators are equal with opposite signs. Therefore one of the coordinates of the common intercept is positive, and the other negative. The same situation occurs if $v_0<v_1$ and $v_0<v_2$.

If one of the modifiers acts (at the given substrate concentration) as an inhibitor, and the other as an activator, then both coordinates of the common intercept are negative. E.g., if $v_1>v_0>v_2$, then $db_1-ae_1<0<db_2-ae_2$, from where $\frac{b_1}{e_1}<\frac{a}{d}<\frac{b_2}{e_2}$, i.e. $b_1e_2<b_2e_1$, whence i_1^o = negative/positive < 0, and i_2^o = positive/negative < 0.

Case III., c>0:

$$i_1 = \frac{(wd-a) + (we_2-b_2)i_2}{(e_2-wb_2) + (c-wf)i_2}$$

- hyperbolae, possibly with a straight line (parallel with one of the coordinate axes) among them.

2. Method of Yagi and Ozawa(1960)

If s = constant and $i_2/i_1 = x$ = constant, then in case I.

$$\frac{1}{v_{12}} = \frac{a}{d} + \frac{b_1 + b_2x}{d}.i_1 + \frac{cx}{d}.i_1^2 .$$

3. Method of Yonetani and Theorell(1964)

In case I.

$$\frac{1}{v_{12}} = \frac{a + b_2i_2}{d} + i_1.\frac{b_1 + ci_2}{d}$$

If c=0, then, in plot A, $1/v_{12}$ vs. i_1 at different fixed values of i_2 are parallel straight lines with slope b_1/d.
If c>0, the straight lines have a common intercept with coordinates

$$x_A = -\frac{b_2}{c} , \quad y_A = \frac{1}{d}(a - \frac{b_1b_2}{c}) .$$

Similarly, in the plot of $1/v_{12}$ versus i_2 at different fixed concentrations i_1 (plot B), if c>0, the straight lines have a common intercept

$$x_B = -\frac{b_1}{c} , \quad y_B = y_A .$$

Returning to the original notations,

$$x_A = -\frac{\frac{1}{K_{02}} + \frac{K_0}{s}.\frac{1}{K_2}}{\frac{1}{\beta K_{01}K_{02}} + \frac{K_0}{s}.\frac{1}{\alpha K_1K_2}} .$$

x_B can be expressed quite similarly, with index 1 instead of 2,

and inversely.

$$y_A = y_B = \frac{1}{V_m}\{(1 + \frac{K_0}{s}) - \frac{(\frac{1}{K_{01}} + \frac{K_0}{s}\cdot\frac{1}{K_1})\cdot(\frac{1}{K_{02}} + \frac{K_0}{s}\cdot\frac{1}{K_2})}{\frac{1}{\beta K_{01}K_{02}} + \frac{K_0}{s}\cdot\frac{1}{\alpha K_1 K_2}}\}$$

If I_1 is purely competitive, then $K_{01}=\infty$. If I_2 is not of uncompetitive type, then

$$x_B = -\frac{\frac{K_0}{s}\cdot\frac{1}{K_1}}{\frac{K_0}{s}\cdot\frac{1}{\alpha K_1 K_2}} = -\alpha K_2 .$$

If I_2 is of uncompetitive type, and the EI_1I_2 complex exists, but not the ESI_1I_2, then $c = \frac{K_0}{s}\cdot\frac{1}{K_1 K_{12}}$, whence $x_B = -K_{12}$.

Similarly, if the ESI_1I_2 complex exists, but not EI_1I_2, then $c = \frac{1}{K_{02}K_{021}}$, and $x_A = -K_{021}$.

If I_2 is purely uncompetitive, and I_1 is not competitive, then $K_2=\infty$, EI_1I_2 does not exist, and $x_A = -\beta K_{01}$.

If both I_1 and I_2 are noncompetitive, then $K_{01}=K_1$ and $K_{02}=K_2$. So

$$x_A = -K_1\cdot\frac{1 + \frac{K_0}{s}}{\frac{1}{\beta} + \frac{K_0}{s}\cdot\frac{1}{\alpha}}, \quad y_A = \frac{1}{V_m}\cdot\frac{(\frac{1}{\beta} - 1) + \frac{K_0}{s}\cdot(\frac{1}{\alpha} - 1)}{\frac{1}{\beta} + \frac{K_0}{s}\cdot\frac{1}{\alpha}}\cdot(1 + \frac{K_0}{s}) .$$

Division of y_A by x_A yields immediately Eq. (4).
If $\alpha=\beta$, then x_A reduces to $-\alpha K_1$.

4. Generalized method of Hunter and Downs (1945)

Let $i_2/i_1 = x = \text{const}$ and $s = \text{const}$. $y = i_1\cdot\frac{v_{12}}{v_0 - v_{12}}$ is to be calculated, and plotted against i_1.

Case I.: $$y = \frac{a}{(b_1 + b_2x) + i_1cx}$$

For $c = 0$ y is constant, while for $c>0$ y declines to zero as i_1 tends to infinity.

Case II.: $$y = \frac{ad + i_1e_2ax}{\{b_1d + x(b_2d - e_2a)\} + i_1cdx}$$

For $c = 0$: a straight line (with positive slope, if $v_2<v_0$).
For $c > 0$: a hyperbola or a constant.

Case III.: $$y = \frac{ad + i_1a(e_1 + e_2x) + i_1^2afx}{\{(b_1d - ae_1) + x(b_2d - ae_2)\} + i_1x(cd-af)}$$

For $c = 0$ y vs. i_1 is a straight line (with positive slope, if

$v_1 < v_0$ and $v_2 < v_0$). For $c>0$ the plot generally does not yield a straight line. However, if $f=0$ and $cd^2 > e_1(b_1d - ae_1)$, then there exists a single x value, at which y is constant. If $f>0$, then y vs. i_1 yields a straight line, namely

$$y = \frac{ad}{(b_1d - ae_1) + x(b_2d - ae_2)} + i_1 \cdot \frac{af}{cd - af} ,$$

in that very specific case when

$$a(e_1 + e_2x) = \frac{ad}{(b_1d - ae_1) + x(b_2d - ae_2)} \cdot x(cd - af) + \\ + xaf \cdot \frac{(b_1d - ae_1) + x(b_2d - ae_2)}{x(cd - af)} .$$

This is a second-degree equation in x, so this relationship may prove true for at most two values of x. If the plotting is performed for several i_2/i_1 ratios, the cases $c=0$ and $c>0$ can be clearly distinguished. (Plotting at several fixed s's serves equally well for this distinction).

5. Generalized method of Webb(1963)

$\frac{v_0}{v_0 - v_{12}}$ is to be plotted against $1/i_1$, at constant i_2/i_1 ratio and fixed s. Since $\frac{v_0}{v_0 - v_{12}} = 1 + \frac{v_{12}}{v_0 - v_{12}}$, this plot yields a straight line in the same cases when the generalized Hunter-Downs method does.

6. Immediate method for case I.

$$\frac{1}{v_{12}} - \frac{1}{v_2} - \frac{1}{v_1} + \frac{1}{v_0} = \frac{a + b_1i_1 + b_2i_2 + ci_1i_2}{d} - \frac{a + b_2i_2}{d} \\ - \frac{a + b_1i_1}{d} + \frac{a}{d} = \frac{c}{d} \cdot i_1i_2 .$$

If $c=0$, this expression equals zero. If $c>0$, then, with our original notations $\frac{c}{d} = \frac{1}{V_m} \cdot (\frac{1}{\beta K_{01} K_{02}} + \frac{K_0}{s} \cdot \frac{1}{\alpha K_1 K_2})$.

Therefore both α and β can be determined from the plot of c/d versus 1/s.

7. Determination of α and β from secondary plots in case I.

$$\frac{1}{v_{12}} = \frac{1}{V_m}(1 + \frac{i_1}{K_{01}} + \frac{i_2}{K_{02}} + \frac{i_1i_2}{\beta K_{01}K_{02}}) + \frac{1}{s} \cdot \frac{K_0}{V_m}(1 + \frac{i_1}{K_1} + \frac{i_2}{K_2} + \frac{i_1i_2}{\alpha K_1 K_2})$$

$1/v_{12}$ vs. 1/s, at fixed i_1 and i_2, is a straight line, with ordinate intercept $a = \frac{1}{V_m}(1 + \frac{i_1}{K_{01}} + \frac{i_2}{K_{02}} + \frac{i_1i_2}{\beta K_{01}K_{02}})$

and with slope $b = \frac{K_0}{s}(1 + \frac{i_1}{K_1} + \frac{i_2}{K_2} + \frac{i_1 i_2}{\alpha K_1 K_2})$.

8. Case II.: saturation with the partial inhibitor

$$\frac{1}{v_{12}^{/sat2/}} = \frac{1}{V_2}(1 + \frac{i_1}{\beta K_{01}}) + \frac{1}{s}.\frac{K_0 K_{02}}{V_2}.(\frac{1}{K_2} + \frac{i_1}{\alpha K_1 K_2})$$

This equation is analoguous to the expression of initial velocity in the presence of a pure inhibitor, therefore all methods, generally applied for the analysis of a pure inhibitor, can be used here.

In the plot of $1/v_{12}^{/sat2/}$ vs. $1/s$ the ordinate intercept is $a = \frac{1}{V_2}(1 + \frac{i_1}{\beta K_{01}})$, and the slope is $b = \frac{K_0 K_{02}}{V_2}(\frac{1}{K_2} + \frac{i_1}{\alpha K_1 K_2})$

The rate expression in function of i_1 is as follows:

$$\frac{1}{v_{12}^{/sat2/}} = \frac{1}{V_2}(1 + \frac{K_0}{s}.\frac{K_{02}}{K_2}) + i_1.\frac{1}{V_2}(\frac{1}{\beta K_{01}} + \frac{K_0}{s}.\frac{K_{02}}{\alpha K_1 K_2})$$

9. Case II.: without saturation

$$\frac{1}{i_1}(\frac{1}{v_{12}} - \frac{1}{v_1}) = \frac{\frac{1}{K_{01}}(1 + \frac{i_2}{\beta K_{02}}) + \frac{K_0}{s}.\frac{1}{K_1}(1 + \frac{i_2}{\alpha K_2})}{V_m + V_2.\frac{i_2}{K_{02}}} = a + b.\frac{1}{s}$$

$$a = \frac{1}{K_{01}}.\frac{1 + \frac{i_2}{\beta K_{02}}}{V_m + V_2.\frac{i_2}{K_{02}}} , \quad b = \frac{K_0}{K_1}.\frac{1 + \frac{i_2}{\alpha K_2}}{V_m + V_2.\frac{i_2}{K_{02}}} ,$$

$$a_0 = \frac{1}{V_m K_{01}} , \quad \frac{a}{a - a_0} = \frac{V_m K_{01} K_{02}}{V_2 - V_m/\beta}.(\frac{1}{i_2} + \frac{1}{\beta K_{02}}) ,$$

$$c = -a/b = \frac{-K_1}{K_0 K_{01}}.\frac{1 + \frac{i_2}{\beta K_{02}}}{1 + \frac{i_2}{\alpha K_2}} , \quad c_0 = -\frac{K_1}{K_0 K_{01}} ,$$

$$\frac{c}{c - c_0} = \frac{1}{\frac{1}{\alpha K_2} - \frac{1}{\beta K_{02}}}(\frac{1}{i_2} + \frac{1}{\beta K_{02}}) ,$$

$$\frac{1}{c - c_0} = -\frac{K_0 K_{01}}{K_1(\frac{1}{\beta K_{02}} - \frac{1}{\alpha K_2})}(\frac{1}{i_2} + \frac{1}{\alpha K_2}) .$$

10. Case III.

$$\frac{1}{v_{12}^{/sat2/}} = \frac{\frac{1}{K_{02}}(1 + \frac{i_1}{\beta K_{01}}) + \frac{1}{s}.\frac{K_0}{K_2}(1 + \frac{i_1}{\alpha K_1})}{\frac{1}{K_{02}}(V_2 + V_3.\frac{i_1}{\beta K_{01}})}$$

The same equation in other form:

$$\frac{1}{v_{12}^{/sat2/}} = \frac{\left(\frac{1}{K_{02}} + \frac{K_0}{s}\cdot\frac{1}{K_2}\right) + i_1\left(\frac{1}{\beta K_{01}K_{02}} + \frac{K_0}{s}\cdot\frac{1}{\alpha K_1 K_2}\right)}{\frac{V_2}{K_{02}} + i_1\cdot\frac{V_3}{\beta K_{01}K_{02}}}$$

$1/v_{12}^{/sat2/}$ vs. i_1 is a straight line, if $\frac{V_3}{\beta K_{01}K_{02}} = 0$. In this case the slope of $1/v_{12}^{/sat2/}$ vs. $1/s$ is $b = \frac{K_0K_{02}}{V_2K_2}\left(1 + \frac{i_1}{\alpha K_1}\right)$, and the ordinate intercept is $a = \frac{1}{V_2}\left(1 + \frac{i_1}{\beta K_{01}}\right)$.

If $V_3/\beta K_{01}K_{02} \neq 0$, then in the plot of $1/v_{12}^{/sat2/}$ against $1/s$ the abscissa intercept is

$$c = -\frac{K_2}{K_0K_{02}}\cdot\frac{1 + \frac{i_1}{\beta K_{01}}}{1 + \frac{i_1}{\alpha K_1}},$$

and the ordinate intercept is

$$a = \frac{1 + \frac{i_1}{\beta K_{01}}}{V_2 + V_3\cdot\frac{i_1}{\beta K_{01}}}.$$

Hence

$$\frac{1}{a - a_0} = \frac{V_2^2\cdot\beta K_{01}}{V_2 - V_3}\left(\frac{1}{i_1} + \frac{V_3}{V_2\beta K_{01}}\right),$$

$$\frac{a}{a - a_0} = \frac{V_2\cdot\beta K_{01}}{V_2 - V_3}\left(\frac{1}{i_1} + \frac{1}{\beta K_{01}}\right),$$

$$\frac{1}{c - c_0} = \frac{K_0K_{02}}{K_2\left(\frac{1}{\beta K_{01}} - \frac{1}{\alpha K_1}\right)}\cdot\left(\frac{1}{i_1} + \frac{1}{\alpha K_1}\right),$$

$$\frac{c}{c - c_0} = \frac{1}{\left(\frac{1}{\alpha K_1} - \frac{1}{\beta K_{01}}\right)}\left(\frac{1}{i_1} + \frac{1}{\beta K_{01}}\right).$$

REFERENCES

Atkinson, D.E. (1966). Ann. Rev. Biochem. 35, 85.

Berezin, I.V., Martinek, K. (1967). Teoret. Eksp. Khim.(Kiev) 3, 458.

Berezin, I.V., Vill', H., Martinek, K., Jazimirsky, A.K. (1967a). Mol. Biol. (Moscow) 1, 719.

Berezin, I.V., Vill', H., Martinek, K., Jazimirsky, A.K., Hludova, M.S. (1967b). Mol. Biol. (Moscow) 1, 843.

Fajszi, Cs., Keleti, T. (1975). In: Mathematical models of metabolic regulation, eds. S.Lakatos and T.Keleti (Akadémiai Kiadó, Budapest).

Frieden, C. (1964). J. Biol. Chem. 239, 3522.

Hunter, A., Downs, C.E. (1945). J. Biol. Chem. 157, 427.

Keleti, T., Fajszi, Cs. (1971). Math. Biosciences 12, 197.

Loewe, S. (1957). Pharmacol. Rev. 9, 237.

Mares-Guia, M., Shaw, E.J. (1965). J.Biol. Chem. 24o, 1579.

Reynolds, C.H., Morris, D.L., McKinley-McKee, J.S. (197o). Eur. J. Biochem. 14, 14.

Semenza, G., von Balthazar, A.-K. (1974). Eur. J. Biochem. 41, 149.

Silonova, G.V., Livanova, N.B., Kurganov, B.I. (1969). Mol. Biol. (Moscow) 3, 768.

Slater, E.C., Bonner, W.D.,Jr. (1952). Biochem. J. 52, 185.

Stadtman, E.R. (197o). In: The enzymes, ed. P.D.Boyer (Academic Press, New York, London) 3rd edition, vol. I.,p.397.

Webb, J.L. (1963). Enzyme and metabolic inhibitors (Academic Press, New York), vol. I.

Wermuth, B., Brodbeck, U. (1973). Eur. J. Biochem. 37, 377.

Yagi, K., Ozawa, T. (196o). Biochim. Biophys. Acta 42, 381.

Yonetani, T., Theorell, H. (1964). Arch. Biochem. Biophys. 1o6, 243.

Symp. Biol. Hung. 18, pp. 105–119 (1974)

KINETIC BASIS OF ENZYME REGULATION. THE TRIPLE-FACED ENZYME-INHIBITOR RELATION AND THE INHIBITION PARADOX.

Cs. Fajszi and T. Keleti

Institute of Biophysics, Biological Research Center of the Hungarian Academy of Sciences, Szeged and Enzymology Department, Institute of Biochemistry, Hungarian Academy of Sciences, Budapest, Hungary

In the past little attention was paid to the simultaneous action of more than one modifier. However, it is of special interest to study the effect of two or more modifiers on the same enzyme, since in the cell, where all or nearby all metabolites are present simultaneously this situation can prevail very often. In the most simple case the following possibilities arise: one inhibitor (or activator) and one liberator, or two inhibitors (or activators) interact on the same enzyme. In both cases we should consider the interaction of three metabolites (in the simplest case of a one-substrate reaction).

1) The liberator action.

First the liberator action should be considered. The liberator is a substance which may neutralize the action of the inhibitor (or activator), i.e. which liberates the enzyme from inhibition (or activation), (Keleti 1967). The liberator alone is supposed to have no effect on enzymatic activity (i.e. it is not an activator or inhibitor). A number of different liberators are already known: metabolites ordinarily present in the living organisms (e.g. amino acids, ATP, specific immunoglobulins, etc.).

The resulting effect of the interaction of these metabolites may be very different, as the inhibitor may be competitive, non-competitive or uncompetitive with the substrate and similarly the liberator may be competitive, non-competitive and uncompetitive with the inhibitor. Consequently their interaction may result in different effects depending

on the type of inhibition and liberation, on the mutual relation between the Michaelis and dissociation constants of substrate, inhibitor and liberator, on their relative concentrations and on the relative magnitude of maximum velocities in the presence and absence of inhibitor and/or liberator. Therefore the interaction of a substrate, an inhibitor and a liberator may result in either unaffected initial velocity or inhibition or activation.

Let us present as an example the case of non-competitive liberator and competitive inhibitor. One will have competitive inhibition if $K_S/K_S' \leq 1$, independent of the value of $[L]$, (where $K_S = [E][S]/[ES]$, $K_S' = [EIL][S]/[EILS]$, and E, S, I and L are the enzyme, substrate, inhibitor and liberator, respectively). However, if $K_S/K_S' > 1$, one will find competitive inhibition if $0 \leq [L] < [L']$, ($[L'] = K_S K_L'/(K_S - K_S')$, where $K_L' = [EI][L]/[EIL]$), competitive activation if $[L] > [L']$ or, if $[L] = [L']$, the initial velocity will be independent of $[I]$, (Fig. 1).

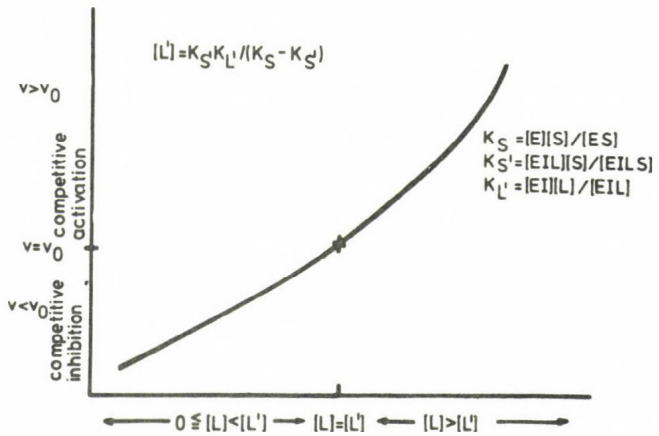

Fig. 1. The interaction of a non-competitive liberator and a competitive inhibitor on a one-substrate enzyme.
$K_S/K_S' > 1$.

2)The double inhibitions.

Similar peculiar effects can be obtained by analysing the different types of double inhibitions (Keleti and Fajszi 1971). Assuming that both inhibitors, independently of each other, can be purely or partially competitive or non-competitive or purely uncompetitive with the substrate, we will have 17 different types of interaction. The simultaneous presence of two inhibitors may result in the simple summation of the two individual inhibitions in only special cases. Ordinarily, the two inhibitors act either antagonistically or synergetically (Keleti and Fajszi 1971).

The two inhibitors act synergetically if $\underline{a}(1/v_o v_{12} - 1/v_1 v_2) = D > 0$, antagonistically if $D < 0$ and there is the special case of simple summation of their effect if $D=0$ (v_o, v_1, v_2 and v_{12} are the initial velocities in the absence of inhibitors, in the presence of the first, of the second and of both inhibitors, respectively and $\underline{a}$ is a positive term, cf. Appendix 1).

a)The triple-faced enzyme-inhibitor relation.

We will present here the case of triple-faced enzyme-inhibitor relation, which means that in a given enzyme-substrate-inhibitor system, depending on the substrate concentration, the interaction may change from $D > 0$, through $D=0$ to $D < 0$ ("D decreases") or vice versa ("D increases"). It is called characteristic substrate concentration $[S_o]$, where $D=0$ and below and above which $D \gtrless 0$.

As an example we present the case of two purely competitive inhibitors. If the interaction constant of the two inhibitors on the free enzyme $\alpha = \infty$ (cf. Appendix 2), i.e. the binding of one inhibitor excludes the binding of the other, we have $D < 0$, i.e. antagonism. If $0 < \alpha < 1$, i.e. the binding of one inhibitor facilitates the binding of the other or $\alpha = 1$, i.e. the binding of the two inhibitors is independent of each other, we will have $D > 0$, i.e. synergy. However, if $1 < \alpha < \infty$, i.e. the binding of one inhibitor hinders the binding of the other, we will have the case of the triple-faced enzyme-inhibitor relation, with the characteristic substrate concentration $[S_o] = K_o(\alpha - 1)$. Namely, in this case

if $[S] < K_0(\alpha - 1)$ then $D < 0$, if $[S] = K_0(\alpha - 1)$ then $D = 0$ and if $[S] > K_0(\alpha - 1)$ then $D > 0$, (Fig.2).

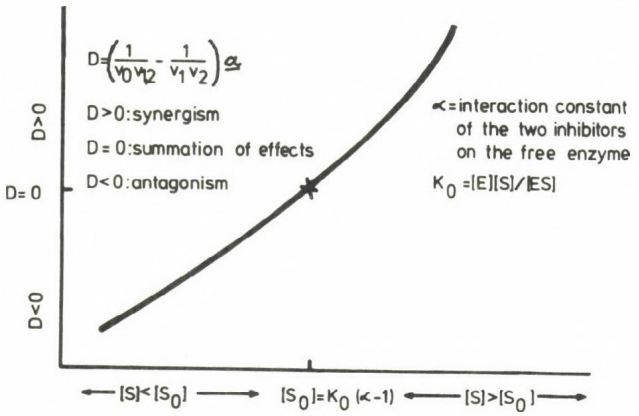

Fig.2. The triple-faced enzyme-inhibitor relation in the case of two purely competitive inhibitors.
$1 < \alpha < \infty$.

Table 1 presents the cases of triple-faced enzyme-inhibitor relations and the corresponding characteristic substrate concentrations.

b) Synergism and antagonism.

In general, the synergism or antagonism does not depend on the substrate concentration (or in the case of two partial inhibitors on their concentrations) but on the type of inhibition and the interaction constant. These cases are summarized in Table 2.

There are certain interactions of inhibitors which result in a v_{12} greater than v_1, i.e. the initial velocity in the presence of both inhibitors is greater than in the presence of only one inhibitor. This extreme of the antagonism between the two inhibitors may occur only if at least one of the inhibitors is partial inhibitor and also depends on the characteristic substrate concentration and the characteristic inhibitor concentration $[I_{1(o)}]$, (Table 3).

Table 1

Some cases of the triple-faced enzyme-inhibitor relations

Inhibition type* of I_1	of I_2	Necessary conditions	$[S_o]$	D
C	C	$1<\alpha<\infty$	$K_o(\alpha-1)$	Incr.
C	U**	$K_{12}>K_{o2}$	$K_oK_{o2}/(K_{12}-K_{o2})$	Decr.
NC	NC	$\alpha<1, \beta>1$	$K_o(1/\alpha-1)/(1-1/\beta)$	Decr.
		$\alpha>1, \beta<1$	$K_o(1/\alpha-1)/(1-1/\beta)$	Incr.
U	U	$1<\beta<\infty$	$K_o/(\beta-1)$	Decr.
C	pC	$1<\alpha<\infty, K_{o2}/K_2>\alpha$	$K_o(\alpha-1)K_2K_{o2}/(K_{o2}-\alpha K_2)$	Incr.
NC	pC	$0<\alpha<1, 1<\beta\leq\infty$	$K_oK_{o2}(1-1/\alpha)/K_2(1/\beta-1)$	Decr.
		$1<\alpha\leq\infty, 0<\beta<1$	as above	Incr.
NC	pNC	$\alpha<1, \beta>1$	$K_o(1/\alpha-1)/(1-1/\beta)$	Decr.
		$\alpha>1, \beta<1$	as above	Incr.
U	pC	$0<\beta<1, K_2/K_{o2}<\beta$	$K_oK_{o2}(1/\beta K_{o2}-1/K_2)/(1-1/\beta)$	Incr.
U	pC**	$\beta=1, 1/K_{21}<(1/K_{o1})(1-K_2/K_{o2})$	$K_o/[(K_{21}/K_{o1})(1-K_2/K_{o2})-1]$	Decr.

The table contains only some selected examples of the possible triple-faced enzyme-inhibitor relations, where the expression of $[S_o]$ is relatively simple.

*Inhibition types: C=purely competitive, NC=purely non-competitive, U=purely uncompetitive, pC=partially competitive, pNC=partially non-competitive. Pure inhibition means that the complexes containing the inhibitor are completely inactive, in partial inhibitions the complexes containing the inhibitor are less active than the enzyme-substrate complex without inhibitor (Dixon and Webb 1964, Keleti and Telegdi 1966).

**Special case, cf. Keleti and Fajszi (1971).

Table 2

Some cases of synergism or antagonism in double inhibitions

Inhibition type of I_1	I_2	Necessary conditions	Interaction
C	C	$\alpha = \infty$	$D < 0$
		$0 < \alpha \leqq 1$	$D > 0$
NC	NC	$0 < \alpha < 1, 0 < \beta < 1$ or $0 < \alpha < 1, \beta = 1$	
		or $\alpha = 1, 0 < \beta < 1$	$D > 0$
		$\alpha = 1, \beta = 1$	$D = 0$
		$\infty > \alpha > 1, 0 > \beta > 1$ or $\infty > \alpha > 1, \beta = 1$	
		or $\alpha = 1, \infty > \beta > 1$	$D < 0$
C	NC	$0 < \alpha < 1$	$D > 0$
		$\alpha = 1$	$D = 0$
		$\infty \geqq \alpha > 1$	$D < 0$
C	U	in all cases	$D < 0$
C	U*	$K_{12} \leqq K_{o2}$	$D > 0$
U	NC	$0 < \beta < 1$	$D > 0$
		$\beta = 1$	$D = 0$
		$1 < \beta \leqq \infty$	$D < 0$
U	U	$0 < \beta \leqq 1$	$D > 0$
		$\beta = \infty$	$D < 0$
C	pC	$1 < \alpha \leqq \infty, K_{o2}/K_2 \leqq \alpha$	$D < 0$
		$0 < \alpha \leqq 1, K_{o2}/K_2 > \alpha$	$D > 0$
C	pNC	$0 < \alpha < 1$	$D > 0$
		$\alpha = 1$	$D = 0$
		$\infty \geqq \alpha > 1$	$D < 0$
NC	pC	$0 < \alpha < 1, 0 < \beta \leqq 1$ or $\alpha = 1, 0 < \beta < 1$	$D > 0$
		$\alpha = 1, \beta = 1$	$D = 0$
		$1 < \alpha \leqq \infty, 1 \leqq \beta \leqq \infty$ or $\alpha = 1, 1 < \beta \leqq \infty$	$D < 0$
NC	pNC	$0 < \alpha < 1, 0 < \beta < 1$ or $0 < \alpha < 1, \beta = 1$	
		or $\alpha = 1, 0 < \beta < 1$	$D > 0$
		$\alpha = 1, \beta = 1$	$D = 0$
		$\infty > \alpha > 1, \infty > \beta > 1$ or $\infty > \alpha > 1, \beta = 1$	
		or $\alpha = 1, \infty > \beta > 1$	$D < 0$
U	pC	$1 \leqq \beta \leqq \infty, K_2/K_{o2} \leqq \beta$	$D < 0$
		$0 < \beta < 1, K_2/K_{o2} \geqq \beta$	$D > 0$

Table 2 (continued)

Inhibition type of I_1	Inhibition type of I_2	Necessary conditions	Interaction
U	pC*	$\beta=1, 1/K_{o1}K_{o2}+(1/K_2)(1/K_{21}-1/K_{o1})\geqq 0$ or $0<\beta<1, \beta\leqq K_2/K_{o2}$ or $K_{21}\leqq K_{o1}$ or $\beta\leqq K_2K_{21}/K_{o2}(K_{21}-K_{o1})$	$D>0$
U	pNC	$0<\beta<1$	$D>0$
		$\beta=1$	$D=0$
		$1<\beta\leqq\infty$	$D<0$
pC	pC	$\alpha=\beta=\infty$	$D<0$
		$\alpha=\beta=1$	$D>0$
pC	pNC	$\alpha=\beta=\infty$ or $\alpha=\beta=1, V_2<V_3$	$D<0$
		$\alpha=\beta=1, V_2=V_3$	$D=0$
		$\alpha=\beta=1, V_2>V_3$	$D>0$
pNC	pNC	$\alpha=\beta=\infty$ or $1<\alpha=\beta<\infty, V_1V_2\leqq(1/\alpha)V_mV_3$	$D<0$
		$\alpha=\beta=1$	the sign of D equals that of $V_1V_2-V_3V_m$
		$0<\alpha=\beta<1, V_1V_2\geqq(1/\alpha)V_mV_3$ or $\alpha=\beta=1, V_1V_2>V_mV_3$	$D<0$
		$\alpha=\beta=1, V_1V_2=V_mV_3$	$D=0$

The table contains only some selected examples.
Inhibition types, see Table 1.
$D>0$ means synergy, $D<0$ antagonism and $D=0$ that the effect of the two inhibitors is the simple sum of the effect of the inhibitors added separately.

*Special case, cf. Keleti and Fajszi (1971).

Table 3

Cases of double inhibitions where $v_{12} \geq v_1$.

Inhibition type of I_1	I_2	case	Necessary conditions		
C	pC	a	$\alpha > K_{o2}/K_2$	$[I_1] > [I_{1(o)}]$	independent of $[S]$
NC	pC		$\alpha \geqq K_{o2}/K_2, 1 < \beta \leqq \infty$ or $\alpha > K_{o2}/K_2$,		
		b	$0 < \beta < 1$	$[I_1] > [I_{1(o)}]$	$[S] < [S_o]$
		c	$\beta = 1, \alpha > K_{o2}/K_2$	$[I_1] > [I_{1(o)}]$	independent of $[S]$
		d	$\alpha < K_{o2}/K_2, 1 < \beta \leqq \infty$	$[I_1] > [I_{1(o)}]$	$[S] > [S_o]$
U	pC	e	$1 < \beta \leqq \infty$	$[I_1] > [I_{1(o)}]$	independent of $[S]$
U	pC*	f	$1 < \beta \leqq \infty$	independent of $[I]$	$[S] > [S_o]$
C	pNC	g	$\alpha > V_m/V_2$	$[I_1] > [I_{1(o)}]$	independent of $[S]$
NC	pNC	h	$\beta \leqq V_m/V_2, \alpha > V_m/V_2$	$[I_1] > [I_{1(o)}]$	$[S] < [S_o]$
		i	$\beta > V_m/V_2, \alpha \leqq V_m/V_2$	$[I_1] > [I_{1(o)}]$	$[S] > [S_o]$
		j	$\beta > V_m/V_2, \alpha > V_m/V_2$	$[I_1] > [I_{1(o)}]$	independent of $[S]$
U	pNC	k	$\beta > V_m/V_2$	$[I_1] > [I_{1(o)}]$	independent of $[S]$
pNC	pNC	l	$\alpha = \beta = \infty, V_2 > V_1$	$[I_1] > [I_{1(o)}]$	independent of $[S]$

Inhibition types, see Table 1.

The characteristic concentrations of the inhibitor and the substrate, see Table 3 (continued).

The cases summarized in Table 4 of course are also the members of this table.

*Special case, cf. Keleti and Fajszi (1971).

Table 3 (continued)

case	$[I_{1(o)}]$	$[S_o]$
a	$K_1(K_{o2}/K_2-1)/(1-K_{o2}/\alpha K_2)$	
b	$K_1(K_o/[S])(K_{o2}/K_2-1)/[(K_o/[S])(1-K_{o2}/\alpha K_2)-(1/\beta-1)]$	$K_o(1-K_{o2}/\alpha K_2)/(1/\beta-1)$
c	$K_1(K_{o2}/K_2-1)/(1-K_{o2}/\alpha K_2)$	
d	$K_1(K_o/[S])(K_{o2}/K_2-1)/[(K_o/[S])(1-K_{o2}/\alpha K_2)-(1/\beta-1)]$	$K_o(1-K_{o2}/\alpha K_2)/(1/\beta-1)$
e	$K_oK_{o1}(K_{o2}/K_2-1)/[S](1-1/\beta)$	
f		$K_oK_{o1}(K_{o2}/K_2-1)(1/[I_1])+K_{o2}/K_2K_{21}/(1-1/\beta)$
g	$K_1(1+[S]/K_o)[(V_m-V_2)/(V_2-V_m/\alpha)]$	
h,i	$K_1(V_m-V_2)(1+K_o/[S])/[(V_2-V_m/\beta)+(V_2-V_m/\alpha)(K_o/[S])]$	$K_o(V_2-V_m/\alpha)/(V_m/\beta-V_2)$
j	$K_1(V_m-V_2)(1+K_o/[S])/[(V_2-V_m/\beta)+(V_2-V_m/\alpha)(K_o/[S])]$	
k	$K_{o1}(1+K_o/[S])(V_m-V_2)/(V_2-V_m/\beta)$	
l	$K_1(V_m-V_2)/(V_2-V_1)$	

c) The inhibition paradox.

The most interesting case of the possible interactions of two inhibitors is the inhibition paradox when the initial velocity in the presence of two inhibitors is higher than without any inhibitor ($v_{12} > v_o$). The inhibition paradox means that the interaction of two inhibitors results in activation. This effect also depends on the characteristic substrate and inhibitor concentrations and can be found in the cases of two partial inhibitors. Fig.3 presents the inhibition paradox in a special case of two partially competitive inhibitors when $[I_{1(o)}]$ and $[I_{2(o)}]$ are independent of $[S]$, and in the case of two partially non-competitive inhibitors when both $[I_{1(o)}]$ and $[I_{2(o)}]$ are functions of $[S]$.

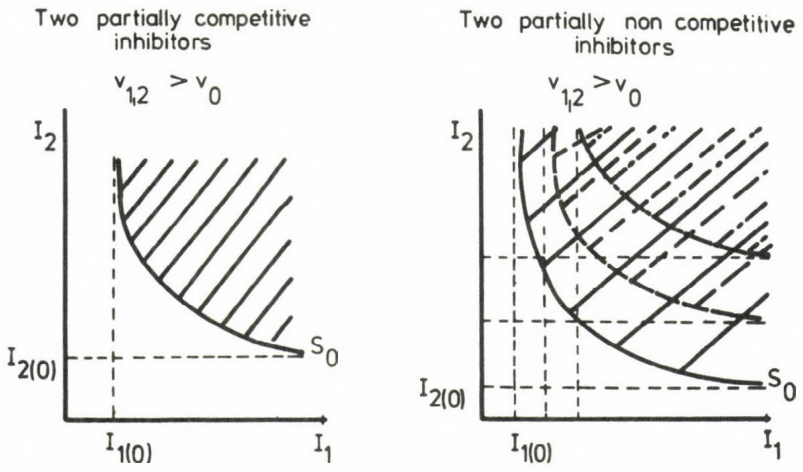

Fig.3. The inhibition paradox in some special cases of two partially competitive or non-competitive inhibitors.
The hatched area represents that concentration range of I_1, I_2 and S where the inhibition paradox appears.

Table 4 summarizes the cases of inhibition paradox and the corresponding characteristic substrate and inhibitor concentrations.

In the case of two partially competitive inhibitors the necessary condition $\alpha/\beta > K_{o1}K_{o2}/K_1K_2$ is equivalent with $K_o > K_{12o}$, i.e. the dissociation constant of the ES complex is higher than the dissociation constant of S from the quaternary complex EI_1I_2S. One can assume that, probably due to steric changes caused in the enzyme by the binding of I_1 and I_2, the EI_1I_2 complex is more able to bind S, than the free enzyme. The characteristic inhibitor concentrations are independent of the substrate concentration.

In the case of one partially competitive, one partially non-competitive inhibitor there are 5 different possibilities:

1. $V_3=V_m$, $1/\beta K_{o1} > 1/\alpha K_1$. Since $K_o=K_{2o}$, the latter condition means that $K_o > K_{12o}$. The dissociation constant of ES complex equals that of S from the EI_2S complex.

Table 4

Some cases of double inhibitions where $v_{12} \geq v_o$.-

Inhibition type of I_1	I_2	case	necessary conditions
pC	pC	a	$\alpha/\beta > K_{o1}K_{o2}/K_1K_2$
pNC	pNC	b	$\beta/\alpha < V_3/V_m, V_3 < V_m, \beta/\alpha = K_{12o}/K_o, [S] < [S_o]$
pC	pNC	c	$V_3 < V_m, \beta < \infty, V_3/V_m > \beta K_{o1}/\alpha K_1 = K_{12o}/K_{2o}$

Inhibition types, see Table 1.

The characteristic concentrations of the inhibitors and the substrate, see Table 4 (continued).

Table 4 (continued)

case	$[I_{1(o)}]$	$[I_{2(o)}]$	$[S_o]$
a	$(1/K_1-1/K_{o1})/(1/\beta K_{o1}K_{o2}-1/\alpha K_1K_2)$	$(1/K_2-1/K_{o2})/(1/\beta K_{o1}K_{o2}-1/\alpha K_1K_2)$	
b	$(V_m-V_2)[([S]+K_o)/[S]]/(1/K_1)[(1/\beta)(V_3-V_m)+(K_o/[S])(V_3/\beta-V_m/\alpha)]$	$(V_m-V_1)[([S]+K_o)/[S]]/(1/K_2)[(1/\beta)(V_3-V_m)+(K_o/[S])(V_3/\beta-V_m/\alpha)]$	$K_o(V_m\beta/\alpha-V_3)/(V_3-V_m)$
c	$\beta K_{o1}(V_m-V_2)(1+K_o/[S])/[(K_o/[S])(V_3-V_m\beta K_{o1}/\alpha K_1)-(V_m-V_3)]$	$V_m(K_o/[S])\cdot\beta K_2K_{o1}(1/K_1-1/K_{o1})/[(K_o/[S])\cdot(V_3-V_m\beta K_{o1}/\alpha K_1)-(V_m-V_3)]$	$K_o(V_m\beta K_{o1}/\alpha K_1-V_3)/V_3-V_m)$

The characteristic I_1 concentration depends on $[S]$, however, $[I_{2(o)}]$ is independent of $[S]$.

2. $V_3 > V_m, \beta < \infty. \alpha/\beta = V_mK_{o1}/V_3K_1$, i.e. $K_o = K_{2o} < K_{12o}$, the dissociation constant of S from the complex EI_1I_2S is higher than that of S from EI_2S, but the simulta-

neous binding of I_1 and I_2 causes such a change in the active center of the enzyme that the complex containing the inhibitors catalyzes the transformation of the substrate at a higher rate than the free enzyme. Both characteristic inhibitor concentrations are the function of the substrate concentration.

3. $V_3 > V_m$, $\beta < \infty$, $\alpha/\beta < V_m K_{01}/V_3 K_1$, i.e. $K_{12o} > K_o(V_3/V_m) > K_o$. This case is similar to that of 2. However, the inhibition paradox manifests itself only if $[S] > [S_o]$.

4. $V_3 > V_m$, $\beta < \infty$, $K_{12o}/K_o < V_3/V_m$. This case is similar to 2. However, the characteristic concentration of I_1 has a minimum and a maximum value if $[S] \rightarrow 0$, or $[S] \rightarrow \infty$, respectively and these values depend on the ratio of βK_{01} and αK_1. The characteristic value of I_2 has a maximum value if $[S] \rightarrow 0$, and declines to zero as $[S] \rightarrow \infty$.

5. $V_3 < V_m$, $\beta < \infty$, $K_{12o}/K_o < V_3/V_m$. This case is similar to 3, however, should be $[S] < [S_o]$.

Consequently, if we have one partially competitive and one partially non-competitive inhibitor, if $V_3 > V_m$, we have always such $[I_{1(o)}]$ and $[I_{2(o)}]$, where $v_{12} > v_o$. If $V_3 \leqq V_m$, to have $v_{12} > v_o$ should be $\beta K_{01}/\alpha K_1 = K_{12o}/K_{2o} = K_{12o}/K_o < V_3/V_m \leqq 1$.

In the case of two partial non-competitive inhibitors we have the same 5 possibilities, with similar consequences.

These considerations suggest that the special problems of the "three-body system" should be taken into consideration in enzyme-catalyzed reactions when *in vivo* modulations of metabolic pathways are investigated. Namely, as presented above the simultaneous action of three ligands on one enzyme may result in unexpected effects. These effects may change in the function of the concentrations of the ligands and the liberation or inhibition may turn into activation. These effects may have role in the kinetic mechanism of enzyme regulation.

One of the most effective regulatory mechanisms of metabolic pathways is the oscillation of the concentrations of the metabolites. Assuming a linear chain of at least three enzymes, where the substrate of the first enzyme

is an inhibitor or liberator and the product of the third enzyme is the inhibitor of the second one, we can obtain oscillations in the case of liberator action or if the conditions of inhibition paradox prevail. In the case of triple-faced enzyme-inhibitor relation, however, one may have only damped oscillation.

References

Dixon, M., Webb, E. L. (1964) Enzymes. Longmans, Green and Co. London

Keleti, T. (1967) J. Theor. Biol. 16 337-355

Keleti, T., Fajszi, Cs. (1971) Math. Biosci. 12 197-215

Keleti, T., Telegdi, M. (1966) Enzymologia 31 39-50

Appendix 1

Initial velocity in reciprocal form:

$$1/v_o = K_s/V[S] + 1/V$$

where $K_s = [E][S]/[ES]$, V=maximum velocity.

Purely competitive inhibition:

$$1/v_i = (K_s/V[S])(1+[I]/K_I) + 1/V$$

where $K_I = [E][I]/[EI]$.

Partially competitive inhibition:

$$1/v_i = (K_s/V[S])\left[K'_I/([I]+K'_I)\right] + (K'_s/V[S])\left[[I]/(K'_I+[I])\right] + 1/V$$

where $K'_I = [ES][I]/[EIS]$, $K'_s = [EI][S]/[EIS]$.

Purely non-competitive inhibition:

$$1/v_i = (K_s/V[S])(1+[I]/K_I) + (1/V)(1+[I]/K_I)$$

Partially non-competitive inhibition:

$$1/v_i = \left[(K_I+[I])/(V'K_I+V''[I])\right]\left[1+K_s/[S]\right]$$

where V' is the maximum velocity of the breakdown of ES complex, V" that of ESI complex.

Purely uncompetitive inhibition:

$$1/v_i = K_s/V[S] + (1/V)(1+[I]/K'_I)$$

Double inhibition with two pure inhibitors:

$$1/v_{12} = (1/V_m)(1+[I_1]/K_{o1}+[I_2]/K_{o2}+[I_1][I_2]/\beta K_{o1}K_{o2}) + (K_o/V_m[S])(1+[I_1]/K_1+[I_2]/K_2+[I_1][I_2]/\alpha K_1K_2)$$

Double inhibition with one pure and one partial inhibitor:

$$1/v_{12} = \left[1+[I_1]/K_{o1}+[I_2]/K_{o2}+[I_1][I_2]/\beta K_{o1}K_{o2}+(K_o/[S])(1+[I_1]/K_1+[I_2]/K_2+[I_1][I_2]/\alpha K_1K_2)\right]/(V_m+V_2[I_2]/K_{o2})$$

Double inhibition with two partial inhibitors:

$$1/v_{12}=\left[1+[I_1]/K_{o1}+[I_2]/K_{o2}+[I_1][I_2]/\beta K_{o1}K_{o2}+(K_o/[S])(1+\right.$$
$$\left.+[I_1]/K_1+[I_2]/K_2+[I_1][I_2]/\alpha K_1K_2)\right]/(V_m+V_1[I_1]/K_{o1}+$$
$$+V_2[I_2]/K_{o2}+V_3[I_1][I_2]/\beta K_{o1}K_{o2})$$

The meaning of the constants in the double inhibitions, see Appendix 2.

$$1/v_ov_{12}-1/v_1v_2=d$$

where v_1 and v_2 are the v_i-s of purely or partially competitive or non-competitive or uncompetitive inhibitions and v_{12} is the double inhibition either with two pure or partial or with one pure and one partial inhibitors. In these latter cases $K_s=K_o$, $K_I=K_1$ or K_2, $K'_I=K_{o1}$ or K_{o2}, $K'_s=K_{1o}$ or K_{2o}, $V=V'=V_m$, $V''=V_1$ or V_2.

Since, in the case of two pure inhibitors the factor $\underline{a}=[I_1][I_2]/V_m^2$ is always positive, we analyze the sign of $dV_m^2/[I_1][I_2]=D$. In the case of one or two partial inhibitors the meaning of $\underline{a}$ is a complex expression, but always positive.

D, the parameter of interaction between the ligands, indicates the synergy or antagonism between the inhibitors. $D>0$ means synergy, $D<0$ antagonism and $D=0$ a simple addition of the effects of the two inhibitors as determined separately.

Appendix 2

$K_o=[E][S]/[ES]$ $K_1=[E][I_1]/[EI_1]$

$K_2=[E][I_2]/[EI_2]$ $K_{o1}=[ES][I_1]/[ESI_1]$

$K_{o2}=[ES][I_2]/[ESI_2]$ $K_{1o}=[EI_1][S]/[ESI_1]$

$K_{2o}=[EI_2][S]/[ESI_2]$ $K_{12}=[EI_1][I_2]/[EI_1I_2]$

$K_{21}=[EI_2][I_1]/[EI_1I_2]$ $K_{o12}=[ESI_1][I_2]/[ESI_1I_2]$

$K_{o21}=[ESI_2][I_1]/[ESI_1I_2]$ $K_{12o}=[EI_1I_2][S]/[ESI_1I_2]$

V_m=maximum velocity of the breakdown of the complex ES

V_1=maximum velocity of the breakdown of the complex ESI_1

V_2=maximum velocity of the breakdown of the complex ESI_2

V_3=maximum velocity of the breakdown of the complex ESI_1I_2

$\alpha=K_{12}/K_2=K_{21}/K_1$=intercation constant of the two inhibitors on E

$\beta=K_{o12}/K_{o2}=K_{o21}/K_{o1}$=interaction constant of the two inhibitors on ES complex.

$\alpha = 1$ or $\beta = 1$ means that the binding of I_1 is independent of I_2.

$\alpha = \infty$ or $\beta = \infty$ means that the binding of I_1 excludes that of I_2.

$1 < \alpha < \infty$ or $1 < \beta < \infty$ means that the binding of I_1 hinders that of I_2.

$0 < \alpha < 1$ or $0 < \beta < 1$ means that the binding of I_1 facilitates that of I_2.

II. MODELLING OF METABOLIC PATHWAYS

Symp. Biol. Hung. 18, pp. 123–142 (1974)

REGULATION OF KEY ENZYMES: STRATEGY IN REPROGRAMMING OF GENE EXPRESSION

GEORGE WEBER, NOEMI PRAJDA and JIM C. WILLIAMS

Laboratory for Experimental Oncology and Department of Pharmacology
Indiana University School of Medicine, Indianapolis, Indiana, USA 46202

INTRODUCTION

The biochemical strategy of gene expression is manifested, in a large part at least, in the regulation of the activity, amount and isozyme pattern of key enzymes. The concept of regulation of the rate and direction of metabolism through control of key enzymes was developed in this Laboratory in studying hormonal regulation and the clinical and biochemical syndromes in metabolic diseases (Weber, 1959, 1963; Weber et al., 1965, 1966, 1971). The experimental evidence obtained in this Laboratory supported the concept that the biochemical pattern in endocrine and nutritional regulation of metabolism could be understood in the control of opposing and competing key enzymes in antagonistic and competing synthetic and degradative pathways. The principles learned in these investigations were also applied to studies on the sequential unfolding of the pattern of gene expression that occurs in regeneration and in neoplasia (for review see Weber, 1974).

Previous studies pointed out the operational advantage of this concept that proposed a pattern of behavior and control mechanisms for the various key enzymes, the operation of which was readily subject to experimental testing. Thus, this concept provided a set of predictions for the anticipated antagonistic behavioral pattern of key enzymes in physiological and pathological conditions, such as in hormonal regulation (steroid and insulin action, in diabetes, etc.), in metabolic diseases (Glycogen Storage Disease), in differentiation and in neoplasia. A useful insight yielded by this approach proved to be the experience that from determining a single pair of such antagonistic enzymes, e.g., phosphofructokinase/fructose-1,6-diphosphatase, one was able to predict the behavior of other antagonistic pairs of key enzymes in carbohydrate metabolism (glucose-6-phosphatase/glucokinase, pyruvate carboxylase/pyruvate kinase) under various conditions entailing alterations in homeostatic balance. The experimental and conceptual studies led to the formulation of the general theory of the molecular correlation concept which was first tested in examining the behavior of carbohydrate metabolism under various conditions involving reprogramming of gene expression (Weber, 1973). The special theory of the molecular correlation concept refers to studies on the alterations of gene expression in neoplasia (Weber, 1974). Detailed investigations carried out in this Laboratory demonstrated that the regulation of the rate and direction of opposing pathways of synthesis and degradation through control of antagonistic key enzymes was applicable not only to carbohydrate but also to

Table 1

Pleiotropic action of insulin on hepatic enzymes of different metabolic pathways

FUNCTIONS INCREASED	ENZYMES INDUCED
Glycogenesis	Glycogen synthetase
Glycolysis	Glucokinase (high K_m isozyme) Phosphofructokinase Pyruvate kinase (high K_m isozyme)
Lipogenesis	Citrate cleavage enzyme Acetyl CoA carboxylase Fatty acid synthetase
NADPH production	Glucose-6-phosphate dehydrogenase 6-Phosphogluconate dehydrogenase Malate enzyme
Pentose phosphate pathway	Transaldolase Transketolase
Thymidine incorporation into DNA	DNA polymerase
Thymidine degradation to CO_2	Thymidine phosphorylase
FUNCTIONS DECREASED	**ENZYMES SUPPRESSED**
Gluconeogenesis	Glucose-6-phosphatase Fructose-1,6-diphosphatase Phosphoenolpyruvate carboxykinase Pyruvate carboxylase
Urea cycle	Ornithine carbamyltransferase Arginine synthetase Argininosuccinase

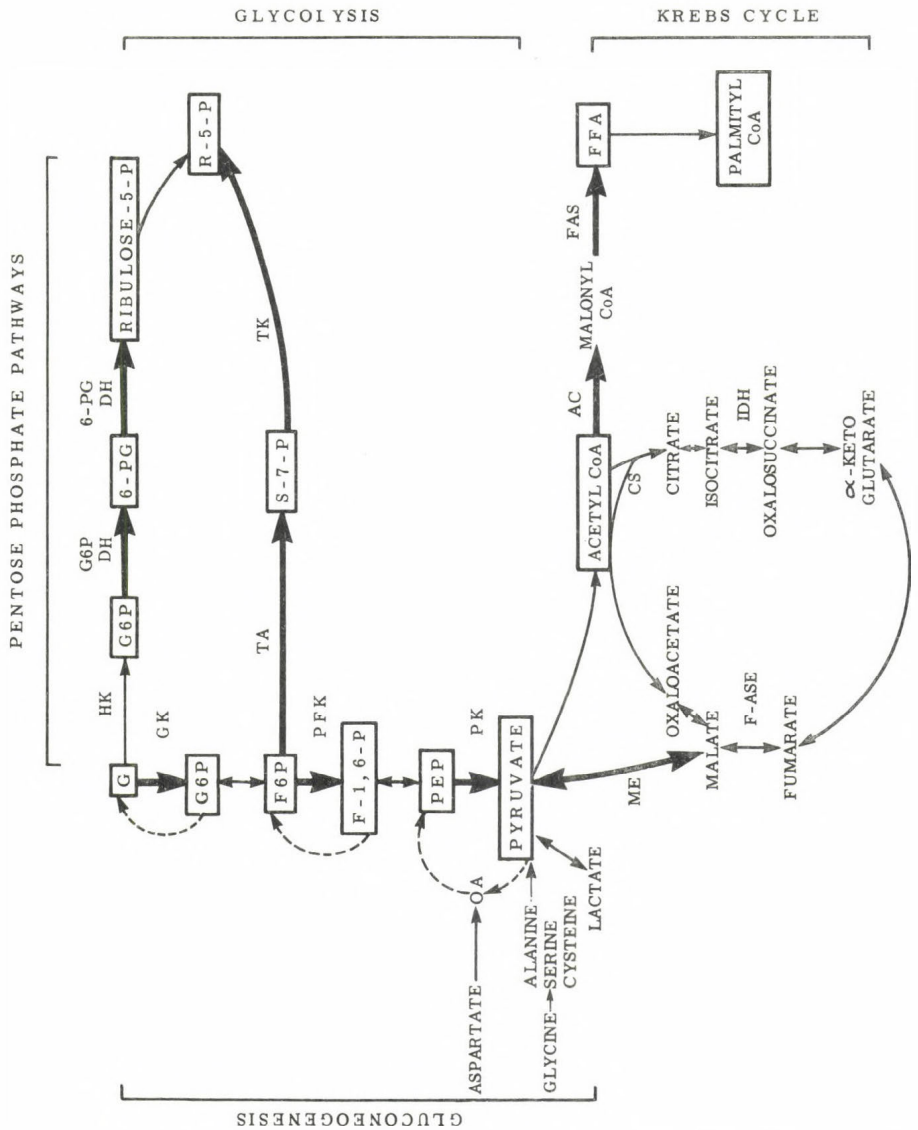

Fig. 1. Insulin: integrative action at the hepatic enzyme level.

GK=Glucokinase, PFK=Phosphofructokinase, PK=Pyruvate kinase, HK=Hexokinase, G6P DH=Glucose-6-phosphate dehydrogenase, 6-PG DH=6-Phosphogluconate dehydrogenase, IDH=Isocitrate dehydrogenase, F-ASE=Fumarase, ME=Malic enzyme, AC=Acetyl CoA carboxylase, CS=Citrate synthase, TA=Transaldolase, TK=Transketolase.

pyrimidine, DNA, ornithine, and membrane cAMP metabolism (Weber et al., 1971, 1972, 1973, 1974; Ferdinandus et al., 1971; Williams-Ashman et al., 1972).

The purpose of this presentation is to examine in more detail the key enzyme concept, the selective advantages and economy the key enzymes provide for the organism and the applicability of these principles to purine metabolism and the utilization of UDP.

MATERIALS AND METHODS

The conceptual significance of the role of key enzymes in the regulation of metabolism and in the control of gene expression was outlined elsewhere (Weber, 1973). The description of the strains and conditions of animals used, the type of tumor and the partial hepatectomy and the preparation of extract for enzyme assays were cited elsewhere (Weber, 1974). The methods for the assays of the various key enzymes and overall metabolic pathways were given previously (Weber, 1974; Weber et al., 1965, 1966, 1971). The discussion of the experimental procedures, the tumor work and the expression and evaluation of the enzymatic data are provided elsewhere (Weber, 1974).

RESULTS AND DISCUSSION

Pleiotropic Action of Insulin on Hepatic Key Enzymes

It was discovered earlier in this Laboratory that the integrative action of insulin at the molecular level in the liver entailed an antagonistic action on the biosynthesis of groups of key enzymes opposing each other in gluconeogenesis and in glycolysis. Subsequent work pointed out that the hepatic action of insulin involved reprogramming of gene expression and evidence was provided that this process included a shift in the isozyme pattern of the key glycolytic enzymes (for review see Weber, 1975). Recently, we obtained extensive evidence by measuring the activity and the immunoprecipitable isozyme concentration of PFK that the concentration of this enzyme was decreased in low insulin states (starvation, diabetes) and high insulin states (refeeding, insulin administration) restored the concentration of PFK to normal level (Dunaway & Weber, 1974, 1974a; Weber, 1975a). The determination of PFK concentration by two independent methods strongly supported the conceptual view we proposed for the integrative action of insulin at the molecular level. Further investigations in this Laboratory and in other Centers revealed that there are also characteristic alterations in enzyme activity of the pentose phosphate pathway, glycogenesis, thymidine metabolism and the urea cycle that occur in diabetes and insulin returns the activities to normal range. Table 1 and Figure 1 summarize the array of enzymes induced and those suppressed by insulin action.

It was proposed elsewhere that the reprogramming of gene expression occurring as a result of insulin administration that restores enzyme activities to normal range might operate through determining the expression of master genes capable of exerting pleiotropic action on groups of functionally related key enzymes operating in different metabolic pathways (Weber et al., 1974). There are other levels of controls where pleiotropic regulation might be achieved and these alternative possibilities were discussed in a recent paper by Weber et al. (1974). The term pleiotropy, as it refers to reprogramming in gene expression through hormonal influences or in

neoplasia, was also discussed in the same article. The importance of the multienzyme alterations is relevant for the present discussion which deals with the biochemical strategy of the cell as it is expressed through regulation of key enzymes.

Through the operation of hormonal influences, adaptation in a mammalian system has reached the highly advanced integrated state that provides selective advantages for the system. When experimentally or clinically endocrine alterations occur such as in diabetes, marked quantitative and qualitative shifts take place in the ratios of key enzymes in different pathways. Administration of the hormone that was in short supply, e.g., insulin, is capable of restoring the homeostatic balance to normal range. Thus, the reprogramming of gene expression in endocrine alterations has a reversible nature and the alterations themselves appear to be not heritable. The situation is entirely different in neoplasia where the alterations in gene expression that occur appear to be irreversible and heritable. In the following we will examine the behavior of key enzymes in two areas that we have been studying recently: purine and pyrimidine metabolism.

Regulation of Purine Metabolism: Control of Glutamine PRPP Amidotransferase Activity

The opposing pathways of synthesis and degradation of IMP are shown in Figure 2. In this Figure we emphasize that the origin of the de novo synthesis of IMP starts at the product of the pentose phosphate pathways, ribose-5-phosphate. Previous work from this Laboratory emphasized this strategic link between carbohydrate and purine metabolism accomplished by PRPP synthetase that converts ribose-5-phosphate into PRPP (Weber et al., 1974). These studies resulted in the discovery that PRPP synthetase was increased in the rapidly growing tumors (Heinrich et al., 1974); thus, the reaction involved in the de novo synthesis of PRPP was increased, leading to a heightened potential for IMP production. With the discovery of the increased PRPP synthetase activity it became of immediate interest to elucidate the behavior of the enzyme that utilizes PRPP into the de novo purine biosynthesis: glutamine PRPP amidotransferase, amidophosphoribosyltransferase, EC 2.4.2.14, (amidotransferase).

The comparison of the kinetic behavior of the liver and hepatoma amidotransferase and the development of an assay system applicable to kinetic conditions of rat liver and hepatomas was published recently from this Laboratory (Katunuma and Weber, 1974; Weber et al., 1975). An analysis of the molecular properties of amidotransferase from normal rat liver and from rapidly growing hepatomas is of interest in evaluating the role of this key enzyme in metabolic regulation.

Figure 3 indicates that the affinity of the normal liver amidotransferase to PRPP yields a sigmoid curve, whereas the hepatoma enzyme exhibits Michaelis-Menten kinetics. These results indicate that the liver enzyme had very low activity at a PRPP concentration of less than 1 mM, but in the same substrate range the hepatoma amidotransferase activity was high. Thus, the tumor enzyme was more readily saturated by PRPP at the low level that may occur in the tissues (Weber et al., 1975; Prajda et al., 1975).

The biological significance to the neoplastic transformation is also determined by the responsiveness of the tumor enzyme to physiological regulatory signals. Earlier work by Katunuma and Weber showed that the amidotransferase in the rapidly growing hepatoma was much less sensitive to the action of the physiological inhibitor, AMP (1974).

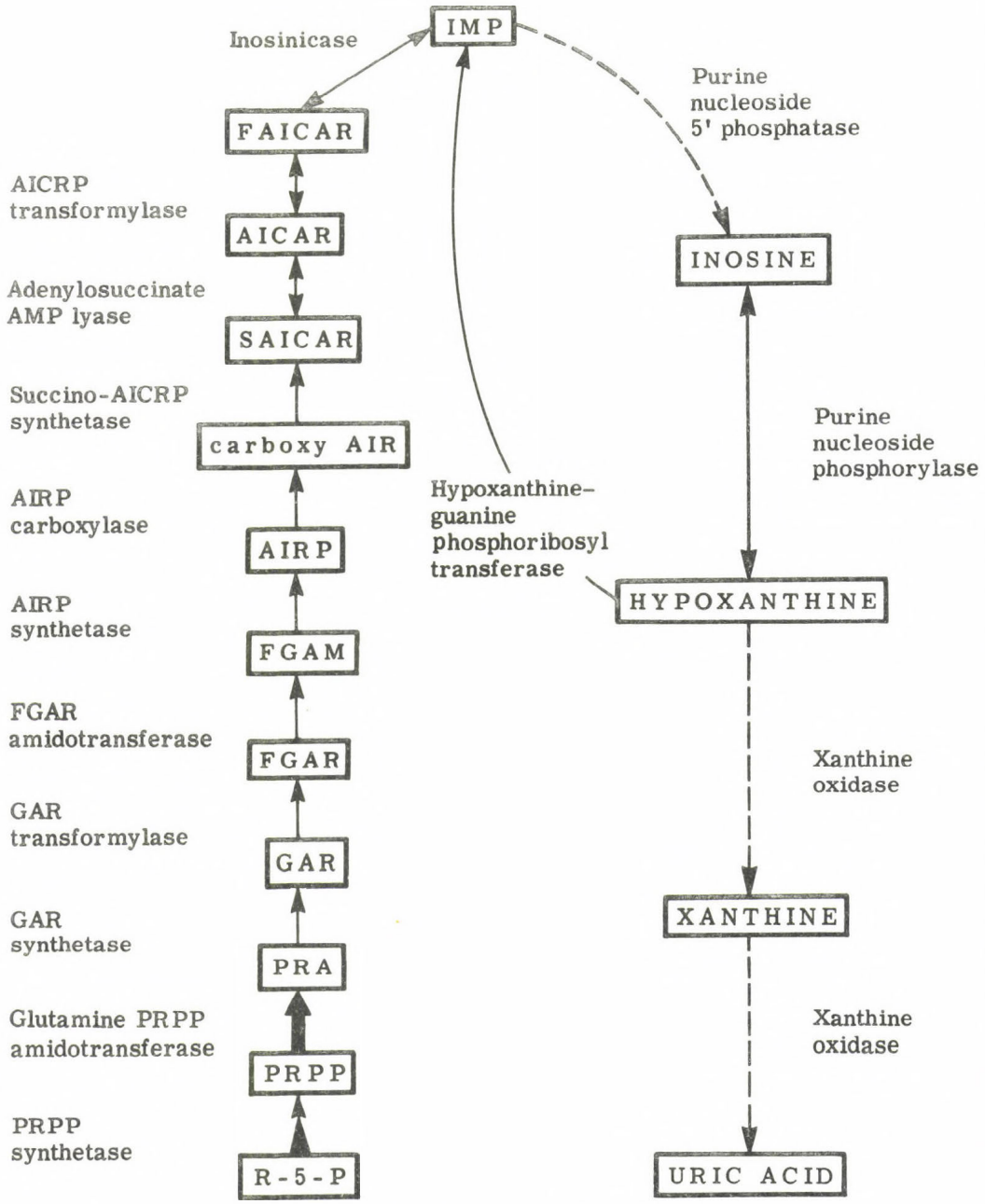

Fig. 2. Metabolic imbalance in purine biosynthesis in rapidly growing hepatomas. PRPP synthetase was increased in rapidly growing hepatomas and amidotransferase was elevated in all hepatomas; the catabolic enzymes, 5'-nucleotidase and xanthine oxidase, were decreased in rapidly growing hepatomas. The resulting metabolic imbalance favors purine biosynthesis and should prevent recycling of metabolites into the catabolic pathway.

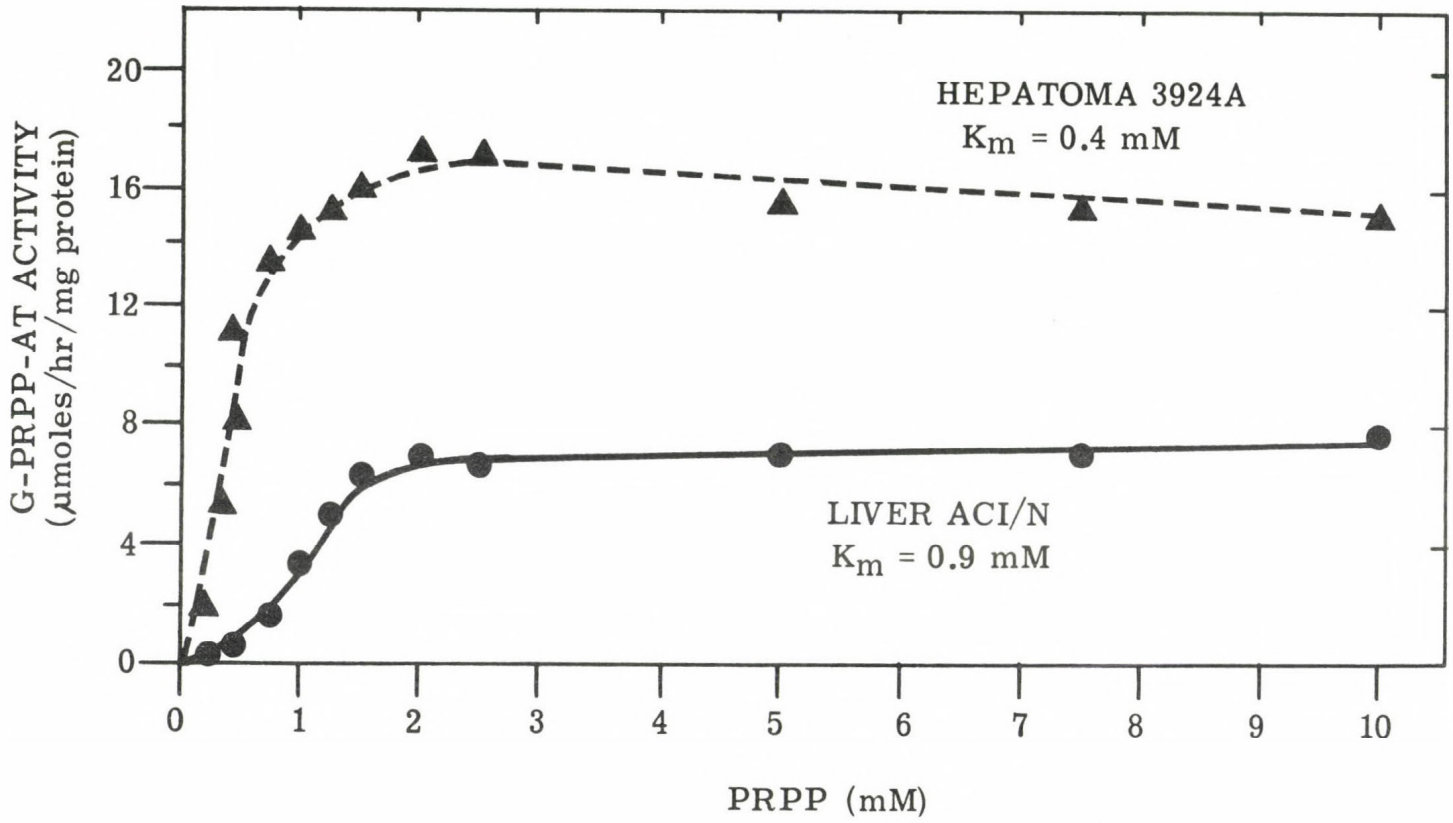

Fig. 3. Comparison of the affinity of amidotransferase to PRPP in liver and hepatoma 3924A.

Extensive studies carried out recently in this Laboratory demonstrated that amidotransferase activity was increased in all the hepatomas irrespective of their growth rate or degree of differentiation (Fig. 3) (Katunuma & Weber, 1974; Weber et al., 1975; Weber & Prajda, 1975). Current work of Prajda et al. (1975a) showed that the amidotransferase activity was also increased in kidney tumors.

Biological Significance and Selective Advantage Achieved Through Reprogramming of Gene Expression as Manifested in Activity and Molecular Properties of Amidotransferase

As shown in Figure 4 all hepatomas contain more amidotransferase activity than the liver; thus the cancer cells should have an increased capacity for purine biosynthesis through the de novo pathway. This enhanced potential is further increased by the higher affinity of the hepatoma enzyme to the substrate PRPP and thus the tumor enzyme is more readily saturated by the substrate. Furthermore, the hepatoma amidotransferase is less sensitive to feedback regulation as manifested by the decreased sensitivity to AMP. Thus, in the hepatoma there is more amidotransferase activity, the enzyme can operate at lower PRPP concentrations and may well be deinhibited at physiological AMP levels. These alterations in amidotransferase activity and molecular properties reveal reprogramming of gene expression that should confer selective biological advantages to neoplastic cells. As the increase in amidotransferase activity is present in all hepatomas, irrespective of their growth rates and malignancy, the reprogramming of gene expression manifested in the ubiquitous rise in this enzyme activity appears to be linked with the neoplastic transformation itself (Katunuma & Weber, 1974; Prajda et al., 1975, 1975a; Weber et al., 1975; Weber & Prajda, 1975).

Effect of Regeneration on Hepatic Amidotransferase Activity

The regenerating liver is a useful model in the analysis of the processes of the reprogramming of gene expression and the informational flow in the mammalian cell. To examine the linkage of amidotransferase to induced proliferative response the activity of this enzyme was studied at different intervals after partial hepatectomy and the results were compared with those obtained in sham operated control animals. The results in Figure 5 show that the specific activity of amidotransferase rose after partial hepatectomy and it was significantly increased at 24, 48 and 72 hours after operation. The peak increase of 164% was observed at 48 hours after partial hepatectomy. The enzyme activity returned to normal at 96 hours. This experiment indicates that amidotransferase activity, and probably its synthesis and degradation, are linked with cellular proliferation. However, the alterations in the neoplastic liver are distinguished from those in the regenerating liver, because in the partially hepatectomized animals amidotransferase exhibits sigmoid kinetics towards PRPP whereas, as outlined above in the hepatomas, the enzyme showed hyperbolic kinetics.

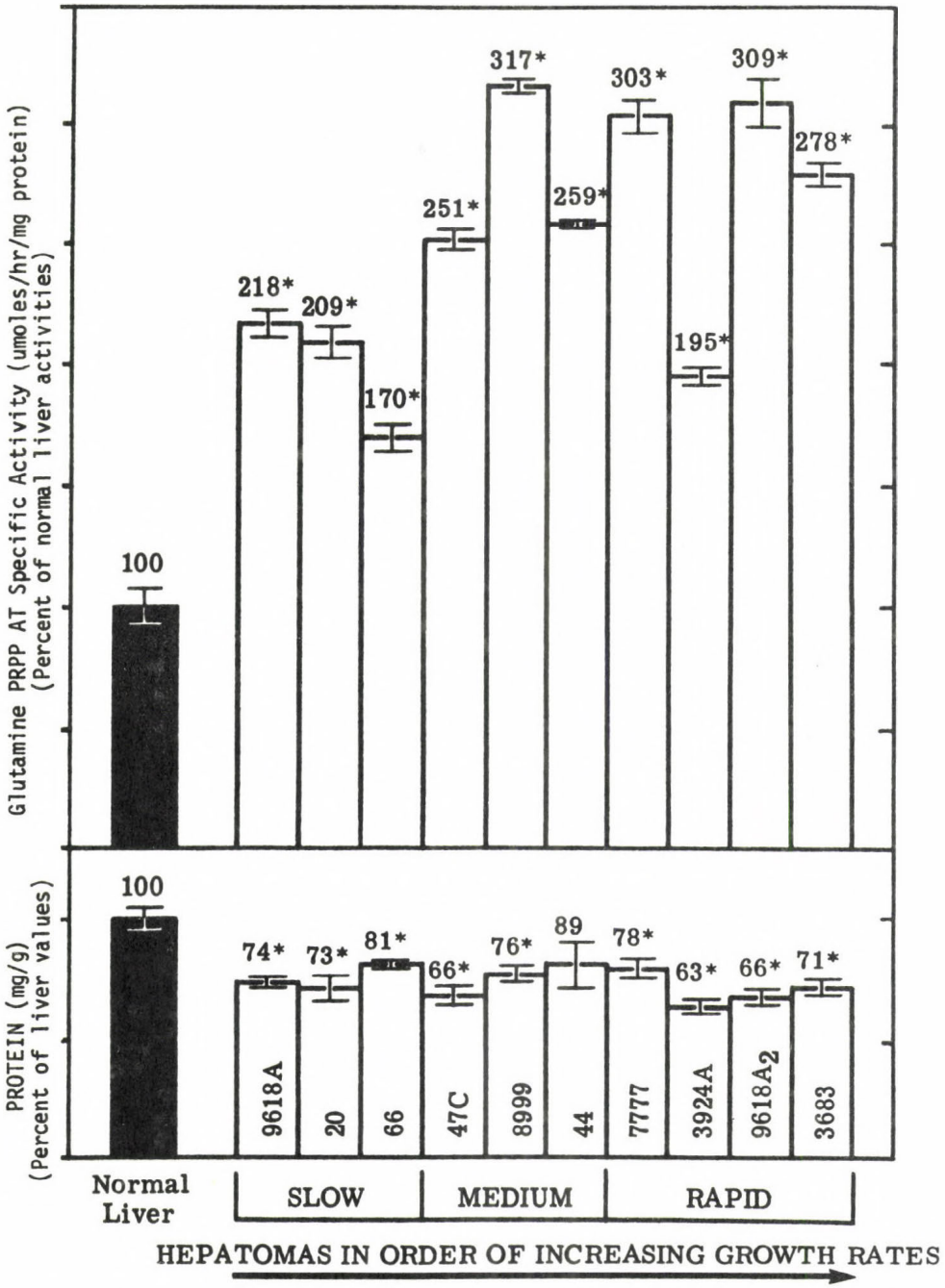

Fig. 4. Increased amidotransferase activity in hepatomas of different growth rates. The protein concentration of the supernate, in which the enzyme activity was measured, is also shown for comparison.

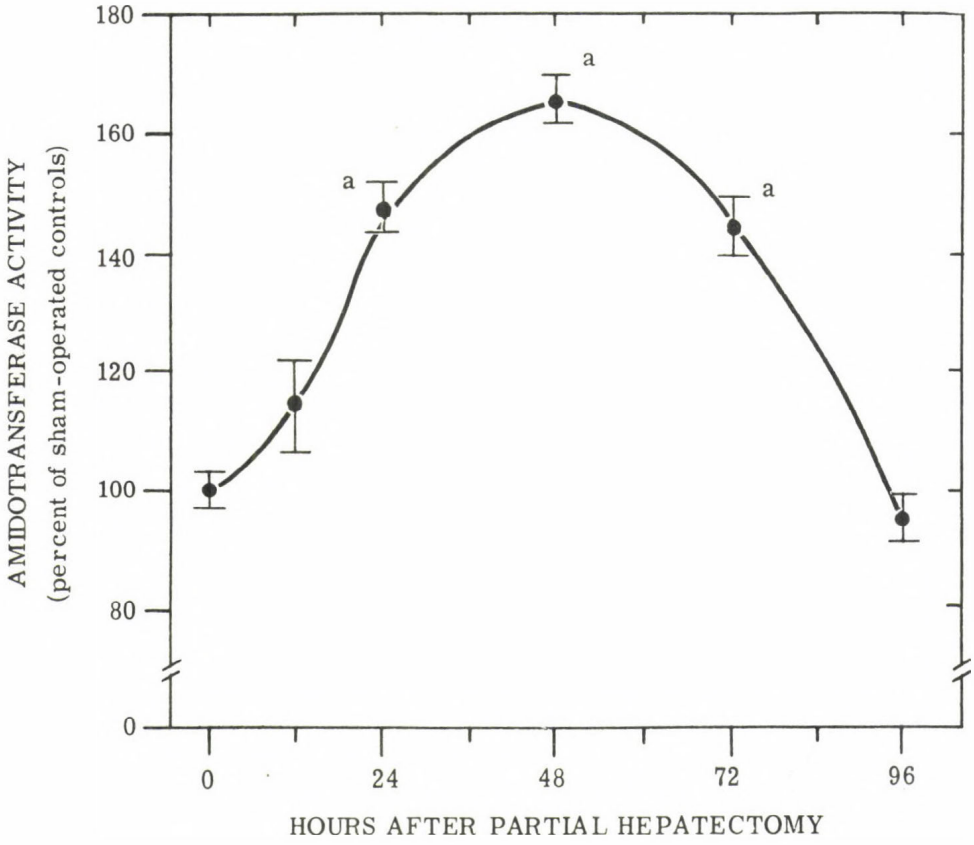

Fig. 5. Effect of liver regeneration on specific activity of amidotransferase. Activity was measured in umoles per hr/mg protein and expressed as percentages of the sham-operated controls

Integrated Pattern of Alterations in Key Enzyme Activities in Neoplasia in Carbohydrate and Purine Metabolism

The reprogramming of gene expression in neoplasia is manifested in an integrated imbalance in the activities of key enzymes in opposing and competing pathways of glycolysis, gluconeogenesis, pentose phosphate metabolism, and in purine synthesis and catabolism. The activities of the key enzymes of glycolysis are increased whereas the opposing key enzymes for gluconeogenesis are decreased in parallel with the growth rate of the hepatomas. In contrast, the activities of the key enzymes for pentose phosphate pathways, G-6-P dehydrogenase and transaldolase (Weber et al., 1974) and the key enzyme of purine de novo synthesis, the amidotransferase, are increased in all the hepatomas examined (Katunuma & Weber, 1974). Thus, in liver neoplasia there are key enzymes that characterize the degrees of expression of neoplastic transformation (the key glycolytic and gluconeogenic enzymes) and there are other enzymes that are discriminants for the neoplastic transformation per se (glucose-6-phosphate dehydrogenase, transaldolase, amidotransferase). The integrated pattern of the key enzymes of carbohydrate and purine metabolism and their behavior in hepatomas are summarized in Figure 6.

The experimental results indicate that there is an increased potential for glycolysis and a decreased potential for recycling. There is a heightened capacity for the biosynthesis of pentose phosphates and for de novo purine biosynthesis. In contrast, the degradative potential for IMP declines. This alteration in the reprogramming of gene expression should confer selective advantages to cancer cells. The integrated pattern revealed in our studies points out the applicability of the molecular correlation concept and the key enzyme concept to purine metabolism (Weber, 1974; Weber et al., 1975).

Studies on Reprogramming of Gene Expression as Manifested in Enzymes Involved in UDP Utilization

Previous work showed that there is an increased potential for pyrimidine biosynthesis and a decreased capacity for degradation of the pyrimidines in the hepatomas (Ferdinandus et al., 1971). This metabolic imbalance was manifested in the increased activities of the key enzymes of UDP biosynthesis, aspartate transcarbamylase and dihydroorotase (Sweeney et al., 1974) and in the decrease in the activity of the rate-limiting enzyme of pyrimidine catabolism, dihydrouracil dehydrogenase (Queener et al., 1971). UDP is at an important metabolic crossroad and its utilization is dependent on ribonucleotide reductase that routes it into de novo DNA biosynthesis and UDP kinase that channels it into RNA biosynthesis and potentially this reaction could also contribute to the de novo DNA biosynthesis as shown in Figure 7. The studies of Elford et al. (1970) demonstrated that ribonucleoside reductase (EC 1.17.4.1) was increased in parallel with the growth rate of the hepatomas.

The molecular correlation concept predicts that in the neoplastic cells reprogramming of gene expression is likely to occur where enzymes antagonize each other either by opposing each other's direction of action or by their competition for the same substrate. To test the applicability of this concept to UDP metabolism we have carried out a systematic investigation of the behavior of UDP kinase (nucleoside diphosphate kinase; ATP:UDP

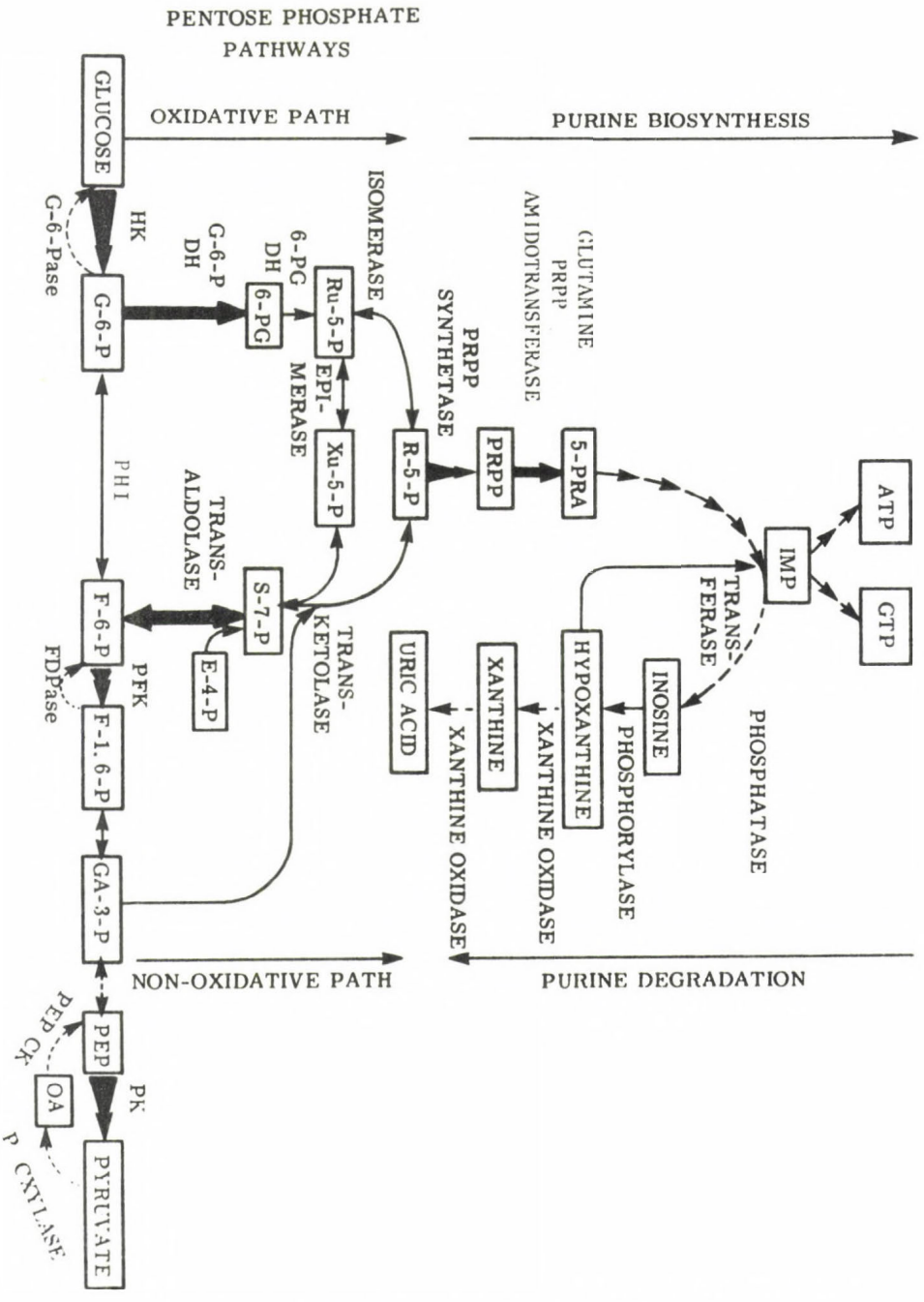

Fig. 6. Integrated pattern of glycolysis, gluconeogenesis, pentose phosphate pathways, purine synthesis and degradation as manifested in rapidly growing hepatomas.

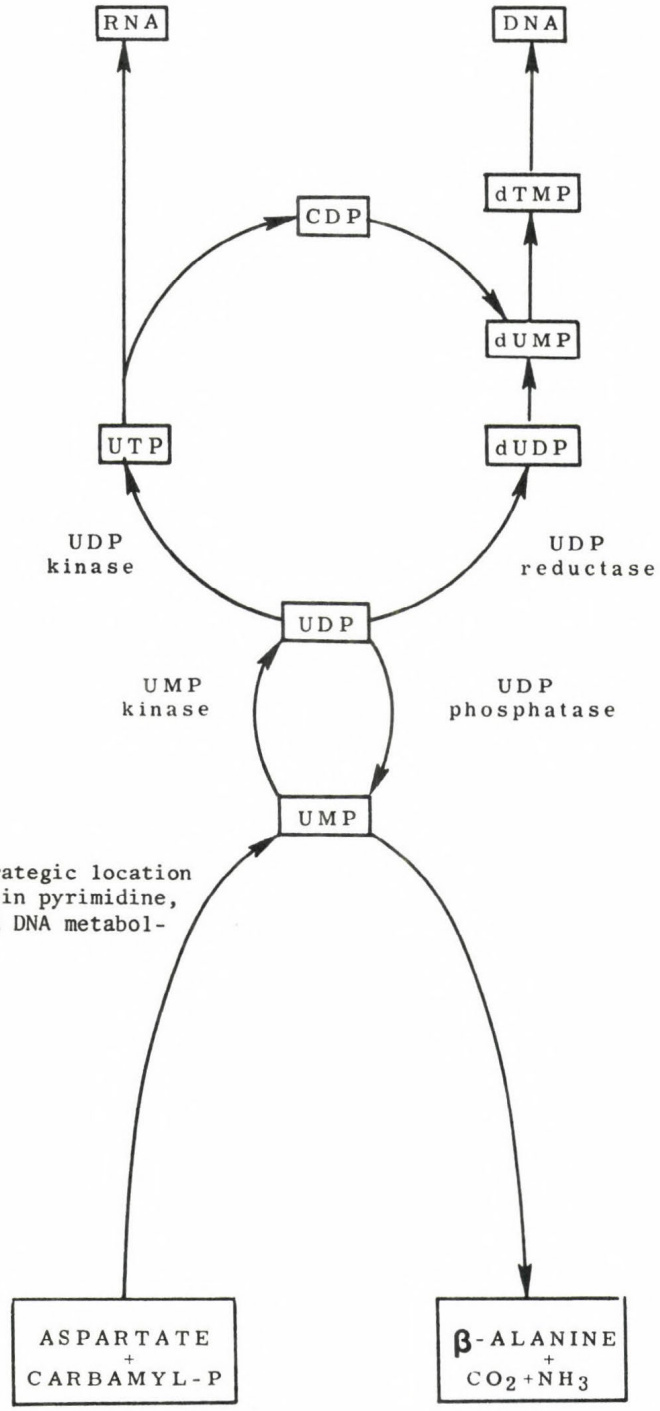

Fig. 7. Strategic location of UDP in pyrimidine, RNA and DNA metabolism.

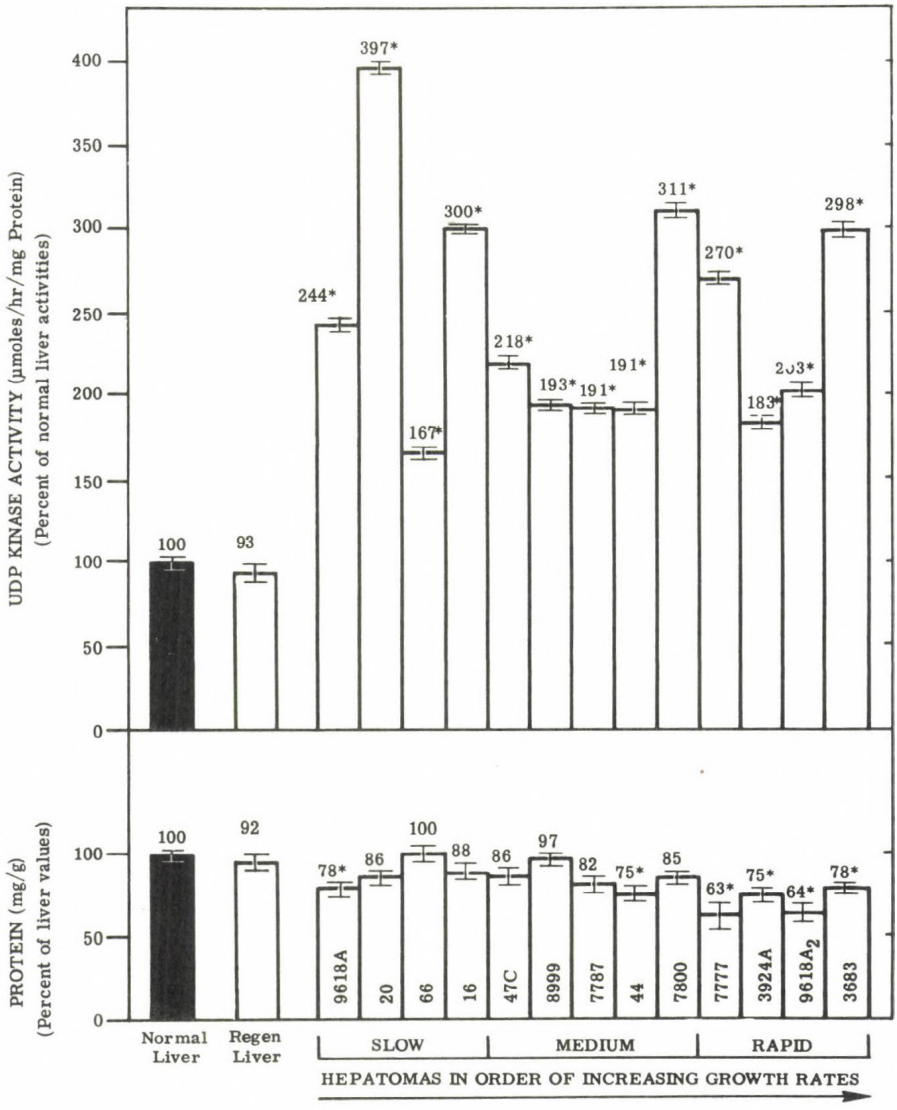

Fig. 8. Increased UDP kinase specific activity in hepatomas of different growth rates. The protein concentration of the supernate, in which the enzyme activity was measured, is also shown for comparison (Williams et al., 1975).

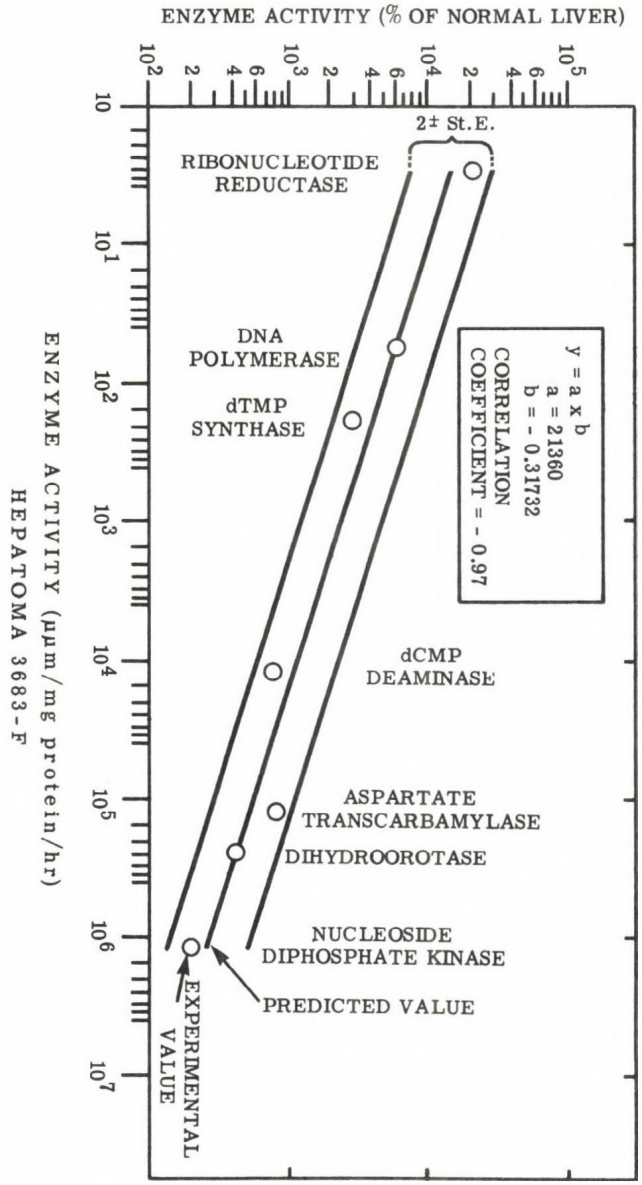

Fig. 9. Correlation of enzyme activity in normal resting adult liver with the extent of increase of respective enzyme activities in the rapidly growing hepatoma 3683F.

phosphotransferase (EC 2.7.4.6). Kinetic studies were conducted to ensure proportionality of UDP kinase activity with amount of enzyme added under optimum kinetic conditions for rat liver and hepatomas. The details of our assay method were described recently by Williams et al. (1975). The UDP kinase specific activity was expressed in umoles of substrate metabolized per mg protein per hour. The kinetic characteristics of UDP kinase activity from crude enzyme preparations of rat liver and hepatomas were similar (Williams et al., 1975). The UDP kinase specific activity was markedly increased in all liver neoplasms irrespective of tumor growth rate or degree of differentiation (Figure 8). Current studies also showed that UDP kinase activity was increased in 2 primary human hepatomas as compared to the histologically normal samples from the human host liver as controls.

Our demonstration that UDP kinase activity was increased in all hepatomas, irrespective of the degree of tumor malignancy, suggests that the reprogramming of gene expression in malignant transformation is linked with an increase in the expression of this UTP-synthesizing enzyme activity. In this Laboratory we recently discovered four such transformation-linked elevations in enzyme activities, and they all relate to a heightened potential in the channeling of precursors to strategic biosynthetic processes. Thus, the rise in the activities of glucose-6-phosphate dehydrogenase and transaldolase should provide an increased capacity for routing glycolytic intermediates into pentose phosphate biosynthesis (Weber et al., 1974). The third alteration discovered in all hepatomas was an increased activity of glutamine PRPP amidotransferase which should also result in an increased potential for purine and nucleic acid biosynthesis (Katunuma & Weber, 1974; Weber et al., 1975; Prajda et al., 1975). In turn, the increased UDP kinase activities reported here should provide an increased potential for production of RNA and for de novo DNA biosynthesis (Williams et al., 1975). These elevations in the activities of the key enzymes of pentose phosphate biosynthesis, de novo purine production and RNA and DNA biosynthesis signal a reprogramming of gene expression that should confer selective biological advantages to the neoplastic cells.

Mathematical Model of Altered Metabolic Regulation in Neoplastic Cells

In previous work it was recognized that the lower the activity of an enzyme was in the adult resting rat liver, the higher it increased in the rapidly growing hepatomas (Weber, 1974). The mathematical expression of these experimental observations and the plotting of the results from this publication are given in Figure 9. The predicted value for the increase of the activity of nucleosidediphosphate kinase in the rapidly growing hepatoma was tested and the values observed fit well into the range mathematically predicted by the equation in Figure 9.

The Key Enzyme Concept: Identifying Features of Key Enzymes

It was recognized in this Laboratory that the regulation of the rate and direction of opposing pathways of intermediary metabolism is achieved by controlling the operation of certain enzymes. These enzymes that appear to be playing a key role in metabolic regulation thus were named key enzymes (Weber et al., 1965). The key enzyme concept proved to be a conceptual breakthrough in the analysis and understanding of the regula-

tion and behavior of enzyme pattern in endocrine and nutritional conditions. The key enzymes were also relevant to our understanding of the unfolding of gene expression in differentiation and in the reprogramming of gene expression that occurs in the neoplastic transformation and in the progression of the neoplastic state. As a result of experimental and conceptual progress in our investigations a number of the features which characterize key enzymes were recognized in this Laboratory and representative examples are given in Table 2. As our progress in gaining an insight into the identifying features of key enzymes develops, it is hoped that a deeper understanding will be reached of the properties, regulation and function of the key enzymes and the interpretive value of this concept (Weber, 1976).

CONCLUSION

Metabolic regulation and adaptation in the mammalian system are achieved through control of the concentration, activity, and isozyme pattern of key enzymes that oppose and compete with each other at strategic crossroads of intermediary metabolism. Through controlling the antagonistic and competing key enzymes and by adjusting the ratios of the opposing key enzymes and isozymes, metabolic regulation achieved an integration of the rate and direction of opposing metabolic pathways. This integrative action at the molecular level results in the capacity of the mammalian system to adapt to endocrine and nutritional circumstances. The ability of the organism to regulate the key enzyme systems confers selective advantages to the biological systems as a whole.

In regeneration, differentiation and neoplasia, the reprogramming of gene expression is also targeted through alterations in the concentration, activity, molecular properties, and isozyme pattern of key enzymes.

SUMMARY

The regulation of key enzymes was examined in investigating the strategy of reprogramming of gene expression in normal and neoplastic cells.

1. The pleiotropic action of insulin in integrating the activity, amount and isozyme pattern of a series of hepatic key enzymes in glycolysis, pentose phosphate pathway, glycogen, lipid, and thymidine metabolism was examined.
2. The regulation of purine metabolism was studied in investigating the control of the key purine synthesizing enzyme, glutamine PRPP amidotransferase. This enzyme was markedly increased in all hepatomas irrespective of their growth rate and malignancy. The normal liver enzymes showed sigmoid kinetics whereas in rapidly growing hepatomas the enzyme had hyperbolic kinetics; the sensitivity of this hepatoma enzyme to feedback inhibition was decreased. These alterations confer selective advantages to the hepatoma cells. In the regenerating liver the amidotransferase activity increased to 164% of the activity of sham-operated controls; however, in the regenerating liver, the molecular properties of the enzyme were similar to the normal liver and it showed sigmoid kinetics towards the substrate PRPP.

Table 2

Identification of key enzymes

FEATURES OF KEY ENZYMES	EXAMPLES IN VARIOUS METABOLIC AREAS
I. PLACE IN PATHWAY	
1. First in a reaction sequence	Pyruvate carboxylase; TdR kinase
2. Last in a reaction sequence	Glucose-6-phosphatase; DNA polymerase
3. Pathways in themselves	Glucose-6-phosphatase; adenylate cyclase
4. Operate on both sides of reversible reaction pools	TdR kinase; dihydrothymine dehydrogenase
5. One-way enzyme opposed by another one-way enzyme	Phosphofructokinase; fructose-1,6-diphosphatase
II. REGULATORY PROPERTIES	
6. Rate-limiting in pathway	PEP carboxykinase; ribonucleotide reductase
7. Possesses relatively low activity in the pathway	Pyruvate carboxylase; DNA polymerase
8. Target of feedback regulation	Amidophosphoribosyltransferase; TdR kinase
9. Target of multiple controls	Pyruvate kinase; ribonucleotide reductase
10. Exhibits allosteric properties	Aspartate carbamyltransferase
11. Interconvertible enzymes	Glycogen phosphorylase
12. Isozyme pattern provides added adaptive features	Glucokinase; hexokinase
III. BIOLOGICAL ROLE	
13. Involved in overcoming thermodynamic barriers	Four key gluconeogenic enzymes
14. Governs one-way reactions	Glucokinase; ribonucleotide reductase
IV. INTRACELLULAR COMPARTMENTATION	
15. Localized in particulate fraction when other enzymes in same pathway are in cytoplasm	Uricase; glucose-6-phosphatase

3. An integrated pattern of the alterations in key enzyme activities in neoplasia was examined in carbohydrate, pentose phosphate, and purine metabolism.

4. Studies were carried out in analyzing the reprogramming of gene expression as manifested in enzymes involved in UDP utilization. The results indicated that UDP kinase activity was increased in all hepatomas irrespective of the growth rate and malignancy of the liver tumors. This alteration in gene expression confers selective advantages to the hepatoma cells.

5. The identifying features of the key enzymes were outlined and examples were given for the applicability of the concept to key enzymes in various pathways of intermediary metabolism.

ACKNOWLEDGMENTS

The research work outlined in this paper was supported by grants from the United States Public Health Service, National Cancer Institute, Grant Nos. CA-13526 and CA-05034.

REFERENCES

Dunaway, Jr., G. A. and Weber, G. (1974). Arch. Biochem. Biophys. 162, 620.
Dunaway, Jr., G. A. and Weber, G. (1974a). Arch. Biochem. Biophys. 162, 629.
Elford, H. L., Freese, M., Passamani, E. and Morris, H. P. (1970). J. Biol. Chem. 245, 5228.
Ferdinandus, J. A., Morris, H. P. and Weber, G. (1971). Cancer Res. 31, 550.
Heinrich, P. C., Morris, H. P. and Weber, G. (1974). FEBS Letters 42, 145.
Katunuma, N. and Weber, G. (1974). FEBS Letters 49, 53.
Prajda, N., Katunuma, N., Morris, H. P. and Weber, G. (1975). Submitted for publication.
Prajda, N., Morris, H. P. and Weber, G. (1975a). Submitted for publication.
Queener, S. F., Morris, H. P. and Weber, G. (1971). Cancer Res. 31, 1004.
Sweeney, M. J., Parton, J. W. and Hoffman, D. H. (1974). Advan. Enzyme Regulation 12, 385.
Weber, G. (1959). Rev. Can. Biol. 18, 245.
Weber, G. (1963). Advan. Enzyme Regulation 1, 1.
Weber, G. (1973). Advan. Enzyme Regulation 11, 79.
Weber, G. (1974). In: The Molecular Biology of Cancer, ed. H. Busch (Academic Press, N.Y.) p. 487.
Weber, G. (1975). In: Proc. Ninth FEBS Meeting, Budapest 1974, vol. 32, Symp. on Mechanism of Action and Regulation of Enzymes (ed. T. Keleti) Akademiai Kiado, Budapest, and North-Holland, Amsterdam.
Weber, G. (1976). Biochemical Strategy of the Cancer Cell, to be published.
Weber, G. and Prajda, N. (1975). Proc. Am. Assoc. Cancer Res. 16, in press.
Weber, G., Singhal, R. L. and Srivastava, S. K. (1965). Advan. Enzyme Regulation 3, 43.
Weber, G., Singhal, R. L., Stamm, N. B., Lea, M. A. and Fisher, E. A. (1966). Advan. Enzyme Regulation 4, 59.
Weber, G., Queener, S. F. and Ferdinandus, J. A. (1971). Advan. Enzyme Regulation 9, 63.

Weber, G., Ferdinandus, J. A., Queener, S. F., Dunaway, Jr., G. A. and Trahan, L. J.-P. (1972). Advan. Enzyme Regulation 10, 39.
Weber, G., Queener, S. F. and Morris, H. P. (1972a). Cancer Res. 32, 1933.
Weber, G., Trevisani, A. and Heinrich, P. C. (1974). Advan. Enzyme Regulation 12, 11.
Weber, G., Prajda, N. and Williams, J. C. (1975). Advan. Enzyme Regulation 13, 3.
Williams, J. C., Weber, G. and Morris, H. P. (1975). Nature 253, 567.
Williams-Ashman, H. G., Coppoc, G. L. and Weber, G. (1972). Cancer Res. 32, 1924.

Symp. Biol. Hung. 18, pp. 143–158 (1974)

REGULATION OF METABOLIC PATHWAYS BY COOPERATIVITY AND COMPARTMENTATION OF METABOLITES

H. Frunder, A. Horn, G. Cumme,
W. Achilles and R. Bublitz
Institute of Physiological Chemistry,
Friedrich Schiller University, Jena, GDR

INTRODUCTION

In our group, out of the diversity of regulatory mechanisms in action in the living cell, we analyzed the importance of metal metabolite complexes for metabolic regulation. The reasons for this selection are based on the well known fact that most metabolites form complexes with intracellular cations like potassium and magnesium ions. Thus, single metabolite pools are not homogeneous entities, but distributed among a heterogeneous mixture of free, protonated and complexed species. Furthermore, there are well documented examples (Purich and Fromm, 1972) indicating that different species of one metabolite act in opposition even on the same enzyme.

Our starting point along the metal complex line should be a theoretical study to determine whether complex formation can be a principal mechanism of control in intact cells, where total metal ion concentrations are usually fairly constant while variation in metabolite levels is much wider.

RESULTS

As the first step let us assume one metal ion M and one ligand L forming a metal ligand complex ML. The total metal ion concentration is kept constant at 1 mM and the total ligand concentration varied from zero to 2 mM.

In Fig. 1 we may distinguish two regions. The transition area between them is centered at a total ligand concentration which corresponds approximately to the total metal ion concentration kept constant at 1 mM. In the left region the total ligand concentration is smaller than the total metal ion concentration, and the free ligand L increases with a relatively small slope. In the right region the total ligand concentration surpasses the total metal ion concentration, and therefore, L increases with a slope of nearly one. The behaviour of the free metal ion concentration M is quite opposite. Lastly, the complex ML increases linearly in the left region and approaches its saturation value in the right region.

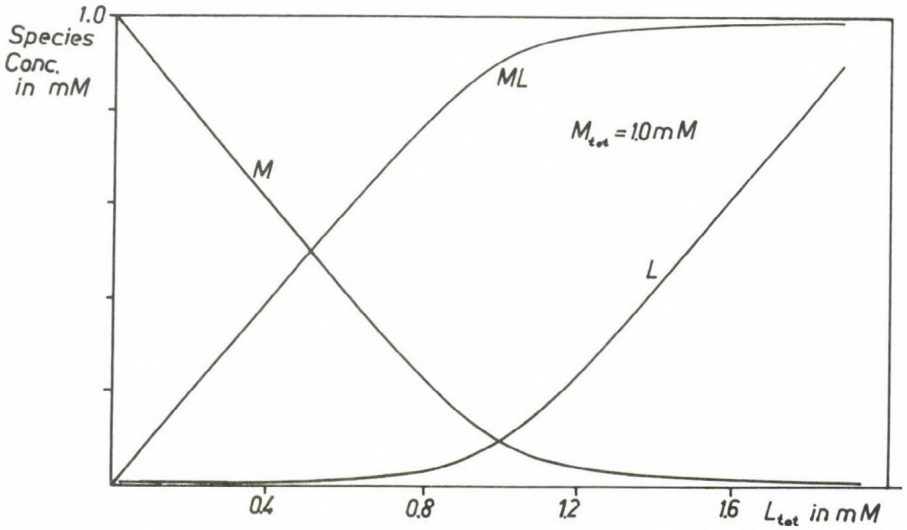

Fig. 1. Concentrations of free metal ion M, free ligand L and of the ML complex as function of the total ligand concentration L_{tot}. The complex formation constant of the ML complex is assumed to be 10^5 M^{-1}.

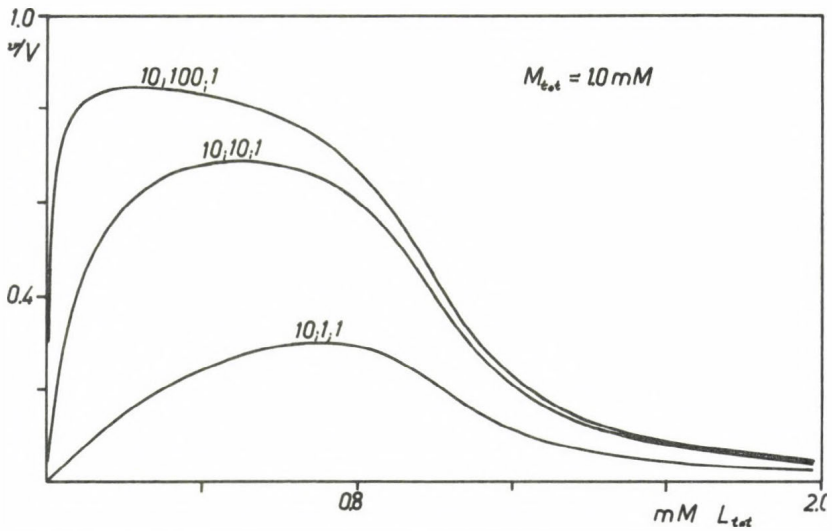

Fig. 2. Activity (v/V) of a hypothetical enzyme as function of the total ligand concentration L_{tot}. M is assumed to act as activator, ML as substrate and L as non-competitive inhibitor. The total metal ion concentration is kept constant at 1 mM. The binding constants (in mM^{-1}) of the different complex species with the enzyme are indicated at the curves in the order M, ML and L.

If the different species act in a different manner upon the same enzyme, then it may be shown that relatively small changes of the total ligand concentration in the critical area may cause marked changes in enzyme activity, provided that there are suitable binding constants for the different complex species with the enzyme (Fig. 2).

The enzyme activity is inhibited more or less strongly as soon as the total ligand concentration approaches that of the constant total metal ion. This behaviour indicates that theoretically, a weak variation of the total metabolite concentration within a critical area can cause a great velocity variation through metal ligand complex formation.

This situation led us to the conclusion that an enzyme might be more clearly characterized in terms of single species concentrations rather than in terms of total metabolite concentrations as reported by most authors in the past (G. Cumme et al., 1973 a,b).

In order to achieve a simple experimental situation, we vary the concentration of a selected single species, keeping constant as many other species as possible and interpret the measured enzyme activity as a function of the varied species concentration. In doing so, the following principles must be taken into account. From the complex equilibrium

$$\frac{[ML]}{[M]\ [L]} = B \quad \text{(B denotes the complex formation constant)}$$

follows: When L is kept constant and ML is varied, then M varies proportionally. The constant ratio ML/L can be altered by fixing L at another constant level. At constant M, ML and L vary proportionally and, if ML is kept constant, the two other species vary inversely.

In order to make clear the principles of our evaluation we use the same hypothetical enzyme as characterized in the legend of Fig. 2. Additionally, a second free ligand L^X acts as competitive inhibitor against ML. The corresponding rapid equilibrium rate equation for this enzyme has the following form:

$$v/V = \frac{K_1 K_2 [M] [ML]}{(1+K_1[M])(1+K_2[ML]+ K_3[L^X])(1+K_4[L])} \qquad \text{Eq. (1)}$$

The numerical values chosen for the different K's are in mM^{-1}: $K_1 = 1$; $K_2 = 40$; $K_3 = 20$; $K_4 = 20$. The complex formation constant $B = \frac{[ML]}{[M]\ [L]}$ is 5 mM^{-1}.

In Fig. 3 the test conditions are set up so that M is kept constant at different levels and v/V is plotted against L. Curve shapes with maxima are obtained because the denominator of the rate equation is of second order, and the numerator of first order in L. Fixing constant M at lower levels, the maxima shift to the right, that is to higher concentrations of L.

The explanation is: The ML term in the second sum of the denominator needs higher L concentrations in order to dominate, if M is small. Or in other words, ML substituted by M · L · B becomes smaller at low M. Thus, one needs higher L concentrations before the second sum of the denominator becomes considerably greater than one.

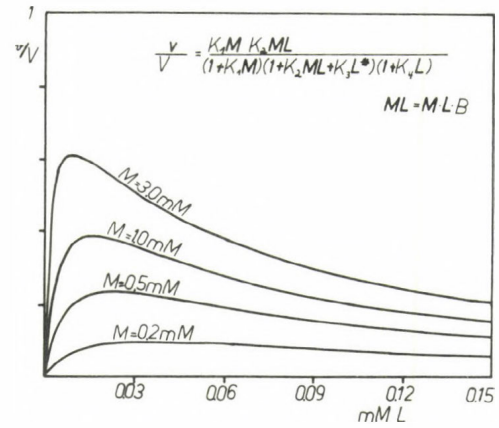

Fig. 3. v/V plotted against L at different fixed levels of M. L^x = zero.

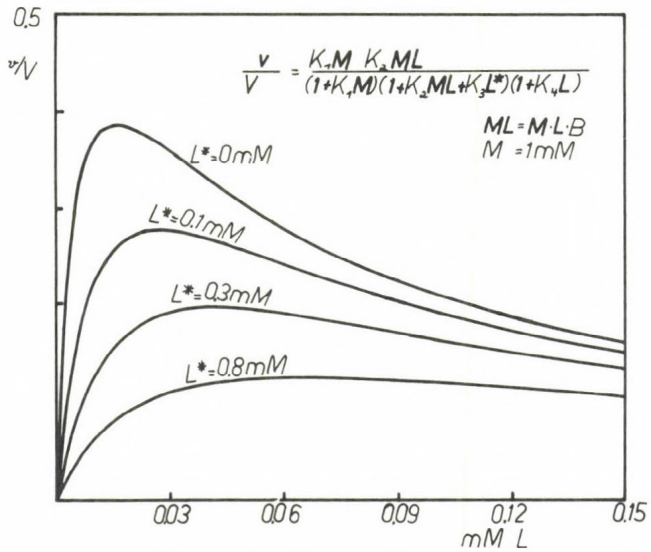

Fig. 4. v/V plotted against L at different fixed concentrations of L^x. M = 1 mM = constant.

Next, we set up the same conditions, namely M is kept constant and L is varied, now however at different constant concentrations of L^X inhibiting the enzyme competitively against ML. Fig. 4 shows curve shapes with maxima. The maxima shift to the right when increasing the constant level of L^X, because the ML term of the denominator needs higher L concentrations in order to dominate.

In Fig. 5, v/V is plotted against ML at constant levels of M. The maxima shift to the right at increasing constant M, since L is now lowered. Or in other words, substituting L in the last sum of the denominator by $\frac{ML}{M \cdot B}$, one sees that this term dominates later, if the level of M is increased. However, one has to take care not to use very high levels of M. Otherwise, the maxima go far to the right and can easily be overlooked if one does not examine the whole range of relevant physiological concentrations.

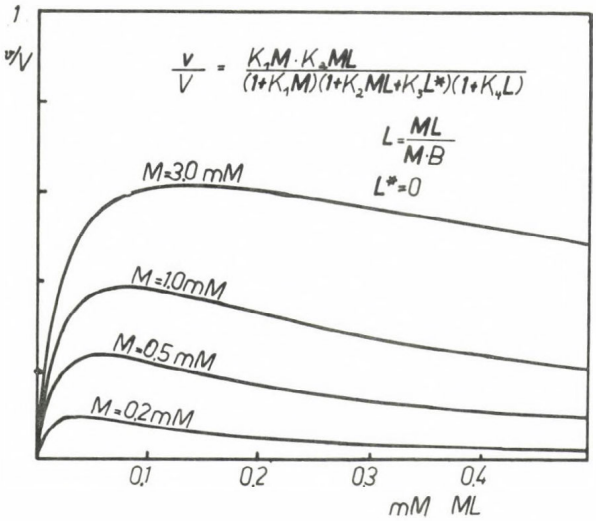

Fig. 5. v/V plotted against ML at different fixed concentrations of M.

In Fig. 6 no maxima are observed, since both numerator and denominator are second order in M. However, the fact that the order is higher than one leads to a sigmoidicity seen at low concentrations of ML. When using an appropriate scaled double reciprocal plot, which expands the area of very low ML concentrations, we get parabolas (Fig. 7), much more evident at higher fixed levels of L, that is at a higher ratio ML/M. When using an excess of M, which leads to very low levels of L, then the parabolas approach straight lines, and interactions of M with the enzyme can be overlooked.

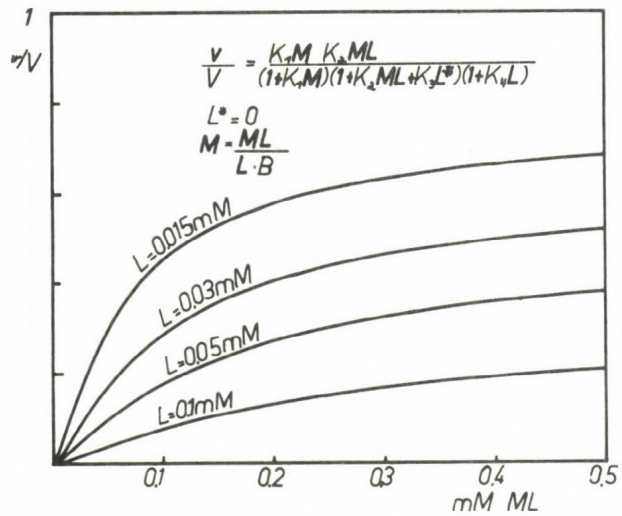

Fig. 6. v/V plotted against ML at different fixed concentrations of L.

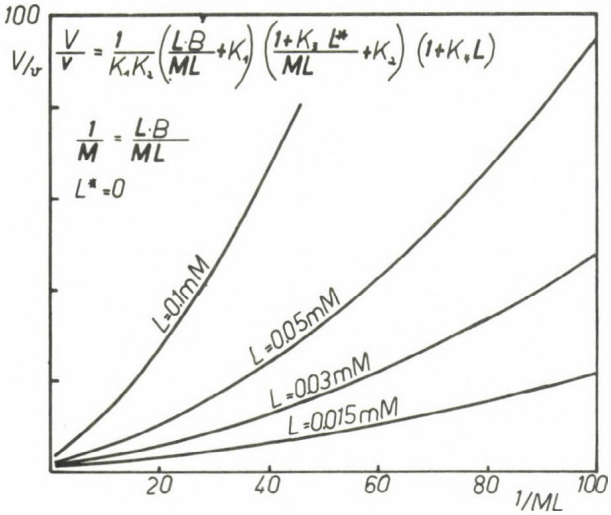

Fig. 7. V/v plotted against 1/ML at different fixed concentrations of L.

All these examples demonstrate that the occurrence of different curve shapes and of shifts of maxima and minima can be used in order to evaluate the effects of different complex species on a real enzyme.

According to this scheme purified pyruvate kinase from human erythrocytes was characterized, first varying the different ADP species whilst keeping all other species constant, then varying the phosphoenolpyruvate and potassium concentrations, and lastly performing competition experiments between the ADP and phosphoenolpyruvate species. The rapid equilibrium rate equation, based on about 1500 single determinations of the enzyme activity while varying the different complex species of the substrate side, has the following form (Eq.(2)):

$$v/V = \frac{k_1 k_3 k_4 k_6 [Mg^{2+}][Mg\,ADP][PEP][k^+]}{(1+k_1[Mg^{2+}])(1+k_7[Mg^{2+}]+k_3[MgADP])(1+k_2[kADP]+k_4[PEP]+k_5[kPEP])(1+k_6[k^+])}$$

The binding constants K_1 - K_7 were fitted by the Marquardt procedure. Their numerical values with the ranges are listed in Table 1.

Table 1.

Numerical values and ranges for the binding constants of the complex species of the substrate side of pyruvate kinase from human erythrocytes

	For binding of:	Binding constants in mM^{-1}	Range
K_1	Mg^{2+} on the activator side	6	5 - 24
K_2	KADP on the PEP side	3	1 - 4
K_3	MgADP on the substrate side	2	1 - 5
K_4	PEP on the substrate side	1.5	0.6 - 2.5
K_5	KPEP on the PEP side	15	8 - 22
K_6	K^+ on the K^+-side	0.004	0.002 - 0.006
K_7	Mg^{2+} on the MgADP side	1.5	1 - 2

The model chosen uses MgADP and non-complexed phosphoenolpyruvate as substrates and Mg^{2+} and K^+ions as activators. The potassium complexes of phosphoenolpyruvate and ADP act as competitive inhibitors against phosphoenolpyruvate, and Mg^{2+}, beside its action as activator, influences the enzyme activity as competitive inhibitor against the substrate MgADP. Thus, not only one but several complex species of the substrate side of pyruvate kinase modulate the enzyme activity at several binding places. As it can be easily derived from the association constants for the different enzyme complexes, shown in Table 1, the numerical values of the corresponding dissociation constants are very close to the concentrations found in erythrocytes, thus predestinating all species for control.

Due to interdependences via complex equilibria a change in any species alters the whole complex pattern and the enzyme activity through many simultaneous effects on all binding sides.

As to the influence of the products of the pyruvate kinase on enzyme activity we have at present only limited data. ATP in micromolar concentrations reduces the enzyme activity to about one fourth of the activity in the absence of ATP[1]. However, this inhibition is completely abolished by micromolar concentrations of fructosediphosphate and especially fructose-6-phosphate. That means, the ATP inhibition observed in vitro probably has no effect on the enzyme activity in intact erythrocytes.

With regard to the terms "substrate", "activator" and "inhibitor", these terms cannot always be applied uniquely, when complex forming effectors are involved. Let us consider the following two models:

In model 1 K^+ acts as activator, phosphoenolpyruvate as substrate and the potassium complex of phosphoenolpyruvate as competitive inhibitor against non-complexed phosphoenolpyruvate

$$\frac{K^+(3) \quad PEP(2)}{KPEP(1)} \text{ (model 1)}; \qquad \frac{KPEP(1)}{PEP(2) \quad K^+(3)} \text{ (model 2)}$$

In model 2 the functions all of the three species are interchanged, i.e. the potassium phosphoenolpyruvate complex acts as substrate, phosphoenolpyruvate as competitive inhibitor against potassium phosphoenolpyruvate and potassium ions as non-competitive inhibitor.

The corresponding two rapid equilibrium rate equations (Eqs. (3) and (4)) are as follows:

$$v = \frac{V_1 \cdot K_2 \cdot K_3 \, [K^+] \, [PEP]}{(1+K_3 \, [K^+])(1+K_1 \, [KPEP] + K_2 \, [PEP])} \text{ for model 1, and}$$

$$v = \frac{V_2 \cdot K_1 \, [KPEP]}{(1+K_3 \, [K^+])(1+K_1 \, [KPEP] + K_2 \, [PEP])},$$

and after substitution

$$v = \frac{V_2 \cdot K_1 \cdot B \, [K^+] \, [KPEP]}{(1+K_3 \, [K^+])(1+K_1 \, [KPEP] + K_2 \, [PEP])} \text{ for model 2}$$

[1] at physiological phosphoenolpyruvate concentrations

Both Eqs. differ only in the product of three constants of the numerator. Taking V_1 for the Eq. (3) for model 1 and V_2 for the Eq. (4) for model 2, so that the product

$$V_1 \cdot K_2 \cdot K_3 = V_2 \cdot K_1 \cdot B,$$

then one obtains equal velocities at equal effector concentrations for both models. Thus, both models cannot be distinguished, even by the most painstaking kinetic or binding studies. That means that a given mathematical relation between the effector concentrations and the enzyme activity is not uniquely describable in terms of what species acts as substrate, activator or inhibitor.

However, from any of such Eqs. we may deduce the exact stoichiometry of the reactive enzyme complex and in advantageous cases the effector competition for the different binding sites of the enzyme. Defining an enzyme in terms of stoichiometries and competitions leads despite its missing uniqueness to a unique description of the behaviour of the enzyme as a member of a metabolic pathway. And this is the main aim of our modelling.

An obvious disadvantage of the method used is that the total concentrations which are necessary for each determination of the enzyme activity must be calculated from the prescribed single species concentration, making use of the possibly incomplete pattern of metal ligand complexes and their complex formation constants, which are known only within certain ranges of error. ± 0.1 pK unit error of the complex formation constant, which holds for many constants, may produce ± 10 % error in the concentrations of the non-complexed species and ± 20 % error in the concentrations of the complexed species. This points to the urgent need of developing methods for the direct experimental determination of different complex species.

On the other hand, the advantages are also evident. The method used greatly simplifies the interpretation of velocity changes as consequences of concentration changes, because well defined linear relations exist between the concentrations of the varied complex species and because the concentrations remain constant for the majority of species.

APPLICATION TO ENZYME SEQUENCES

We might proceed from purified enzymes, which can be treated in vitro as one likes, to enzyme sequences in intact cells. Here, further interactions come up in the ensemble of all cell constituents.

The most important one to be discussed is the competition of all metabolites for the intracellular metal ions, which show fairly constant levels of their total concentrations while the metabolite levels vary much more. This causes marked changes in the complex pattern.

The second main problem we have to envisage in enzyme sequences in intact cells is the possibility of compartmentation of metabolites and metal ions within the cell.

As to magnesium we know from a recent paper (Romero, 1974), that about 10 % of the total red cell magnesium is bound to the inner surface of the erythrocyte membrane.

We also have definite knowledge as to metabolite compartmentation in red cells, especially through the work of Rapoport s group in Berlin (Berger et al., 1973; Gerber et al., 1973). From their data we know that about 40 % of the total 2,3-biphosphoglycerate and 15 % of the total ATP are bound to hemoglobin in oxygenated red cells at normal pH.

With this information at hand we undertook a computer study to investigate the influence of complex formation on the coupling of different enzymes of glycolysis in intact erythrocytes. For this purpose we chose two kinases, about which we have the most reliable and detailed information.

The first one selected is red cell hexokinase as a prototype of an ATP consuming kinase. Here, kinetic data with regard to magnesium complexes are available (Purich and Fromm, 1972; Gerber et al., 1974). The second kinase is red cell pyruvate kinase as a prototype of an ATP producing kinase with kinetic data as shown above.

The first step consists of building a simplified model of the substrates and main effectors of both kinases under simulated in vivo conditions. Then, by a computer we calculated the alterations of the complex pattern induced by increasing or decreasing total 2,3-biphosphoglycerate and ATP-concentrations within a physiologically reasonable range, all other total metabolite concentrations being kept constant.

Table 2 gives the metabolite concentrations used in this study. They correspond approximately to the total metabolite concentrations and the intracellular conditions found experimentally.

Table 2.

Basic data used for the model study with effectors of hexokinase and pyruvate kinase

Intraerythrocytic conditions, i.e. KCl = 130 mM; NaCl = 10 mM; pH 7.2; I = 0.16; oxygenated hemoglobin = 5 mM; 37° C.

Metabolites	Total concentrations in mM/l red cell water
ATP	1.7 and 3.0
2,3-biphosphoglycerate	7.0 (varied between 3.5 and 14.0)
ADP	0.3
AMP	0.05
phosphoenolpyruvate	0.025
$MgCl_2$	2.0 (and 3.0)

We used two different total magnesium concentrations as indicated in Table 2. In addition, we used a new method for the experimental determination of free magnesium ion concentrations in "thick" hemolysates (Achilles et al., 1975). These hemolysates were obtained by using Triton X-100 or ultra sound to disrupt a cell suspension with a hematocrit of > 95 %. They maintained a normal ATP level for at least half an hour. The experimental figures on the free magnesium ion concentration in these hemolysates correspond better with the calculated data when using 2 mM total magnesium (Scheidt et al., 1975).

Thus, the apparently arbitrary choice of a total magnesium ion concentration of 2 mM (as used in Fig. 8 - 10) seems reasonable. This is based, firstly on the fact that part of the total magnesium binds to the cell membrane (Romero, 1974) and, secondly, on omission of some magnesium binding metabolites of the red cell in our simplified model, as characterized in Table 2.

We chose 2,3-biphosphoglycerate and ATP changes because they can be correlated with well documented data from the literature on the rate of glycolysis in intact erythrocytes. At small 2,3-biphosphoglycerate levels the normal glycolytic rate is doubled. If 2,3-biphosphoglycerate has twice its normal concentration, the glycolytic rate is about 50 % of its normal value. In both cases, the other metabolite concentrations show practically no change (Deuticke et al., 1971; Ponce et al., 1971).

For calculations of the changes of the whole complex pattern induced by increasing total 2,3-biphosphoglycerate or total ATP we used the complex formation constants and the binding constants of 2,3-biphosphoglycerate, MgATP and "ATP" with oxygenated hemoglobin, as shown in Table 3 and 4.

Table 3.

log of the complex formation constants used for the calculation of the complex pattern under intraerythrocytic conditions (those of the protonated species in brackets)

	H^+	Mg^{2+}	K^+	Na^+
DPG	8.21 (6.63)	3.87 (7.05)	1.93 (7.23)	1.93 (7.27)
ATP	6.95	4.96 (4.84)	1.15	1.18
ADP	6.73	3.54 (5.16)	0.74	0.83
AMP	6.37	1.70	0.20	0.46
PEP	6.36	2.33	0.65	0.71

Table 4.

log of the binding constants between oxygenated hemoglobin MgATP, ATP and 2,3-biphosphoglycerate (ATP and 2,3-biphosphoglycerate indicating the sum of all other species except the magnesium complexes under intraerythrocytic conditions, according to Gerber et al. (1973))

MgATP	ATP	2,3-biphosphoglycerate
1.59	2.56	2.40

Fig. 8 displays the calculated shifts of three important complex species, when total 2,3-biphosphoglycerate is increased from 3.5 to 14 mM.

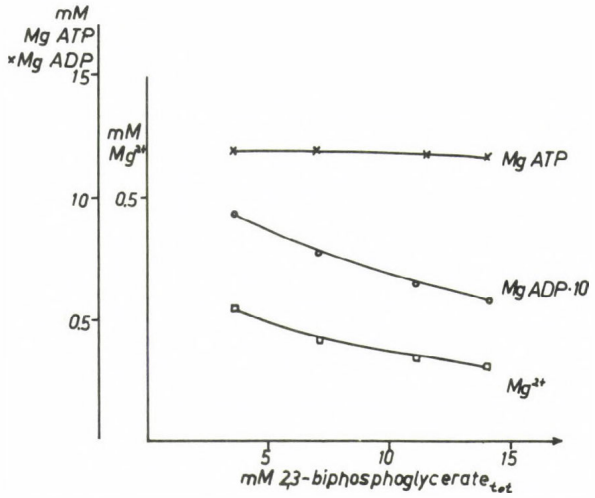

Fig. 8. Changes in the concentration of MgATP, MgADP and Mg^{2+} induced by increasing total 2,3-biphosphoglycerate, all other total metabolite concentrations (Table 2) being kept constant.

Contrary to intuitive expectations, MgATP, the substrate of hexokinase, remains fairly constant. This is caused firstly by the high affinity of ATP to Mg^{2+} and the lower affinity of 2,3-biphosphoglycerate to Mg^{2+}. Secondly, by increasing 2,3-biphosphoglycerate, MgATP, initially bound to oxygenated hemoglobin, is released to a certain extent by competition with 2,3-biphosphoglycerate. On the other hand, MgADP, one substrate of pyruvate kinase, decreases markedly with increasing 2,3-biphosphoglycerate. Lastly, Mg^{2+}, which activates both kinases, also falls.

Here, one should emphasize that the changes observed at the level of a single species are relatively small. However, several species act simultaneously on one enzyme and their concentrations are altered coincidently. Thus, one has to expect cooperative effects on the enzyme activities by transformation of the signal 2,3-biphosphoglycerate via complex equilibria into many subsignals, capable of altering the enzyme activity considerably although the total concentrations of the substrates of both kinases remain absolutely constant.

Of course, with hexokinase a direct inhibitory effect of 2,3-biphosphoglycerate has to be taken into account. As to pyruvate kinase, this is not the case. 2,3-biphosphoglycerate inhibition of pyruvate kinase is caused by binding of the activator Mg^{2+} to 2,3-biphosphoglycerate. Thus, direct inhibition of pyruvate kinase was not included in the pyruvate kinase effector pattern.

Table 5.

Dissociation constants for the different enzyme complexes of red cell hexokinase (glucose present in saturating amounts)

	mM	
$K_{Mg^{2+}}$	= 0.77	(activator)
K_{MgATP}	= 1.03	(substrate)
$K_{2,3\text{-biphosphoglycerate}}$	= 3.44	(competitive inhibitors against MgATP)
K_{ATP}	= 1.00	

In order to quantitate the effects of the 2,3-biphosphoglycerate induced changes of the complex pattern on the activities of hexokinase and pyruvate kinase, the initial velocities were calculated for both kinases with the association and dissociation constants, respectively, for the different enzyme complexes as shown in Table 2 and 5 and the calculated complex pattern shown in part in Fig. 9.

As is to be expected, the initial velocities of both kinases decrease concomitantly as 2,3-biphosphoglycerate increases. The hexokinase decrease is more pronounced than is the pyruvate kinase. The calculated inhibition of both kinases corresponds roughly to the observed inhibition of the glycolytic flux in intact cells with increasing 2,3-biphosphoglycerate, the total concentrations of ATP, ADP, phosphoenolpyruvate and magnesium remaining constant.

Of course, not all interactions that might occur in intact cells are taken into account in our model. But the cooperative behaviour of both kinases in the simplified model, where we compare only the initial velocities under the influence of a few effectors, points to the importance

of a multistep control of both enzymes via complex formation.

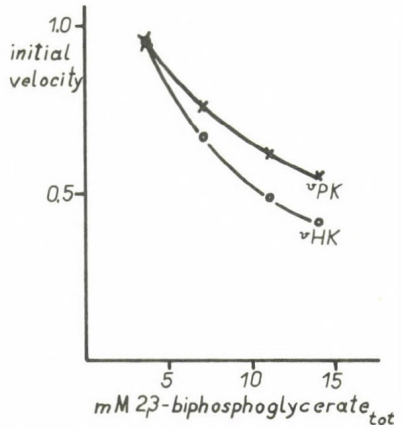

Fig. 9. Initial velocities of red cell hexokinase and pyruvate kinase (arbitrary units) at increasing total 2,3-biphosphoglycerate and constant total concentrations of all other metabolites.

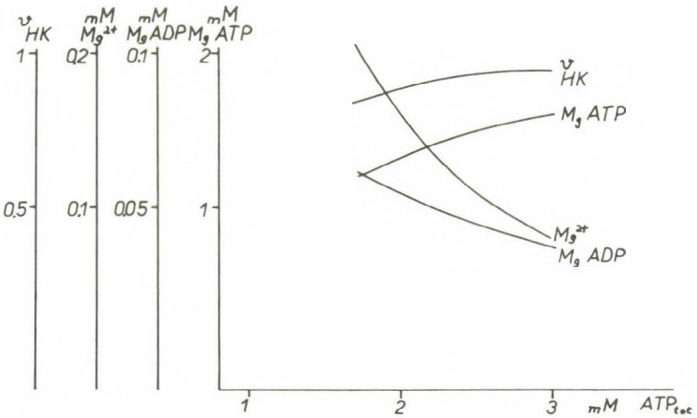

Fig. 10. Changes in concentrations of Mg^{2+}, MgADP and MgATP induced by increasing total ATP from its normal value of 1.7 mM to 3 mM. The calculated initial velocity of hexokinase (v_{HK}) is also plotted, using the dissociation constants stated in Table 5.

The second example deals with another metabolic situation, namely doubling total ATP without changing the other metabolite levels. This can easily be achieved by a few hours incubation of erythrocytes with adenosin or inosine. Under these conditions there are normal 2,3-biphosphoglycerate levels and also normal overall glycolysis (Rubinstein et al., 1972).

Fig. 10 gives the changes of three complex species by increasing total ATP above normal.

The level of MgATP increases only slightly, due firstly to the fixed amount of total magnesium, which is 2 mM, and secondly due to an increased binding of ATP, not complexed with magnesium ions to oxygenated hemoglobin. MgADP and Mg^{2+} decrease considerably. The steep increase of total ATP with a concomitant slight increase of MgATP alters the hexokinase activity only minimally. This is caused mainly by the decreasing level of free magnesium ions which is inhibiting for the hexokinase. The result of this example corresponds to unaltered glycolysis in intact cells when total ATP rises above normal.

SUMMARY

1. Complex formation has to be taken into account for enzyme kinetic measurements with complex forming substrates and effectors. However, an experimentally determined relation between the effector concentrations and the enzyme activity cannot be uniquely described in terms of what species acts as substrate, activator or inhibitor. From this relation we may deduce only the stoichiometry of the reactive enzyme complex and the effector competition for the different binding sites of the enzyme. This is sufficient for a unique description of the behaviour of an enzyme as a member of a metabolic pathway.
2. Complex formation is in action for a multistep control of enzyme sequences in intact cells. It works as a preset control, which links several enzymes of a sequence to each other by interactions at the metabolite level.
3. Complex formation might also be important for the integration of different metabolic functions in compartmentalized cells. This, however, remains to be elucidated.

REFERENCES

Achilles, W., Scheidt, B. Hoppe, H. and Cumme, G.A. (1975). Acta Biol. Med. Germ., submitted to publication.

Berger, H., Jänig, G.-R., Gerber, G., Ruckpaul, K. and Rapoport, S.M. (1973). Eur. J. Biochem. 38, 553.

Cumme, G.A., Horn, A. and Achilles, W. (1973a). Acta Biol. Med. Germ. 31, 343.

Cumme, G.A., Horn, A., Bublitz, R. and Achilles, W. (1973b). Acta Biol. Med. Germ. 31, 771.

Deuticke, B., Duhm, J. and Dierkesmann, R. (1971). Pflügers Arch. 326, 15.

Duhm, J., Deuticke, B. and Gerlach, E. (1968). in "Metabolism and Membrane Permeability of Erythrocytes and Thrombocytes" (G. Thieme Verlag, Stuttgart) p. 69.

Gerber, G., Berger, H., Jänig, G.-R. and Rapoport, S.M. (1973). Eur. J. Biochem. 38, 563.

Gerber, G., Preissler, H., Heinrich, R. and Rapoport, S.M. (1974). Eur. J. Biochem. 45, 39.

Ponce, J., Roth, S. and Harkness, D.R. (1971). Biochim. Biophys. Acta 250, 63.
Purich, D.L. and Fromm, H.J. (1972). Biochem. J. 130, 63.
Romero, P.J. (1974). Biochim. Biophys. Acta 339, 116.
Rubinstein, D., Lerner, M.W. and Novosad, F. (1972). in "VI. Internationales Symposium über Struktur und Funktion der Erythrozyten" (Akademie Verlag, Berlin) p. 363.
Scheidt, B., Achilles, W., Frunder, H. and Winnefeld, K. (1975). Acta Biol. Med. Germ., submitted to publication.

Symp. Biol. Hung. 18, pp. 159–171 (1974)

Near-Equilibrium Reactions and the Regulation of Pathways

Jens Georg Reich
Zentralinstitut für Molekularbiologie
Bereich Methodik und Theorie
Berlin-Buch (DDR)

I. Introduction

The term "near-equilibrium relation" has been used in several papers by Krebs (ref.1-3), but a similiar concept has been applied in earlier work already by other authors (ref.4-6). The basic idea is simple: If the catalytic capacity of an enzyme in the cell is much higher than that of the other enzymes which react with common substrates, then it will bring its own reaction partners very close to thermodynamic equilibrium.
In the context of dehydrogenases, this principle has been used very widely to study and interpret the redox state of pyridine nucleotides in various compartments of the living cell (ref.7.). There are numerous papers, especially in the physiological field, which make use of metabolite ratios for the study of the intermediary metabolism.
Usually the application ot the idea is of technical nature. One uses the equilibrium in order to calculate one inaccessible quantity from another one which is more easily available. A theoretical treatment of the equilibrium principle is still lacking, although several papers (e.g. 8,9) provide the necessary apparatus. My Dobogokö lecture is intended as an outline of a theoretical treatment of the near-equilibrium problem with the aim to make some of the tacit implications of the usual argumentation explicit and available for criticism.

II. Equilibrium and Characteristic Time of the Single Reaction

II.1. Equilibrium and Reversibility

The concept as shortly outlined in the introduction presupposes the validity of the formalism of equilibrium thermodynamics, in particular that any reaction is principally reversible provided that the chemical potential of the reactant is reversed, and that a unique equilibrium exists, as defined by the equilibrium mass action ratio. Furthermore, it implies that for a reaction (example)

$$A + B \rightleftharpoons P + Q \qquad (1)$$

with actual mass action ratio

$$G = \frac{P \cdot Q}{A \cdot B} \qquad \text{(letters for concentrations)} \tag{2}$$

the velocity of the enzyme catalyzed reaction can be written down as function of the deviation from equilibrium. In Cleland's standard notation (ref.10):

$$v = \frac{V_1 V_2 (AB - PQ/K_{eq})}{C} \qquad \begin{array}{ll} v, V_1, V_2 & - \text{ mM/min} \\ A, B, P, Q & - \text{ mM} \\ K_{eq} & - \text{ dimensionless} \\ C & - \text{ mM}^3/\text{min}, \end{array} \tag{3}$$

where C is a kinetic term which depends on the concentration of the reactants and on the catalytic mechanism. To give an example, for a rapid equilibrium random bi bi mechanism C reads:

$$C = V_2 K_b K_{ia} + K_b V_2 A + K_a V_2 B + V_2 AB + K_q V_1 P/K_{eq} + K_p V_1 Q/K_{eq} + V_1 PQ/K_{eq} \tag{4}$$

where the K's are in mM.
Within the cell, the parameters K_{eq}, V_i and the K's may be considered as approximately constant, while the reactants A, B, P, Q are variables. They are kept in the same concentration range (millimolar) and only rarely vary by more than one order of magnitude under different metabolic conditions. This means that, if K_{eq} is high or low enough (say, 10^7 or 10^{-7}), either the second or the first term (respectively) of the bracket which stands in eq. (3) is negligible (as compared to its companion). Such reactions are called quasiirreversible. It is well known that many key reactions of metabolism are of this type. They are irreversible because the reversal of the chemical potential is practically not possible.
All other reactions must in practice be considered as reversible.

Their rate equation has the full form of eq. (3). Now a reaction is said to be near-equilibrium if the actual ratio G does not depart too far from the equilibrium value K_{eq}. For several reasons the biochemical practician does not set the limit too narrow and speaks of near-equilibrium when G and K_{eq} are in the same range, say

$$0.3 < G/K_{eq} < 3. \tag{5}$$

II.2. Rapid and Slow Reactions

A further implication of the basic concept is that the individual reaction can be classified as rapid or slow. This presupposes a time scale for comparison. The actual range of the velocity of a reaction cannot be taken as measure, because in the steady-state all reactions proceed with about the same net velocity. A time scale can be obtained, however, when the rate with which the reaction tends to equilibrium is considered.

To this purpose the rate equation (3) is rearranged. Without loss of generality one can choose the reaction direction such that $AB > PQ/K_{eq}$. Dividing (3) by

V_2AB one has

$$v = \frac{V_1}{D} \quad (1 - G/K_{eq}) \tag{6}$$

with a dimensionless quantity

$$D = C/V_2AB \geq 1 \ . \tag{7}$$

Equation (6) was derived for a special example, but it can be shown that any steady-state rate equation can be formulated in the same manner. The catalytic mechanism manifests itself in the form of the term D. V_1 is the maximal capacity of the reaction in the direction of net reaction: D can be considered as a brake which reduces this maximal velocity to the actual capacity V_1/D. The bracket is a driving-force term and depends on the thermodynamic properties of the reaction. Thus the rate equation consists of three terms: kinetic term, affinity term and thermodynamic term (V_1, D, bracket).

Now consider the actual situation with given A, B, P, Q and the pertinent equilibrium defined by $\overline{A}, \overline{B}, \overline{P}, \overline{Q}$ whose mass action ratio equals K_{eq}. This unique equilibrium can be attained by a reaction step d such that

$$\overline{A} = A - d \ ; \ \overline{B} = B - d \ ; \ \overline{P} = P + d \ ; \ \overline{Q} = Q + d. \tag{8}$$

Inserting this into (6), one obtains, neglecting d in comparison to A, B, P, Q, after some manipulation

$$v = V_1/D \cdot (1/\overline{A} + 1/\overline{B} + K_{eq}/\overline{P} + K_{eq}/\overline{Q}) \cdot d, \tag{9}$$

or, as a characteristic time

$$t^+ = d/v = D/V_1/ \ (1/\overline{A} + 1/\overline{B} + K_{eq}/\overline{P} + K_{eq}/\overline{Q}). \tag{10}$$

The reaction, if undisturbed, tends to equilibrium within a time of order t^+ (see ref. 8). This time is a measure of fastness or slowness of a reaction.

It is important to note that authors usually consider a reaction as fast if V_{max} is high enough. Eq. (10) shows that this is only part of the truth. t^+ depends also on D and on the bracket term. The expression looks involved, but can be usually simplified in the practical case. So, for instance, the bracket is mostly dominated by one of its terms, say $1/\overline{A}$, since one of the partners is considerably smaller (like NADH for cytoplasmic dehydrogenases). Also D is usually approximated by one of its terms. If the enzyme is saturated by its partners, this dominating term will be unity, otherwise it will be a quantity of the form $K/\overline{B}$. Thus two limiting cases may be distinguished, one with the enzyme saturated:

$$t^+ \approx \overline{A}/V_1 \quad \text{(A-smallest metabolite)}, \tag{11}$$

the other one with unsaturated enzyme:

$$t^+ \approx L/V_1, \tag{12}$$

where L is an affinity parameter (either constant or of form $K \cdot \bar{A}/B$), which can be very high in the case of low affinity to the enzyme or of excess inhibition by substrate. Such cases are by no means rare (e.g. GAPDH inhibited by substrate (ref. 11-13), or LDH inhibited by abortive complex (Kurganov's calculation, personal communication). Therefore a high V_{max} as the only sign of a rapid enzyme can lead astray. One should always investigate the kinetic situation under cellular conditions.

III. Interaction of Rapid Enzyme with Slow Neighbours

So far we have treated the isolated reaction and its tendency towards equilibrium. In the cell no reaction is isolated. This offsets the equilibrium continuously and even drives its position away. To study this motion we will take a very simple model example, a fast dehydrogenase whose substrate partakes at a slow side pathway:

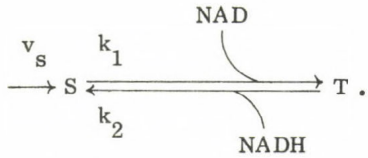

(13)

Let us assume that the rate equation of the fast dehydrogenase has the following simple form:

$$w = k_1 \cdot (NAD) \cdot (S) \, (1 - G/K_{eq}) \tag{14}$$

$$G = (NADH) \cdot (T)/((NAD) \cdot (S)) \, .$$

The side flux is slow, which is equivalent to

$$\varepsilon \equiv \frac{v_s}{k_1 \cdot NAD \cdot S} \ll 1 \, . \tag{15}$$

In the stationary state ($v_s - w = 0$):

$$\tilde{\varepsilon} - (1 - \tilde{G}/K_{eq}) = 0 \tag{16}$$

with the stationary values $\tilde{S}, \tilde{T}, \widetilde{NAD}$, and $\widetilde{NADH}$ inserted into ε and G. It follows that

$$\tilde{G} = K_{eq} \, (1 - \tilde{\varepsilon}) \, , \tag{17}$$

or

$$\frac{\widetilde{NADH}}{\widetilde{NAD}} = \tilde{S}/\tilde{T} \cdot K_{eq} \, (1 - \tilde{\varepsilon}), \tag{17a}$$

which demonstrates that the cofactor ratio can be approximated by the substrate ratio to accuracy $1-\bar{\varepsilon}$ where $\bar{\varepsilon}$ is the stationary ratio between drift flux and actual capacity of the dehydrogenase. The wording "actual" is of importance, because authors usually take the maximal capacity as indicator of an equilibrium enzyme (ref. 2, 6). Generally the actual capacity is given by an expression of form V_1/D (see previous section).

If we compare the accuracy expression (17) with the practical requirements (eq. (5)), we see that already a moderate excess capacity (3-5 fold of flux) is sufficient to establish near equilibrium conditions. Thus the potential activity of a candidate for an equilibrium enzyme need not be astronomical. This is of importance for the judgment of the metabolic character of several enzymes (e.g. malic enzyme (ref. 2)). On the other hand, one must have very strong arguments to reject an enzyme as candidate if his activity is high as compared with flux and no evident strong inhibition brings its potential down to the flux value.

IV. Temporal Hierarchy of Cofactor-Coupled Fast Reactions

Usually a considerable number of fast and slow reactions take part at the interconversion of a cofactor pair like NAD-NADH or ATP-ADP. Since the substrates pertain to different pathways, this introduces a very characteristic temporal organization. We propose to study this with a model example:

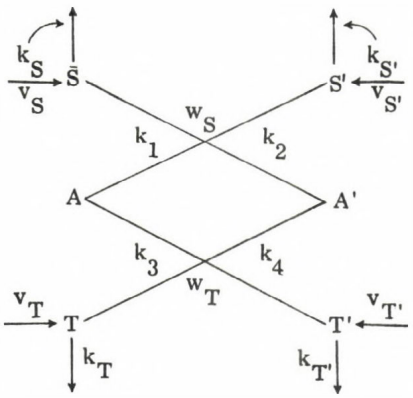

(18)

The following simplifying assumptions are assumed valid: i) substrate levels higher than cofactor levels:

$$A + A' \equiv A_o \ll S, T, T', S' \tag{19}$$

This holds especially in the general case when a big number of enzymes is connected to the cofactor pair.

ii) the side fluxes are slow and the cofactor reactions rapid, i.e.

$$k_1 A_o S \gg v_S, k_S$$

$$k_2 A_o S' \gg v_{S'}, k_{S'} \quad \text{etc. for all metabolites.} \tag{20}$$

iii) The reactions are described by simple rate laws:

$$w_s = k_1 \cdot A \cdot S - k_2 \cdot A' \cdot S' \tag{21a}$$

$$w_T = k_3 \cdot A \cdot T - k_4 \cdot A' \cdot T' \tag{21b}$$

$$v_d = k_S \cdot S \quad \text{(side drift from S)}, \tag{21c}$$

and expressions similiar to (21 c) for the side drift of the rest of metabolites.

These considerations lead to the system of equations

$$\begin{aligned} dS/dt &= v_s - k_S \cdot S - w_S \\ dS'/dt &= v_{S'} - k_{S'} \cdot S' + w_S \\ dT/dt &= v_T - k_T \cdot T - w_T \\ dT'/dt &= v_{T'} - k_{T'} \cdot T' + w_T \\ dA/dt &= - (w_S + w_T) \\ A' &= A_o - A , \end{aligned} \tag{22}$$

whose treatment in the given dimensional form is somewhat inconvenient. Therefore dimensionless variables are introduced (Greek letters):

$$\tau = k_S t; \qquad \sigma = S \cdot k_S/v_S; \qquad \sigma' = S' \cdot k_{S'}/v_{S'},$$

$$\theta = T \cdot k_S/v_S; \qquad \theta' = T' \cdot k_S/v_S \tag{23}$$

$$\alpha = A/A_o; \qquad K_s = k_1/k_2 ; \qquad K_T = k_3/k_4 \quad \text{(equil. constants)}.$$

The following scaling factors are convenient

$\mu = k_3/k_1$ (ratio of capacity of dehydrogenases);

$$\varepsilon_1 = k_s/(k_1 A_o) \ll 1 \text{ (fast dehydrogenase, see (20))}; \tag{24}$$

$\varepsilon_2 = k_s A_o/v_s \ll 1$ (because of small cofactor concentrations).

With these new variables, the system (22) can be restated in dimensionless form. We write down only the equations for α and σ, since for the other metabolites they are similiar in form as that for σ :

$$d\alpha/d\tau = -\frac{1}{\varepsilon_1}\,\frac{1}{\varepsilon_2}\left\{\alpha\sigma - \frac{(1-\alpha)\sigma'}{K_S} + \mu\alpha\theta - \mu\,\frac{(1-\alpha)\,\theta'}{K_T}\right\} \tag{25a}$$

$$d\sigma/d\tau = 1 - \sigma - \frac{1}{\varepsilon_1}\left\{\alpha\sigma - \frac{(1-\alpha)\sigma'}{K_S}\right\} \tag{25b}$$

The properties of these equations in different time scales will now be studied.

IV.1. First Time Scale: Ultrarapid Equilibration of Cofactor

Introducing the very short time scale $\tau^* = \tau / \varepsilon_1 \varepsilon_2$, one has

$$d\alpha/d\tau^* = -\alpha\left\{\sigma + \frac{\sigma'}{K_S} + \mu\theta + \mu\,\frac{\theta'}{K_T}\right\} + \left\{\frac{\sigma'}{K_S} + \mu\,\frac{\theta'}{K_T}\right\} \tag{26}$$

while the other variables σ, σ', θ, θ' get equations of the form

$$d\sigma/d\tau^* = \varepsilon_1\varepsilon_2(1-\sigma) - \varepsilon_2\left\{\alpha\sigma - \frac{(1-\alpha)\sigma'}{K_S}\right\} \tag{27}$$

which reduce to σ, σ, θ, and θ' = const. because of the small ε' s.
The further analysis of equation (26) will be given in summarized form:

i) α approaches its steady-state value $\tilde{\alpha}$, as defined by $d\alpha / d\tau^* = 0$, in a first-order reaction.

ii) The rate constant of this process is a weighted sum of rapid reactions ($\mu + 1$). In a metabolic system with many rapid reactions it would be a very fast process.

iii) The cofactor ratio $\tilde{\alpha} / (1 - \tilde{\alpha})$ lies between the equilibria $K_T\ \theta / \theta'$ and $K_S\ \sigma / \sigma'$ of the individual reactions. It would approach one of them if either $\mu \to 0$ or $\mu \to \infty$.

iv) $\tilde{\alpha}$ is unique if the cofactor reactions are monotonous in α; otherwise it may happen that two different steady-states of the cofactor ratio are possible. This could exert great influence on the velocity of the further equilibration. This is a further point while anomalies in the kinetics of fast enzymes should be carefully studied.

IV.2. Second Time Scale: Rapid Exchange between Metabolites

Once α has reached $\tilde{\alpha}$ it behaves as a slowly drifting steady-state parameter. The essential motion is now on the still rather short time scale $\tau^+ = \tau / \varepsilon_1$. Insertion of $\tilde{\alpha}$ in (25 b) and transition to τ^+ results in:

$$d\sigma/d\tau^+ = - \frac{\sigma\theta' - \frac{\sigma'\theta}{K_\Omega}}{M} + \varepsilon_1 (1 - \sigma) \tag{28a}$$

with

$$K_\Omega = K_S/K_T \text{ (overall equilibrium of two reactions)} \tag{28b}$$

$$M = \frac{K_T}{\mu}\sigma + \frac{K_T}{K_S\mu}\sigma' + K_T\theta + \theta' \quad \text{(kinetic term).} \tag{28c}$$

Analysis of these expressions reveals:

Neglecting the small ε_1-drift, one has the kinetic pattern of a combined essential reaction

$$\sigma + \theta' \overset{K_\Omega}{\rightleftharpoons} \sigma' + \theta \tag{29}$$

This means that the material is directly rearranged between the pathways which feed the metabolites. There is a new kinetic term M which expresses the catalytic function of the cofactor. The special form of the result (29) depends on the simple form of the original reactions (eq. 21). But even if the constituent reactions have the full Cleland form (eq. 3), the same result is obtained only M can no longer be stated explicitly.

IV.3. Third Time Scale: Drift of Metabolic Equilibria

Once the fast reactions which together perform the cooperative reaction (29), namely w_S and w_T, have attained their combined steady-state, all metabolites have near-equilibrium values, which are defined by $d\sigma/d\tau^+ = 0$ and so on for the other metabolites. The side fluxes (see scheme 18) maintain a slow drift of the steady-state of the system. Only a sudden burst of incoming metabolic material (e.g. sudden lactate affluence from glycolysis) is capable to excite the equilibrium such that all the time scales just analyzed come once more into play.

It should be pointed out that on the third, slow scale the old variables (metabolites) are no longer independent. The essential variables of the slow scale become

transparent after introduction of (S + A' + T), (T + T') and (S + S') into the motion equations:

$$d(S + T + A')/dt = v_S + v_T - k_S S - k_T T \tag{30A}$$

$$d(T + T')/dt = v_T + v_{T'} - k_T T - k_{T'} T' \tag{30b}$$

$$d(S + S')/dt = v_S + v_{S'} - k_S S - k_{S'} S'. \tag{30c}$$

It is seen that the motion is slow. The right-hand sides are uniquely determined by the state of the new variables. The metabolic interpretation of these equations is that two of them (30 b and c) represent the motion of carriers (e.g. common backbone of lactate and pyruvate), while the first one concerns the motion of the chemical material attached to them (like H_2 to the lac-pyr system), in other words of the occupancy of the carriers.

Thus on the slow scale a system of carriers and attached metabolic equivalents (H_2, energy-rich bonds etc.) appears as the essential substructure of the metabolic network. The system is connected by fast reactions which on a faster time scale establish near-equilibrium of the partners. The near-equilibrium is a state where the degree of occupancy of the carriers is thermodynamically equivalent (e.g. same redox potential). This does not mean that the actual occupancy is identical. Therefore greatly differing metabolic ratios are compatible with equilibrium, depending on the standard potential of the respective reactions (see ref. 1-3, 7).

V) Fast Reactions in Metabolic Systems

In metabolic systems fast and slow processes are interconnected so that a clear separation of the time levels is not possible on the basis of the original biochemical variables (metabolites). Since the detailed technique to perform the required transformations and limit transitions has been the object of my paper at the FEBS-Meeting in Budapest (to be published in Biosystems), I quote only a rather simple example and proceed with several summarizing statements on the regulation of metabolic pathways.

V.1.) Transformation to Essential Motion: Adenine Nucleotides

Consider the following, somewhat embryonic model of energy metabolism, where the designations u, v, w indicate rate equations of (respectively) very fast, fast and slow characteristic time (see section II.2):

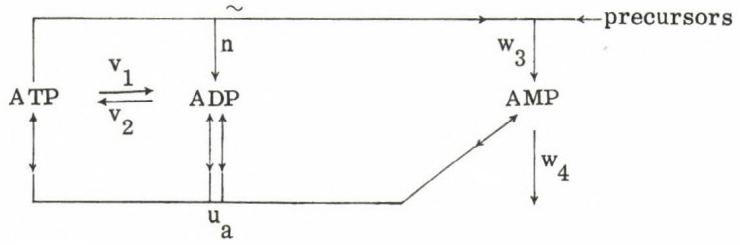

(31)

where

v_1 - rate of ATP-consumption (fast, 10^0 min)
v_2 - rate of ATP-generation (fast, 10^0 min)
u_a - rate of adenylate kinase (very fast, 10^{-1} min)
w_3 - rate of adenylate synthesis from precursor (slow, 10^1 min)
w_4 - rate of adenylate decay (slow, 10^1 min).

The system of differential equations reads

$$\begin{aligned} da_3/dt &= -v_1 + v_2 + u_a - nw_3 \\ da_2/dt &= v_1 - v_2 - 2u_a + nw_3 \\ da_1/dt &= u_a + w_3 - w_4 \end{aligned} \tag{32}$$

where the precise stoichiometry (value of n ATP required to make one new AMP-backbone) depends on the precursor and on the chosen metabolic pathway. System (32) displays the mixture of velocity scales which is typical for metabolic systems. Introduction of a new set of essential variables

$$\begin{aligned} a &= a_3 + a_2 + a_1 && \text{(sum of adenylate nucleotide)} \\ s &= 2a_3 + a_2 && \text{(sum of energy-rich bonds)} \\ p &= a_3 + a_2 && \text{(sum of energy containing nucleotides)} \end{aligned} \tag{33}$$

and differentiation of them results in

$$\begin{aligned} da/dt &= w_3 - w_4 && \text{(motion of energy carriers, slow)} \\ ds/dt &= v_2 - v_1 - nw_3 && \text{(energy balance, fast)} \\ dp/dt &= - u_a && \text{(energy distribution, very fast)} \end{aligned} \tag{34}$$

with essentially three time levels and one essential motion on each of them. Reduction of the order of the system is therefore possible after choice of the time scale at which the biochemist is interested to study his phenomena. For instance, if the energy balance is to be studied, all rate equations have to be transformed into the time scale of the v's:

$$\begin{aligned} da/dt &= \varepsilon_1 (w_3 - w_4) \\ ds/dt &= v_2 - v_1 - \varepsilon_1 nw_3 \\ dp/dt &= - \frac{1}{\varepsilon_2} v_a \end{aligned} \qquad (v_i \text{ of equal order}). \tag{35}$$

Now the transitions $\varepsilon_1 \to 0$ (i.e. a= constant) and $\varepsilon_2 \to 0$ (which sets adenylate kinase to equilibrium: the transformation is of the type to which Tikhonov's theorem can be applied (see ref. 14,15)) display the essential motion of s, where the right-hand sides depend on a_3, a_2, a_1 which can be calculated from the actual state of the essential variable s, and from the value of the essential parameters a and K_{eq} (adenylate kinase).

V.2) Near-Equilibrium Reactions: Summary and Conclusions

1.) Metabolic Systems are obviously organized such that the motion can be approximately classified according to logarithmic time scales. The scale of an individual reaction is to be understood as the time in which it, if left alone, would run to equilibrium (approximately).

2. If at a specified time level a reaction is fast, it will keep near-equilibrium of its partners whatever the metabolic drift will be. The fastness depends not only on V_{max} but also on the kinetic state of the enzyme which must not be neglected therefore. The equilibrium assumption, if so established, may be used to calculate concentrations or concentration ratios of otherwise not measurable metabolites.

3. The accuracy of the equilibrium assumption depends on the time scale of the side flux (slow drift) and on the actual capacity of the enzyme. The latter is composed of a kinetic term (V_{max}) and an affinity term (D). If the accuracy requirements are moderate, the ratio between the slow and the fast reactions need not be astronomical, a capacity excess of 3 to 5 is sufficient to maintain a state not far from equilibrium.

4. Within the cell, the equilibrium of the fast reaction is continuously disturbed ("excited", ref.8), and it is of importance to study the time course of equilibration. For one fast reaction in the environment of slow ones this analysis has been outlined in section IV. The principal event is fast equilibration of the reaction followed by slow drift of the equilibrium.

5. The matter becomes more complicated when several fast reactions cooperate in a metabolic knot via common substrates or cofactors. The fast time scale now splits into an ultrafast and a fast component. The very rapid phase comprises cofactors which are involved in several or all fast reactions. They go into a preequilibrium whose position need not be unique if the fast reactions do not depend monotonously on the cofactor. Thus several preequilibria may exist.

Whatever the preequilibrium, a further still fast phase comprises the approach to equilibrium of the individual metabolites. The final near-equilibrium of all fast reactions is unique, only the velocity of the approach to it is dependent on the different possible preequilibria just mentioned.

6. A set of fast reactions imposes a subset of near-equilibrium relations (NER, for short) among the original metabolites like NAD, NADH, ATP, Lac, Pyr, GAP, FDP etc. These cease to be independent variables on the slow metabolic scale. The real structure of the motion must therefore be expressed by new equations in essential variables and parameters. The latter are combinations of the phenomenological quantities. The typical new variables in a system where approximate NER hold is the pool, either in the form of a carrier pool (like AMP, Pyr, oxaloacetate etc.) or as metabolic pools of material attached to the carriers (e.g. energy-rich bonds or H_2-equivalents etc.). Sometimes the degree of occupation of carrier places (i.e. a ratio metabolic pool over carrier) may be an essential variable (such as energy-charge (ref.16) or degree of reduction (ref.17)).

7. The motion of the essential variables is described by a set of (slow) differential equations (e.g. ds/dt in (35)). The mathematical difficulty is that their right-hand sides are usually not known as explicit functions of the essential variables, but rather of phenomenological quantities, namely the metabolites. The latter are uniquely determined by the former (in a mathematical sense) through a set of linear relations (definition equations like (33)) and through an additional set of NER which, however, are linear in the chemical potential of the metabolites (i.e. in the log of their concentrations).

8. At any change of the metabolic situation, the substructure of NER becomes rearranged nearly instantaneously. Since, by way of common substrates and cofactors, the fast reactions form a complicated topological network, near-equilibrium of combined reactions ("super-reactions") is established. We will study an illustrative example:

$$1/2\ \mathrm{AMP} + (\mathrm{GAP\text{-}DOAP\text{-}FDP}) + \mathrm{Pyr} + \mathrm{P_i} = 1/2\ \mathrm{ATP} + \mathrm{Lac} + (\mathrm{PGS\text{-}PEP}), \qquad (36)$$

the partners of which are near-equilibrium when, as usually, GAPDH, LDH, PGK and adenylate kinase are fast.

9. Such combined equilibria introduce a rigid stoichiometric linkage into the system of metabolites. One consequence of this is buffering of metabolites, in particular of small ones. If in eq. (36), for instance, AMP is the smallest metabolite, then an attempt to remove it would turn out futile, because the loss would be replaced by a small step from right to left in the equilibrium.

10. A further curious consequence might be the possibility to rally metabolic material without damaging effects to the metabolic system. So in the same example the injection of lactate (or P_i) would have no other direct consequence than a slight increase (or decrease) of AMP to reestablish the equilibrium. Due to the stoichiometric linkage this small change would not affect the other partners.

11. Of course, to quite distant metabolic sensors this change in a small metabolite like AMP could be a signal to react to the sudden affluence. In a recently submitted paper (ref.17) we have called this the pointer property of certain small metabolites (like AMP or NADH or NADP) which triggers counter-measures in the case of imminent danger.

It is seen that distance effects are not a monopoly of allosteric systems, but rather may be brought about by equilibrium relations.

12. As we have pointed out in detail in ref. 17, the experimental approach to the metabolic importance of fast reactions has to be different from the usual concept which "sticks" too much to the original biochemical variables. So, for instance, adenylate deaminase's function is quite incomprehensible if its kinetics is always measured with single metabolites which never occur isolated in vivo. Atkinson (ref. 18) has shown how the matter becomes immediately transparent when the true variables are varied (adenylate content and energy charge).

13. Thus the NER have consequences which are not trivial and to my mind not sufficiently understood. Since the kinetic requirements for a NER are not too restrictive (see point 3), it can be expected that whole pathways may consist of them and that important distance signals are cinveyed from pathway to pathway. To my mind these facts require some conceptual rearrangement in our understanding of the regulation of pathways.

References

1.) Veech, R.L., Eggleston, L.V. and Krebs, H.A.: Biochem.J.115 (1969) 609.
2.) Krebs, H.A. and Veech, R.L.: Equilibrium Relations between Pyridine Nucleotides and Adenine Nucleotides and their Roles in the Regulation of Metabolic Processes. In: Advances in Enzyme Regulation, vol.7 (1969) 397-413. G. Weber ed. Pergamon Press, Oxford.
3.) Veech, R.L., Raijman, L. and Krebs, H.A.: Biochem. J. 117 (1970) 499.
4.) Holzer, H., Schultz, G. and Lynen, F.: Biochem. Z. 328 (1955) 252.
5.) Bücher, Th. and Klingenberg, M.: Angew. Chemie 70 (1958) 552.
6.) Hohorst, H., Kreutz, F.H. and Bücher, Th.: Biochem. Z. 332 (1959) 18.
7.) Gumaa, K.A., McLean, P. and Greenbaum, A.L.: Compartmentation in Relation to Metabolic Control in Liver. In: Essays in Biochemistry, vol. 7 (1970), pp.39-85, P.N. Campbell and D. Greville eds., Academic Press, New York.
8.) Higgins, J.: Dynamics and Control in Cellular Reactions. In: Control of Energy Metabolism, Chance, B., Estabrook, R.W. and Williamson, J.R., eds., Academic Press, New York-London 1965.
9.) Bücher, Th. and Rüssmann, W.: Angew. Chemie 75 (1964) 881.
10.) Cleland, W.W.: Biochim. Biophys. Acta 67 (1963) 104.
11.) Furfine, C.S. and Velick, S.F.: J. Biol. Chem. 240 (1965) 844.
12.) Greene, F.C. and Feeney, R.E. : Biochim. Biophys. Acta 220 (1970) 430.
13.) Orsi, B.A. and Cleland, W.W.: Biochemistry 11 (1970) 102.
14.) Tikhonov, A.N.: Matematiceskij Zbornik 22 (64) (1948) 193.
15.) Reich, J.G. and Selkov, E.E.: FEBS Letters 40 (1974) S 119 (suppl.)
16.) Atkinson, D.E. and Walton, G.M.: J. Biol. Chem. 242 (1967) 3241.
17.) Kothe, K., Sachsenröder, Ch. and Reich, J.G.: Redox Metabolism of Glutathione in the Erythrocyte, submitted to Acta Biol. Med. Germ. (1975)
18.) Chapman, A.G. and Atkinson, D.E.: J. Biol. Chem. 248 (1973) 8309.

Symp. Biol. Hung. 18, pp. 173–212 (1974)

THE REGULATORY PRINCIPLES OF THE GLYCOLYSIS OF ERYTHROCYTES IN VIVO AND IN VITRO

R. HEINRICH[&] and T.A. RAPOPORT[§]

[&]Humboldt-Universität zu Berlin, Institut f. physiologische und biologische Chemie, Berlin, DDR

[§]Akademie der Wissenschaften der DDR, Zentralinstitut f. Molekularbiologie, Bereich Bioregulation, Berlin- Buch, DDR

INTRODUCTION

The approach of this paper to set up a model of a metabolic system is guided by the following principles:
1) The interaction with experiments is essential for model building, verification and predictions. Idealized models which are not confronted with real experiments are suitable to disclose generalities of regulation but without assurance that they are applicable to the conditions of any real cell.
2) The model should involve as few parameters as possible. Otherwise, they give little insight in the regulatory structure of the system. Simplification of models is possible in view of two principles of model reduction. Firstly, there exist a time hierarchy in metabolic systems. Some variables are so slow that they remain almost constant during a specified time period, other are so fast that they are always in a steady state. A powerful method for the reduction of the number of the variables is provided by the Tichonov-Theorem (Tichonov, 1948; Park, 1974). Parameter reduction results from the fact that the rate laws of the constituent enzymes essential for the metabolism need not include the details of the enzyme mechanisms. It is, for example, sometimes possible to use only first order rate constants in the kinetic equations of enzymes if the substrate concentrations are

always small compared to the corresponding half saturation constants. Furthermore, reactions which are catalyzed by very fast enzymes may be considered to be nearly in equilibrium and are fully characterized by their equilibrium constants.
3) It is necessary to consider the system as a whole, not parts or single steps. Omission of any of the important interactions or stochiometries leads to discrepancies with the experimental data.

The paper gives a mathematical model of the glycolysis of erythrocytes. The erythrocyte glycolysis was chosen for the modelling since 1. it is uncontaminated by other interfering pathways, 2. no intracellular compartments exist and 3. all enzyme concentrations are practically constant.

The present model extents a previous one by explicite inclusion of synthesis and breakdown of ATP in a manner similar to the simplified system of Sel'kov (1973). This was done although many experimental uncertainties concerning the ATP-consuming processes exist. It is hoped that the theoretical results of this paper will stimulate further experiments in this direction. A second goal of the investigation was the detailed analysis of the differences between the conditions in vivo and in vitro. Both steady states and time dependent processes were analyzed.

Abbreviations

G6P, glucose 6-phosphate; F6P, fructose 6-phosphate; FP_2, fructose 1,6-bisphosphate; GAP, glyceraldehyde 3-phosphate; DHAP, dihydroxyacetone phosphate; triose-P, triose phosphate (sum of GAP and DHAP); 1.3 P_2G, 1,3-bisphosphoglycerate; 3 PG, 3-phosphoglycerate; 2 PG, 2-phosphoglycerate; P-Pyr, phosphoenolpyruvate; Pyr, pyruvate; Lac, lactate; 2,3 P_2G, 2,3-bisphosphoglycerate.

1. Confinement of the model

Fig.1 shows the scheme for the glycolytic model. It includes both the ATP- producing reactions catalyzed by the phosphoglycerate kinase and pyruvate kinase and the ATP- consuming reactions catalyzed by hexokinase, phosphofructokinase and ATPases. Since there are several enzymes in red cells which degrade ATP (Nakao, 1974) the term "ATPase" refers not only to the Na^+- K^+- ATPase but to the sum of all ATP- consuming reactions. The system includes furthermore the NAD^+-NADH- coupling of the reactions of glyceraldehyde-P dehydrogenase and lactate dehydrogenase. It takes into account several actions of metabolites as inner effectors of enzymes: the G6P- inhibition of the hexokinase, the ATP- inhibition and AMP- and ADP-activation of the phosphofructokinase and the 2.3 P_2G- inhibition of the 2.3 P_2G- mutase. A characteristic feature of the glycolysis of erythrocytes is the 2.3 P_2G- bypass (Rapoport & Luebering, 1950,1951).

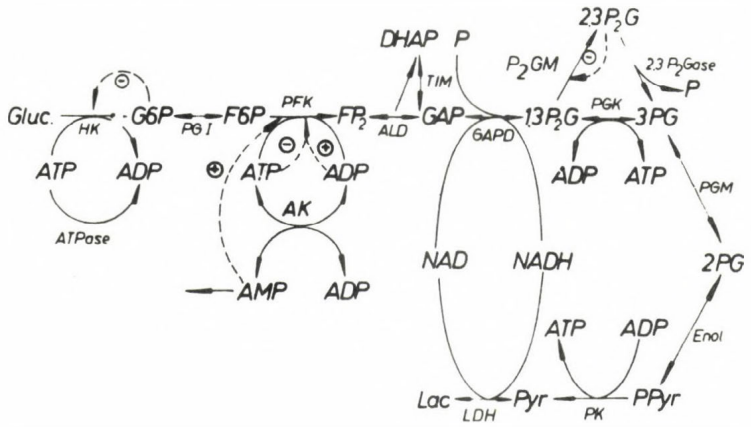

Fig.1. Scheme of the glycolysis of erythrocytes considered for the modelling

The following assumptions were made for the modelling (for justification see Rapoport et al,1974) :

a) One group of enzymes is considered to catalyze very fast reactions so that an approximate equilibrium between the reaction partners is maintained under all conditions. This group of enzymes includes the phosphoglucoisomerase, aldolase, triose-P isomerase, glyceraldehyde-P dehydrogenase, phosphoglycerate kinase, phosphoglycerate mutase, enolase, lactate dehydrogenase and the adenylate kinase.
The following equilibrium relations hold

$$q_{PGI} = \frac{(F6P)}{(G6P)}\ ,\quad q_{Ald} = \frac{(GAP)}{(FP_2)}\ ,\quad q_{TIM} = \frac{(GAP)}{(DHAP)}\ ,$$

$$P_i \cdot q_{GAPD} = q'_{GAPD} = \frac{(1.3P_2G)(NADH)}{(GAP)(NAD^+)}\ ,\quad q_{PGK} = \frac{(3\ PG)(ATP)}{(1.3P_2G)(ADP)} \qquad (1)$$

$$q_{PGM} = \frac{(2PG)}{(3PG)}\ ,\quad q_{Enol} = \frac{(P\text{-}Pyr)}{(2PG)}\ ,$$

$$q_{LDH} = \frac{(Lac)(NAD^+)}{(Pyr)(NADH)}\ ,\quad q_{AK} = \frac{(ADP)^2}{(ATP)(AMP)}\ .$$

A fixed ratio of the concentrations of FP_2 and triose-P was assumed in accord with experimental data. Actually, the equilibrium assumption for the reactions catalyzed by aldolase and triose-P isomerase should lead to a quadratic relation (Rapoport et al, 1974).

b) The other enzymes are considered to catalyze practically irreversible reactions: hexokinase, phosphofructokinase, pyruvate kinase, 2.3 P_2G- mutase, 2.3 P_2G- phosphatase and ATPase. These enzymes are described by kinetic equations (**Table** 1). In most cases descriptive rate laws were used which lack a mechanistical basis.

c) The reactions of the hexokinase and phosphofructokinase are subsumed as one subsystem with a single response to the adenine nucleotides (Rapoport et al,1974).It is assumed that G6P and F6P are always in a steady state. This approximation is justified since the relaxation time of the phosphofructokinase is relatively short.The descriptive rate law given in **Table** 1 is the result of 1. the action

Table 1.

Rate laws assumed for the various enzymatic steps of the model

enzyme	rate law	parameters
hexokinase-phosphofructo-kinase-system	$v_{HK-PFK} = \frac{V_m(ATP)}{K_m+(ATP)}$	V_m, K_m
pyruvate kinase	$v_{PK} = k_{PK}(ADP)(P\text{-}Pyr)$	k_{PK}
2.3 P_2G mutase	$v_{P_2GM} = \frac{k_{P_2GM}(1.3P_2G)}{1+(2.3P_2G)/K_{P_2G}}$	k_{P_2GM}, K_{P_2G}
2.3 P_2G-phosphatase	$v_{P_2Gase} = k_{P_2Gase}(2.3P_2)+C$	k_{P_2Gase}, C
ATPase	$v_{ATPase} = k_{ATPase}(ATP)$	k_{ATPase}

of ATP as the substrate of the hexokinase, 2. of the activating influence of AMP and ADP and the inhibiting effect of ATP on the phosphofructokinase, and 3. of the G6P- inhibition of the hexokinase.

d) For the 2.3 P_2G- phosphatase two terms are assumed, one proportional to its substrate 2.3 P_2G and one independent of it. This assumption is based on the fact that there are several enzymes which degrade 2.3 P_2G (Harkness et al,1970; Rose et al,1970) one of which, the actual 2.3 P_2G-phosphatase, probably works at its V_{max} (Rose & Liebowitz,1970).

e) Complex formation of some metabolites with Mg^{2+} and the binding of anions to hemoglobin was neglected. Both effects have a slight but significant influence on metabolite concentrations (Gerber et al,1973; Berger et al, unpublished results) .

f) Two conservation quantities are taken into account: the sum of the pyridine nucleotides and that of the adenine nucleotides

$$N = (NAD^+) + (NADH) \tag{2}$$

$$A = (AMP) + (ADP) + (ATP) . \tag{3}$$

It is assumed that the processes changing these sums are slow compared to all other reactions included in the model.

g) Inorganic phosphate is taken as an outer parameter which is controlled by the experimenter.

h) Glucose is assumed to be saturating for the hexokinase.

These assumptions are supported by experimental data with the exception of the nonglycolytic ATP- consuming processes which are poorly characterized.

The time dependent changes of the concentrations of the metabolites are described by a set of ordinary differential equations. By consideration of the fluxes which produce and remove the metabolites and taking into account the equilibria (1) one obtains the following equations of motion

$$\frac{d}{dt}(2FP_2+triose-P+1.3P_2G+3PG+2PG+P-Pyr) = 2v_{HK-PFK} - v_{P_2GM} + v_{P_2Gase} + v_{PK} \tag{4}$$

$$\frac{d}{dt}(ATP-AMP- 3PG-2PG-P-Pyr) = -2v_{HK-PFK} - v_{P_2Gase} + 2v_{PK} - v_{ATPase} \tag{5}$$

$$\frac{d}{dt}(2.3P_2G) = v_{P_2GM} - v_{P_2Gase} \tag{6}$$

$$\frac{d}{dt}(Pyr+Lac) = v_{PK} + v_{exchange} \tag{7}$$

Eq. (5) is the result of three differential equations

$$\frac{d(ATP)}{dt} = -2v_{HK\text{-}PFK} + v_{PK} + v^{+}_{PGK} - v^{-}_{PGK} + v^{+}_{AK} - v^{-}_{AK} - v_{ATPase}$$

$$\frac{d(AMP)}{dt} = v^{+}_{AK} - v^{-}_{AK}$$

$$\frac{d}{dt}(3PG + 2PG + P\text{-}Pyr) = v^{+}_{PGK} - v^{-}_{PGK} + v_{P_2Gase} - v_{PK}$$

where the + and - signs indicate the forward and backward reactions, respectively. From these three differential equations the slow motion is extracted described by eqn.(5) (Tichonov,1948; Park,1974).
Introducing the kinetic equations of **Table** 1 the right hand sides of the **Eqs.** (4)-(7) become functions of the metabolite concentrations and the parameters of the enzymes. The differential equations are nonlinear. The metabolite concentrations are determined not only by differential equations (4)-(7) but also by the equilibrium relations (1) and by the conservation equations (2) and (3).

2. The in vivo- system of glycolysis

2.1. The steady states

2.1.1. Steady state equations and general features of the solutions

The steady state solutions for the metabolites can be obtained by setting the time- derivatives on the left side of the differential equations (4)-(7) equal to zero.
The steady state concentrations of pyruvate and lactate can be calculated from Eq. (7) and depend on the term $v_{exchange}$ which is determined by other tissues of the body. Owing to the equilibria at the glyceraldehyde-P dehydrogenase and lactate dehydrogenase the concentrations of FP_2 and triose-P depend also on processes outside of the erythrocytes. On the other hand, since the concentrations of pyruvate and lactate do not appear in **Eqs.** (4)-(6) they do not influence the steady state levels of the other glycolytic metabolites.

One may call therefore the metabolic system described by Eqs. (4)-(6) the "core" of glycolysis. It is essentially the energy metabolism of this pathway.
The steady state equations have now the following form

$$\frac{2V_m(ATP)}{K_m+(ATP)} - \frac{k_{P_2GM}(1.3P_2G)}{1+(2.3P_2G)/K_{P_2G}} + k_{P_2Gase}(2.3P_2G) + C - k_{PK}(ADP)(P\text{-}Pyr) = 0 \qquad (8)$$

$$\frac{k_{P_2GM}(1.3P_2G)}{1+(2.3P_2G)/K_{P_2G}} - k_{P_2Gase}(2.3P_2G) - C = 0 \qquad (9)$$

$$-\frac{2V_m(ATP)}{K_m+(ATP)} - k_{P_2Gase}(2.3P_2G) - C + 2k_{PK}(ADP)(P\text{-}Pyr) - k_{ATPase}(ATP) = 0 \qquad (10)$$

In these equations the variables are ATP, ADP, 1.3 P_2G, 2.3 P_2G and P-Pyr. By use of the equilibria (1) P-Pyr can be expressed by 1.3 P_2G, ATP and ADP. Furthermore, 2.3P_2G and 1.3 P_2G can be eliminated from Eqs. (8)-(10) yielding an equation for ATP and ADP

$$\frac{2V_m(ATP)}{K_m+(ATP)} - \frac{q_{Enol}q_{PGM}q_{PGK}\,k_{PK}\,(ADP)^2}{k_{P_2GM}(ATP)}\left(\frac{2V_m(ATP)}{K_m+(ATP)} - k_{ATPase}(ATP)\right)\left(1 + (k_{P_2Gase}K_{P_2G})^{-1}\left(\frac{2V_m(ATP)}{K_m+(ATP)} - k_{ATPase}(ATP) - C\right)\right) = 0 \qquad (11)$$

Finally, ADP can be expressed as a function of ATP using the conservation sum for the adenine nucleotides and the equilibrium of the adenylate kinase

$$(ADP) = \frac{q_{AK}(ATP)}{2}\left(\sqrt{1 + \frac{4}{q_{AK}}\left(\frac{A}{(ATP)} - 1\right)} - 1\right) \qquad (12)$$

There are several solutions for the Eqs. (11) and (12). One with (ATP) equal to zero is trivial. Dividing Eq. (11) by (ATP) the resulting expression may be transformed into a polynomial in the ATP- concentration the roots of which are further solutions. The degree of the polynomial, however, is rather high. Another procedure is much simpler. The implicite equation for (ATP) is solved for a parameter (**Table** 1) as a function of the ATP- concentration. This yields for example for k_{ATPase} and V_m a quadratic or for k_{P_2GM} a linear relation. With their help steady state lines for the metabolite concentrations can be constructed. The concentrations of $2.3P_2G$, $1.3P_2G$ and P-Pyr can be obtained from the solutions for ATP.

Typical steady state curves of the metabolite concentrations are given in **Figs.**2 and 3. All curves have common characteristics. The first feature is that there is only a limited range for the parameter values for which steady states exist. Beyond a critical value only the trivial steady state exists corresponding to zero concentrations of ATP, ADP and the phosphoglycerates. There is a sharp change of the steady state values at the critical point (bifurcation point). One should keep in mind that the time needed for the critical change cannot be inferred from the curves. The steady state space is limited by the permissible values of both variables and parameters. The reasons are of complex nature. One is the existence of a conservation restriction for the adenine nucleotides which confines their variations. Another reason is the special structure of the energy system. Thus, the following flux equation is easily derived from Eqs. (8)-(10)

$$v_{P_2GM} = 2v_{HK\text{-}PFK} - v_{ATPase} \qquad (13)$$

If either v_{ATPase} is increased (by change of k_{ATPase}) or $v_{HK\text{-}PFK}$ decreased (by change of e.g. V_m) too strongly

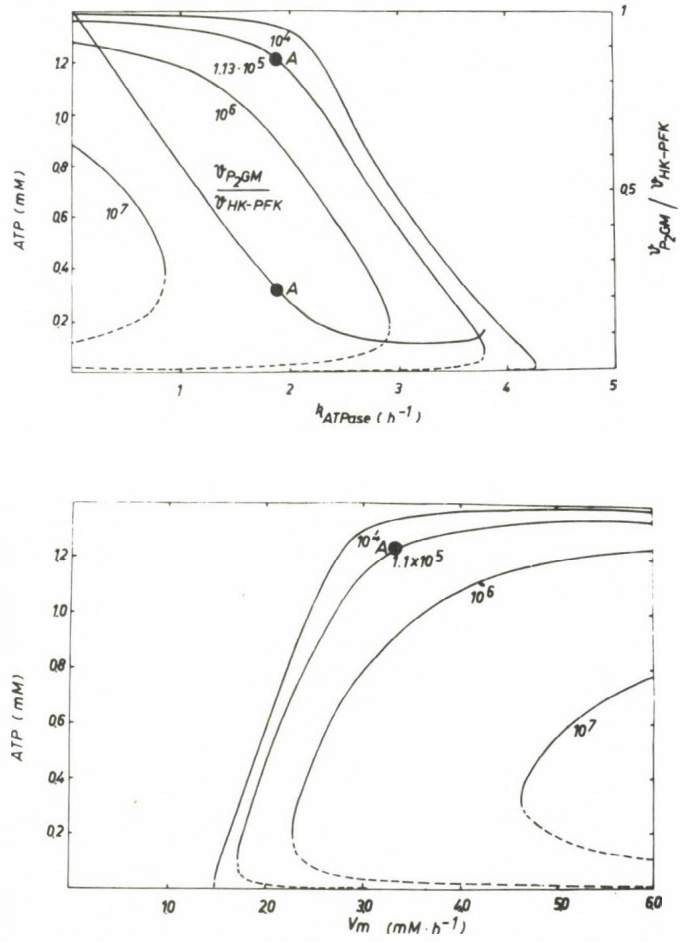

Fig.2. ATP- level and flux through the 2.3 P_2G- bypass as functions of the rate constants of the ATPase and of the hexokinase- phosphofructokinase- system (Figs.2a,b)

The parameter of the 2.3 P_2G- mutase (k_{P_2GM}) was varied (numbers in the figure in h^{-1}). The other parameter values are those given in **Table** 2. Unstable steady states are indicated by dotted lines. v_{P_2GM}/v_{HK-PFK} gives the share of the total flux which flows through the 2.3 P_2G- bypass. This curve was plotted with k_{P_2GM} = 1.1 x 10^5 h^{-1}. The points A indicate the in vivo state of the system.

negative values for the bypass- flux arise which are of course irrealistic. Therefore, k_{ATPase} and V_m are limited in their range. A second characteristicum is the existence of multiple steady states. For a given parameter combination there exist three steady states, one of which is (ATP) equal to zero. The third feature is the occurence of stable and unstable steady states. "Stable" means that the system after some arbitrarily small perturbation from the steady state will return to it (for definitions and details see appendix). Steady states found in vivo must correspond to stable steady states of the model. A mere steady state analysis without investigation of the stability properties may be quite misleading since it might refer to an unstable state which has no correspondence in reality.

2.1.2. The 2.3 P_2G- bypass acts as an "energy buffer"

The ATP- level is influenced in an opposite manner by the ATPase- constant (k_{ATPase}) and by the V_m- value of the hexokinase- phosphofructokinase- system (Fig.2). It may be seen that the ATP- level falls with increasing k_{ATPase}. However, there is a region in the curves where the ATP- concentration is relatively constant. This is brought about by the 2.3P_2G- bypass which acts as an "energy buffer". If the ATP- consumption increases the share of the flux through the bypass decreases so that more ATP can be produced at the phosphoglycerate kinase step. At low fluxes through the bypass an increase of the ATPase- constant cannot be compensated by a reduction of the ATP- waste of the bypass and therefore the ATP- concentration falls (Fig.2a). Identical effects are produced by a decrease of the V_m - value of the hexokinase-phosphofructokinase- system.
The 2.3 P_2G- bypass may be considered as an example of a futile cycle. It may be suggested that futile cycles in general may serve as "energy buffers" in cells.

2.1.3. Fitting of the in vivo- model to experimental data

Table 2 contains the parameter values which give the best correspondence between predicted and observed metabolite concentrations in the in vivo- steady state. It was used for the calculation of all curves except where indicated otherwise. This parameter set gives the point A in Fig.2 at which the glycolysis is expected to work in vivo.

Table 2.

Parameter combination best fitting the in vivo data

The data refer to pH 7.2, 37°C and 1 mM inorganic phosphate. For the equilibrium constants q_{Enol}, q_{PGM}, q_{PGK} and q_{AK} the values 0.18, 2.8, 600 and 0.5, respectively, were used. For K_{P_2G} a value of 40 /uM was used in approximate aggreement with data given by Rose (1973)

parameter	best value for the parameter	metabolite	calculated concentration (/uM)	measured concentration (/uM)
V_m	3170 /uM h^{-1}	ATP	1184	1200
K_m	1400 /uM	ADP	167	185
k_{ATPase}	1.92 h^{-1}	AMP	43	50
k_{PK}	0.67 /uM^{-1} h^{-1}	2.3 P_2G	4900	4700
k_{P_2GM}	1.1 x 10^5 h^{-1}	1.3 P_2G	0.6	0.5
k_{P_2Gase}	0.1 h^{-1}	3 PG	52	60
C	110 /uM h^{-1}	2 PG	10	15
		P-Pyr	27	26
		flux (/uM h^{-1})	1480	1350

The best parameter set is in fair agreement with data on the isolated enzymatic steps (unpublished results). Furthermore, the model describes satisfactorily the changes of metabolites found in pyruvate kinase deficient red cells and the species variations among erythrocytes from different animals. This shows that the model may represent the in vivo-situation.

2.1.4. Control properties of the in vivo steady states

2.1.4.1. Control of the levels of the metabolites

The influence of an enzyme E_j on the metabolite concentration S_i can be expressed by an element of the control matrix S_{ij} (Heinrich & Rapoport, 1974)

$$S_{ij} = \frac{\partial \ln S_i}{\partial \ln v_j} \qquad (14)$$

A positive value indicates that activation of the enzyme leads to an increase of the level of the metabolite while a negative value has the opposite meaning. Some rules for the calculation of the control matrix are given in the appendix. In Table 3 some calculated elements of the control matrix at the "in vivo- point" are given. The elements of the control matrix for the remaining metabolites can be easily calculated from those given in the table. For equilibrium enzymes the elements are zero. The following qualitative conclusions can be drawn from the data of Table 3.
The ATP- concentration is mainly determined by the hexokinase-phosphofructokinase- system and by the ATP-consuming processes. Other enzymes have little influence on the ATP- level. The 2.3 P_2G- concentration is mainly controlled by the same enzymes. Additionally, the 2.3 P_2G- phosphatase has a significant influence, while the 2.3 P_2G- mutase has only little effect. This is explained in the following manner. The flux through the bypass is determined by Eq. (13) so that it is a strict function of the ATP- level. The 2.3 P_2G-mutase has an insignificant influence on the ATP- concentration so that its variation will not produce great changes of the flux through the bypass. Consequently, the 2.3 P_2G-concentration will also be little affected. Any change of the rate constant of the 2.3 P_2G-mutase is counterbalanced by a corresponding inverse change of the 1.3 P_2G- concentration (see Fig.3). This example demonstrates that the whole system must be analyzed rather than parts or even

single steps. The P-Pyr- level is influenced by all enzymes, especially by the hexokinase- phosphofructokinase- system and by the ATPases.

Table 3.

Control matrix at the "in vivo- point"

enzyme	ATP	2.3 P_2G	P-Pyr
hexokinase-phosphofructo-kinase-system	0.80	4.88	4.70
ATPase	- 0.70	- 3.83	- 3.22
pyruvate kinase	0.10	- 0.10	- 0.63
2.3 P_2G-mutase	- 0.10	0.10	- 0.42
2.3 P_2G-phosphatase	- 0.10	- 1.05	- 0.43

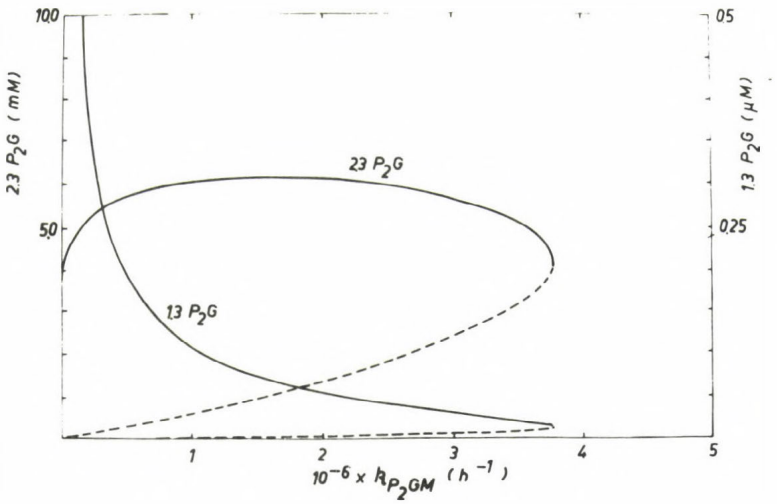

Fig.3. 2.3 P_2G- and 1.3 P_2G- levels as functions of the rate constants of the 2.3 P_2G- mutase

The dotted lines indicate unstable steady states

2.1.4.2. Flux control

The control strength C_i has been defined as a measure of the influence of an enzyme on the overall flux in the following way (Heinrich & Rapoport, 1974)

$$C_i = \frac{\partial \ln v_g}{\partial \ln v_i} \qquad (15)$$

v_g denotes the total flux, v_i the flux through the enzyme E_i. By use of the procedure given in the appendix the numerical values given in **Table** 4 were calculated for the control strengths at the "in vivo- point".
The hexokinase- phosphofructokinase- system which is favoured for flux control by its position in the glycolytic chain (Heinrich & Rapoport,1974) has a control strength greater than unity.Activation of the hexokinase- phosphofructokinase-system leads to ATP- increase so that its control strength is higher than it would be without feedback. ATPase, 2.3 P_2G-phosphatase and 2.3 P_2G- mutase have negative control strengths. Activation of these enzymes leads to a decrease in the overall flux caused by a diminished ATP- level (see **Table** 3). The enzymes of the bypass have small control strengths owing to their small elements in the control matrix. Pyruvate kinase has a small positive control strength.

Table 4.

Control strengths of the glycolytic enzymes

enzyme	C_i
hexokinase-phospho-fructokinase-system	1.37
ATPase	- 0.33
pyruvate kinase	0.04
2.3 P_2G- mutase	- 0.04
2.3 P_2G- phosphatase	- 0.04

2.1.5. Optimality of the location of the in vivo- point

Fig.4 gives plots of the ATP- concentrations versus the rate of the ATP- consuming processes (i.e. $k_{ATPase}x$ (ATP)) for erythrocytes of various species. All curves display a maximum with respect to the ATPase- rate. This can be explained as follows. At high ATP- levels an increase of k_{ATPase} which means an increase of v_{ATPase} will cause small changes in the ATP- concentration owing to the compensation by the 2.3 P_2G- bypass (see section 2.1.2.). If the share of the bypass has reached low values the decrease of the ATP- concentration results in a decreased ATP- synthesis and therefore the rate of the ATPase must also decrease.It is seen in **Fig.**4 that in all species the "in vivo- point" is located at the maximum. This is especially surprising as the rate constants among the species differ by more than one order of magnitude. A similar, but arbitrarily chosen change of the rate constant of the 2.3 P_2G- mutase can lead to quite a different position of the working point (dotted line in **Fig.**4). Thus, the location of the "in vivo- point" does not seem to be fortuitous but rather the result of an evolutionary adaption. The cells of the various species differ with respect to the absolute work they can do, but they all perform at maximal efficiency, i.e. they do maximal work at minimal glucose consumption.
The in vivo- point appears to represent a compromise between a high ATP- level, i.e. high glycolytic flux and ATP- production, on the one hand, and on the other a small share of the ATP- wasting 2.3 P_2G- bypass (10 - 20% of the total glycolytic flux, see **Fig.**2a).

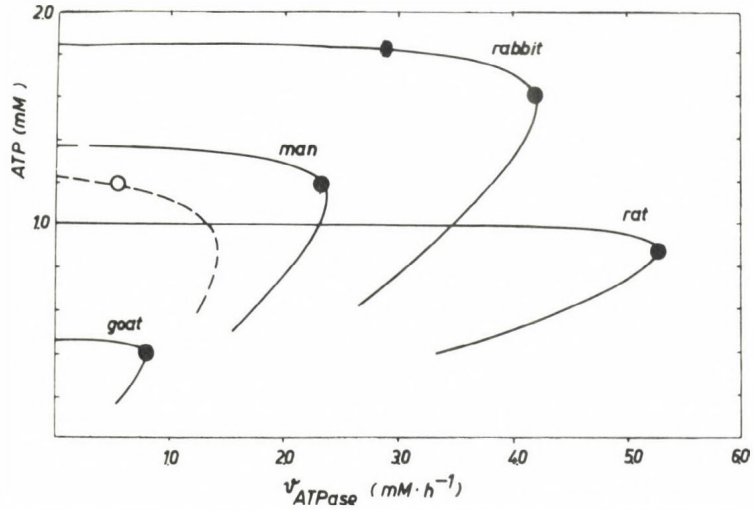

Fig.4. The ATP- concentration as a function of the rate of the nonglycolytic ATP- consuming processes (v_{ATPase}) for erythrocytes from various species

The parameter values for the erythrocytes from man are given in Table 2, those for the other species are the following (given in the order rat, rabbit, goat; Jacobasch, 1970) : V_m = 6340, 4440, 950 /uM h^{-1}; k_{PK} = 0.36, 1.04, 0.33 /uM$^{-1}h^{-1}$; k_{P_2GM}= 4.95 x 10^4, 1.4 x 10^5, 3.85 x 10^3 h^{-1}; k_{P_2Gase}= 0.04, 0.087, 0.047 h^{-1}; C = 45, 96, 52 /uM$^2h^{-1}$; A = 1020, 1870, 462 /uM; K_m = 1020, 1870, 462 /uM. All other parameters have the same values as given in **Table** 2. It was assumed that in all cells 85% of the total adenine nucleotides are present as ATP. The points give the "in vivo- points" for the cells. The dotted line gives a simulated situation where the parameter k_{P_2GM} had a value of 1.1 x 10^6 h^{-1} but all other values are identical to those given in **Table** 2.

2.2. The time- hierarchy of the glycolytic system

For small deviations of the metabolite concentrations S_i from their steady state values S_i^o the dynamics of the system is determined by linear differential equations. The solutions are of the general form

$$S_i(t) = S_i^o + \sum_{k=1}^{m} c_k A_i^k e^{\lambda_k t} \qquad (16)$$

where λ_k and A_i^k are the eigenvalues and the eigenvectors, respectively, of the Jacobian of the linearized system. The coefficients c_k depend on the starting conditions of the time- dependent process. The reciprocal real parts of the eigenvalues have the dimension of a time and characterize the slowness of the relaxation process. The eigenvalues are complex functions of the kinetic parameters of the enzymes so that they usually cannot be attributed to the relaxation of isolated single reactions. In **Fig.**5 the calculated eigenvalues of the in vivo equation system (4)-(6) are plotted versus k_{ATPase}. Numerical values for the "in vivo- point" are also given in the legend.

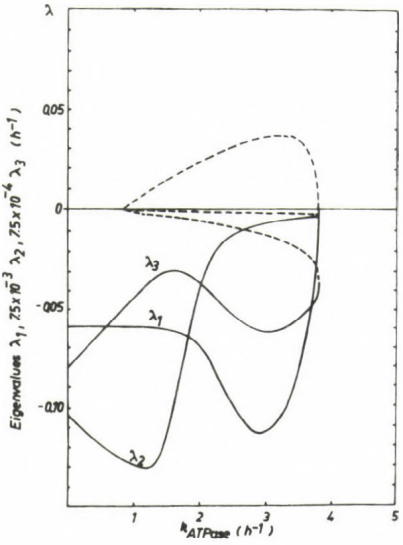

Fig.5.
Eigenvalues of the glycolytic system (λ) as functions of the rate constant of the ATPase

At the in vivo- point the eigenvalues have the following values: $\lambda_1 = -0.068\ h^{-1}$; $\lambda_2 = -6.46\ h^{-1}$; $\lambda_3 = -45.84\ h^{-1}$.

The eigenvalues are real. At the bifurcation point the smallest eigenvalue changes its sign and is therefore responsible for the existence of the unstable branches in the

steady state curves. The three eigenvalues are of different orders of magnitude. This expresses the fact that the glycolysis of erythrocytes exhibits a pronounced time- hierarchy. The most important feature is the great difference between the two smallest eigenvalues (by a factor of 100 at the "in vivo- point").

In **Table** 5 the characteristic times (Heinrich & Rapoport, 1974) of the glycolytic enzymes are given. It is seen that they vary over almost four orders of magnitude. This is further proof for the time- hierarchy of the glycolytic system. It is evident that the slowness of the 2.3 P_2G- phosphatase is responsible for the slow movement with the relaxation time $1/\lambda_1$.

Table 5.

Characteristic times of some enzymatic steps included in the model at the in vivo- point

The characteristic times (τ) were calculated from the rate laws $v(S_i)$. τ is for a one- substrate reaction $(dv/dS)^{-1}$ and for a two- substrate reaction $(\partial v/\partial S_1 + \partial v/\partial S_2)^{-1}$.

enzyme	characteristic time
hexokinase- phospho-fructokinase- system	1.5 h
ATPase	0.5 h
pyruvate kinase	28 s
2.3 P_2G- mutase	3.9 s
2.3 P_2G- phosphatase	10 h

The reciprocal eigenvalues give the relaxation times of the eigenstates of the whole system. A comprehensive quantity suitable for the characterization of the relaxation of individual metabolites is provided by the following expression

$$T_i = \frac{\int_0^\infty t(S_i(t) - S_i^o)dt}{\int_0^\infty (S_i(t) - S_i^o)dt} \qquad (17)$$

T_i are called the mean transition times of the metabolites. The transition times of isolated enzymatic steps coincide with their characteristic times. Transition times may also be calculated for experimental conditions with great deviations of the metabolite levels from their steady state values. In such a case it is advantageous to replace the upper limit in the integrals by the time at which the deviations from the steady state values fall below the experimental error. The applicability of expression (17) is limited by the requirement that the functions $S_i(t) - S_i^o$ do not change their signs during the process. Otherwise, negative weights would occur in the integrals. Therefore, this definition is meaningless for processes which involve damped oscillations, overshoots or undershoots (Heinrich & Rapoport, 1975).

Owing to the great differences between the eigenvalues of the linearized system the differential equations (4)-(7) are "stiff".Ordinary numerical integration methods, e.g. the classical Runge- Kutta- method, require very small step sizes which are comparable to the reciprocal value of the greatest eigenvalue λ_3. An increase of the step size would lead to instabilities of the integration procedure. Therefore, the numerical integration of slow processes with a time constant of about $1/\lambda_1$ require much computer time. Application of the Tichonov- theorem provides a simple method to deal with the stiffness of differential equation systems (Tichonov,1948). The time derivatives of equations which describe very fast movements of metabolite pools are set equal to zero, i.e. these pools are considered to be in the steady state. Thus, only the differential equations describing slow movements remain for the integration and the other equations serve only as an algebraic subsystem which has to be solved simultaneously.

Park has given a simple criterion to discriminate between slow and fast variables (Park 1974). It is essentially based on a comparison of the net flux $v_n = v_i^+ - v_i^-$ and the corresponding outward flux v_i^- of the pools. If the ratio of these quantities is smaller than a given ε (e.g. $\varepsilon = 10^{-2}$)

$$\left| \frac{v_i^+ - v_i^-}{v_i^-} \right| < \varepsilon \qquad (18)$$

the time derivatives of the corresponding pools can be set equal to zero. By use of this criterion the following result is obtained for the glycolytic system of erythrocytes. Under in vivo- conditions Eq. (4) describes a very fast movement of the pool

$$P_1 = 1.3P_2G + 3PG + 2PG + P\text{-}Pyr \qquad (19)$$

After excursion of the metabolites it is nearly in the steady state after a few minutes. The pool

$$P_2 = ATP - AMP - 3PG - 2PG - P\text{-}Pyr \qquad (20)$$

also approaches the steady state after about half an hour. By combination of the differential equations (4) and (5) and considering the conservation equation for the adenine nucleotides the pool

$$P_2' = 2\ ATP + ADP + 1.3\ P_2G \qquad (21)$$

is obtained which is also a fast variable of the system. If one considers longer time periods only the differential equation (6) for $2.3\ P_2G$ remains for integration.

If for some of the metabolites the criterion (18) is fulfilled and for others does not the corresponding states are called "quasi- steady states" of the metabolic system. Another definition of quasi- steady states which is sometimes more advantageous for practical purposes refers to the relative changes of the metabolite concentrations under transient conditions. Then it is required that in the quasi-steady state some of the metabolite concentrations show only small relative variations with respect to time.

3. The in vitro- system of glycolysis

The differentiation between in vivo- and in vitro- conditions is necessary because of two facts. 1. Under in vitro- conditions one has a closed system in which lactate and pyruvate are not exchanged with other tissues and for which the conservation restriction holds (Rapoport et al,1974)

$$T = (NAD^+)+(1.3P_2G)+(2.3P_2G)+(3PG)+(2PG)+(P\text{-}Pyr)+(Pyr) \quad (22)$$

The question is whether approximately time- independent states of subsystems may exist within a closed nonequilibrium system. 2. A related question is whether relatively time-independent metabolite levels can be observed within periods of a few hours which are usual for in vitro experiments.

3.1. The differential equations for the closed system

For the closed in vitro system the term for the exchange of lactate and pyruvate must be dropped in Eq. (7). In Eq. (4) the concentrations of FP_2 and triose-P can be expressed by the concentrations of P-Pyr, ATP, ADP and lactate

$$\frac{d}{dt}\left(\frac{Q_1(P\text{-}Pyr)(ATP)(Lac)}{(ADP)(Pyr)} + (1.3P_2G) + Q_2(P\text{-}Pyr) \right) =$$

$$= 2v_{HK\text{-}PFK} - v_{P_2GM} + v_{P_2Gase} - v_{PK} \quad (23)$$

with

$$Q_1 = \frac{1 + 2/q_{Ald} + 1/q_{TIM}}{q_{PGK}q_{PGM}q_{Enol}q'_{GAPD}q_{LDH}} \quad , \quad Q_2 = 1 + \frac{1}{q_{Enol}}\left(1 + \frac{1}{q_{PGM}}\right) \quad (24)$$

By use of the conservation Eqs. (2) and (22) the time derivative of pyruvate can be expressed by P-Pyr, $2.3P_2G$, $1.3P_2G$ and the pyridine nucleotides. Eq. (7) becomes

$$\frac{d(Lac)}{dt} = v_{PK} + \frac{1-Y_1}{1+\frac{(Pyr)}{(Lac)}Y_1}\left(Q_2\frac{d(P\text{-}Pyr)}{dt} + \frac{d(2.3P_2G)}{dt} + \frac{d(1.3P_2G)}{dt}\right) \quad (25)$$

where

$$Y_1 = \frac{(NAD^+)(NADH)}{(NAD^+)(NADH) + (Pyr)\ N} \qquad (26)$$

Differentiation of the left side of Eq. (23) yields after some rearrangements

$$\frac{d(1.3P_2G)}{dt} + (Q_2+F_1)\frac{d(P\text{-}Pyr)}{dt} = 2v_{HK\text{-}PFK} - v_{P_2GM} + v_{P_2Gase} - v_{PK}(1+F_2) - F_3\frac{d(ATP)}{dt} - F_4\frac{d(2.3P_2G)}{dt} \qquad (27)$$

with

$$F_1 = \frac{(ATP)Q_1}{(ADP)(Pyr)}\left((Lac) + (P\text{-}Pyr)\left(Q_2 + \frac{L}{q_{Enol}q_{PGM}q_{PGK}}\right)\right)$$

$$F_2 = \frac{Q_1(P\text{-}Pyr)(ATP)(Lac)(1-Y_1)}{(ADP)(Pyr)((Lac)+(Pyr)Y_1)} \qquad (28)$$

$$F_3 = \left(1-\frac{d(ADP)}{d(ATP)}\frac{(ATP)}{(ADP)}\right)\frac{Q_1(P\text{-}Pyr)}{(ADP)(Pyr)}\left((Lac)+\frac{(P\text{-}Pyr)\ L}{q_{Enol}q_{PGM}q_{PGK}}\right)$$

$$F_4 = \frac{Q_1(P\text{-}Pyr)\ L}{(ADP)(Pyr)}$$

$$L = \frac{(ATP)(1-Y_1)((Lac)+(Pyr))}{(ADP)((Lac)+(Pyr)Y_1)}$$

Eq. (27) differs from the respective in vivo Eq. (4) by the occurrence of terms F_1 - F_4. At pH 7.2 assuming normal metabolite levels the terms have the following numerical values

$$F_1 = 2.8\ ;\ F_2 = 0.033\ ;\ F_3 = 0.21\ ;\ F_4 = 0.35$$

Most of these quantities are not small enough to be neglected. Their magnitude can be decreased by high levels of pyruvate (Eq. (28)). The differential Eqs. (5) and (6) for (ATP - AMP - 3PG - 2PG - P-Pyr) and 2.3 P_2G remain unchanged for the in vitro situation.

Obviously, the in vitro- system has no steady state solution in contrast to the in vivo situation since **Eq.** (25) cannot be set equal to zero; lactate increases steadily.

3.2. Existence of quasi- steady states in the closed system for all glycolytic metabolites except for lactate, FP_2 and triose-P

The following considerations demonstrate the existence of quasi- steady states in vitro. Setting the time derivatives in the differential **Eq.** (27) equal to zero one obtains an equation similar to that for the steady state in vivo (**Eq.** (8)) with the difference that it contains the term F_2

$$2v_{HK-PFK} - v_{P_2GM} + v_{P_2Gase} - v_{PK}(1+F_2) = 0 \qquad (29)$$

If F_2 were constant a steady state could be expected for the adenine nucleotides, phosphoglycerates and for pyruvate (see **Eqs.** (5),(6) and (22)). The constancy of F_2 depends on the term

$$Y_2 = \frac{(Pyr)\,N}{(NAD^+)(NADH) + (Pyr)\,N} \qquad (30)$$

which is influenced by the concentrations of the pyridine nucleotides. By use of the equilibria (1) and the conservation **Eq.** (2) the following expression is obtained for NAD^+

$$(NAD^+) = \frac{N}{1 + (Lac)/((Pyr)q_{LDH})} \qquad (31)$$

Since under in vitro conditions lactate increases steadily the concentration of NAD^+ decreases and consequently the term Y_2 cannot be constant. However, if the condition $NAD^+ \gg$ NADH (or vice versa) is fulfilled the influence of the time dependent changes of this system is negligible (Y_2 tends to unity). For erythrocytes at pH 7.2 (NAD^+) is always much higher than (NADH)so that F_2, and consequently the

adenine nucleotides, phosphoglycerates, may be approximately constant. Pyruvate is also time- independent owing to the conservation sum for the oxidized metabolites. The case of $NAD^+ \ll$ NADH can only be expected if lactate tends to **infinity** The computer curves shown in Fig. 6 verify these conclusions. Metabolites which are not influenced in vivo by the exchange of lactate and pyruvate reach constant values in vitro too. The accumulation of lactate is accompanied by an increase of FP_2 and triose-P. This is explained by the NAD^+ - NADH-coupling of the lactate dehydrogenase and glyceraldehyde-P dehydrogenase which leads to the following relation

$$(GAP) = \frac{(1.3P_2G)\ (Lac)}{q_{LDH} q_{GAPD}\ (Pyr)} \qquad (32)$$

where $1.3P_2G$ and pyruvate are constant with time. Since part of the flux from the hexokinase- phosphofructokinase- system is used to accumulate FP_2 and triose-P, the glucose consumption must be higher than the corresponding lactate formation. The quasi- stationary character of the state shown in **Fig.** 6 is apparent from the slow decrease of NAD^+.

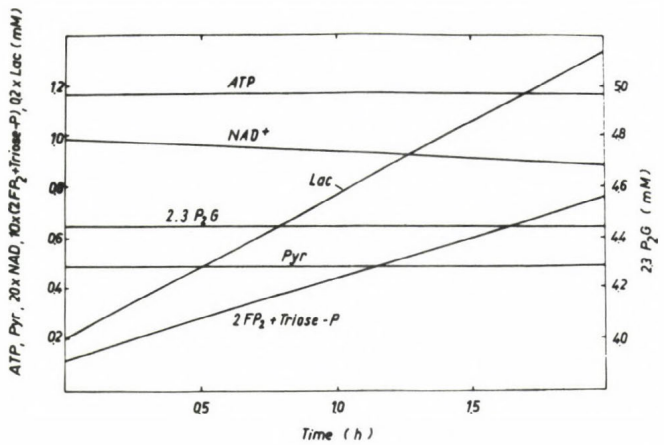

Fig.6. In vitro quasi- steady state behaviour of the glycolytic metabolites

A conservation sum of T = 5 mM was assumed. For Q_1 a value of 3.6×10^{-2} was used. N was set at 50/uM.

3.3. Constraints by the oxidation equivalents

The differences in the concentrations of the adenine nucleotides and phosphoglycerates in the quasi-steady state from those in vivo depend only on the magnitude of the term F_2 (**Eq.** (29)). At pH 7.2 only small deviations from the in vivo conditions are calculated. For the limiting case of infinite pyruvate levels there are no constraints imposed by oxidation equivalents and F_2, as well as the accumulation rate of FP_2 and triose-P, tend to zero. Consequently, the adenine nucleotides and phosphoglycerates attain the in vivo values. Even their time- dependent behaviour is identical with that in vivo if the pyruvate level is infinite since all terms which may cause deviations (cf. **Eq.** (28)) become vanishingly small.
The restriction by the conservation sum of oxidation equivalents becomes more apparent if the hexokinase- phosphofructokinase- system is activated. Whereas in the unconstraint in vivo system 2.3 P_2G and the other oxidized phosphoglycerates would increase greatly, the changes are limited in vitro by the amount of oxidation equivalents available in the system. The increase of 2.3 P_2G is compensated mainly by a decrease of pyruvate. This in turn leads to a higher rate of accumulation of FP_2 and triose-P. The increased flux in the upper part of glycolysis results in a more pronounced discrepancy between glucose consumption and lactate formation. Under such conditions ATP may even decrease despite of a higher glucose consuption. The accumulation of FP_2 and triose-P may be regarded as a futile "cycle" which buffers ATP- changes. This is a similar effect as described for the 2.3 P_2G- bypass (see section 2.1.2.).

3.4. Quasi- steady states at unrelaxed 2.3 P_2G- levels

In this section it will be shown that quasi- steady states may be observed even if 2.3 P_2G is not relaxed.
Fig.7 gives a simulated experiment in which the hexokinase-phosphofructokinase- system was activated by a factor of two

in the presence of excess of oxidation equivalents (left side of **Fig.**7). P-Pyr changes rapidly and reaches a quasi-steady state with a half- time of about five minutes. ATP does not change much and is also constant after about 0.5 h. 2.3 P_2G increases continously after an initial lag phase. It should be noted that the quasi- steady state levels of the metabolites can differ considerably from their values in the in vivo steady state. For instance, the level in the quasi- steady state of P-Pyr (left side of **Fig.**7) is lower than the true steady state value by a factor of four.
On the right side of **Fig.**7 the inverse experiment was simulated; the hexokinase- phosphofructokinase- system was brought back to its original activity. Again P-Pyr changes rapidly reaching approximately its initial level within 0.5 hours. ATP and 2.3 P_2G change only insignificantly. The figure demonstrates that the increase of 2.3 P_2G during the period of flux activation cannot be reversed in a comparable time interval of restored original conditions.
The quasi- steady state solutions for the levels of the adenine nucleotides and phosphoglycerates can be calculated assuming specified 2.3 P_2G- levels and unlimited amounts of oxidation equivalents. The **Eqs.** (4) and (6) are set equal to zero and the 2.3 P_2G- concentration is considered as a parameter (cf. section 2.2). The resulting quasi- steady state curves are shown in **Fig.**8 for different values of 2.3 P_2G. For comparision the in vivo steady state curve is plotted. The quasi- steady state has only one stable solution. The variation of the 2.3 P_2G- level influences relatively little the ATP- level. Changes of 2.3 P_2G as large as 2mM affect the ATP- concentration to less than 5%. Therefore, the metabolite concentrations remain relatively constant during the quasi- steady state period even for large changes in2.3 P_2G. The comparision of the curves in **Fig.**8 shows that ATP is more constant in the quasi- steady state than it is in the in vivo- steady state. This means that the glycolytic system can tolerate ATP- overconsumption for a short time better than it can do for longer periods of time.

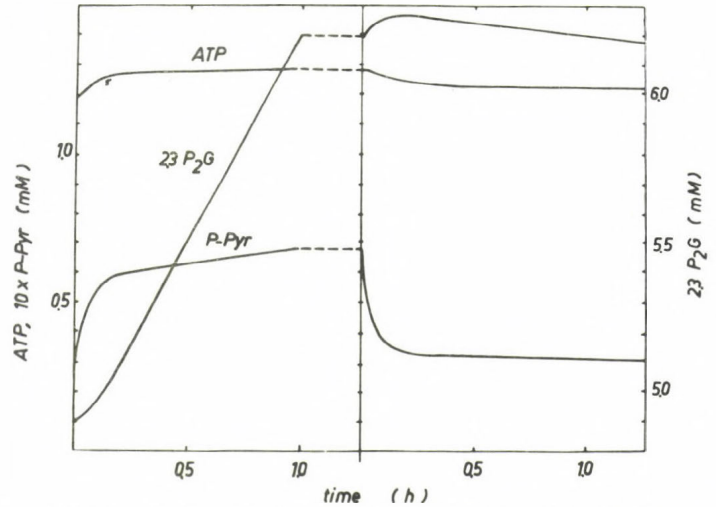

Fig.7. Time dependent behaviour of glycolytic metabolites after activation of the hexokinase-phosphofructokinase- system (left side) and after restorement of the original conditions (right side)

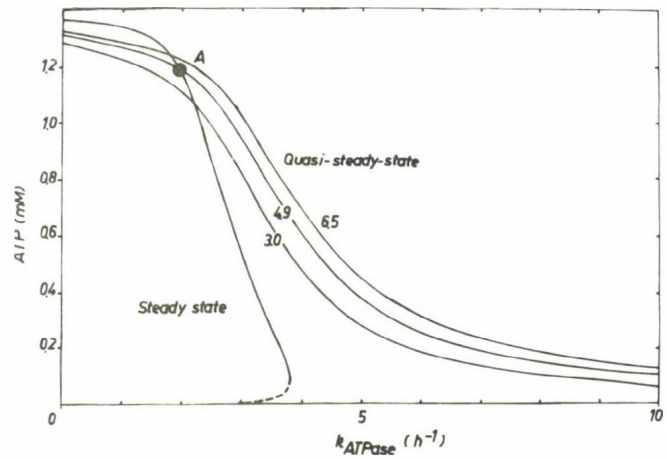

Fig.8. Quasi- steady state concentrations of ATP as a function of the rate constant of the ATPase

The 2.3 P_2G- level was varied as indicated (numbers in mM). The in vivo- steady state curve for ATP is given for **comparison**. It intersects the quasi- steady state curve corresponding to the steady state level of 2.3 P_2G (4.9 mM) at the in vivo- point A.

Two mechanisms are responsible for the ATP-constancy in quasi- steady states. One is the effect of "energy buffering" discussed in section 2.1.2. for transitions between in vivo steady states. A second mechanism is the formation of ATP in the reaction of the pyruvate kinase at the expense of 2.3 P_2G. While in the true steady state formation and degradation of 2.3 P_2G are always equal, in the quasi- steady state more 2.3 P_2G is degraded than formed. The second mechanism is responsible for the flatter curve of ATP in quasi- steady states as compared to in vivo steady states.
The control properties of the quasi- steady states at unrelaxed 2.3 P_2G- levels correspond to those of our previous model (Rapoport et al, 1974). The flux control in the quasi-steady state is exerted almost entirely by the hexokinase-phosphofructokinase- system. The explanation is that ATP is practically uninfluenced by the activities of the enzymes so that no significant feedback to the first enzyme exists.

3.5. Modelling of blood preservation conditions

This section gives an example which shows that the model may describe time dependent processes.
At this stage of analysis only the simplest conditions of blood preservation could be dealt with, i.e. lowering of pH and temperature. For the modelling it was assumed that the restriction by oxidation equivalents can be neglected owing to the pyruvate production from 2.3 P_2G in the course of storage. Breakdown of adenine nucleotides via AMP- degradation was taken into account. The following rate law was assumed

$$\frac{dA}{dt} = - k_{AMP}(AMP) \qquad (33)$$

Resynthesis of adenine nucleotides can be neglected (Nakao, 1974). The stiffness of the differential equations poses difficulties owing to the long periods of time that have to

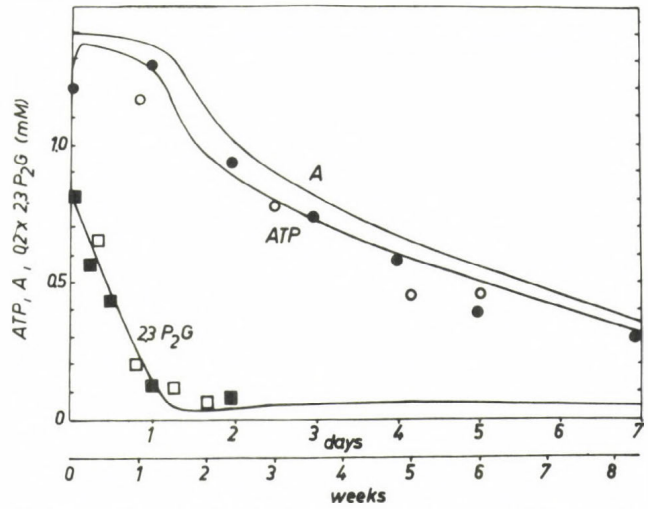

Fig.9. Time dependent changes of some glycolytic metabolites under blood storage conditions at 25°C and 4°C

The cells were incubated in ACD- medium. The points represent experimental values. Closed symbols correspond to 25°C, open symbols to 4°C (●, ○ ATP, ■, □ , 2.3 P_2G). The following parameter values were used at 25°C : V_m = 1080/uM h^{-1}, K_m = 1400/uM, k_{ATPase}=0.8 h^{-1}, k_{PK}= 0.34/uM$^{-1}h^{-1}$, k_{P_2GM}= 1000 h^{-1}, k_{P_2Gase}= = 310/uM h^{-1}, K = 200/uM, K_{P_2G} = 40/uM.

be considered. The integration was performed essentially by the method proposed by Park (1974) using the differential **Eqs.** (4)-(7) and (33). When the right hand side of **Eq.**(4) approached zero it was excluded from the integration and served only as an algebraic subsystem. The same procedure was followed for **Eq.** (5). Thus, only two differential equations remained (**Eqs.** (7) and (33)) which resulted in a large economy of computer time.

Fig.9 gives representative computer curves and experimental points for both 25°C (Bartel et al,1972) and 4°C (Stigge,

unpublished data). For the 2.3 P_2G- phosphatase the rate law assumed was slightly modified (cf. **Table** 1)

$$v_{P_2Gase} = \frac{k_{P_2Gase}(2.3\ P_2G)}{K + (2.3\ P_2G)} \qquad (34)$$

Obviously, the model describes the experimental observations with the only possible exception of the sum of the adenine nucleotides for which no data were available. The lowering of the temperature below 37°C causes a general proportional slowing down of all enzymatic steps. In keeping with this conclusion, the form of the curves did not differ between 25°C and 4°C. The parameter values given in the legend to Fig.9 were obtained from the standard set of **Table** 2 by use of a temperature coefficient of about two. In addition to temperature, pH and possibly other factors also exert effects which necessitated additional parameter changes, the most important of which were an inhibition of the hexokinase-phosphofructokinase- system and of the 2.3 P_2G- mutase (Jacobasch & Raderecht, **1967**; Rose, 1973). The most interesting feature of **Fig.** 9 is the behaviour of ATP which increases initially, remains constant for a certain period of time and decreases steadily thereafter. The constancy of ATP at a high level is produced mainly by the 2.3 P_2G-degradation which yields ATP at the pyruvate kinase reaction.
Variation of the kinetic parameters of the enzymes showed that the most important factors responsible for a constant ATP- level over long periods are a) the difference between the rate constants of ATP- production and -consumption and b) the inhibition of the 2.3 P_2G- mutase reaction.

4.Discussion

The analysis of this model shows that only four essential variables are sufficient to characterize the glycolytic system of erythrocytes. From the standpoint of methodical convenience these may be ATP, 2.3 P_2G, 3 PG and lactate.Of course, there may be substitutions, such as AMP or ADP for

ATP, P-Pyr, 2PG and 1.3 P_2G for 3PG or the flux for lactate. Compared with the previous proposal (Rapoport et al, 1974) G6P is omitted since it is only of importance for the elucidation of the interrelations between the hexokinase and phosphofructokinase.

The aggreement of theory and experiment indicates that the most important interactions between metabolites and enzymes are included in the model.

The model reconfirms the previous conclusions that in the steady state the equilibrium enzymes phosphoglycerate kinase and glyceraldehyde-P dehydrogenase have no influence on either flux or metabolites of glycolysis while pyruvate kinase which does affect some intermediates has little influence on the flux. This is in contrast to various intuitive assumptions (Reinauer & Bruns, 1964; Minakami, 1968). It should be emphasized that the role of an enzyme under steady state conditions must be distinguished from that in a transient process. Enzymes with high control strengths need not control in a transient process and vice versa. This is illustrated by the fact that the 2.3 P_2G- phosphatase which has only a small control strength exerts a strong influence on transient processes.

So far the role of the ATP- consuming processes in regulating the glycolysis has been largely neglected both in theoretical and experimental work. From the present study it emerges, however, that ATP- consuming processes are of great importance.

Some principles of the regulation of the important metabolite ATP are revealed. ATP is kept approximately constant in the cell by three mechanisms. Firstly, the 2.3 P_2G- bypass acts as an "energy buffer" so that a change in the ATP- consumption is compensated by a variation in the ATP- waste of the bypass. Secondly, the metabolite 2.3 P_2G acts as an energy source as it may yield ATP for a certain period of time at the pyruvate kinase step in case of ATP- overconsumption. A third mechanism is observed in vitro, where ATP- changes can be buffered by variations in the accumulation rate of

FP_2 and triose-P. The first and third mechanism are regulations of energy consuming processes while the second one refers to an energy producing process.

An unexpected biological regularity has turned up, i.e. that the ATP- consumption rate assumes its maximal value at the in vivo steady state. This holds for various species independent of their values of 2.3 P_2G, ATP or glycolytic flux. It appears as if, given the need for ATP- consumption, the whole glycolytic system is composed in such a manner as to yield maximal efficiency. This must represent an evolutionary adaptation which involves the whole set of elements which constitute the glycolytic system rather than one single factor. It appears strange, however, that any activation of the ATPases should produce a lowered ATP- consumption unless the parameters of the glycolytic enzymes are changed by outer effectors, such as H^+-, P_i- or NH_4^+- ions. Possibly erythrocytes are not faced with great changes of their ATP- need. In this respect erythrocytes are not representative of other cells which are geared for great changes in the ATP- need, e.g. those of muscle. In these cells glycogenolysis is highly sensitive to the breakdown products of ATP, AMP and P_i, so that a higher response to changes in the ATP- consumption exists. A preliminary modelling of such a system indicates that the rate of ATP- consumption may vary over a wide range (unpublished results). A similar behaviour is shown by the erythrocyte system during periods of time in which a quasi-steady state obtains. An activation of the ATPase may lead to an increased ATP- consumption for several hours. The fundamental difference shown in this paper between the conditions in vivo and in vitro has been largely neglected before. So far there has been no general concept to what extent the situation of cells in vitro corresponds to that in vivo and how in vitro experiments should be set up to approximate the conditions in vivo. Whereas a steady state exists in vivo to a high degree of approximation it cannot be realized in vitro. Within certain periods of incubation, i.e. between about 0.5 and 2 hours, a quasi- steady state may be achieved, a con-

dition which is favourable for both theoretical and experimental analysis. Two kinds of quasi- steady states can be observed in vitro. One can be reached during the short incubation periods for all glycolytic metabolites except for lactate, FP_2 and triose-P at low levels of oxidation equivalents. A second type of quasi- steady states which is limited to adenine nucleotides and phosphoglycerates can be observed, however, at high levels of oxidation equivalents during the short periods of incubation. It is defined by unrelaxed 2.3 P_2G- levels.

The analysis revealed a pronounced time- hierarchy of the glycolytic reactions of erythrocytes which is mainly due to the slow 2.3 P_2G- phosphatase- reaction. For the investigation of the hierarchical structure of a system the eigenvalues seem to be the best representation. The Tichonov-theorem offers the key for the simplification of the stiff differential equations by allowing one to eliminate fast movements.

Time- hierarchies are a general feature in nature. Any theoretical or experimental approach requires a confinement of the system to be investigated with respect to the time ranges. These restrictions determine the experimental methods to be applied as well as the structure of the models assumed.For the present model the lower boundary of time constitute rapid reactions which were not considered explicitly. These include three types of processes. Firstly, reactions on the level of single enzymes which are usually fast enough to be in a steady state in the metabolic time range. Secondly, glycolytic reactions near to equilibrium and thirdly, the steady state aggregation of some enzymes, i.e. of the hexokinase and phosphofructokinase. The upper boundary are slow processes such as renewal of the adenine or nicotineamide moieties. By these boundaries the time range of the model analyzed in this paper is set between one minute and 1 -2 days.

Appendix

1. Stability properties of a system

The time- dependent behaviour of the metabolite concentrations S_i is given by a set of ordinary differential equations

$$\frac{dS_i}{dt} = f_i(S_1, \ldots, S_m; p_k) \qquad (A\ 1)$$

p_k are the parameters of the system. The differential equations are in general nonlinear. In the neighbourhood of a stationary point ($f_i = 0$; $i = 1,2,\ldots,m$) the functions f_i can be expanded in Taylor series. Neglecting terms higher than first order the following linear system of differential equations is obtained

$$\frac{d(\Delta S_i)}{dt} = \sum_I I_{il} \Delta S_l \qquad (A\ 2)$$

with $\Delta S_i = S_i(t) - S_i^o$. S_i^o are the metabolite concentrations at the stationary point. I_{il} is the Jacobian of the system. The system is stable if the eigenvalues of the Jacobian have all negative real parts (see e.g. Willems, 1973), otherwise it is unstable. The eigenvalues are the roots of the characteristic polynomial

$$\det (I_{il} - \delta_{il}) = 0 \qquad (A\ 3)$$

δ_{il} is the Kronecker symbol ($\delta_{il} = 1$ if $i = l$ and zero otherwise). The constant term of the polynomial is equal to the determinant of I_{il}. The roots can either be calculated explicitly for a given stationary point or the signs of the real parts can be checked by application of the Routh-Hurwitz- criterion (e.g. Willems, 1973).

In general, for a given parameter combination more than one set of metabolite concentrations fulfills the conditions $f_i = 0$, i.e. there exist multiple steady states. In that case a plot of a metabolite concentration versus a parameter

of the system displays several branches. Two of these branches may have a common bifurcation point. At such points the system of equations $f_i = 0$ has no unique solution. According to a fundamental theorem of implicite functions the determinant of the Jacobian and consequently at least one eigenvalue becomes zero at the bifurcation point. In general, one of the eigenvalues will change its sign so that at least one of the two branches will be unstable.

2. Relations between the Jacobian, the control matrix and the effector strengths

The functions f_i are connected with the fluxes v_j producing and removing the metabolite S_i in the following manner

$$f_i = \sum_j w_{ij} v_j \qquad (A4)$$

w_{ij} is the stochiometric matrix of the system (Park, 1974). The Jacobian can be rewritten as

$$I_{il} = \sum_j w_{ij} \frac{\partial v_j}{\partial S_l} = \sum_j w_{ij} v_j S_l^{-1} \frac{\partial \ln v_j}{\partial \ln S_l} \qquad (A 5)$$

or

$$I_{il} = \sum_j w_{ij} v_j S_l^{-1} X_{jl} \qquad (A 6)$$

The elements of the matrix X_{jl} give the sensitivities of the fluxes v_j to changes of the metabolite concentrations; they are the effector strengths (Heinrich & Rapoport, 1974).
An important relation is deduced if one analyzes the change of a steady state to a new one under the influence of an enzyme E_r. If differential changes are considered a Taylor expansion can be used neglecting terms higher than first order

$$f_i(v_r+dv_r) = f_i(v_r) + \sum_j \frac{\partial f_i}{\partial S_j} dS_j + \frac{\partial f_i}{\partial v_r} dv_r = 0 \qquad (A 7)$$

$$(f_i(v_r) = 0)$$

One obtains

$$\sum_j \frac{\partial f_i}{\partial S_j} \frac{\partial S_j}{\partial v_r} + \frac{\partial f_i}{\partial v_r} = 0 \qquad \text{(A 8)}$$

or

$$\sum_j I_{ij} \frac{\partial S_i}{\partial v_r} + \frac{\partial f_i}{\partial v_r} = 0 \qquad \text{(A 9)}$$

Since

$$\frac{\partial S_j}{\partial v_r} = \frac{\partial \ln S_j}{\partial \ln v_r} \frac{S_j}{v_r} = S_{jr} \frac{S_j}{v_r} \qquad \text{(A10)}$$

Eq. (A 9) gives a relation between the control matrix and the Jacobian of the system. The elements of the control matrix can be calculated by inversion of the Jacobian. At the bifurcation point the determinant of I_{ij} is zero so that the terms S_{jr} tend to infinity.

3. Control of steady states

Eq. (A 8) can be used to calculate the control matrix and the control strengths. Rearrangement of the equation gives

$$\sum_l \sum_j w_{il} v_l \frac{\partial \ln v_l}{\partial \ln S_j} \frac{\partial \ln S_j}{\partial \ln v_r} + \sum_l w_{il} v_l \frac{\partial \ln v_l}{\partial \ln v_r} = 0 \qquad \text{(A11)}$$

or by use of the abbreviations for the effector strengths (X_{lj}) and control matrix elements (S_{jr})

$$\sum_l \sum_j w_{il} v_l X_{lj} S_{jr} + \sum_l w_{il} v_l \delta_{lr} = 0 \qquad \text{(A12)}$$

The fluxes and the effector strengths can be calculated from the steady state equations and the rate laws of the isolated enzymes, respectively. The matrix w_{il} is known from the stochiometric structure of the system. Thus, the elements of the control matrix S_{jr} may be obtained by solving the n x m equations of type (A12). If the control matrix is known the control strengths of the enzymes can be obtained by use of the equation

$$C_i = \frac{\partial \ln v_g}{\partial \ln v_i} = v_g^{-1} \left(\sum_j v_j \delta_{ij} + \sum_j \sum_k v_j X_{jk} S_{ki} \right) \quad \text{(A13)}$$

The sum over j contains all fluxes which contribute to the total flux.

The calculation of the control strengths may be simplified by application of the following fundamental theorems.

a) The sum of the control strengths is equal to unity

$$\sum_i C_i = 1 \quad \text{(A14)}$$

This summation theorem expresses the fact that a simultaneous activation or inhibition of all enzymes by the same factor leads to an equal response in the total flux and does not change the metabolite concentrations.

b) Kacser & Burns (1973) proved a theorem which connects the control strengths with the effector strengths of the metabolites

$$\sum_i C_i X_{ik} = 0 \quad (k = 1, \ldots, m) \quad \text{(A15)}$$

The theorem follows from the consideration that differential changes in the concentration of a metabolite S_k can be compensated by variations of the kinetic parameters of the enzymes which are influenced by this metabolite so that the flux remains unaltered.

For metabolic systems in which the number of enzymes exceeds the number of metabolites only by one (e.g. linear enzymatic chains) theorems a) and b) suffice for the calculation of the control strengths. In case of branches in the system the number of enzymes can exceed that of the metabolites by more than one and the control strengths of at least (n - (m+1)) enzymes must be calculated by means of **Eqs.** (A12) and (A13). The remaining control strengths can be obtained by the theorems a) and b).

References

Bartel,U., Manitz,L., Matthes,G. & Weber,F. (1972) Dissertation an der medizinischen Fakultät d. wiss. Rates d. Humboldt- Universität zu Berlin

Gerber,G.,Berger,H.,Jänig,G.-R. & Rapoport,S.M. (1973) Eur.J.Biochem.38, 563-571

Harkness,D.R.,Thompson,W.,Roth,S. & Grayson,V. (1970) Arch. Biochem. Biophys. 138, 208- 219

Heinrich,R. & Rapoport,T.A. (1974) Eur.J.Biochem. 42,89- 95

Heinrich,R. & Rapoport,T.A. (1975) BioSystems, in press

Jacobasch,G. & Raderecht,H.J. (1967) Acta biol.med.germ. 17, 275- 284

Jacobasch,G. (1970) Thesis Dr. s.c.,Biowiss.Fakultät d. Humboldt-Universität zu Berlin

Kacser,H. & Burns,I.A. (1973) in: Rate Control of Biological Processes (Davies,D.D.,ed.),pp.65- 104,Cambridge University Press

Minakami,S. (1968) in: Metabolism and Membrane Permeability of Erythrocytes and Thrombocytes (Deutsch,E., Gerlach,E. & Moser,K.,eds.),pp.10-15, Georg Thieme Verlag, Stuttgart

Nakao,M. (1974) in: Cellular and Molecular Biology of Erythrocytes (Yoshikawa,H. & Rapoport,S.M.,eds.) pp.35-54, University Press,Tokyo

Park,D.J.M. (1974) J.theor.Biol. 46, 31-74

Rapoport,S.M. & Luebering,J. (1950) J.Biol.Chem.183,507-516

Rapoport,S.M. & Luebering,J. (1951) J.Biol.Chem.189,683-694

Rapoport,T.A.,Heinrich,R.,Jacobasch,G. & Rapoport,S.M. (1974) Eur.J.Biochem. 42, 107-120

Reinauer,H. & Bruns,F.H. (1964) Biochem. Zeitschrift 340, 503-521

Rosa,R.,Gaillardon,J. & Rosa,J. (1975) VIIth International Berlin Symposium on the Structure and Function of Erythrocytes 1973 (Rapoport,S.M. & Jung,F., eds.) Akademie Verlag,Berlin, in press

Rose,Z.B. & Liebowitz,J. (1970) J.Biol. Chem. 245,3232-3241
Rose,Z.B. (1973) Arch.Biochem.Biophys. 158,903-910
Sel'kov,E.E. (1975) VIIth International Berlin Symposium on Structure and Function of Erythrocytes 1973 (Rapoport,S.M. & Jung,F.,eds.) Akademie Verlag, Berlin, in press
Tichonov,A.N. (1948) Mat.Sb. 22,(64), 193
Willems,J.L. (1973) Stabilität dynamischer Systeme, Oldenburg Verlag,München,Wien

III. MODELLING OF CELLS AND ORGANISMS

Symp. Biol. Hung. 18, pp. 215–226 (1974)

KINETIC MODELLING OF DIFFERENTIATION IN THE CELLULAR SLIME MOLD

B. WRIGHT

Boston Biomedical Research Institute
Boston, Ma. USA

INTRODUCTION

I would like to begin by making some general observations about the nature of differentiation. For purposes of illustration, consider eye pigment accumulation in the fly. A variety of time scales are represented (Fig. 1). Evolution is measured in years, the life cycle in days, and

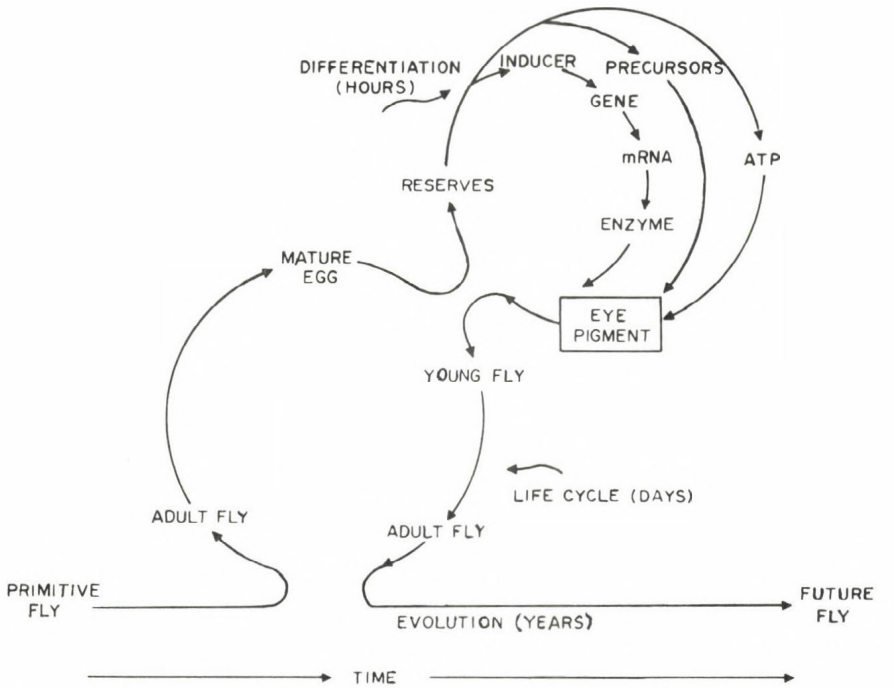

Fig. 1. The sequence of events preceeding eye pigment accumulation in the fly.

the sequential events immediately preceeding pigment synthesis in hours. Does the activation of the gene indicated 'cause' differentiation? If it occurs close in time to pigment accumulation, most people would say it does 'cause' differentiation. But what if the mRNA is already in the mature egg, and gene activation occurs during egg maturation or even earlier, during evolution? Each event is only one in an inevitable series, which could be traced back in time through the evolution of this system. To pick any one event and call it a 'cause' denies this history of successive events. No cellular component has the intrinsic ability to act alone; all components are equally essential to pigment accumulation. No component (gene, inducer, ATP, precursor) is more essential or important than the others. Gene activation, whenever it occurs, has no more claim as 'the basis' of differentiation than precursor availability--less so, in fact, as enzymes are catalysts and usually in great excess. Precursor availability limits the rate of most reactions *in vivo*. Perhaps we should put less emphasis on correlations at the genetic and enzymatic level, and attempt to describe the relationships between the many variables essential to differentiation. Only then can we hope to learn which ones are critical at particular points in time.

I would like to use Fig. 2 to discuss various kinds of rate-limiting events which could occur and affect differentiation in this system. Let us say an enzyme of energy metabolism is impaired and that ATP production is limiting. This may affect the distance the fly can fly. However, if

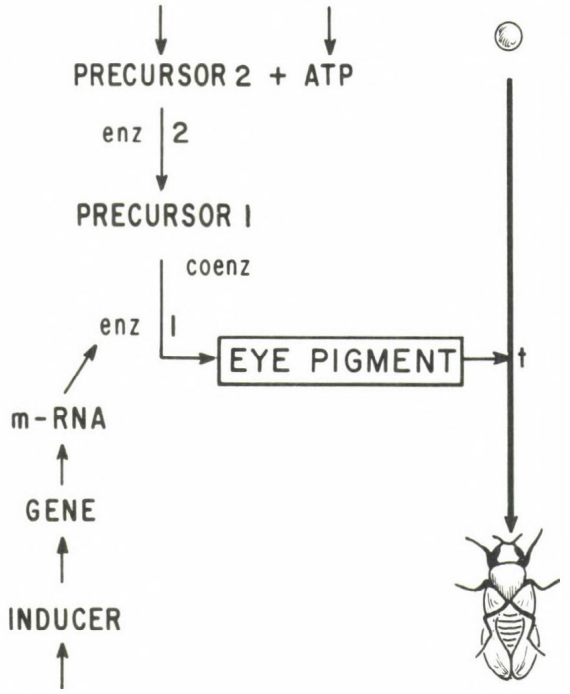

Fig. 2. Possible rate-limiting events controlling eye pigment accumulation during differentiation in the fly.

ATP availability is in great excess compared to precursor 2, pigment formation will not be affected. With respect to differentiation, then, the enzyme impaired is vital and essential, but not unique or critical (i.e., rate-limiting). If ATP availability is limiting for the synthesis of precursor 1 and pigment accumulation is affected, the enzyme is critical, but not unique to differentiation. Now consider enzyme 2, which is essential and unique to differentiation. If this enzyme is in great excess, impairing its activity will not affect pigment synthesis, and it is a unique but not a critical enzyme. On the other hand, if enzyme 2 limits the rate of precursor 1 formation, it is critical to differentiation. We shall now turn to the subject of the rest of this presentation, a microbial model system called the cellular slime mold.

RESULTS AND DISCUSSION

The carbohydrate metabolism of Dictyostelium discoideum is a very simple and convenient system for the analysis of critical variables controlling a differentiation process. The fact that cytodifferentiation occurs in

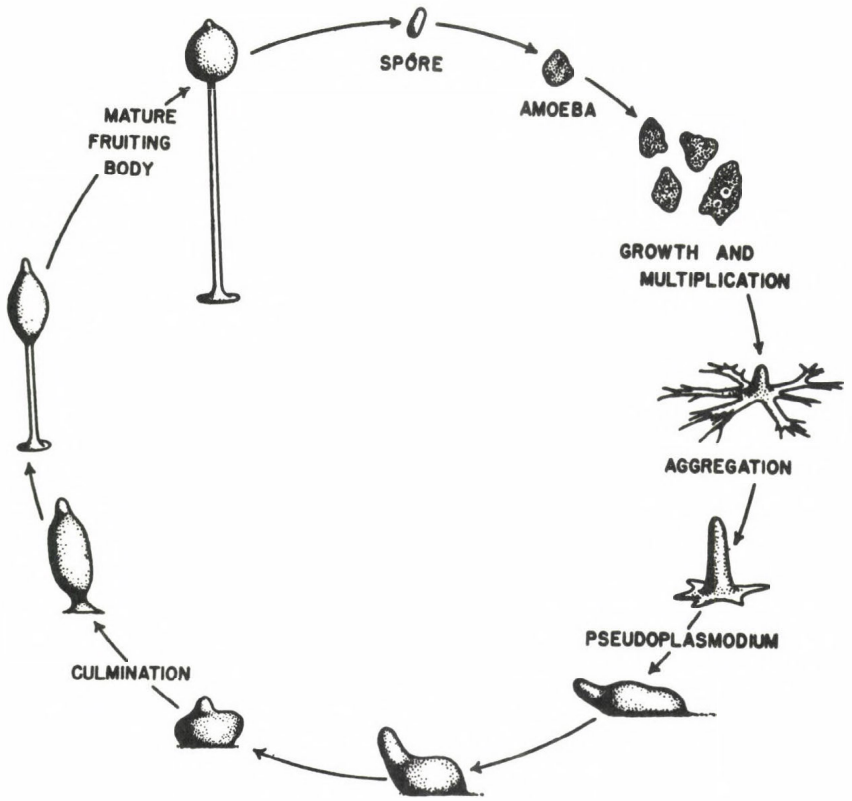

Fig. 3. The life cycle of the cellular slime mold, Dictyostelium discoideum.

the absence of cell division under starvation conditions, also makes this system particularly amenable to quantitative analysis. As indicated in Fig. 3, unicellular amoebae stream together to form multicellular aggregates. Each aggregate then undergoes a transformation (culmination) which results in the formation of a fruiting body or sorocarp, the latter consisting of a spore mass or sorus supported by a cellulose-ensheathed stalk. The entire morphological transformation is complete within 24 hr at 22 C. The major end products which accumulate are trehalose and cellulose (Rosness and Wright, 1974); total carbohydrate remains constant during development, but is rearranged between various metabolic pools and phases. Endogenous glycogen is used as the major source of glucose units for the synthesis of the new end products of differentiation (Table 1).

Table 1.

Approximate saccharide composition during differentiation[1]

Carbohydrate	Stage of differentiation	
	Aggregation	Sorocarp
Soluble glycogen	50	23
Trehalose	0.2	11
α-Cellulose	0	16
β-Cellulose	0	16
Cell wall glycogen	0	6
Mucopolysaccharide[2]	0	5
Glycoprotein[3]	14	-
Glucose	0.2	0
Unknown	35.6	23.0

[1] Rosness and Wright, 1974

[2] White and Sussman, 1961

[3] Gerisch, et al., 1969

The reactions depicted in Figure 4 are all essential to differentiation in this simple microbial system. The accumulation patterns of the metabolites shown have been measured over 900 minutes of differentiation (from aggregation to sorocarp) and most of the reactions have been examined both in vivo and in vitro (Gustafson and Wright, 1972; Killick and Wright, 1974; Pannbacker, 1967; Sargent and Wright, 1971; Wright, 1973). This metabolic network changes over a period of 900 min from one steady state (undifferentiated) to another (differentiated), defined in terms of the accumulation of two specific saccharides, trehalose and cellulose. Correlated with this process are changes in the concentration and flux of various metabolites and changes in the activities of many enzymes. The problem is to determine which of these changes

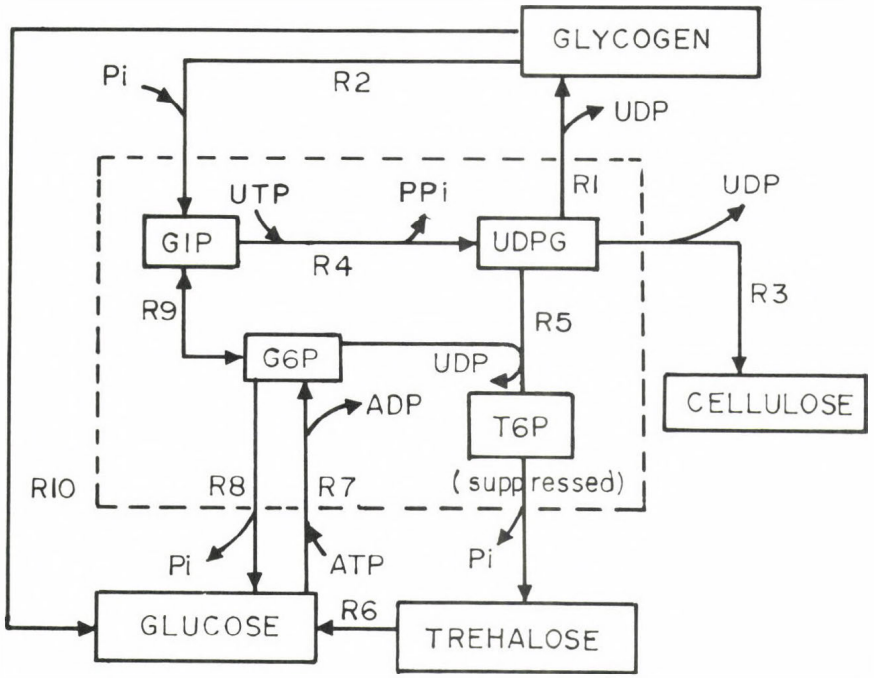

Fig. 4. Kinetic model of metabolic pathways simulated. Abbreviations: Pi, inorganic phosphate; PPi, inorganic pyrophosphate; UDPG, uridine diphosphoglucose; UTP, uridine triphosphate; G1P, glucose-1-phosphate; G6P, glucose-6-phosphate; and ATP, adenosine triphosphate.

---

control the metabolism of differentiation (i.e., are rate-limiting) at particular points in time. The primary aim of the present simulation analysis is to compare the relative influence of three enzymes on the accumulation of trehalose and cellulose. By using kinetic models, it is possible to simulate the effects of changing enzyme activities on this metabolic network. The three enzymes to be examined catalyze the following reactions, indicated in Fig. 4. R2 (glycogen phosphorylase), R4 (UDP-glucose pyrophosphorylase), and R5 (trehalose-6-phosphate synthetase). Although the model simulates metabolic changes over a 900-minute period of differentiation, the period between 630 and 900 minutes (culmination to sorocarp) will be the focus of attention, as all three enzymes are active during this period.

Initially, i.e. at culmination, nearly all of the carbohydrate material considered in the present model is contained in the soluble glycogen pool. After culmination this material is converted to trehalose and cellulose, flowing through a network of small, rapid turnover pools consisting of glucose-1-phosphate (G1P), glucose-6-phosphate (G6P),

trehalose-6-P (T6P), and UDP-glucose (UDPG). At the sorocarp stage, approximately 32 mM cellulose and 11 mM trehalose have accumulated, and the soluble glycogen pool has declined (Table 1).

We assume (along with all enzymologists) that enzyme kinetic mechanisms and constants apply to the intact cell. We incorporate these mechanisms and flux values obtained with isotope studies *in vivo* into a kinetic model and try to mimic the dynamics of the intact cell, i.e., by describing the rates of all reactions indicated in Fig. 4 and the changes in concentration of metabolite pools and end products during differentiation. The user of the program supplies the initial metabolite concentrations (determined experimentally), the kinetic expressions and constants for each reaction shown (determined *in vitro*), the rates of key reactions (determined with isotopes *in vivo*), and activation functions for each enzyme. To define an activation function consider, for example, an initial velocity expression with no significant product inhibition:

$$\text{Rate} = V = V_1 [A/(K_a + A)]$$

V is determined *in vivo*, A is the substrate concentration, and K_a the Michaelis binding constant. The latter is determined *in vitro*, but V_1, or V_{max}, is calculated as the unknown. We therefore call it V_v, to be distinguished from V_{max} as determined *in vitro*. V_v corresponds to the amount of enzyme activity which can change during differentiation, so we make it a function of time ($V_v(t)$). This so called 'activation function' can be arbitrarily changed by the user of the program. In our standard model activation functions are adjusted so that the output of the program over the course of differentiation gives metabolite accumulation patterns and flux values corresponding to the experimental data. Further details of our kinetic modelling approach may be found elsewhere (Gustafson and Wright, 1972; Wright, 1973; Wright and Gustafson, 1972; Wright, *et al.*, 1968).

By using trajectories depicting the concentrations of trehalose and cellulose as a function of time, it is possible to visualize the effects of variations in enzyme activation functions on the outcome of differentiation (i.e., saccharide accumulation) (Wright and Park, 1975). This representation describes carbohydrate metabolism fairly completely, as total carbohydrate (largely trehalose, cellulose and glycogen) is conserved and the glycogen concentration can be calculated by the difference. The term 'speed of differentiation' will mean the rate of movement of the carbohydrate system along its trajectory (length of a trajectory segment/time to travel over the segment). In Figs. 5-7 Part A describes the three activation functions used and Part B the resulting effect on the trehalose/cellulose balance. The encircled case (II) represents the standard model, giving output consistent with all the available data. The diagonal lines indicate equal time periods beginning at 630 minutes (culmination). In the analysis of this metabolic network, it is of particular importance to bear in mind that trehalose synthesis is a bimolecular reaction and is therefore a function of the product of two substrate concentrations. In contrast, the rate of cellulose synthesis is a function only of the UDPG concentration. Thus, when the levels of both UDPG and glucose-6-P change, there results a greater (positive or negative) effect on the rate of trehalose synthesis than on that of cellulose synthesis.

Trehalose-6-P Synthetase: Although this enzyme influences the final trehalose/cellulose balance (Fig. 5), it does not affect the speed of differentiation. That is, trajectories are of comparable length and

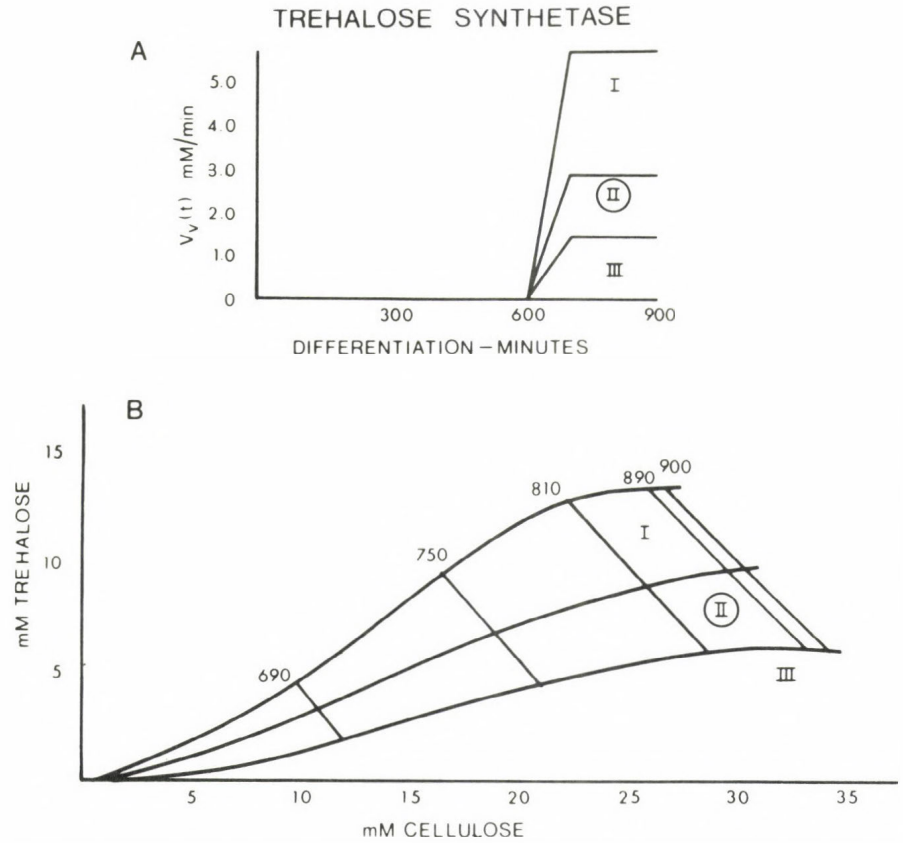

Fig. 5. Trajectories (B) depicting the concentrations of cellulose and trehalose for three activation functions (A) of trehalose synthetase. The standard case, II, is encircled.

Table 2.

UDP-glucose concentration (mM) as a function of changes in $K_v(t)$ for trehalose synthetase

TIME	CASE I	CASE II	CASE III
690	.25	.30	.34
750	.22	.26	.30
810	.16	.19	.22
870	.06	.07	.07

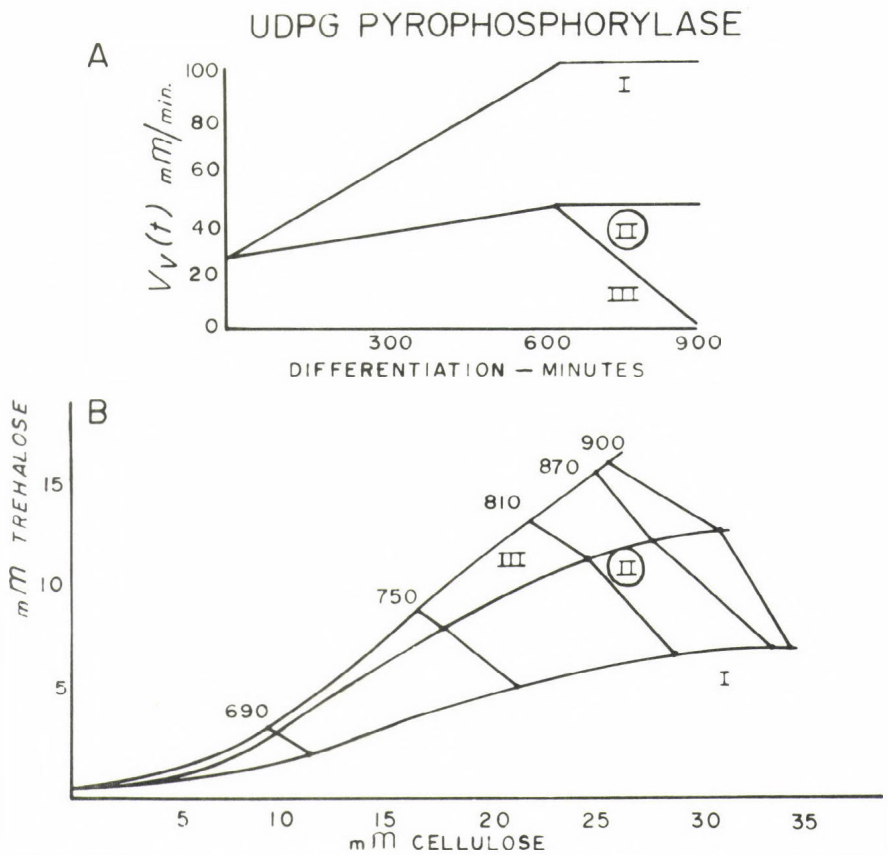

Fig. 6. Trajectories (B) indicating the concentrations of cellulose and trehalose for three activation functions (A) of UDP-glucose pyrophosphorylase. The standard case, II, is encircled (Wright and Park, 1975).

---

the lines connecting similar time points on the trajectories represent equal glycogen concentration. An increase in $K_v(t)$ for trehalose-6-P synthetase lowers the steady-state level of the UDP-glucose pool (Table 2) and slightly lowers the hexose phosphate pool size. The rate of trehalose synthesis is increased and that of cellulose decreased. The final trehalose + cellulose concentration is not affected by the relative rates of synthesis of cellulose and trehalose, but the trehalose/cellulose ratio is increased by high trehalose synthetase activity.

UDP-glucose pyrophosphorylase: As seen in Fig. 6 changes in the activity of UDP-glucose pyrophosphorylase do not affect the speed along the trajectory, but do affect its direction and hence the final trehalose/cellulose ratio. Decreasing this enzyme activity causes the hexose phosphate pools to increase in size (Table 3), thereby increasing the rate of trehalose synthesis. This additional drain on the UDP-glucose pool causes it to decrease in size, but to an extent less than the amount by

Table 3.

Glucose-1-P and UDP-glucose concentration (mM) as a function of changes in $V_v(t)$ for UDP-glucose pyrophosphorylase[1]

	Glucose-1-P[2]			UDP-glucose		
Time	Case I	Case II	Case III	Case I	Case II	Case III
690	.006	.011	.012	.34	.28	.25
750	.004	.008	.012	.20	.25	.20
810	.002	.006	.011	.20	.20	.14
870	.0006	.002	.011	.08	.12	.06

[1] from Wright and Park (1975)

[2] Glucose-6-P = 6 x glucose-1-P

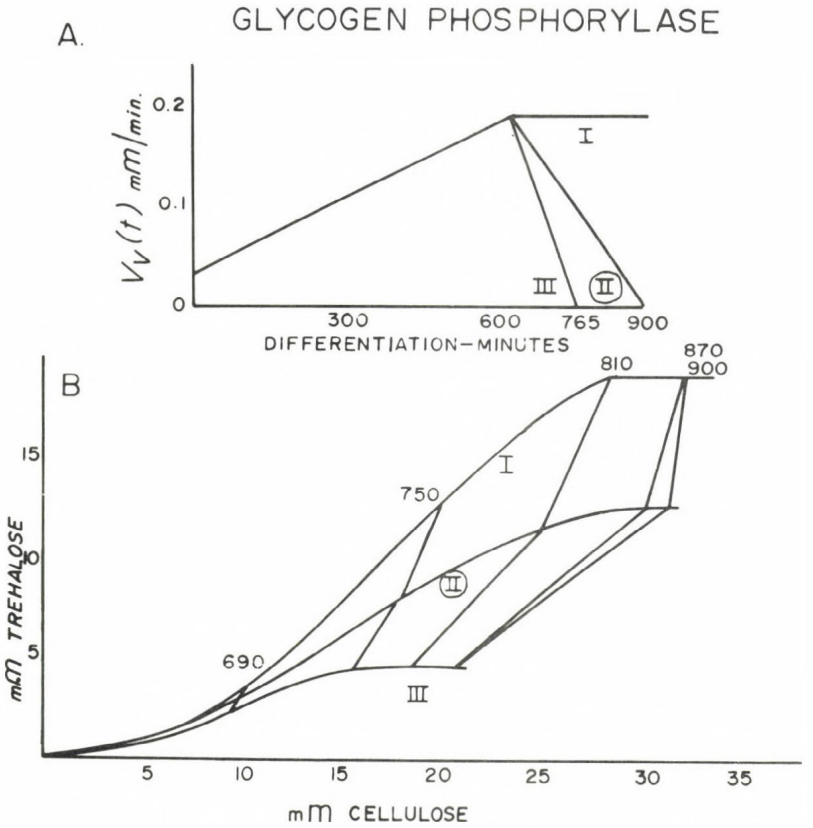

Fig. 7. Trajectories (B) depicting the concentrations of cellulose and trehalose for three activation functions (A) of glycogen phosphorylase. The standard case, II, is encircled (Wright and Park, 1975).

which the hexose phosphate pool increases. Thus, an increase in the rate of trehalose synthesis is seen, accompanied by a corresponding decrease in the rate of cellulose synthesis. The net effect is that decreasing the enzyme activity bends the trajectory toward the trehalose axis and increasing the enzyme activity bends the trajectory toward the cellulose axis. The accumulation of this enzyme during differentiation is not critical in controlling the rate of the reaction it catalyzes (Wright and Gustafson, 1972; Wright, et al., 1968). However, the present analysis suggests that the enzyme levels achieved by 630 min may play a subsequent role in controlling the competition between the synthesis of cellulose and of trehalose for common precursor materials.

Glycogen phosphorylase: Changes in the activity of this enzyme exert strong control over both the speed of differentiation and the cellulose/trehalose ratio (Fig. 7). Both the glucose-1-P and UDP-glucose pool levels are affected (Table 4). The higher the enzyme activity, the higher the substrate levels and the higher the trehalose to cellulose ratio. That is, the bimolecular reaction is favored by an enhanced level of both precursors, only one of which is used for cellulose synthesis. The striking effect of phosphorylase on the speed of differentiation suggests that a mutant strain of D. discoideum which differentiates more rapidly than wild type (Sonneborn, et al., 1963) may have abnormally high enzyme activity.

Predictions arising from the analyses presented here have recently been confirmed experimentally. Hames and Ashworth (1974) studied the effect of the initial glycogen content in an axenic mutant of D. discoideum on the subsequent rate of glycogen breakdown and end product accumulation during differentiation. Cells with high glycogen content had 2-fold higher glycogen phosphorylase activity and higher levels of glucose, glucose-6-phosphate and UDP-glucose. Furthermore, these cells

Table 4

Glucose-1-P and UDP-glucose concentration (mM) as a function of changes in $V_v(t)$ for glycogen phosphorylase[1]

Time	Case I	Case II	Case III	Case I	Case II	Case III
690	.014	.011	.008	.31	.28	.24
750	.014	.008	.003	.30	.25	.14
810	.005	.006	.001	.20	.12	.09
870	.001	.003	.0004	.08	.12	.03

[1] from Wright and Park (1975)

[2] Glucose-6-P = 6 x glucose-1-P

accumulated abnormally high levels of cellulose and trehalose, with the latter being far in excess. This result would be predicted from our model (Fig. 7). The characteristics of the axenic mutant were simulated, and the striking comparison between the predicted and observed values (Wright and Park, 1975) strongly suggests that the 2-fold increase in specific activity of glycogen phosphorylase observed *in vitro* also occurs *in vivo*, and that this change alone is the critical variable controlling the enhanced accumulation of metabolites and end products. In spite of the fact that an increase in the amount of trehalose occurred, no change was seen in the activity of trehalose-6-P synthetase (Hames and Ashworth, 1974). Had one been observed, the simulation analyses indicate that it could not occur *in vivo*. The present and previous studies (Wright and Marshall, 1971) have shown that an increase in the activity of this enzyme would result in a *decrease* in the amount of cellulose, glucose-6-P and UDP-glucose (Fig. 5, Table 2). For this reason, it was predicted that the increase in activity of trehalose-6-P synthetase found *in vitro* prior to culmination could not reflect increased enzyme activity *in vivo* (Sargent and Wright, 1971; Wright and Marshall, 1971). Another example of using kinetic models to judge the relevance of *in vitro* data to the intact cell concerns trehalase activity. Although this enzyme is active in extracts prepared in cells accumulating trehalose, it cannot be active *in vivo*, as the degradation of trehalose during its accumulation would require a higher rate of synthesis than that observed *in vivo* (Sargent and Wright, 1971; Wright and Marshall, 1971). In the case of UDP-glucose pyrophosphorylase, the enzyme level, UDP-glucose, and the rate of UDP-glucose synthesis all increase in parallel prior to culmination. However, simulation studies indicate that the enhanced enzyme level cannot be primarily responsible for the increased rates of either UDP-glucose synthesis or UDP-glucose accumulation (Wright and Gustafson, 1972; Wright, 1973; Wright, *et al.*, 1968).

Predictions such as these derived from the construction and perturbation of kinetic models have now been substantiated experimentally in many instances (Marshall, *et al.*, 1970; Sargent and Wright, 1971; Wright, 1973; Wright and Gustafson, 1972; Wright and Marshall, 1971; Wright, *et al.*, 1968). Such confirmations are most encouraging, as they validate the use of dynamic models in the analysis of biochemical differentiation and strongly suggest a close correspondence between model behavior and the behavior of differentiating cells.

SUMMARY

Biochemical differentiation in the cellular slime mold, *Dictyostelium discoideum* is described. Kinetic models of this system have been constructed, using cellular metabolite levels, reaction rates determined *in vivo*, and enzyme kinetic mechanisms and constants determined *in vitro*. By perturbing these models, insight has been gained as to which variables (enzymes, metabolite flux) are most critical in controlling specific reactions essential to differentiation. Model exploration has also led to specific predictions which can be tested experimentally.

ACKNOWLEDGEMENTS

This work was supported by research grants HD 05357 and HD 04667 from the USPHS, National Institutes of Health.

REFERENCES

Gerisch, G., Malchow, D., Wilhelms, H. and Lüderitz, O. (1969). Eur. J. Biochem. 9, 229.

Gustafson, G.L. and Wright, B.E. (1972). in Critical Reviews in Microbiology, Vol. 1(4), eds. A.I. Laskin and H. Lechevalier (CRC Press, The Chemical Rubber Company, Cleveland) p. 453.

Hames, B.D. and Ashworth, J.M. (1974). Biochem. J. 142, 317.

Killick, K.A. and Wright, B.E. (1974). Ann. Rev. Microbiol. 28, 139.

Marshall, R., Sargent, D. and Wright, B.E. (1970). Biochemistry 9, 3087.

Pannbacker, R.G. (1967). Biochemistry 6, 1283.

Rosness, P., Gustafson, G.L. and Wright, B.E. (1971). J. Bacteriol. 108, 1329.

Rosness, P. and Wright, B.E. (1974). Archiv. Biochem. Biophys. 164, 60.

Sargent, D. and Wright, B.E. (1971). J. Biol. Chem. 246, 5340.

Sonneborn, D.R., White, G.J. and Sussman, M. (1963). Dev. Biol. 7, 79.

White, G.J. and Sussman, M. (1961). Biochim. Biophys. Acta 53, 285.

Wright, B.E. (1973). Critical Variables in Differentiation. Prentice-Hall, Inc., Englewood Cliffs, N.J.

Wright, B.E. and Dahlberg, D. (1967). Biochemistry 6, 2074.

Wright, B.E. and Gustafson, G.L. (1972). J. Biol. Chem. 247, 7875.

Wright, B.E. and Marshall, R. (1971). J. Biol. Chem. 246, 5335.

Wright, B.E. and Park, D.J.M. (1975). J. Biol. Chem., in press.

Wright, B.E., Simon, W. and Walsh, B.T. (1968). Proc. Natl. Acad. Sci. US 60, 644.

Symp. Biol. Hung. 18, pp. 227–256 (1974)

COMPUTER SIMULATION MODELS OF GENE EXPRESSION

K. Bellmann [1], R. Böttner [1], [2]
A. Knijnenburg [1], H. Neumann [2]

1) Central Institute of Cybernetics and Information Processes
Acad. Sci. GDR, 1199 Berlin-Adlershof, Rudower Chaussee

2) Central Institute of Molecular Biology,
Acad. Sci. GDR, 1115 Berlin-Buch, Lindenberger Weg

1. Introduction

The analysis of large scale systems in biology by means of algorithmic simulation has developed to a fruitful tool to get deep insights in the internal machinery of dynamic processes. It is possible to study the integrative behaviour of complex networks, especially in such cases where the types of behavior patterns cannot be forecasted intuitively. Mapping real systems by adequate algorithmic models [general method in model building and adapting see Bellmann et. al. (1974)] using model parameters with very close relations to real system parameters, one gets results about (I) laws and principles that govern dynamic behaviour of the total system on the basis of coordination and interaction of subunits, (II) internal key sites (control variables) with big control effects on the over-all output, (III) tests of hypotheses about the internal structure (structural and functional elements and their interrelations) of the system under investigation. Consequently new experiments can be proposed. - In this contribution some algorithmic simulation models, realized about a discrete time axis and describing the processes of gene expression in molecular terms are presented. They are models of genetic information processing, that are elaborated in the last years [see also model of transcription process in eucaryotes (Bellmann et.al., in press) in procaryotes (Neumann, Kreischer, in press),

model of translation (Knijnenburg, 1974; Knijnenburg, Kreischer, in press), overall model of machinery of protein synthesis from transcription until the active protein (Böttner, 1975), model for evaluation of breeding methods applicated to genetic populations (Bellmann, Dragawzew, in press). Here we give an overlook about transcription, translation and global gene expression models.

2. Transcription model in procaryotes

The purpose of the regulation model of transcription in procaryotes is to analyse the effect of different types of regulation mechanism on the rate of mRNA synthesis. By this model it is possible to give predictions about the behaviour of the system under several experimental conditions, e. g. analysis of the influence of positive and negative control of the transcription rate in the case of polymerase deficite. A further aim is to detect sensible control points in order to change the total behaviour by artificial influences.

A DNA section is called transcriptional unit if

(I) DNA section is transcriptable

(II) DNA section owns (a) a defined beginning (regulation sequence). The regulation sequence contains two parts: promoter region and operator region.
(b) a defined end (end terminator sequence)
(c) one and only one autonomous promoter region (in sense of SZYBALSKI)

The cistron sequence consists of one or several cistrons (structural genes). Cistrons or groups of cistrons can be separated from each other by means of terminators ignored under certain circumstances at the transcription.

The class of transcriptional units of the quantity of all organization types of transcriptional units was selected based on the constructive principle of the "classical" operon. The following definition of the prototype is given:

(I) transcriptional unit with the constructive principle
(a) regulation sequence consists of one promoter and one operator.
(b) cistron sequence isn't interrupted by terminators.
(c) end terminator T

(II) transcription is regulated by
(a) negative control realized by operator-repressor-inducer-interaction
(b) positive control realized by promoter-CAP-cAMP-polymerase-interaction
(c) concentration of the free DNA-dependent RNA-polymerase.

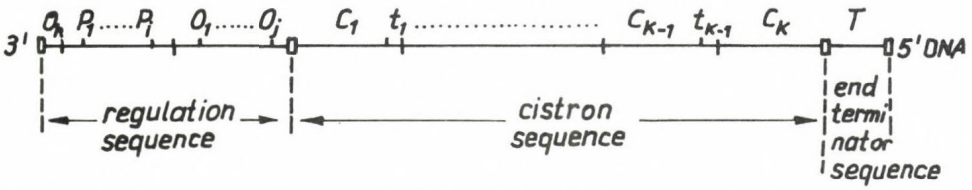

Fig. 1 a Abstract-ideal model of all possible organization types of transcriptional units

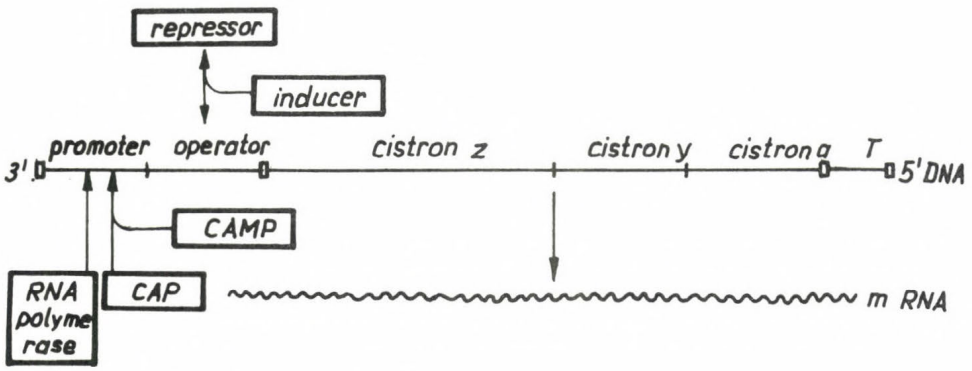

Fig. 1 b The lactose operon

Furthermore acceptances and assumptions are necessary for an exact determination of prototype. They will not be explained. The model is an abstract automaton for description of the system I (b). $\mathcal{A}_p$ is a MOORE automaton defined on the prototype. $\mathcal{A}_p$ is a finite, initial and indeterminate automaton:

$\mathcal{A}_p = {}_{\mathcal{D}f}(X, Y, Z, A, \delta, \mu, z_0)$, where

$X = \{x : x = (IND, IREP, ICAP, IAMP, POL)$

$Y = {}_{\mathcal{D}f} \{0, 1, \ldots, i\}$ number of initiated polymerases

$Z = {}_{\mathcal{D}f} \{0, 1, \ldots, j\}$ number of initiated polymerases on the transcriptional unit

$A = \{A_\delta, A_\mu\}$ algorithm for δ, μ-realization

$\delta : A_\delta^n \circ (X_n \times Z_n) \rightarrow Z_{n+1}$ next state function

$\mu : A_\mu^n \circ z_n \rightarrow Y$ output function

$z_0 \in Z$: initial state $z_0 = 0$,

IND - concentration of inductor = $\begin{cases} 1, & \text{if IND abolishes the repressor effect} \\ 0, & \text{else} \end{cases}$

IREP - concentration of repressor = $\begin{cases} 1, & \text{if repressor can form a complex with operator} \\ 0, & \text{else} \end{cases}$

ICAP - concentration of catabolite activation system = $\begin{cases} 1, & \text{if ICAP is so high that regulation is possible} \\ 0, & \text{else} \end{cases}$

IAMP - concentration of 3', 5'-cyclic AMP = $\begin{cases} 1, & \text{if IAMP is so high that regulation is possible} \\ 0, & \text{else} \end{cases}$

POL - concentration of free DNA-dependent RNA-polymerase. Concentration is given in percentage. POL = 100 corresponds to the concentration at which the polymerases initiate in such a way that they transcribe with a minimal distance. If POL < 100 the probability of initiation decreases (W < 1) and the transcrip-

tional distance between the polymerases is greater than the minimal distance.

The number of initial polymerases was chosen as output Y in order to determine the rate of RNA synthesis ("external" behaviour of system). Number of initial polymerases on the transcriptional unit was chosen as state Z

(I) in order to determine the number of complete synthesized mRNA

(II) in order to learn something about the regulation mechanisms ("internal" behaviour of system).

The algorithmic simulation model is based on the following fundamental parameters:

(I) average transcriptional velocity of the polymerase
(II) length of transcriptional unit and its components
(III) minimal transcriptional distance between two neighborring polimerases reached on optimal system conditions.

These parameters can be determined by comparison of the computer simulated results with the experimental results.

(IV) dependence of the initation probability on the concentration of free RNA polymerase.

To that end experimental investigations are not yet available. Therefore these facts must be estimated indirectly and solution space can be given by means of computer simulation. It is necessary to test this dependence in the experimental investigations.

In Fig. 2 the kinetics of approach to the steady-state rate of the transcription (experimental results) and the predictions computed by the algorithm are shown.

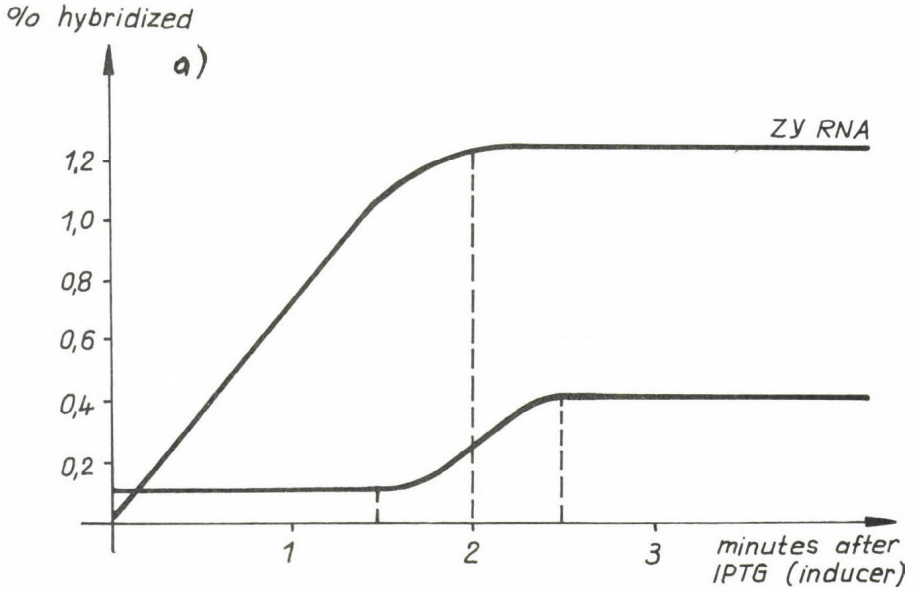

The kinetics of approach to the steady-state rate of lac transcription (Adesnik/Levinthal, Cold Spring Harbor Symp. on quant. Biol., Vol. XXXV, 1970)

b)

results from	time of transcription of Z [sec]	y [sec]	A [sec]
experiments (Adisnik/Levinthal)	~ 90	~ 120	~ 150
computer simulation	97,34	122,33	143,75

Fig. 2 The kinetics of lac transcription

3. An eucaryotic transcription model

In a big lot of in-vitro-experiments always typical patterns of distinct m-RNA fractions were found(see Lindigkeit et.al. 1974). These fractions are characterized by different mean lengths of their molecules in terms of sedimentation coefficients S (5,7,9,11,13,14,17,19,21,23,24,27,29,34 S . From these results it is suggested that on parts of the transcription units special hypothetical structures (transcription blockers) are to be assumed. Because discret sets of m-RNA molecules were found we have to conclude that the transcription blockers are localized in each transcription unit at nearley the same site. The blockers have nearly constant distances between each other (about 500 nucleotides). They give rise to a temporary or final stop of the travelling RNA polymerase. Between two neighbouring blockers the polymerase may travel without any restriction. Due to the RNA-synthesis-stop at distinct blocker sites RNA-chains with discrete lengths occur. The blockers now may be partly removed or inactivited by application of ammonium sulfate. This is the reason why the RNA-molecules synthetized by the travelling polymerase become longer and longer in experiments in which salt is applicated. The situation may be illustrated by Fig. 3. A DNA-template (i.e. transcription unit) T_1 at time t_o with fully acting blocker structures B_o, B_1, ..., B_7 is considered. During a first time intervall a salt conditioned removal of some blockers (as a random process) may happen. B_o is removed and the polymerase runs up to B_1 where it is stopped. Until time t_τ further blockers are removed (further stochastic events) and now it is possible that the polymerase is able to pass through up to B_5. At time t_n a seldom event is shown: all blockers are removed and with this it is possible to synthesize an RNA-molecule of full length.

Supposing

(I) that the removal of the transcription blockers by

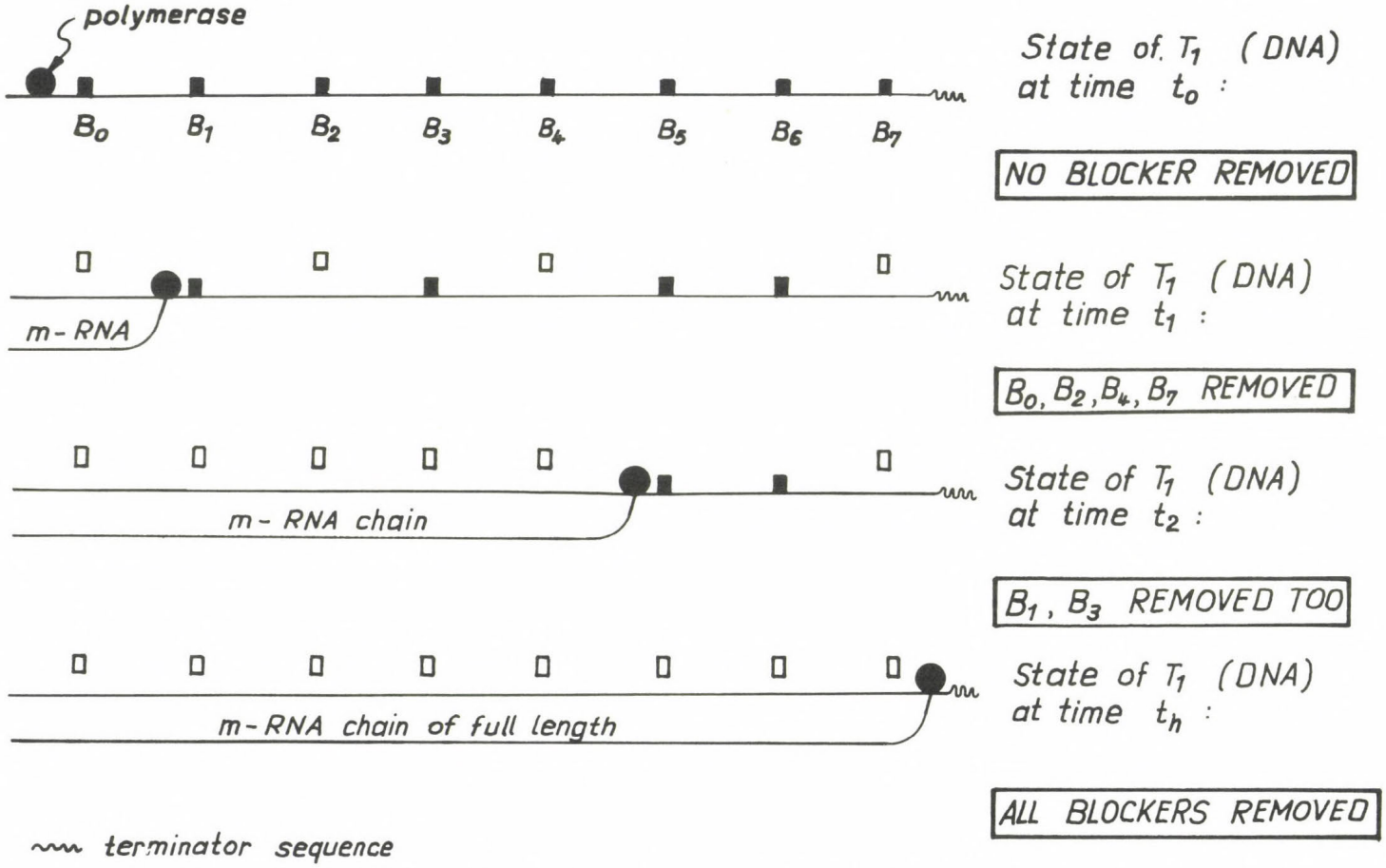

Fig. 3 Scheme of time dependent elongation of a m-RNA molecule synthesized on a single template

salts is a stochastic process realized on each blocker site on each transcriptable template and that a time dependent blocker-removal-probability-function $BRP_i(t)$ is given (or is hypotheticly assumed),

(II) that estimates of the localisation sites of the blockers (expressed in terms of S) are available by estimates from experiments,

(III) that a time dependent function L(t) describing the inactivation (lethality)of polymerase is given (or is hypothetical assumed), and

(IV) that a start distribution of polymerase on the template is given (or is hypothetical assumed)

it may be possible to simulate the transcription process by an adequate algorithmic model in order to test hypotheses, to propose new experimental designs and to get information about the importance of the system elements in the control of the process under investigation. We have to chose parameter types 1. internal (microscopic) basis parameters B_i, by which the real system is characterized and which therefore are to be included in the model. 2. phenomenological, external (macroscopic) parameters P_j, need to fit the model (i.e. the B_i) on the real system.

As a first step we have to discretisize T in small sections of equal length each representing a S unit (about 250 nucleotides).

a = 70 S is a variable value which designates the maximal length of messenger molecules to be expected in the experiments. The time needed by the polymerase to travel from A_i to A_{i+1} is called tact and depends on the 1. basis parameter B 1: velocity of polymerase (VP), i.e. number of synthesized nucleotides per second (e.g. 30).

The 2. basis parameter B 2 is the blocker-position-parameter

$\underline{\bar{x}} = (\bar{x}_1, \ldots, \bar{x}_i, \ldots \bar{x}_b)$, estimated from experiments.

A random binary blocker state variable $D_i(t)$ may be defined now

$$D_i(t) = \begin{cases} 0, & \text{if polymerase is stopped at the ith blocker at time t} \\ 1, & \text{if polymerase is passing the ith blocker at time t} \end{cases}$$

The 3. basis parameter B 3 is the blocker-removal-probability $BRP_i(t)$; it is the probability that $D_i(t) = 1$. The $BRP_i(t)$ are very important variable fuctions being changed in the process of model fitting. Their slope is monoton increasing or decreasing or maximum function.

The 4. basis parameter B 4 is the polymerase-start-distribution $\underline{C} = (C_0, C_1, \ldots C_i \ldots C_b)$, where the C_i are relative amounts of molecules lieing in front of blockers B_i.

The 5. basis parameter B 5 is a non-template-parameter. We have to consider the ratio of active polymerase during the experiment and we define a further random binary variable: state of polymerase at time t:

$$Z(t) = \begin{cases} 1, & \text{if a polymerase is lethal at time t} \\ 0, & \text{if a polymerase is not lethal at time t} \end{cases}$$

P1 represents the time dependent RNA-synthesis-function RNA(t): total amount of synthesized RNA.

P2 represents the over-all-chain-length-distribution appropriate.

$$p(x) = \sum_{i=1}^{b} p(x_i).$$

P1 and P2 are estimable by appropriate experiments.

In Fig. 4 results concerning P2 of a fitted model in comparison with experimental results are demonstrated.

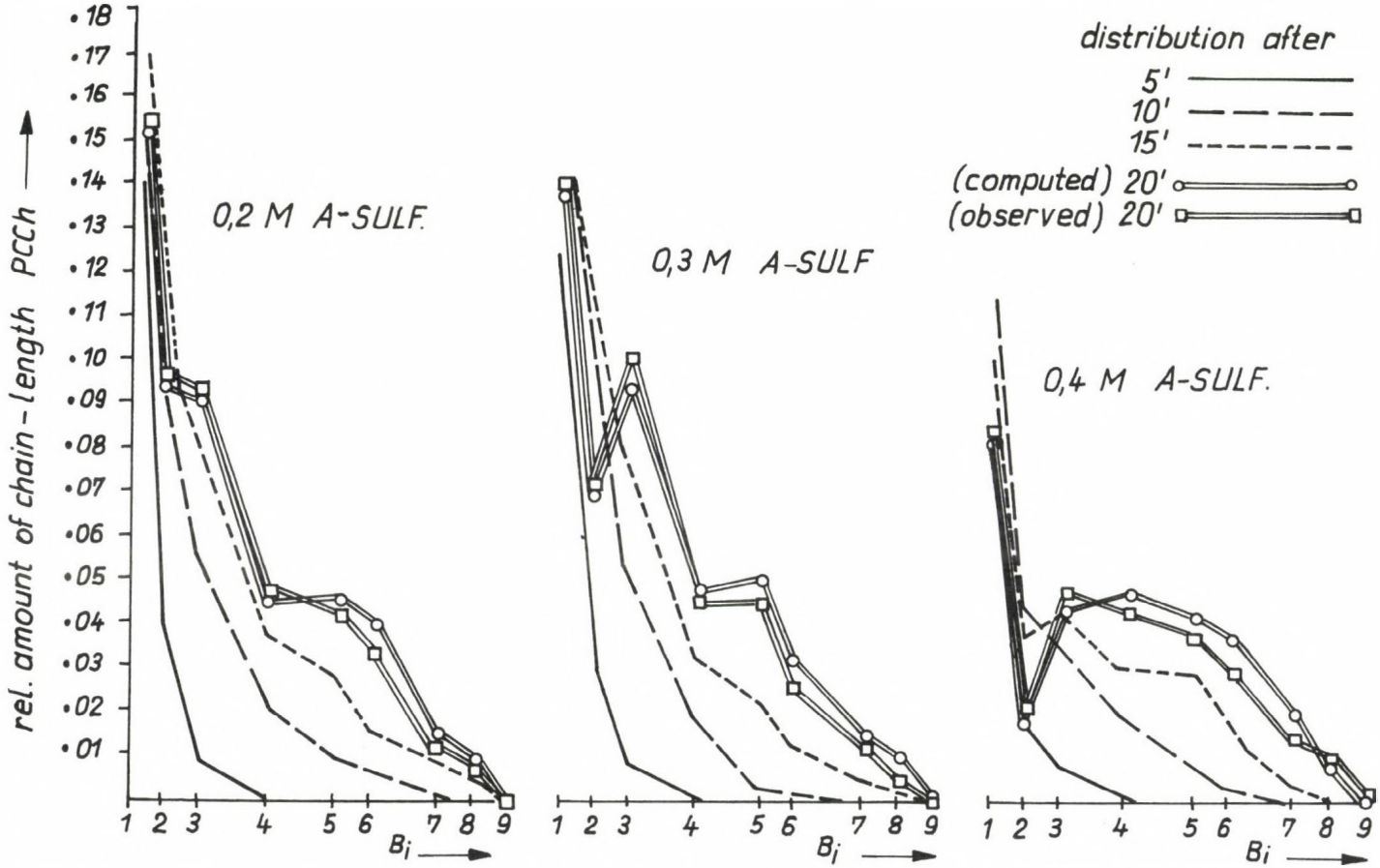

Fig. 4 Observed time dependent chainlengths in the case of 3 ammonium sulfate concentrations in comparison with computer results.

4. Model of the infection process of RNA-bacteriophage S

This model was elaborated to investigate the inherent regulation mechanisms in a defined RNA-bacteriophage prototype system. We hope that this model may serve as an instrument to investigate the regulation of genetic information release in the course of ontogenesis, using a very small and well known transparent biological system. The process of information expression is molecule wise adequate mapped in the computer algorithm.

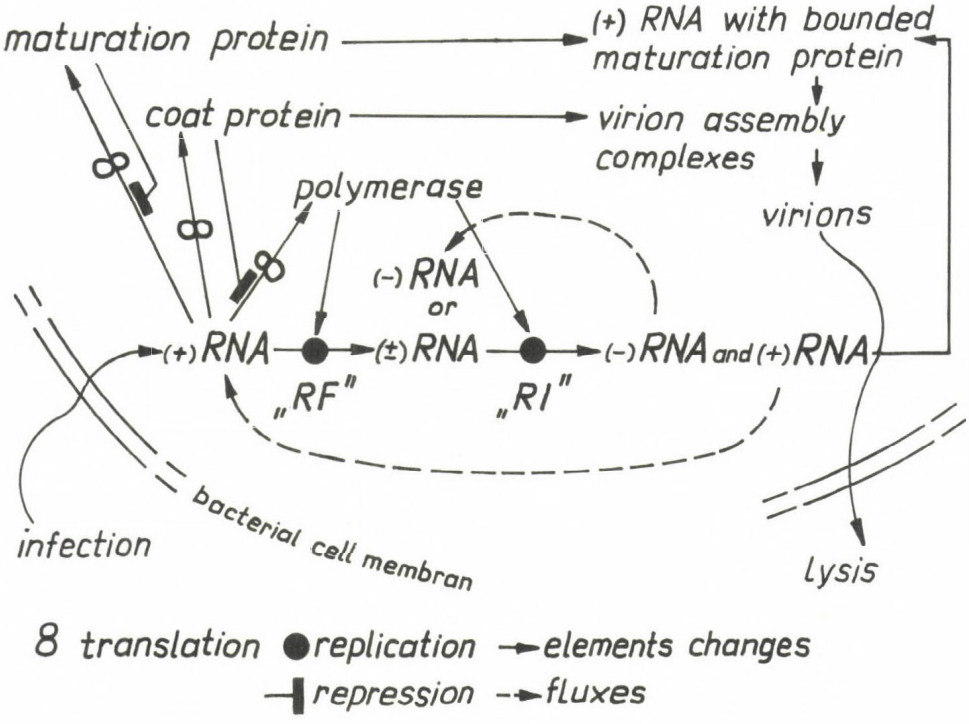

Fig. 5 The RNA bacteriophage replication cycle

Fig. 5 shows the viral system of a definite prototype of the RNA-bacteriophage group. The infection process starts with the penetration of the parental RNA plus strand in the bacteria used by the host cell ribosomes as a messenger. Thus phage specific proteins will be produced by expression of

its three genes of the RNA(+) strand which are maturation protein, coat protein, and polymerase.

The polymerase in connection with cell factors synthesize an RNA strand using the parental strand as template. This complex is called the "replication form" of the viral RNA ("RF"). The replication product is double stranded RNA. The replicating enzyme consists of four subunits one of which is the virus coded polymerase. The same replicating enzyme accepts minus RNA strands as template by loosing two host cell specific subunits. These complexes where the replicase is working at complementary RNA strands is called the "intermediate replication form" ("RI"). Here the replication product is plus RNA. The plus strands may again be translated or replicated or they can go the unidirectional way of virion assembly that begins if maturation protein binds to the nascent RNA plus strands. Virion assembly is the process of continued binding of coat protein molecules to the assembling complex concerning one molecule plus RNA, one molecule maturation protein and the already bounded coat protein molecules. The assembly ends if the coat consists of 180 protein molecules. The viral infection process is terminated by the lysis of the bacterial cell membrane loosing lots of thousands infections particles into the medium. The mathematical model of this system has the purpose to explain the integrative overall behaviour of the viral cycle from the contribution of the single molecular mechanism. In this sense we want that the model is an aid to test chemicals to be worth for repression of viral genoms. Therefore we are to copy the single biochemical mechanism and the system elements on the molecular level. Thus we define the system state as the totality of the numbers of molecules of all the system elements shown in the Fig. 6. The possible relations between the system elements are collected in an algorithm. The different types of this relations in the under part of the scheme are to be seen. This form of the definition of the system state together with the algorithm is sufficient

to describe the viral system as an autonomous initial automaton without output.

The initial state z_0 is characterized by the factum, that at the beginning of the infection process the viral system consists of a single molecule parental phage RNA. A is a stochastic algorithm because it describes a lot of random processes. Above all the stochastic relates to the binding processes (e.g. the binding of ribosomes to plus RNA). The probabilities assumed are based on the real system. Thus G is a stochastic automaton because it turns over from a given state in an other state with a given probability.

$$G = \left[\{ z_T \mid z_T = A^T \circ z_0 , T = 0,1,\ldots, T_{max} \}, A, z_0 \right]$$

T_{max} denotes how many times A must be realized by the automaton. T_{max} may be selected arbitrary or T_{max} will be found by the system itself because the process will be simulated until lysis. The set of all possible system states Z cannot be found completely because of a lot practical and oeconomical reasons. That can be understand immediately if one know that the system includes a large set of different system elements taking the time as a basis which is needed by a ribosomes translation of one codon as the length of one tact. The state declares in each case the numbers of molecules or molecule complexes resp. for all these system elements. A state change consists of a change of these numbers. It is obvious that there are enormous big number of possibilities for one state change. In addition to that several processes are stochastic. If there are only few participants of the reactions it is not possible to operate with expectation values for random events, e.g. the binding of ribosomes to RNA. Therefore the single random event has to be simulated as a "yes" or "no" decision with a certain probability for "yes". This kind of the algorithm leads to a real Monte Carlo simulation. Through that the run time charged is increased, but not overmuch because the random generators work very quickly. The very long run times [up to about

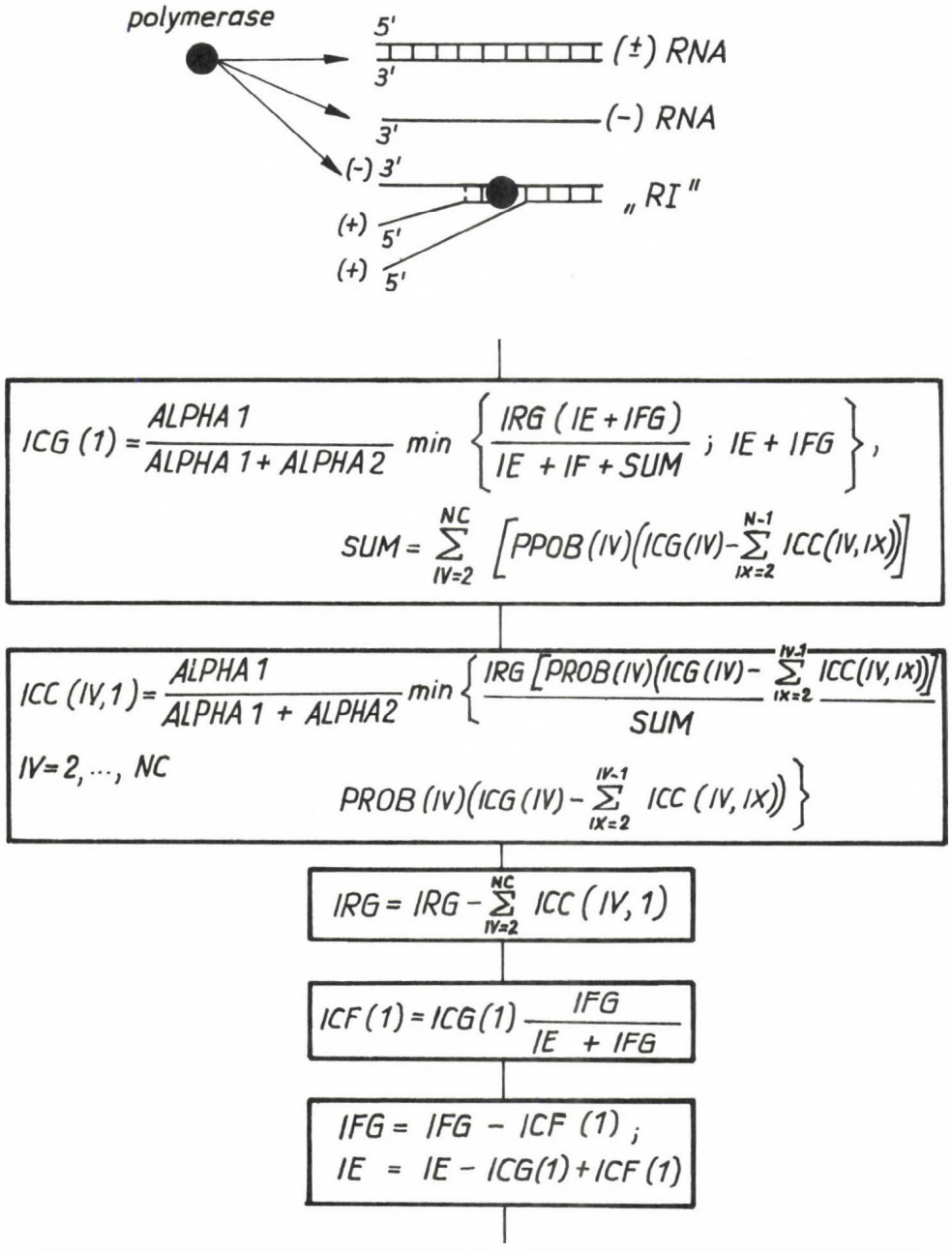

Fig. 6 A concrete cut-out of the program plan: formation of intermediate replication complexes

6 hours by using a computer with 1 million operations per second computer (BESM 6) subunit from the complicated interior logic of the model which concerns the functional relations between the system elements nevertheless. The polymerase (i.e. actually the active replication enzyme) is able to bind themselves to the 3'-end of the minus strand of double stranded RNA and likewise to the 3'-end of a single minus RNA strand or to the 3'-end of the minus strand of an already existing intermediate replication form (Fig. 6). Elected results of simulation experiments with this model have the subsequent form.

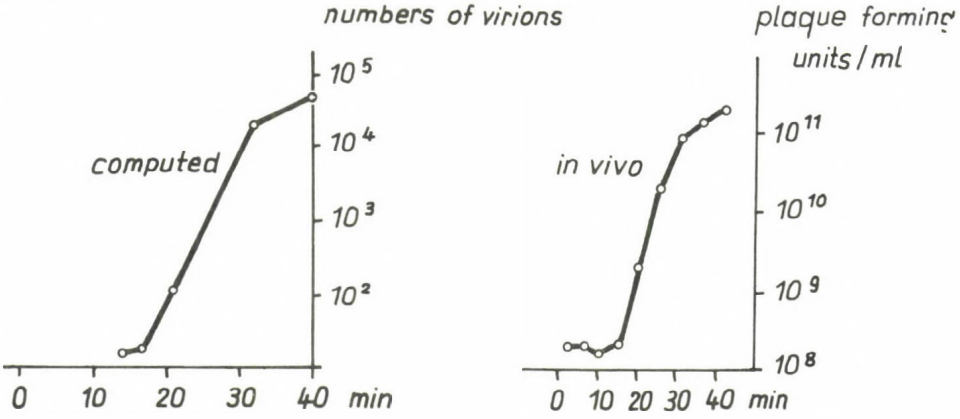

from: Nathans, D., et. al., J. Mol. Biol., 39 (1969) 279 - 292

Fig. 7 The results of the computermodel in comparison with the in vivo results

In Fig. 7 a comparison between in vivo and computed curves is possible. You see that model supplies equivalent results in relation to the results of in vivo measurements.

Stochastic deviations between different runs are not larger than that ones of the real object. All stochastic deviations of the results may be attributed to the stochastic of the defined phage system (not host system) because all host cell influences are assumed as to be constant. The differences of the computer results from the in vivo results at

single points lie within the range of real experiments.

In Fig. 8 the results of two different runs are shown. The differences are due to the three parameters: binding probability of ribosomes to the three binding sites of the three cistrons.

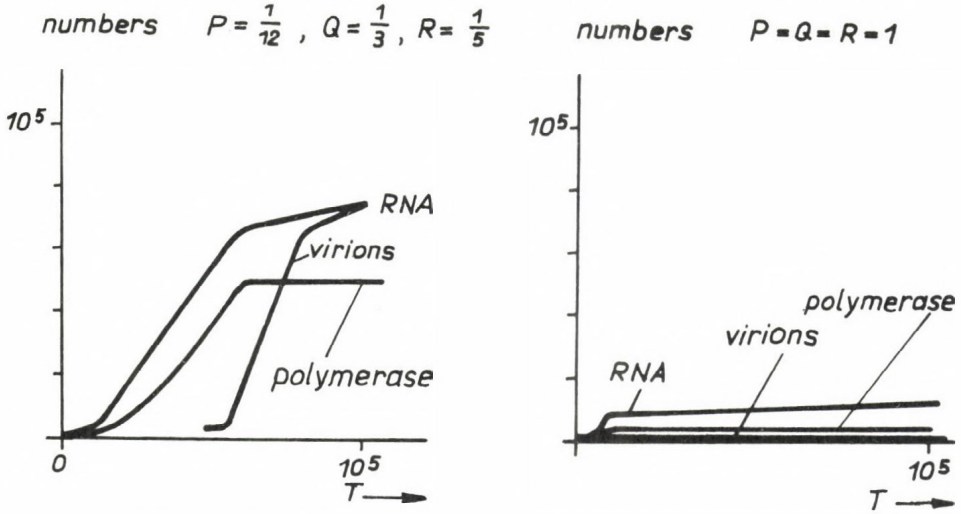

Fig. 8 Two experiments with different probabilities for ribosome binding

The binding of ribosomes
with P to maturation protein binding sites,
with Q to coat protein binding sites,
with R to polymerase binding sites
was simulated.

5. Model of the realization of the genetic information

The first model: we will speak about a compartment model characterized by a set of compartments (pools of molecules) and a set of transfer functions by which the molecule concentrations in the different compartments are changed during the process. In the model the whole process of gene expression beginning from transcription until the activation of the protein is described.

It was developed a model of the control of the realization of the genetic information, using a set of nonlinear difference equations. The aim of the study is to inquire the laws and principles that govern the dynamic behaviour, the coordination and interaction of subunits of gene expression. Gene expression means the total process from transcription to active protein.

This work is necessary for a causal understanding of the complex epigenetic control systems and a systematic interference in the processes of gene expression. By the model it may be possible to interpret experimental results. For instance it is possible to get insight in the site of action of a chemical agent, which is under test, analysing the model and comparing experimental curves with theoretical results, generated by the model.

The study of the dynamic and function of the gene expression requires the decomposition of the epigenetic control system in elementary subsystems, which represent single protein synthesis pathways. Then, the processes of differentiation and development are conceivable as complex overlapping and coordination of elementary processes of gene expression in space and time.

The fundamental subunit, we consider, is the pathway of synthesis of a monocistronic m-RNA-molecule until the finished polypeptide (Fig. 9).

Today it is necessary to consider the following levels of gene expression, which may be all sites for regulation:

1. level of RNA-synthesis (transcription)
2. level of transport of RNA from the nucleus to the cytoplasm
3. level of stabilization of RNA by binding of proteins (formation of informosomes)
4. level of the formation of activ translatable polysomes
5. level of translation
6. level of irreversible and reversible protein modifications

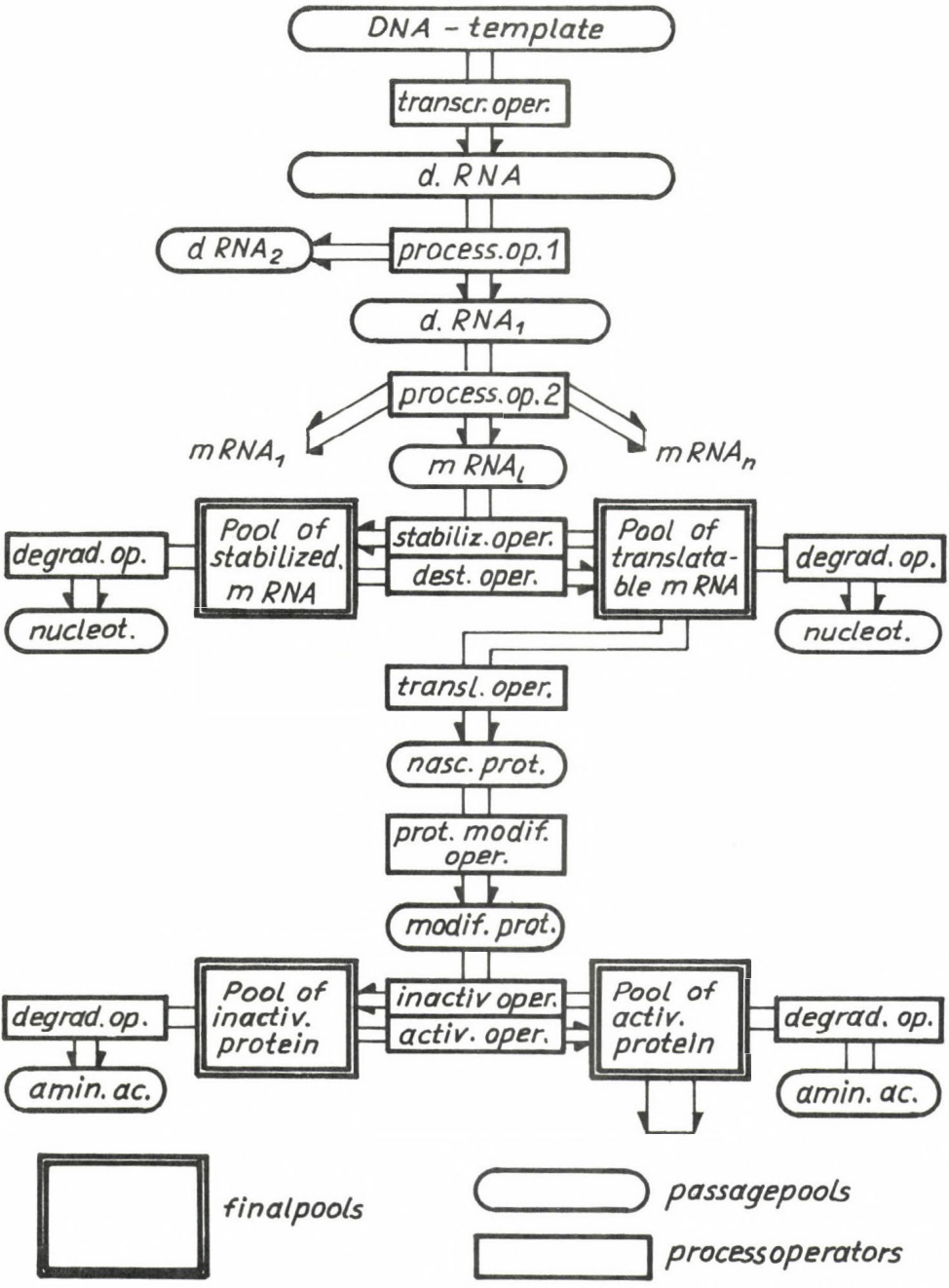

Fig.9 Formalization of a single protein synthesis pathway

7. level of activiation and inactiviation of proteins, caused by conformational changes
8. level of protein degradation.

Some of this regulation levels probable are not relevant in procaryotes, but for the eucaryotics 8 levels are to be taken into account. The molecular mechanism of the single processes are until now not jet fully explained. Nevertheless it is possible to study the dynamic consequences of these processes (which are all time-consuming and which partly yield new memory capacity for the cell (e.g. formation of informosomes) for the total process of gene expression. By a respective choise of parameters one can for instance turn off special subprocesses or modify their behaviour in a rigorous manner, to get common knowledges for procaryotic as well as for eucaryotic systems. If there are experimental data on the system parameters and the topology of interactions of a special system it is possible to inspect special questions of gene expression and its influence by effector molecules.

We abstract from the special mechanisms and physico-chemical details of the single subprocesses for the purpose of their formal characterization, considering only their functional properties (Fig. 10). The change of numbers of molecules is not described on the level of single molecular processes, but by transfer functions with suitable parameters. Because it is in the nature of the processes of synthesis and degradation, we chose the mathematical formulation in form of difference equations, i.e. the time is considered as to be a discrete variable. With it we simultaneously take into account the high complexity of processes of gene expression and obtain a reduction of numerical calculations. For the same reason all parameters of synthesis and degradation are considered as expected values. In that way all other numbers of molecules in the system are expected values too. In principle however it is possible to take into consideration exactly stochastic effects; Monte Carlo simultation is then needed.

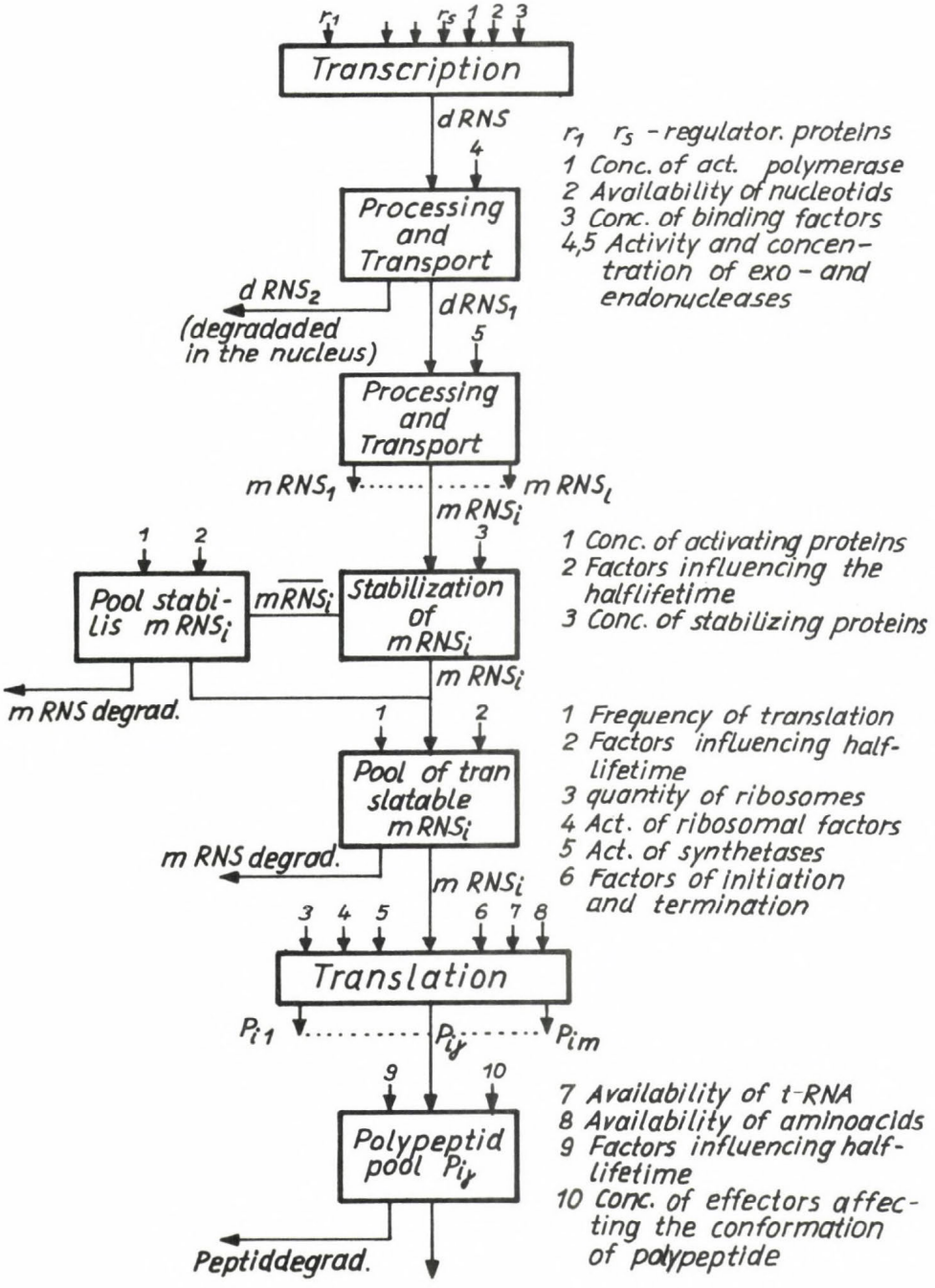

Fig. 10 Scheme of realization of genetic information for an unit of transcription

(1) $x_{oj}(t) = F_{1j}(x_{Aj}(t-i_{1j}), x_{Bj}(t-i_{7j}), x_{cj}(t-i_{8j}), H_j)$

(2) $x_{1j}(t) = c_j \cdot x_{oj}(t - i_{2j})$

(3) $x_{2j}(t) = x_{1j}(t) - b_{1j}(t) \cdot x_{1j}(t) - b_{2j}$

(4) $x_{4j}(t) = b_{1j}(t) \cdot x_{1j}(t) + b_{2j}$

(5) $x_{5j}(t) = \left[1-Z_{x5j}\right] x_{5j}(t-1) + x_{4j}(t-i_{3j}) - b_{3j}(t) x_{5j}(t-1)$

(6) $x_{3j}(t) = h_{1j} \left[1-Z_{xj}\right] x_{3j}(t-1) + x_{2j}(t) + b_{3j}(t) x_{5j}(t) - c_{xj}$

(7) $y_{oj}(t) = F_{2j}(x_{3j}(t-i_{4j}), x_{A1j}(t-i_{6j}), H_{1j})$

(8) $y_{1j}(t) = d_{jyj}(t-i_{5j})$

(9) $y_{2j}(t) = \left[1-Z_{xj}\right] y_{2j}(t-1) + y_{1j}(t) - c_{yj}$

$x_{lj}(t)$ (l=0,1,...5): number of RNA-molecules of sort during the moment t

$y_{mj}(t)$ (m = 0,1,2) : number of protein-molecules of sort m during the moment t

F_{1j}, F_{2j} - nontinear functions, describing the processes of transcription and translation

x_{Aj}, x_{Bj}, x_{cj} - controlvariables of transcription

x_{1j}, x_{A1j} - controlvariables of translation

i_{1j}, ... i_{8j} - delayconstants

H_{1j}, H_j, c_j, b_{1j}, b_{2j}, b_{3j}, z_{x5j}, z_{xj}, z_{yj}, h_{1j}, d_j, c_{yj} - various parameters, specifying the processes

Fig. 11 Model equations for the j unit of gene expression

Fig. 11 shows the system of equations, which follows from the analysis of realization of genetic information, which corresponds to a polypeptide, taking into consideration all idealizations, which are founded on the biological system.

The $x_{lj}(t)$ (l = 0,1,...5) and $y_{mj}(t)$ (m = 0,1,2) are the numbers of macromolecules of sort l or m, which are included at the moment t in the j. unit of gene expression.

The $x_{lj}(t)$ are the various sorts of RNA, which emerge on the

path from the nucleus to the cytoplasm, the $y_{mj}(t)$ on the other hand are the various proteins.

The constants i_{kj} ($k = 1,2,\ldots,8$) are delay constants, characterising the duration of transport processes and the delay of action of the control terms x_{Aj}, x_{Bj}, x_{Cj}(transcription), x_{A1j}, x_{B1j}(translation). The index j ($j = 1,2,\ldots, n$) at all system variables denotes, that it is possible to consider simultaneously n fundamental units of gene expression. With that all parameters will be vectors of dimension n, specifying the special properties of every unit of gene expression. The units can work independently of each other or there is a mutual influence and control at various levels. Just this mutual influence is a typical feature of the control of gene expression of viruses, procaryotes and eucaryotes. In the model the topology of interactions is determined by coupling parameters. They decide, which system variables (usually the protein pool y_2) of which unit of gene expression i ($i = 1\ldots n$) act as control variables x_{Aj}, x_{Bj}, x_{Cj} (for transcription) and x_{A1j} (for translation) of the unit j. The functions F_{1j} and F_{2j} characterize the control behaviour of the transcription or translation processes. They are strong nonlinear functions, which occur frequently in biological systems (e.g. the Michaelis-Menten or Hill kinetics in enzymology).

$$F_{1j}(t) = x_{oAj}(t) \overset{(+)}{\cdot} x_{oBj}(t) \overset{(+)}{\cdot} x_{oCj}(t) + a_{40j}$$

$$F_{2j}(t) = \underbrace{\frac{\left[\frac{x_{A_1j}(t - i_{6j})}{a_{5j}}\right]^{z_j}}{1 + \left[\frac{x_{A_1j}(t - i_{6j})}{a_{5j}}\right]^{P_j}}}_{\text{control term}} a_{9j}\, x_{3j}(t - i_{4j})$$

$$x_{oAj}(t) = \frac{\left[\frac{x_{Aj}(t - i_{1j})}{a_{10j}}\right]^{V_{0j}} a_{11j}}{1 + \left[\frac{x_{Aj}(t - i_{1j})}{a_{10j}}\right]^{W_{0j}}}, \quad x_{oBj}(t) = \frac{\left[\frac{x_{Bj}(t - i_{7j})}{a_{20j}}\right]^{V_{1j}} a_{21j}}{1 + \left[\frac{x_{Bj}(t - i_{7j})}{a_{20j}}\right]^{W_{1j}}}, \quad x_{oCj}(t) = \frac{\left[\frac{x_{Cj}(t - i_{8j})}{a_{30j}}\right]^{V_{2j}} a_{31j}}{1 + \left[\frac{x_{Cj}(t - i_{8j})}{a_{30j}}\right]^{W_{2j}}}$$

They determine the quality of action of the control variables x_A, x_B, x_C, x_{A1} (e.g. repression or induction). One can see the high number of variables in each equation and their strong nonlinearity, which represents essential properties of the biological system.

The strong nonlinearity excludes an analytical solution of the equations. As a numerical solving technique was therefore chosen the computer algorithmisation, i.e. the simultaneous solution of all model equations with a permanent increasing time parameter. Thereby it was possible to construct the model taking into account all essential biological features, without the necessity to have regard for analytical solving techniques.

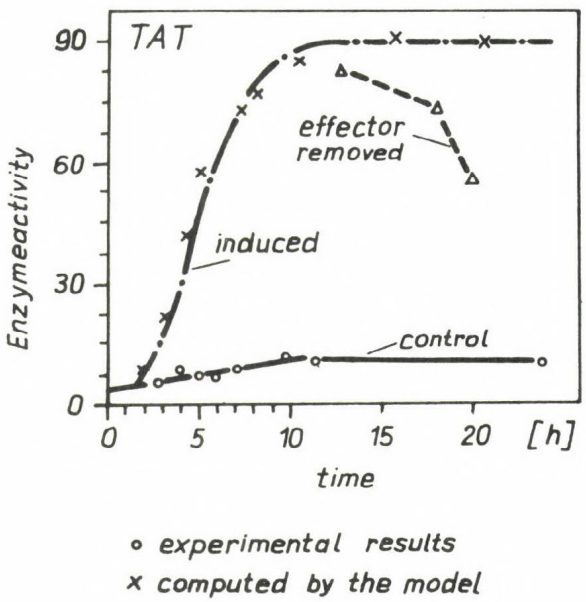

Fig. 12 Experimental and computed results (results of Granner et. al. 1970)

Fig. 12 shows the comparison of an experimental measured kinetic of the induction of the tyrosin-aminotransferase (TAT) in experimental growing rabbit-hepatome cells with a

theoretical curve, generated by computer simulation. Within the bounds of measurability one finds a good correspondence.

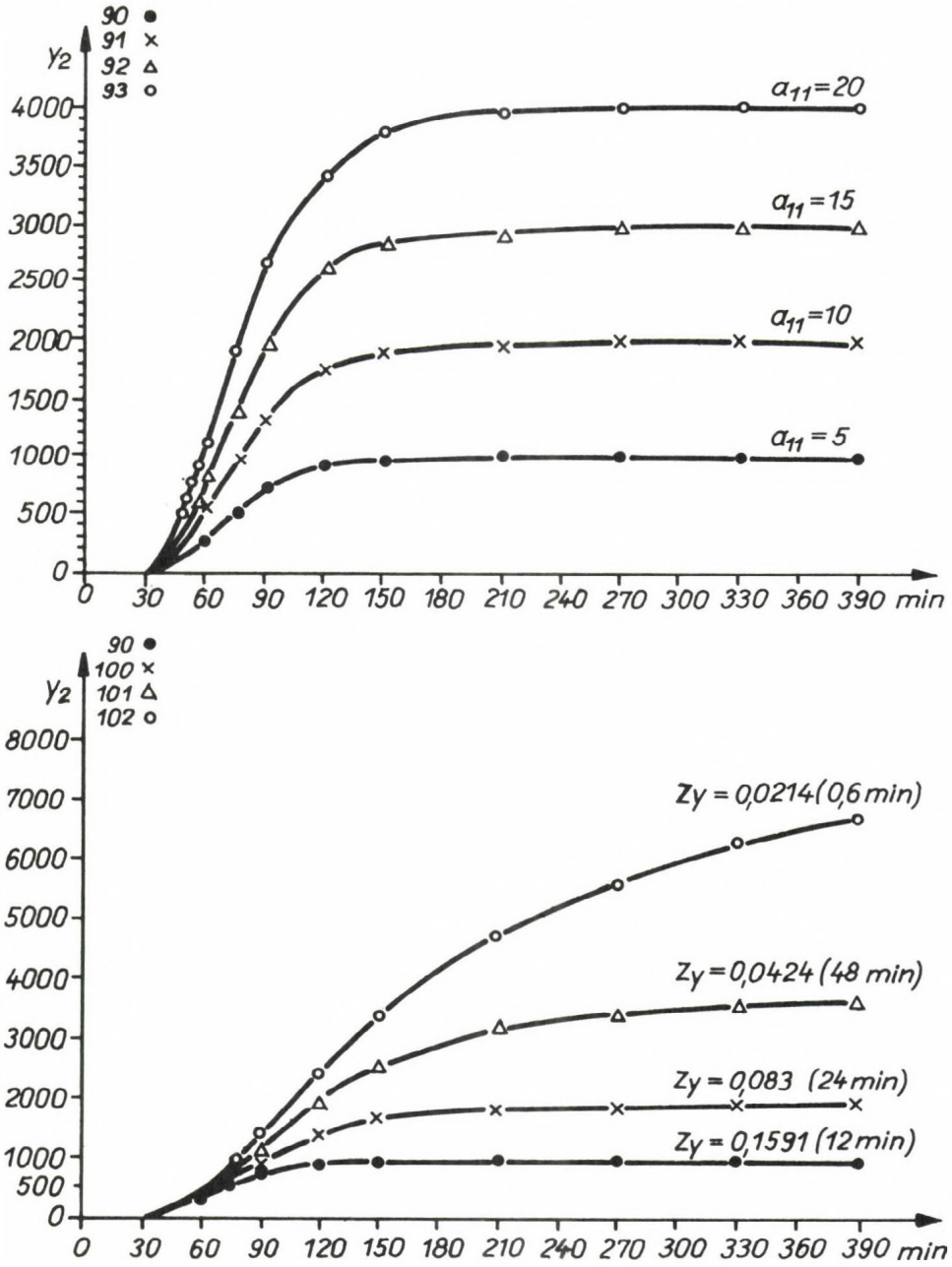

Fig. 13 Effect of variation of different parameters in gene expression: different rate of RNA-synthesis (a) and protein degradation (b).

Fig. 13a shows the influence of the average rate of synthesis of m-RNA on the shape of the induction kinetic of the protein pool and on the value of the stationary number of molecules for a unit of gene expression. The average rate of m-RNA synthesis (a_{11}) is rised in steps of 5 molec./3 min (3 min is the length of a tact) to the final values of 20 molec./3 min. The rate is constant during a single experiment, i. e. it is assumed that there does not exist any control by the factors x_A, x_B or x_C. In Fig. 13 b the dependence of the kinetic of the protein pool from the half life time of the protein is shown. The rate of m-RNA synthesis (a_{11} = 5 molec./ 3 min.), the rate of protein synthesis per m-RNA (5 molec./ 3 min.) and the m-RNA degradation rate (z_x = 0,159) are constant for all curves. One can detect a qualitative difference to Fig. 13a. The curves rise about only at 36 min and are first very close to each other. The rise of the molecule numbers goes on flater than in the curves of Fig. 13a. Therefore one can decide, analyzing the qualitative shape of a family of curves, wether a parameter of synthesis or degradation was varied. The model results are transferable to the real object too. Analyzing experimental measured curves, it is possible to get hints, wether a chemical agent influence the synthesis or degradation of a protein. Therefore the model can be used to interpret experimental results.
Fig. 14 shows the formalized epigenetic network with repression and activation relations of lambda-proteins in the early phase of developing of the lambda phage system. The resp. kinetics are shown in Fig. 15.

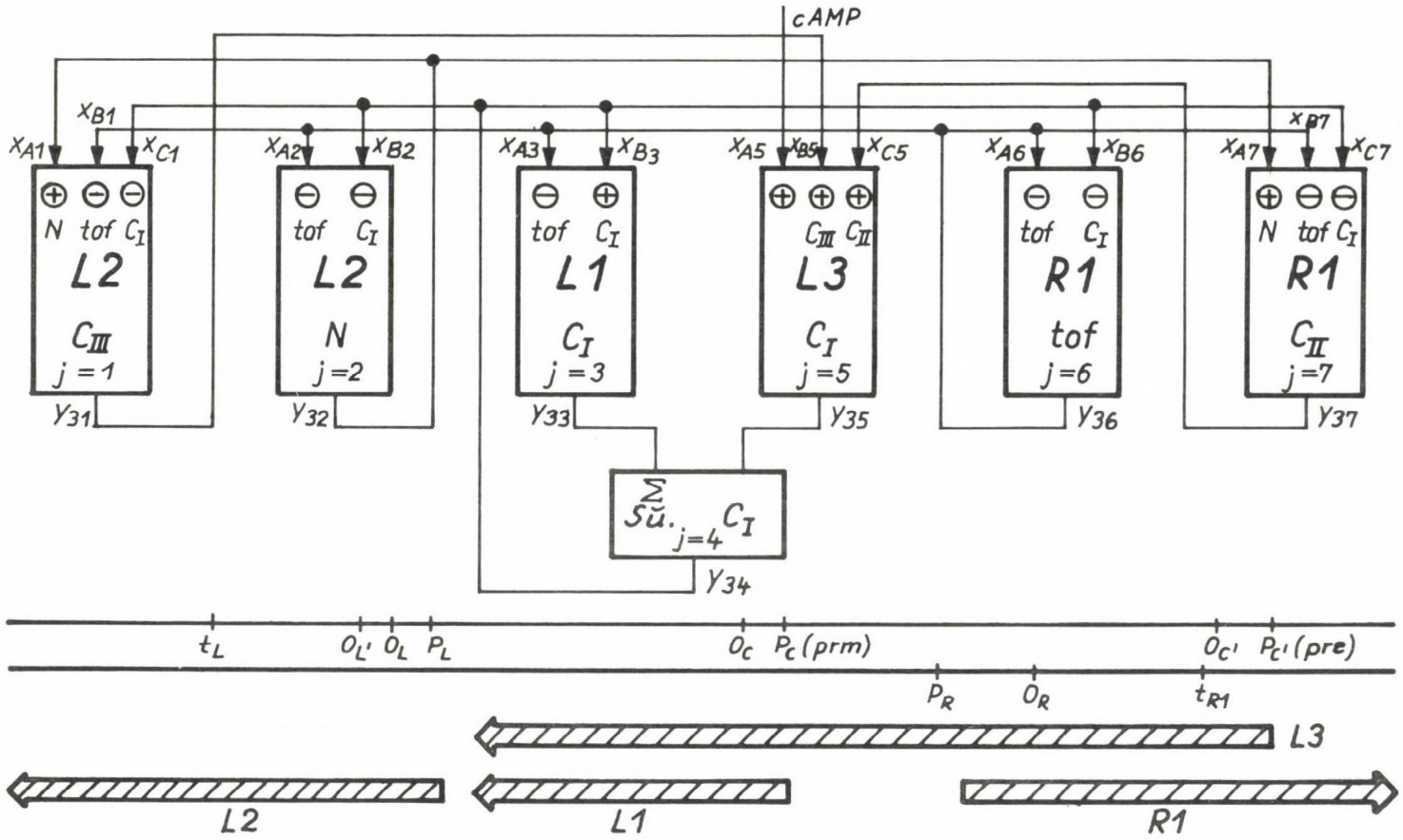

Fig. 14 Regulation of repressor synthesis (C_r) in bacteriophage λ

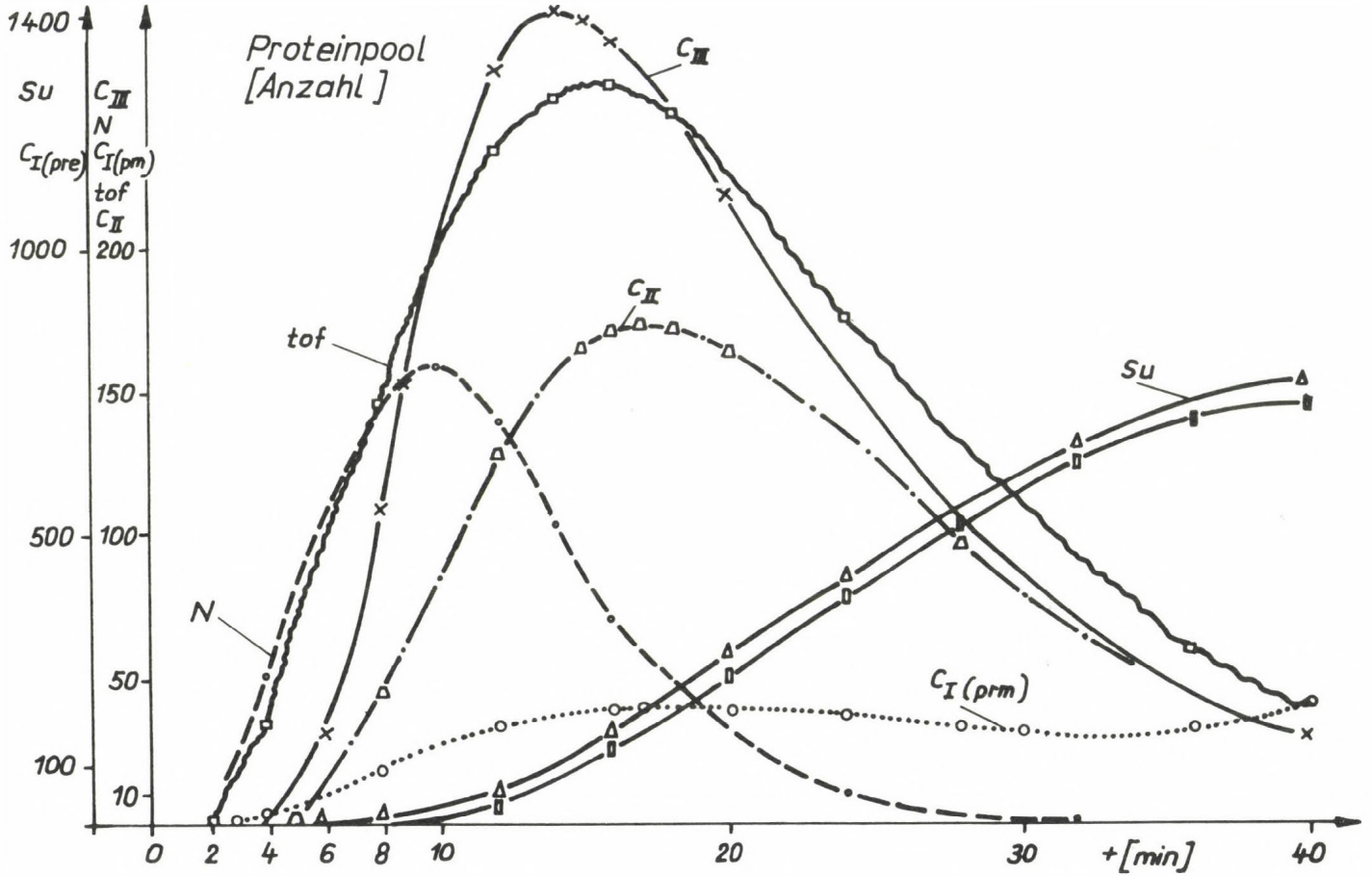

Fig. 15 Kinetic of the λ protein pool during the early phase of developement

A B S T R A C T

Four models of gene expression are described:

(1) Model of protein synthesis in eucaryotes for causal understanding of the complex epigenetic control systems with an application to information realization of Lambda phage. The model is a homomorphic picture of the real processes of gene expression (transcription until activation of proenzymes).

(2) Model of transcription regulation in procaryotes for analysis of the effects of different types of regulation mechanisms on the rate of pre-mRNA synthesis with application to the lac operon of E.coli.

(3) Model for analysis of conformation of nuclear chromatin and the transcription process introducing template and polymerase parameters.

(4) Model for analysis of regulation mechanism of genetic information release in a defined RNA bacteriophage system of the Qβ type.

All models are discrete ones realized by algorithms for simulation studies.

References

Bellmann, K., and V. Dragawzew Genetika (Moskau) in press

Bellmann, K. et al. Proc. 8th Biom. Confer. 1974 Constanta-Romania

Bellmann, K. et al. Biosystems in press

Böttner, R. Mathematisch-kybernetische Modellierung der Regulation der Genexpression. Dissertation Humboldt-Univ. Berlin 1975

Knijnenburg, A.: Algorithmisches Simulationsmodell der RNS-Bakteriophagen-Vermehrung. Dissertation Humboldt-Univ. Berlin 1974

Knijnenburg, A., and U. Kreischer Biom. Zeitschrift in press

Neumann, H., and U. Kreischer, Biom. Zeitschrift in press